Università degli Studi di Ferrara

DOCTORAL COURSE IN
"CHEMICAL SCIENCES"

CYCLE XXXIII

DIRECTOR
Prof. Cavazzini Alberto

Homogeneous and Heterogeneous Lewis Base Organocatalysis for the synthesis of added-value molecules under batch and continuous-flow conditions

Scientific/Disciplinary Sector (SDS) CHIM/06

Candidate
Dott. Brandolese Arianna

Supervisor
Prof. Bortolini Olga

Years 2017/2020

"You must read, you must persevere, you must sit up nights, you must inquire, and exert the utmost power of your mind. If one way does not lead to the desired meaning, take another; if obstacles arise, then still another; until, if your strength holds out, you will find that clear which at first looked dark."

Giovanni Boccaccio

Notes

The thesis is organized in independent chapters with own references and numbering of products.

The works described in Chapters 3 – 7 are related to scientific activities conducted at the University of Ferrara under the supervision of Professor Olga Bortolini. All the projects are focused on the use of N-heterocyclic carbene organocatalysts.

The study reported in Chapter 8 was instead conducted at the University of St Andrews (UK) under the supervision of Professor Andrew D. Smith. The work is based on the use of isothiourea Lewis base organocatalysts. The placement at the University of St Andrews (January 2020 – September 2020) has been supported by funding within the framework "Bando Giovani Ricercatori 2019" (University of Ferrara).

Abbreviations

Ac	Acetyl
ACN	Acetonitrile
Ar	Aromatic
BAF	2,5-Bis(aminomethyl)furan
BHMF	5,5'-Bihydroxymethyl furil
Bn	Benzyl
bs	Broad singlet
BTM	Benzotetramisole
Bu	Butyl
Conv.	Conversion
°C	Celsius
d	Doublet
DABCO	1,4-Diazabicyclo[2.2.2]octane
DAG	Diacylglycerol
DBU	1,5-Diazabicyclo[5.4.0]undec-7-ene
DCM	Dichloromethane
dd	Doublet of doublets
DDA	Decanediamine
ddd	Doublet of doublet of doublets
DES	Deep eutectic solvent
DFF	2,5-Diformylfuran
DHPB	3,4-Dihydro-2*H*-pyrimido[2,1-*b*]benzothiazole
DIPEA	N,N-diisopropylethylamine
DMA	N,N-dimethylacetamide
DMAP	4-Dimethylaminopyridine
DMF	Dimethylformamide
DMSO	Dimethylsulfoxide
dp	Doublet of pentets
dr	Diastereoisomeric ratio
DSC	Differential scanning calorimetry
dt	Doublet of triplets
ee	Enantiomeric excess
er	Enantiomeric ratio
EDA	Ethylendiamine
equiv.	Equivalent(s)
ESI	Electrospray ionisation
Et	Ethyl
ETM	Electron transfer mediator
FDCA	2,5-Furandicarboxylic acid
FF	Furfural
g	Gram(s)
h	Hour(s)
HAD	Hexanediamine
HBTM	Homobenzotetramisole
hept	Heptet
HFIP	Hexafluoro-2-propanol
HMF	5-Hydroxymethylfurfural
HMFCA	5-Hydroxymethyl-2-furancarboxylic acid

HMW	High molecular weight
HOAt	1-Hydroxy-7-azabenzotriazole
HPLC	High performance liquid chromatography
HRMS	High resolution mass spectrometry
Hz	Hertz
i-Pr	*Iso*-propyl
IR	Infrared
IS	Isosorbide
ITU	Isothiourea
J	Coupling constant
KHMDS	Potassium bis(trimethylsilyl)amide
LB	Lewis base
M	Molar
m	Multiplet
m/z	Mass to charge ratio
$M+H^+$ or $M+Na^+$	Protonated molecular ion
Me	Methyl
Me-THF	2-Methyltetrahydrofuran
mg	Milligram(s)
min	Minute(s)
mL	Millilitre(s)
M_n	Number-averaged MW
mol	Mole(s)
mp	Melting point
NHC	N-heterocyclic carbene
NMR	Nuclear magnetic resonance
NPs	Nanoparticles
Nu	Nucleophile
OBFA	5,5′-Oxybis(methylene)bis-2-furaldehyde
OBFC	5,5′-Oxybis(methylene)bis-2-furancarboxylic acid
PAs	Polyamides
PBHMF	Poly(2,5-furandimethylene 2,5-furandicarboxylate)
PCs	Polycarbonates
PEI	Poly(ethylene isophthalate)
PEs	Polyesters
PET	Polyethylene terephthalate
PETA	Poly(*p*-ethylene terephthalamide)
PEOBF	Poly(ethylene 5,5'-(oxybis(methylene)bis(2-furancarboxylate)
PGT	Polyglycerol terephthalate
Ph	Phenyl
PhMe	Toluene
PIF	Poly(isosorbide 2,5-furandicarboxylate)
PIT	Poly(isosorbide)terephthalate
PLA	Polylactic acid
PS	Polystyrene
PS-HyperBTM	Polymer-supported HyperBTM
Pr	Propyl
PUs	Polyurethanes
q	Quartet
qd	Quartet of doublets
ROP	Ring opening polymerization

RT	Room temperature
s	Singlet
s	Selectivity
SCE	Saturated calomel electrode
SEC	Size-exclusion chromatograph
SET	Single electron transfer
t	Triplet
t	*Tert*
T	Temperature
TBD	1,5,7-Triazabicyclo[4.4.0]dec-5-ene
td	Triplet of doublets
TFA	Trifluoroacetic acid
TfOH	Triflic acid
TGA	Termogravimetric analyses
THF	Tetrahydrofuran
TLC	Thin layer chromatography
TM	Tetramisole
TMEDA	Tetramethylethylenediamine
TMS	Trimethylsilyl
TON	Turnover number
TOF	Turnover frequency
t_R	Retention time
TS	Transition state

Table of contents

1. Introduction

1.1 Organocatalysis

Ever since their introduction, organocatalysts emerged as efficient and sophisticated synthetic tools for the synthesis of medicinally and biologically essential molecules from simple starting materials. The concept organocatalysis has been established for the first time at the beginning of the XXI century by MacMillan,[1] underlying the use of small organic molecules as catalysts. Even if this relatively different way of making catalysis was pretty new, its application had been known for more than a century. However, only in the past decades it blossomed mainly thanks to the possibility to promote asymmetric transformations.

Organocatalysts are stable small metal-free molecules, generally cheap and easy to find, that are able to catalyse chemical reactions in a very efficient way.[2] Now, it is widely accepted that this "metal-free catalysis" is one of the main branches of enantioselective synthesis along with enzymatic catalysis and organometallic catalysis. Soon after the conceptualization of the field, the rapid growth of the research on organocatalysis has been promoted by the advent of generic modes of catalyst activation, induction, and reactivity. In fact, most of all organocatalysts can be broadly classified as Lewis bases, Lewis acids, Brønsted bases, and Brønsted acids according to the different mechanisms of action (Figure 1).[3]

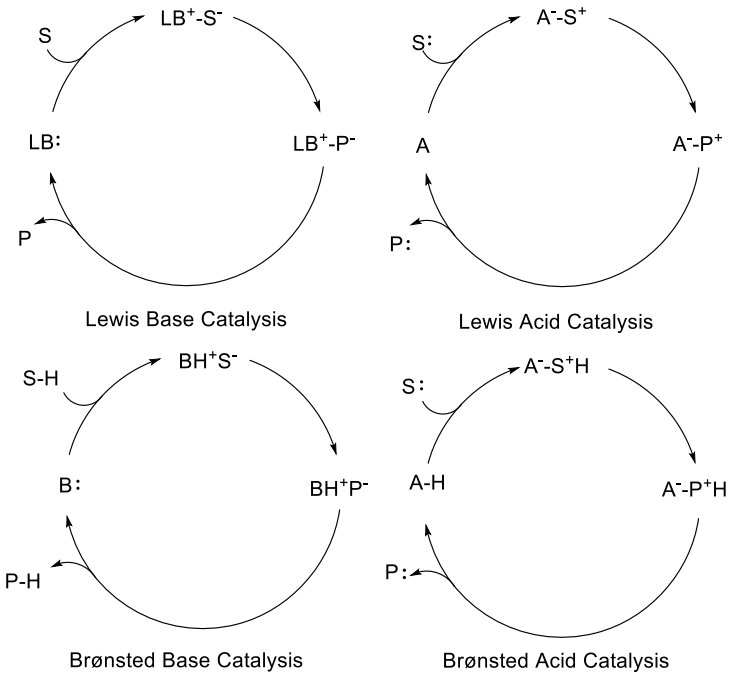

Figure 1. Mechanisms of action of organocatalysts.

Therefore, Lewis base catalyst (LB) initiates the catalytic cycle *via* nucleophilic addition to the substrate (S); the resulting complex undergoes a reaction and then releases the product (P) and

the catalyst for the turnover. Lewis acid catalyst (A) actives the nucleophilic substrate (S) in a similar manner. Brønsted base and acid catalytic cycles are instead initiated *via* deprotonation or protonation, respectively.[3]

Considering the work conducted during the PhD course, the next discussion will be focused on the role of organocatalysts as Lewis bases, in particular on N-heterocyclic carbene (NHC) and isothiourea-based organocatalysts.

1.2 N-heterocyclic carbene: structure and reactivity

N-heterocyclic carbenes (NHCs) represent one of the most spread class of Lewis base organocatalysts. Their use has been grown in the last few years thanks to their peculiar features to be a green and non-toxic alternative to organo-metallic species. Since the pioneering work conducted by Arduengo et al.[4] in 1991 on the isolation of the first free NHC IAd, these compounds have received a huge amount of attention. As studies were conducted on their properties and reactivity, the full potential of NHCs in many different areas such as kinetic resolutions, desymmetrization strategies, polymerization reactions, and the synthesis of natural products and biologically active compounds were revealed. Beside these processes, as strong σ-donors to metal centres, NHCs were at the beginning but as well as nowadays, widely used as ancillary ligands in organometallic chemistry involved in industrially important catalytic transformations.[5]

A carbene is a molecule characterized by a neutral di-coordinated carbon with a sextet of electrons. Two kinds of carbenes can be defined, singlets or triplets, depending upon their electronic structure. When the carbene displays two unshared valence electrons respectively placed on the sp^2 and p orbital, it is called a triplet carbene (Figure 2). Whilst, if the two electrons are placed on the sp^2 orbital (HOMO, highest occupied molecular orbital) with the relative p orbital empty (LUMO, lowest unoccupied molecular orbital), the carbene is called singlet carbene (Figure 2). This is often used as ligands for metal-based catalysis due to their double effect to accept and release electron density.

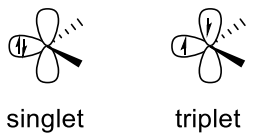

Figure 2. Electronic features of singlet and triplet carbenes.

Unlike classical carbenes, which most often have triplet ground states, NHCs are singlet carbenes. Globally, they present common structural features that play a role in stabilizing the

carbene moiety while variations in their substitution partner or structure result in different properties of the general NHC (Figure 3).[6]

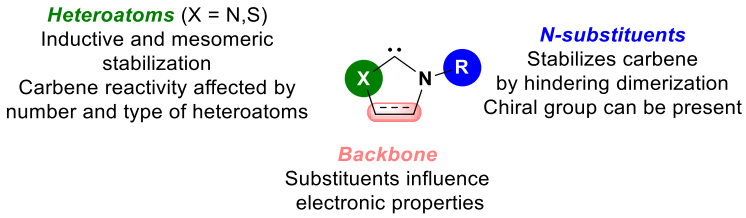

Figure 3. General structural features of NHCs.

Usually, the carbene carbon is situated adjacent to at least one nitrogen atom incorporated into the ring structure. The third bond of the nitrogen atom is established with an aliphatic or aromatic group, (N-substituents) whose role is to stabilize the carbene, minimizing the dimerization (Wanzlick equilibrium) thanks to the steric hindrance. Moreover, chiral groups can also be present. The backbone of the NHCs, instead, could present some substituents that influence the electronic properties without having a minimal steric impact at the carbene centre. The most common NHCs, obtained by *in situ* deprotonation of the corresponding salts, are thiazol-, triazol-, imidazol-, and imidazolin-2-ylidenes (Figure 4).

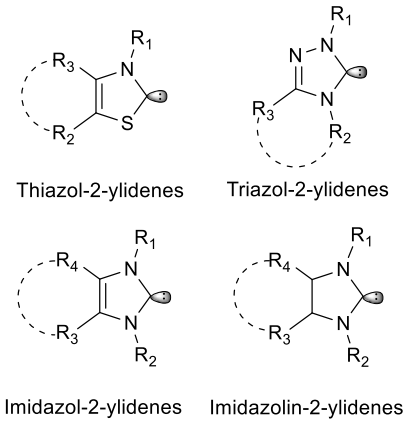

Figure 4. General types of N-heterocyclic carbenes.

Apart from the aforementioned stabilization due to steric clashing between the bulky alkyl or aryl groups frequently present on nitrogen or other substituents situated adjacent to the carbene carbon, a combination of kinetic and thermodynamic factors also occurs. In fact, electronic aspects, depending upon the NHC structure, play a major role in stabilizing the free carbene structure. The lone pair on the nitrogen atom stabilizes the empty *p* orbital of the carbene carbon by resonance, while the electron-withdrawing nature of the heteroatom can remove density from the occupied sp^2 orbital. This effect is well-known as the "push-pull effect" (Figure 5).

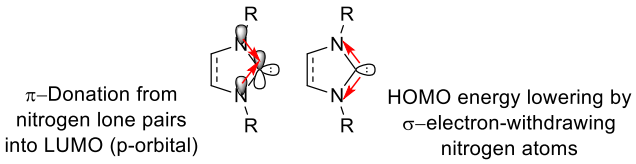

Figure 5. Stabilization of the carbene by push and pull effect.

Of note, these particular electronic features diversify NHCs from common Lewis bases; the latter donate an electron pair while NHCs show at the same time σ basicity and π acidity. For these reasons they represent nowadays the most popular and used organocatalysts for umpolung reactivity.

1.2.1 Umpolung reactivity

The umpolung concept arises from the need to synthetize molecules that could not be obtained by considering their natural polarity. The explanation of normal and umpolung reactivity was introduced by D. Seebach and E. J. Corey[7] to address the necessity of a polarity inversion in a retrosynthetic analysis, therefore providing more flexibility in a synthetic plan. Seebach defined the umpolung as "any process by which the normal alternating donor and acceptor reactivity pattern of a chain, which is due to the presence of O or N heteroatoms, is interchanged".[7] This concept was further rationalized by the identification of the nucleophilic or donor (d) and electrophilic or acceptor (a) sites that are typically used to make or break bonds. Indeed, most of the target molecules in organic synthesis contain heteroatoms such as nitrogen and oxygen as functional group. The presence of these heteroatoms requires an alternating acceptor and donor reactivity upon the carbon skeleton, but if this alternation is inverted by a modification of the substrate, the inversion of the reactivity occurs (Figure 6).

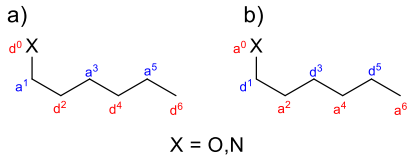

Figure 6. Seebach's umpolung theory: (a) direct reactivity; (b) inverted reactivity.

Therefore, it is possible to classify a direct reactivity and inverted reactivity and labelling the carbon atoms of the chains according to their number and reactivity. As reported in Figure 6b in case of the umpolung reactivity, the carbon next to the heteroatom **X** is called carbon d^1 as well as for all the carbons in odd position $d^{(2n+1)}$. The same convention is also used for the

acceptor carbons, indicated as $a^{(2n)}$. On the other hand, synthons (the retrosynthetic fragmentation structure) labelled as $a^{(2n+)1}$ and $d^{(2n)}$ show a normal reactivity (Figure 6a).
This concept has opened new aspects in synthetic plans broadening the available synthetic strategies. In fact, the umpolung reactivity underlies the latest C-C bond forming methods, such as the benzoin condensation and the Stetter reaction promoted by NHCs catalysis.

1.2.2 Benzoin and Stetter reactions

As already mentioned, the most famous example of umpolung reactivity is the benzoin condensation. This process has its origins in the 1832 with report of Wöhler and Liebig[8] showing that cyanide ion may be used to promote the dimerization of two aldehydes. This reaction is an important approach to create new C-C bonds leading to the formation of an α-hydroxy ketone through the coupling of two molecules of benzaldehyde. Even if the mechanism had been intensively studied, only at the beginning of the XX century it was rationalized (Scheme 1).[9] The reaction starts with the addition of the cyanide ion on benzaldehyde **1** to form the intermediate **2** which undergoes an intramolecular proton transfer to give the species **3**. This transient molecule is intercepted by another molecule of benzaldehyde to generate the adduct **4**. After the final proton transfer to give **5**, the system releases the benzoin **6** and regenerates the cyanide anion which is available for another catalytic cycle.

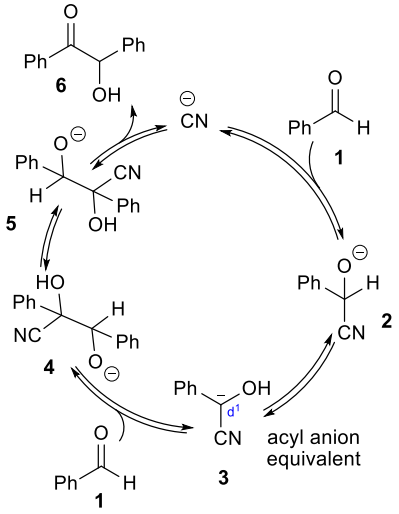

Scheme 1. Mechanism of the cyanide-catalysed benzoin condensation.

In 1943, Ugai and co-workers[10] discovered that thiazolium salts are able to promote this reaction, but only in 1958, upon the work of Lapwort, Breslow proposed a mechanism to explain this process (Scheme 2).[11]

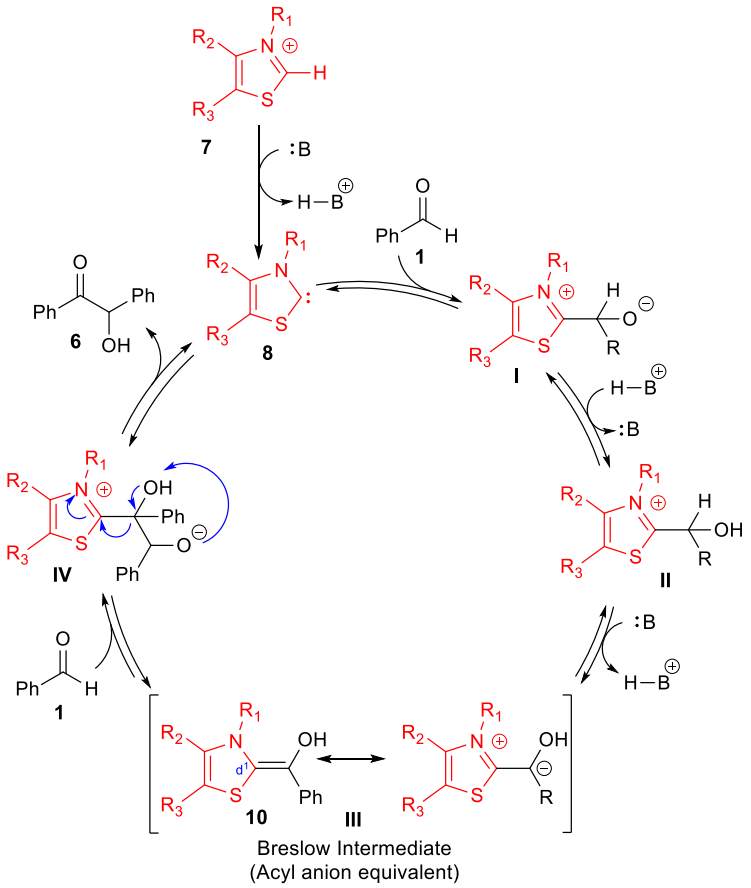

Scheme 2. Proposed mechanism for benzoin reaction catalysed by thiazolium salts.

Deprotonation of the thiazolium salt **7** generates the carbene/ylide **8**. This new species is nucleophilic and attacks a molecule of aldehyde to generate a tetrahedral intermediate (**I**). Protonation of the alkoxide followed by a subsequent deprotonation forms a resonance-stabilized hydroxy-enamine (**III**) with the resulting reversal of polarity (umpolung) on the former carbonyl carbon. This species known as the "Breslow intermediate" attacks another aldehyde molecule to form an unstable intermediate (**IV**), which collapses to eject the benzoin product and the catalyst.[11]

A variety of experiments have been later conducted promoting both the NHC-catalysed homo- and hetero-coupling of aldehydes. Moreover, since the pioneering work conducted by Sheehan and Hunneman,[12] a substantial effort was made to find conditions for highly enantioselective NHC-catalysed homo and hetero-benzoin reactions.[6]

The umpolung of the aldehyde is also the key step for the Stetter reaction. This procedure involves a conjugated addition of an aldehyde to a Michael acceptor such as α,β-unsaturated carboxylic esters, ketones and nitriles (Scheme 3).

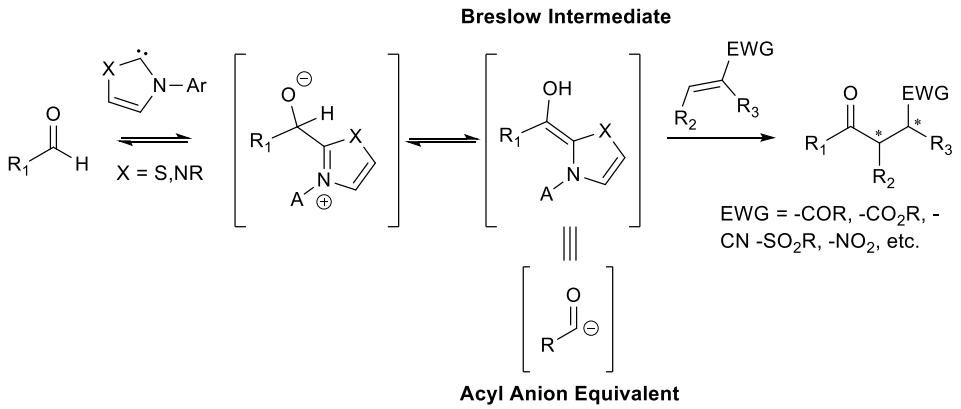

Scheme 3. NHC-catalysed Stetter reaction.

Even if NHCs have been successfully used to promote this umpolung process, during recent years, there has been an increased interest in NHC-catalysed couplings between aldehydes and unconventional electrophiles. The development of new activation modes in NHCs catalysis is important as this provides a platform for developing new reactions. Only recently, in fact, the acyl anion equivalent (Breslow intermediate) reactivity has been complemented with efficient protocols that require oxidative conditions, opening to the investigation of the acyl azolium reactivity.

1.2.3 Oxidative NHC-catalysis

Most of the first published NHC-catalysed processes mimic the reactivity of the naturally occurring Breslow intermediate formed by thiamine pyrophosphate (TPP)-mediated enzymatic transformation of pyruvate to CoASAc (Scheme 4).[13] Indeed, TPP acts as a carbene cofactor and once the enaminol **9** is formed an aerobic or anaerobic pathway can follow. The former pursues an umpolung reactivity, whilst the latter go through an oxidative carbene catalysis. In the disclosed example of the mechanism of pyruvate ferredoxin oxidoreductase, the enaminol **9** is thus oxidized by ferredoxin *via* an additional cofactor characterized by an [Fe_4S_4] cluster through two SET (single electron transfer) steps to afford the acyl azolium intermediate **10** (Scheme 4). Lastly, compound **10** could react as efficient acylation reagent with CoASH to yield CoAS-Ac **11**, which is then used in further chemical and biological transformations.

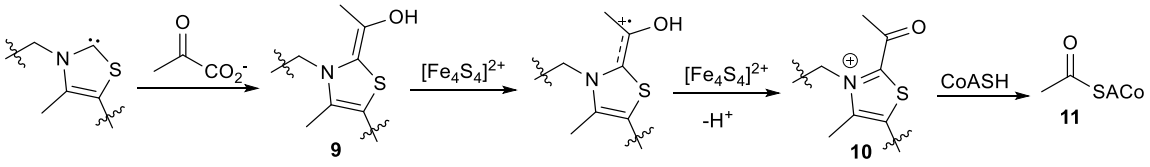

Scheme 4. TPP-mediated enzymatic transformation of pyruvate to CoASAc through oxidative carbene catalysis.

Therefore, inspired by the natural oxidative decarboxylation process described above, the biomimetic oxidation of the Breslow intermediate was extensively studied by chemists. This oxidation can be carried out either by incorporating a redox active functionality into the substrate (internal oxidation) or by using external reagents as oxidants (Scheme 5).[14] The saturated NHC-bound acyl azolium intermediates obtain from the Breslow oxidation are normal polarity intermediates and are frequently involved in several chemical transformation such as transesterification, amidation, and aldehyde oxidations.

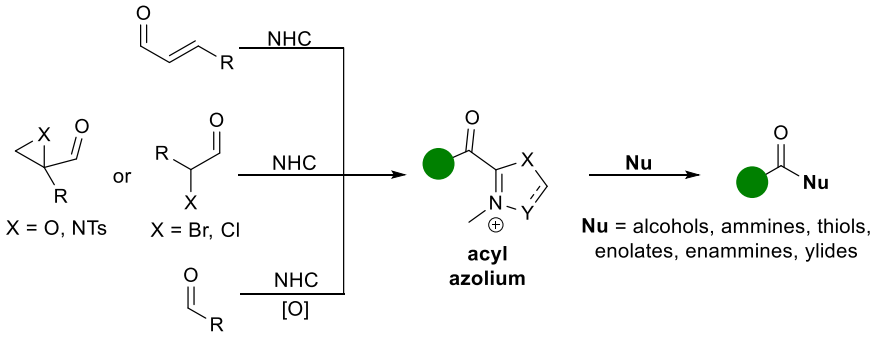

Scheme 5. Oxidation of Breslow intermediate and reactivity of acyl azolium.

The internal oxidation involves substrates that carry a leaving group or unsaturation adjacent to the carbonyl moiety. This process can be redirected to uncommon reaction pathways through two distinct catalytic intermediates: enol and acyl azolium (Scheme 6).

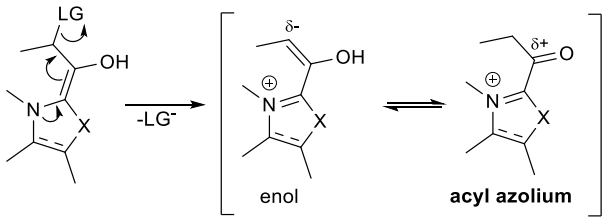

Scheme 6. Enol and acyl azolium intermediates involved in the internal oxidation strategy.

However, considering the purpose of the conducted work, the further discussion will focus on the external oxidation approach highlighting the recent developments in this field.

To oxidize the Breslow intermediate, a range of inorganic and organic oxidants have been used with excellent results. Molecular oxygen was employed as oxidant as well.

The first work involving the use of inorganic oxidants was the Corey's report on a mild cyanide-catalysed oxidative esterification of aldehydes based on the use of MnO_2.[15a] Soon later, Scheidt recognized that this transformation is considerably more efficient if a triazolium carbene replaces the cyanide catalyst (Scheme 7). Mechanistically, two distinct oxidation steps can be identified: firstly, the alcohol oxidation to aldehyde followed by the addition of NHC in order

to generate the Breslow intermediate. Secondly, the enaminol oxidation into the acyl azolium **12**, which rapidly reacts with a molecule of alcohol to give the corresponding ester **13**.[15b]

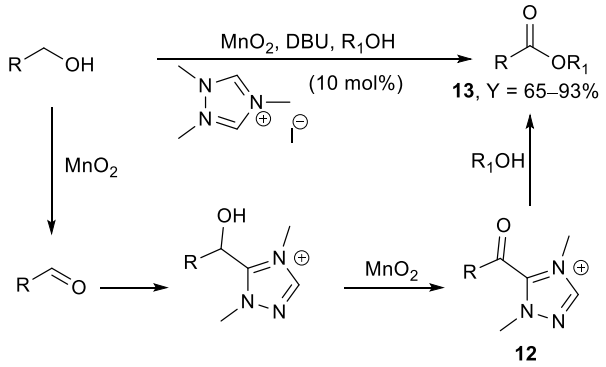

Scheme 7. Oxidation of aldehyde promoted by NHC and MnO_2.

Similar conditions were also used for the desymmetrization of cis-1,2-cyclohexanediol at low temperature using a chiral NHC precursor affording the corresponding ester with 80% enantiomeric excess (*ee*) and 58% chemical yield. Later, the same method was also applied to the one step esterification of unactivated aliphatic aldehydes[16] and cyclopropane aldehydes.[17]

The use of dioxygen in NHC-catalysed oxidations of aldehydes was successfully reported by several research groups.[18] Liu et al. described the oxidation of cinnamyl and aryl aldehydes into carboxylic esters **15** mediated by benzimidazolium pre-catalyst **14** in the presence of different cinnamyl or allyl bromides using air as the terminal oxidant (Scheme 8).[16]

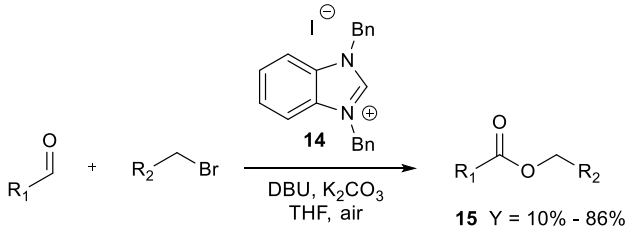

Scheme 8. Aerobic oxidation promoted by NHCs.

Overall, the reactivity trend showed that electron-poor aldehydes are more prone to be oxidized. Soon later, Hui and co-workers extend the process using unactivated alkyl bromides in a similar esterification process.[18b] Along with the rapid growth of examples about the NHC-promoted aerobic oxidation of aldehydes, mechanistic studies were performed too.

The first postulated pathway (Scheme 9) goes through the formation of the zwitterionic peroxy intermediate **17**, obtained by oxygenation of the Breslow intermediate **16**.[18c] The subsequent fragmentation allows the turnover of the carbene catalyst and the corresponding deprotonated peracid **18** is intercepted by a molecule of aldehyde. At this point, carboxylate **20** is generated,

via adduct **19** (oxygenative pathway), and the ester product can be obtained through base-mediated O-alkylation. The supposed mechanism was validated by the Hui's report on the O-alkylation of activated tetrahydrofuran under similar conditions.[18b]

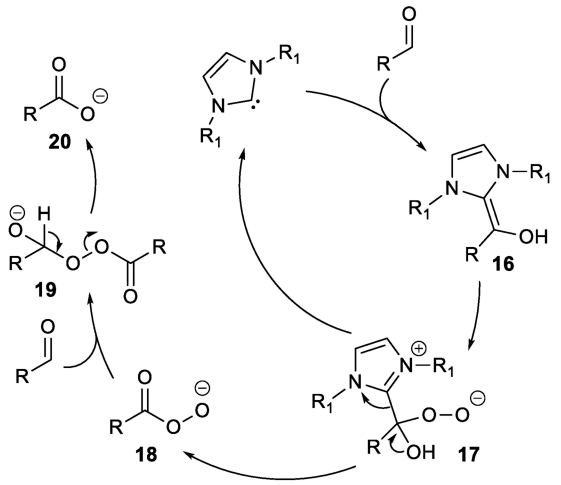

Scheme 9. Mechanism of aerobic oxidation of aldehyde promoted by NHCs.

However, in the presence of alcohol, it has been demonstrated that the oxygenative pathway is in competition with the oxidative one and the favourite pathway is influenced by the stereoelectronic features of the aldehyde substrate (Scheme 10). This dichotomy has been

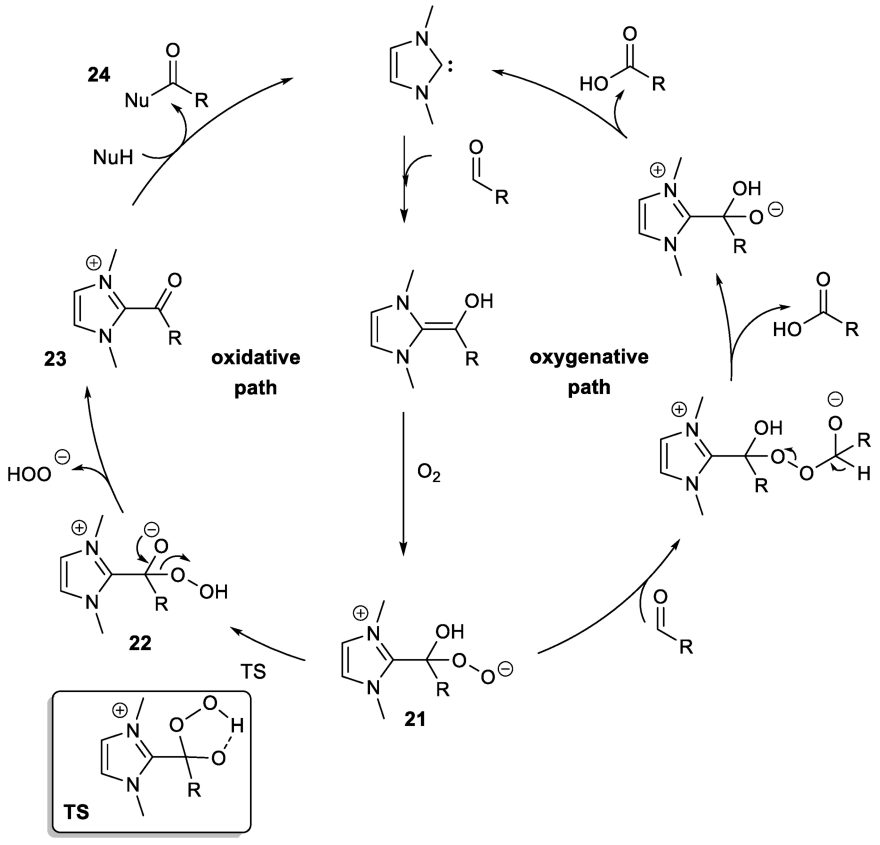

Scheme 10. Dichotomy of the oxygenative and oxidative pathways.

extensively studied and in 2014 Bortolini and co-workers detected several key intermediates involved in the two pathways through ESI-MS analysis.[19] Indeed, the common zwitterionic peroxy species **21** can evolve through either an oxygenative pathway or oxidative pathway. The former is the same reported above, while the latter is characterized by a proton transfer to form the species **22**. The following elimination of hydrogen peroxide anion gives the acyl azolium intermediate **23** that reacts with a nucleophile, such as an alcohol, to afford the corresponding product **24** (Scheme 10).

Nowadays, in place of inorganic oxidants and O_2, organic oxidants represent the most employed reactants in NHC-catalysed oxidative transformations. The organic oxidants initially used were the aromatic nitro and nitroso derivatives[20] and the following mechanism was suggested for the nitro compounds (Scheme 11). Intermediate **26** is generated after the nucleophilic addition of the Breslow intermediate **25** to the nitrogen atom of the nitro compound. At this point **26** is converted into **27** by intramolecular proton transfer and the subsequent fragmentation affords the acyl azolium intermediate which upon nucleophilic trapping with an alcohol or water affords the carboxylic acid derivatives.

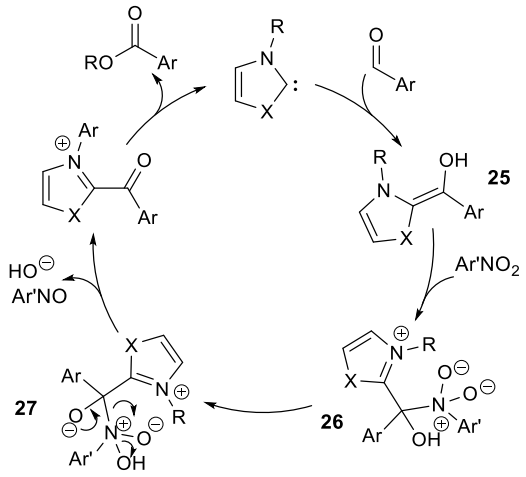

Scheme 11. Suggested mechanism for the NHC-catalysed oxidation of aldehydes with nitroarene as oxidant.

Similarly, nitroso compounds have been used, however two mechanisms on their role as external oxidant have been postulated: an electron-transfer and an ionic reaction. In the redox process, the Breslow intermediate reacts with the nitrosoarene by consecutive double electron transfer from the enaminol **25** to the nitroso functional group. In the ionic pathway, the nitrogen of the nitroso compound undergoes a nucleophilic attack from the Breslow intermediate to form the hydroxy amide **28**.[21] Overall, it has been demonstrated that both mechanisms are possible depending on the substrate (Scheme 12).

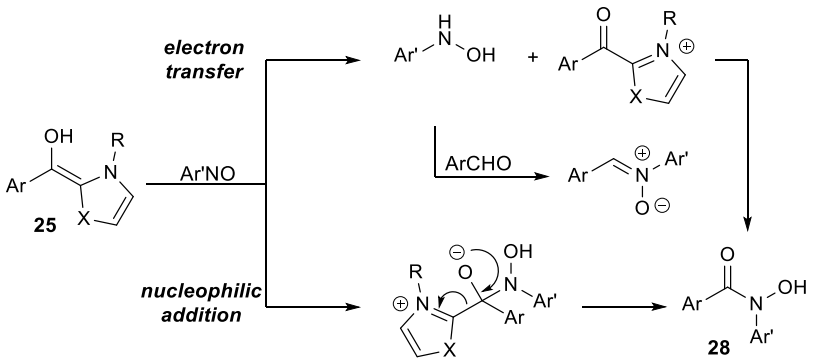

Scheme 12. Dichotomy mechanisms with nitrosoarene as oxidant.

Additionally, a wide range of substrates were converted to hydroxamic acid derivative using a triazolium catalyst and nitrosoarenes as external oxidants.[22]

Anyway, pyruvate dehydrogenase which uses thiamine pyrophosphate (TPP) and flavin adenine dinucleotide (FAD) to obtain acetic acid from pyruvic acid were taken as example for the development of a nonenzymatic version of the process. Methyl tetra-O-acetyl riboflavin (MeFI) was in fact used as electron reservoir for the oxidation of the Breslow intermediate found to be a versatile mediator in NHC-catalysed oxidative reactions. Subsequently other methods were disclosed for the regeneration *in situ* of the mediator, such as an electrochemical one, that avoid the destruction of the NHC in an argon atmosphere at low voltage (−0.3 V).[23]

Other organic oxidants (**30**−**32**) were further tested showing excellent results. Connon, for instance, used a series of organic electron acceptors as oxidants for the esterification of aldehydes promoted by thiazolium precatalyst (Scheme 13).[24]

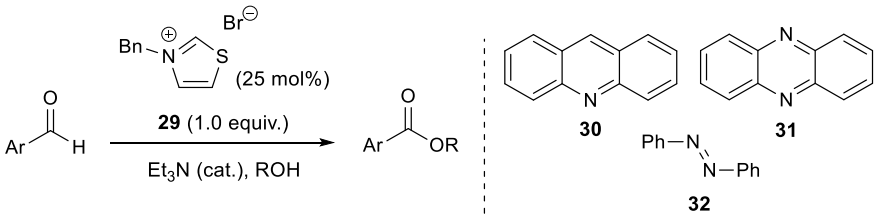

Scheme 13. Oxidative esterification with azobenzene as oxidant.

Inspired by the pyruvate ferredoxin oxidoreductase (PFOR) catalysed processes the biomimetic oxidation of enaminols of type **9** by the organic single- electron transfer (SET) oxidant 2,2,6,6-tertramethyl piperidine N-oxyl radical (TEMPO) has also been investigated. In fact, two oxidizing TEMPO units mimic the role of the oxidizing [Fe_4S_4] cluster in PFOR (Scheme 14).[25] While sluggish reactions were observed for aliphatic aldehydes, the disclosed protocol worked well when aromatic and heteroaromatic aldehydes are converted into the corresponding TEMPO esters. The proposed mechanism involves the formation of the radical cation **34** and

$TEMPO^{-}$, as consequence of a SET of TEMPO to Breslow intermediate. Deprotonation of **34** by $TEMPO^{-}$ leads to radical **35** and TEMPOH. A second SET from **35** to TEMPO gives the acyl azolium **36** which undergoes a nucleophilic attack to form the TEMPO-ester **37** which can be easily converted into any generic esters under acidic conditions.

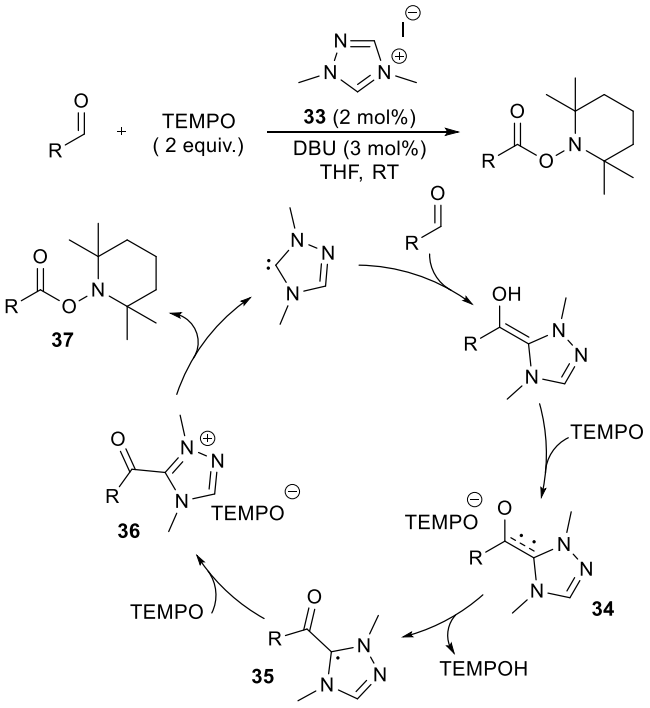

Scheme 14. Biomimetic oxidation of aldehydes with TEMPO.

The further studies on the use of a performant organic oxidant were driven by the search of an organic SET oxidant that is able to oxidize the Breslow intermediate but, in the meantime, its reduced form cannot act as nucleophile. The 3,3',5,5'-tetra-tert-butyldiphenoquinone has been found as one of the optimal oxidants that addresses all the former requirements. Since its introduction, this oxidant has been used in several NHC-oxidative processes. In 2010, Sundén and co-workers proposed the efficient conversion of several aromatic aldehydes into the corresponding esters with low catalytic loading employing cheap triazolium salts (Scheme 15).[26] As expected, the bisphenol **39** formed from **38** by consecutive double SET resulted too bulky to react with the acyl azolium intermediate.

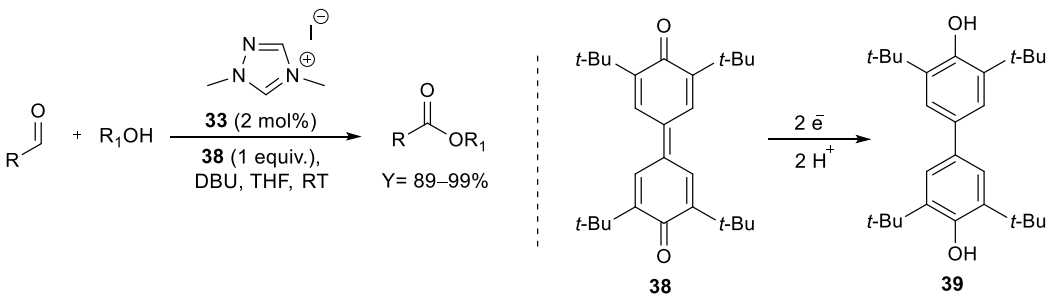

Scheme 15. Oxidative esterification of aldehydes promoted by Kharasch oxidant.

Apart from the previous methods, the NHC-catalysed oxidative reaction in the presence of mediators has acquired a remarkable interest in recent years. Sundén et al., in fact, performed an efficient biomimetic protocol in which iron (II) phthalocyanine (FePc) is employed as electron transport mediator (ETM) and air as the final electron acceptor.[27] The plausible mechanism foresees that the alcohol **40** is converted *in situ* into the Kharasch oxidant **38**, which is continuously regenerated by the FePc. On the other hand, the reduced form of FePc, FePc', is constantly restored by air which acts as the final oxidant. The authors successfully applied this protocol to the esterification of glycerol **41** in the presence of cinnamyl and aromatic aldehydes as the acylating precursors (Scheme 16).

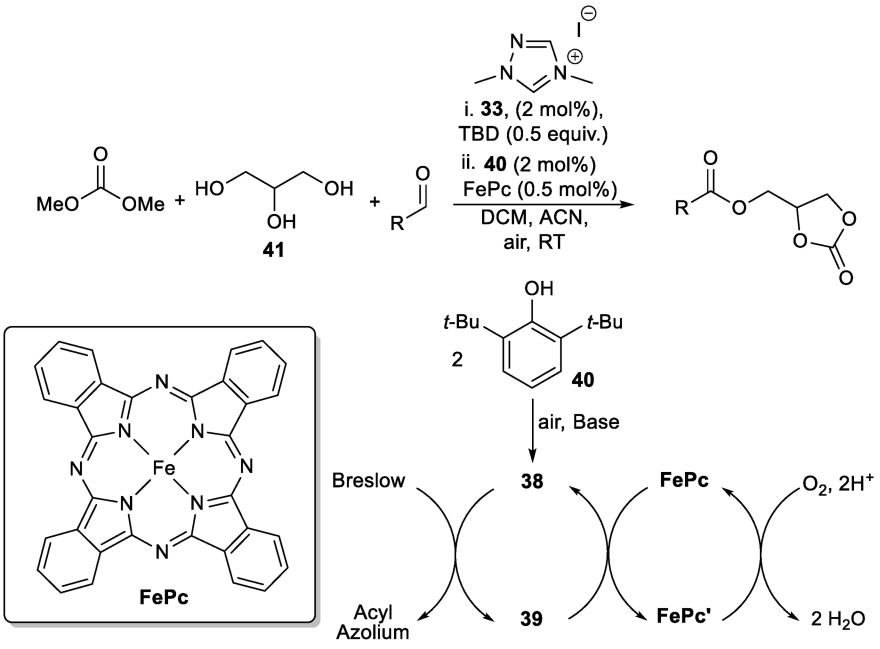

Scheme 16. Glycerol esterification by NHC-catalysed oxidation in the presence of an ETM system.

1.3 Isothiourea catalysis

Isothiourea (ITU) catalysts are pretty new as organocatalysts. In fact, amidines, guanidines and related isothioureas have been often used as strong organic bases. Despite their basicity properties, a number of small molecules containing basic functional group have been shown to act as efficient nucleophilic catalysts.[28] Only in 2006, with Birman's report, chiral ITUs were used in enantioselective processes for the first time.[29] Previously, the group had explored the use of several chiral heterocycles mainly amidines that acted as Lewis bases in enantioselective acyl transfer reactions.[30] Soon later, they turned their attention to tetramisole (TM) **42** and benzotetramisole (BTM) **43** (Figure 7).

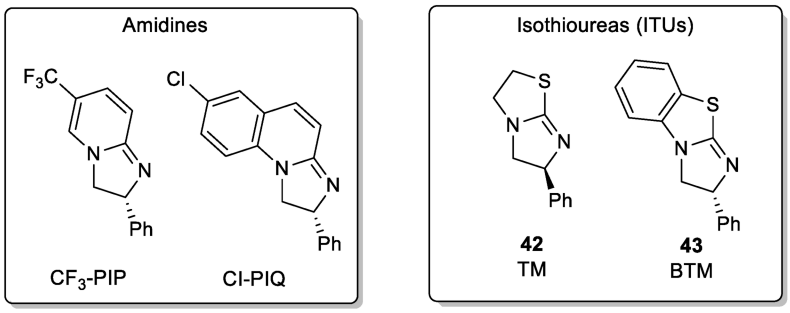

Figure 7. Birman's amidines and isothioureas catalysts.

After the seminal work of Birman, ITUs become one of the most used nucleophilic organocatalyst in a large variety of enantioselective transformation along with chiral DMAP[31] and NHC catalysts. These transformations included C-O, O-Si, C-N, and C-C bond formation, also domino reactions and formal cycloadditions were performed as well.

Rapidly after Birman's introduction of tetramisole **42** and BTM **43**, numerous alternative ITU catalysts were developed (Figure 8). Worth to note, the introduction of the achiral dihydrobenzothiazolo-pyrimidine (DHPB, **44**)[32a] which contains a six-membered ring instead of a five one, leads to a structure with a higher reactivity and improved robustness compared to BTM **43**. In 2008, Birman developed the chiral analogue named homobenzotetramisole (HBTM **45**).[32b] In 2009, Smith[32c] introduced HyperBTM **46**, containing an isopropyl group in the structure. The presence of an additional group plays a role of a conformational lock, in fact the isopropyl group is in a pseudo-equatorial position, forcing the stereodiscriminating phenyl group to adopt a pseudo-axial orientation.[32c]

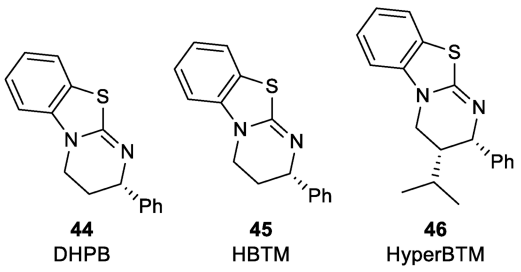

Figure 8. Example of ITU catalysts.

Generally, ITUs activate anhydrides, acyl chlorides and triaryl-silyl chlorides. The main modes of activation could be classified according to the nature of the acylating agent and reaction conditions.[33] As reported in Figure 9, the first studied mechanism includes the formation of an acylisothiouronium species that improves the electrophilicity of the carbon atom of the acyl group. The formation of silylisothiouronium is instead involved in enantioselective silylation and in this case the silicon atom shows an improved electrophilicity. Otherwise, in the event that it is possible to deprotonate the acylisothiouronium moiety, an

acylisothiouronium enolate can be formed. This intermediate presents two adjacent reactive sites: a nucleophilic site centred on the carbon atom in the α-position to the initial C=O bond while the carbon atom of the acyl group still remains an electrophilic centre. Lastly, the α,β-unsaturated acylisothiouronium intermediate with up to three different reactive sites can be formed. This species is produced when the acyl group contains a conjugated double bond and reacts as a Michael acceptor or a dienophile. The carbon atom of the C=O bond remains an electrophilic centre.

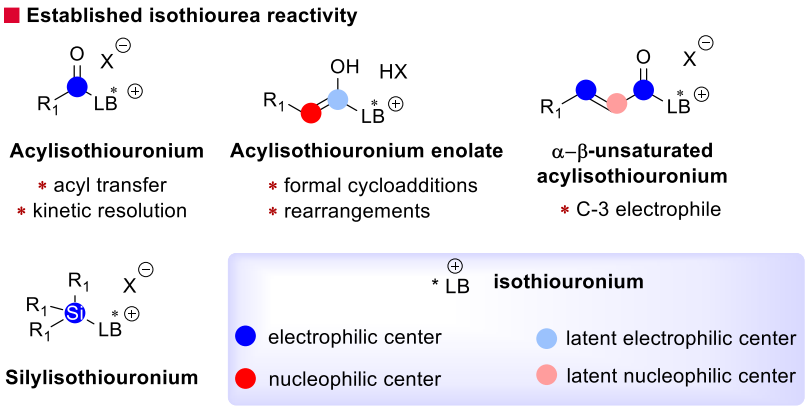

Figure 9. Main activation modes in ITUs catalysis.

As already introduced, the first studied enantioselective transformation was the enantioselective O-acylation. Mechanistically, as well as for DMAP, four partners are involved: the alcohol, the acylating agent, the catalyst, and an auxiliary base (Scheme 17). The reaction proceeds through initial acylation of catalyst to give the acylisothiouronium intermediate. The subsequent acyl transfer from the catalyst to the alcohol leads to the formation of the product and the turnover of the catalyst. The acyl transfer step is the kinetically determining one and the reaction rate is related to the concentration of the acylisothiouronium species.[33] Moreover, in the acyl transfer process the Lewis base catalysis does not apparently proceed through the energy lowering of the LUMO carbonyl bond but through the raising of the alcohol HOMO's energy.[34a] Indeed, it was supposed that the carboxylate counter anion stays close to the acylammonium intermediate **47** because of H-bond stabilization, playing an important role in a concerted process involving deprotonation/formation of the C-O bond.[34b] Finally, the auxiliary base neutralizes the carboxylic acid formed.

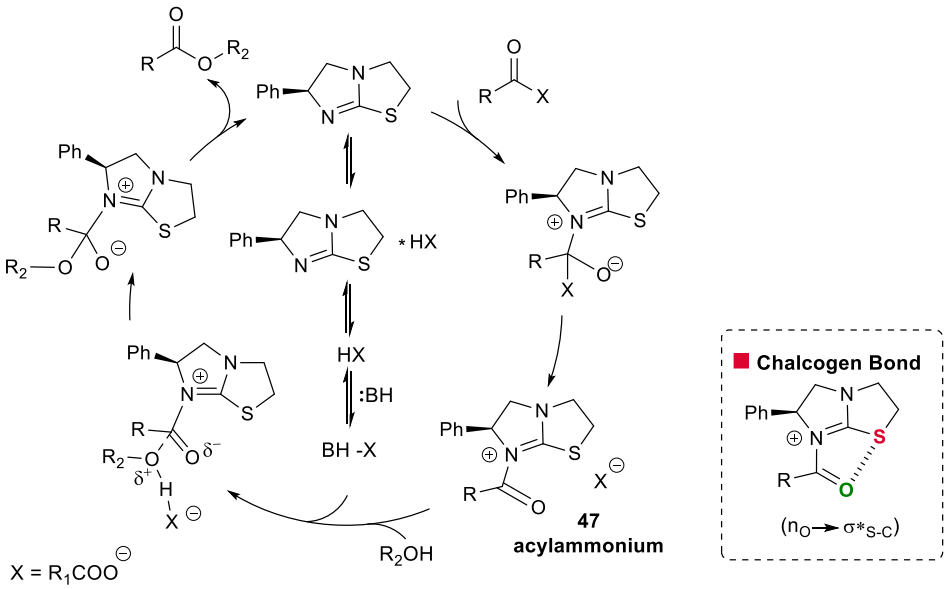

Scheme 17. Mechanism of acyl transfer mediated by Lewis base organocatalyst **42**.

The use of isothioureas in catalysis was initially explored by Birman and Okamoto[29,32a] and later it has been exploited by Smith's group in a numerous enantioselective transformation.[33] In their most common reactions, the N-acyl isothiouronium intermediate is considered responsible to dictate the stereoselectivity in subsequent bond-forming events.[35] As exemplified using HyperBTM catalyst, a common structural feature of the activated intermediate is a 1,5-O•••S ascribed as a chalcogen bond (Scheme 17).[36] This non-bonding interaction, ancillary to covalent bond, is considered to be responsible of the increasing of the electrophilicity of the carbonyl through the interaction with a formally Lewis acidic sulfur atom, and simultaneously it fixes the geometry of the acylated catalyst and proves facial discrimination in subsequent reaction processes. As suggested by the name, chalcogen bonds are considered as secondary interactions specially involving Group 16 elements (O, S, Se, etc.)[36] and present several characteristics similar to their halogen (Group 17) and pnictogen (Group 15) bonding counterparts.[37] According to crystallographic studies, the interatomic distance O-S turned out to be significantly shorter than the sum of the component Van der Waals radii.[35] Moreover, computational analyses revealed that a syn-periplanar 1,5-O•••S relationship is energetically favored.[35] By using a model system bearing a close structural similarity to the N-acylated isothiourea catalysts used within Smith's group, Cockroft et al. investigated the nature of 1,5-Ch•••Ch interactions.[38a] Therefore, experimental and theoretical investigation suggest that this intramolecular chalcogen bond is due to orbital delocalization between a lone pair donor and an antibonding acceptor orbital (e.g., $n_O \rightarrow \sigma^*_{S-C}$).[38b]

1.4 Heterogenization of organocatalyst and flow-mode catalysis

In the last decades, organocatalyst applications increased in academic research whilst in the chemical industry remained limited. The major issues are connected to the high cost and, sometimes to long synthetic procedures and low stability to air and moisture of these catalysts. The high catalytic loading, usually 10−20 mol%, often required in the synthetic protocols represents a problem too. Above all, the recovery and the recyclability of a homogeneous catalyst are the major issue. To face these drawbacks heterogeneous organocatalysts have been introduced. Indeed, recently, wide range of methods have been investigated for the development of heterogeneous catalytic systems in order to facilitate their handling and separation. The immobilized compound can be easily removed from the reaction medium by filtration, decantation, and centrifugation, thus allowing the recycling of the immobilized catalyst. Moreover, studies showed that heterogenization can enhance the stability of the immobilized compounds and in some cases improve the reactivity and selectivity of catalytic reactions.[39] On the other hand, the nature of the support and the immobilization process could impact on the performance of the heterogenized catalysts. In fact these are influenced by the physicochemical nature, porosity and dimensions of the support, by the nature and distance between the catalytic sites and the surface matrix and lastly by the density of the catalytic sites on the surface of the support.[40] The support used should be chemically inert and environmentally benign and the most frequent ones are inorganic,[41] and organic[42] but also nanomaterials and magnetic nanoparticle are employed as well.[41b,43] Generally, another feature can be considered to classify the immobilized catalyst, and it is related to the kind of intermolecular interactions that occur between the support and the catalytically active species. These interactions are covalent bond, non-covalent interactions, and encapsulation. The first one involves a covalent interaction between the catalyst and the support. In the second one, known-as physisorption, the catalyst is adsorbed on the surface of the support *via* weak intermolecular interactions such as hydrogen bonding and electrostatic or van der Waals interactions. Finally, the encapsulation requires the physical entrapment of the catalyst inside of the pores or cavities of support.[40] Along with the formers, which are the most spread methods of heterogenization, more recently metal-organic coordination polymers have been also designed. In this technique, known as self-supporting approach, a coordination occurs between multitopic ligands and metal ions.[40]

The efficiency of the process can be evaluated with the turnover number (TON), a parameter representing the number of moles of substrate that a mole of catalyst can convert before

becoming inactivated. The TON is usually associated with the turnover frequency (TOF), used to refer to the TON per unit time.

As studies were conducted on the use of supported catalyst, questioning about their recyclability and the efficiency of their synthesis were arisen. However, the possibility to discuss of how efficient and recyclable a heterogenous catalyst should be to make its synthesis and use worthwhile are speculative. The comparison between the efficiency of a supported catalyst and a homogenous one which is discarded after a single use should be done for each case of study. Although supported catalyst presents a higher stability respect to the homogeneous analogues, in some case either is not possible to support the catalyst or the immobilization strategy is really high time-demanding thus making the whole process worthless. In principle an immobilization strategy is useful when the catalytic loading for a stated process is really high or to avoid the leaching of catalyst in the product. However, the increasing number of the reported examples conducted in this field represents how important is the possibility to recycle a catalyst, thus paving the way for a more eco-friendly organic synthesis.

Additionally, from a sustainability point of view, the efficiency of a heterogeneous process can be further increased with a flow-mode approach. In fact, along with the spread of immobilization strategy, flow-mode processes flourished, leading to a more efficient chemistry at industrial level. This breakthrough is mainly due to a) large surface-to-volume ratios; b) efficient mass and heat transfer; c) precise mixing; d) intrinsic safety; e) reduced use of solvent and improved stoichiometry; f) scalability; g) reduced footprint and capital investment.[44]

All these features lead to several advantages from a sustainability and safety perspectives. In fact, heterogeneous catalysis in flow implies high efficiency, less waste production, no accumulation of hazardous chemicals, continuous product formation, and easy recovery and reuse of the catalyst.[44] Additionally, the flow-mode synthesis shows other benefits such as the less mechanical degradation of the catalyst, and minimum contact with air and moisture, which may enhance the TON and the productivity of the process. Through this system, it is also possible to suitably control the pressure and temperature parameters and increase the productivity by scaling-up the process through the parallel operation of more reactors (numbering-up approach).

Three different strategies can be applied to perform heterogeneous flow catalysis relying on either packed-bed reactors, monolithic columns, or wall coated flow reactors. Usually, supported catalysts onto an organic or inorganic matrix, with high loading, are preferred for the preparation of packed-bed flow reactors. Note, however, that the particle size checking is important because high backpressure or flow blockage may occur when too small particles are used. The pros on employing this kind of flow reactor involves a high catalytic

loading which affects the kinetics of the reaction, reducing reaction times.[44] In monolithic flow reactors, instead, the solution of reagents flows through a regular or irregular network of polymeric or inorganic materials. Sometimes, this kind of flow system is preferred respect to the former one because the absence of interstitial spacing and the porous nature of the supported catalyst tolerate greater high flow rates and efficient mass transfer. However, pore clogging as well as non-uniformity of radial permeability, and reduced accessibility of the catalytic sites inside the micropores of the heterogenous catalyst could occur.[44] Finally, wall-coated reactors present the immobilized catalyst in the inner wall of the reactor. They show a very good mass transfer with minimal pressure drop or clogging of microchannels. Compared to the other approaches, the catalyst loading is generally lower considering the small amount of catalyst deposited as thin film on the wall of the reactor.[44]

1.4.1 Heterogeneous catalysis promoted by NHCs

As previously introduced, the immobilization of homogeneous catalysts represents a new booming field, thanks to the possibilities to recover and recycle them. Among all the organocatalysts, NHCs played an important role showing an increase of examples of heterogeneous catalysts in the last few years.[45] It is worth emphasizing that the immobilization of the NHCs involves the preparation of the supported pre-catalyst (NHCs precursor) which is later activated in the reaction medium. The operative steps allowing the immobilization of the catalyst usually required the synthesis of the NHC moiety, that can be later heterogenized through the formation of metal-NHC complex (metalation) or through solid phase synthesis, covalent grafting or lastly through the formation of non-covalent interactions. The solid phase synthesis comprises the synthesis of the NHC moiety directly on the supporting material either by quaternization or cyclization, while the covalent grafting involves the formation of a covalent bond between a preformed NHC compound and a suitably functionalized support or self-support.[45]

The immobilization procedure requires different functionalities such as hydroxyl, carboxyl, alkenyl, and alkoxysilyl groups that are commonly introduced into the NHC moieties through the preparation of the respective imidazolium salts (Figure 10).

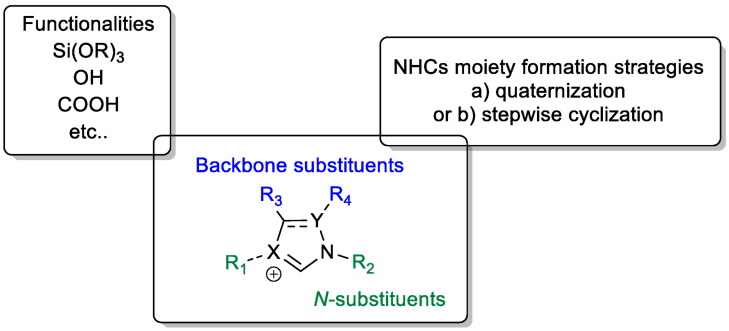

Figure 10. Strategies for the formation of NHC moieties with functional groups.

As summarized in Figure 11, the immobilization process can be classified according to three different aspects: the immobilization method, the immobilization position, and the supporting material.

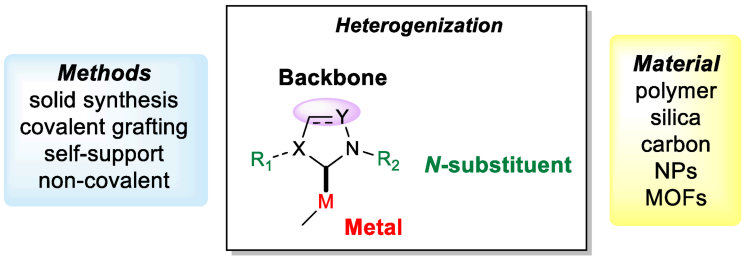

Figure 11. Features of the immobilization of NHCs catalysts.

The predominant methods used for the immobilization procedure are solid synthesis, covalent grafting, and self-support, while other methods such as absorption, entrapment, electrostatic interaction, and π–π stacking are less frequently reported.[46] Recent works also describe the binding of NHCs to metal surfaces such as metal NPs.[47]

The most recurrent used supports are organic polymers and silica-based materials. Besides, carbon-based compounds (i.e. carbon nanotubes, graphene oxide), metal NPs and coordination polymers are also reported in few examples. The immobilization position, instead, is usually determined by the functionalities introduced during the formation of the NHC moiety.

Overall, the effectiveness of NHCs immobilization is evaluated by their activity, selectivity, and yield and on how many different substrates can be converted with respect to the homogeneous catalyst. Great importance is also given to the stability, recyclability of the catalyst and to the nature of the support. As already mentioned, one of the most important benefit of the immobilization is the possibility to remove the catalyst from the reaction medium in an easy way. In some cases, these methods also comprehend the use of a magnetic field when Fe_3O_4 particles are used as supports.[48]

Aside from the several reports on the use of immobilized NHCs in metal-NHCs comlplexes[49], the utilization of heterogeneous NHCs as organocatalysts can be dated back to

2004. Barret reported the Stetter reaction promoted by a triazolium pre-catalyst heterogenized through ROMP gel-support, followed by other works on benzoin condensation.[50]

Along with the greater interest and larger studies conducted on the immobilization of NHCs, flow-mode synthesis started to be explored as well. Based on the aforementioned advantages, flow processes have been implemented for numerous homogenous and heterogeneous reactions including asymmetric transformations using immobilized reagents or catalysts.[51]

One of the first example on continuous flow NHCs application is reported by Monbaliu and co-workers in 2016.[52] The research group developed a system for the generation of a free nucleophilic carbene that was next telescoped with two benchmark NHC-catalysed reactions, i.e. the transesterification of vinyl acetate with benzyl alcohol and the amidation of *N*-Boc-glycine methyl ester with ethanolamine.[52] The NHC-mediated oxidative esterification of several aldehydes was instead reported by Brown and co-workers in the same period.[53] The developed process displayed the formation of Breslow intermediates from aldehydes and a thiazolium salt, their anodic oxidation into the corresponding acyl azolium derivatives, and at the end the esterification reaction in a microreactor. Additionally, an integrated flow system for the synthesis of biodiesel, using polymer supported NHCs catalyst was reported by Lupton.[54]

The heterogeneous umpolung process promoted by immobilized NHCs has been intensively studied by Massi and co-workers.[55] Thiazolium salt pre-catalysts have been immobilized on silica and monolithic polystyrene and their activities were tested under batch conditions for the benzoin condensation of benzaldehyde (Scheme 18a), the acyloin-type condensation of biacetyl (Scheme 18b) and the Stetter reaction of biacetyl with *trans*-chalcone (Scheme 18c). Once the higher performance of the polystyrene monolithic supported NHCs had been established a monolithic microreactor was prepared for the study of the reaction in flow-mode. Overall, it was demonstrated that the polymeric matrix along with the continuous-flow regime leads to an increase of both the stability of the supported catalyst and productivity considering the long-term operativity (up to 7 days) of the system.

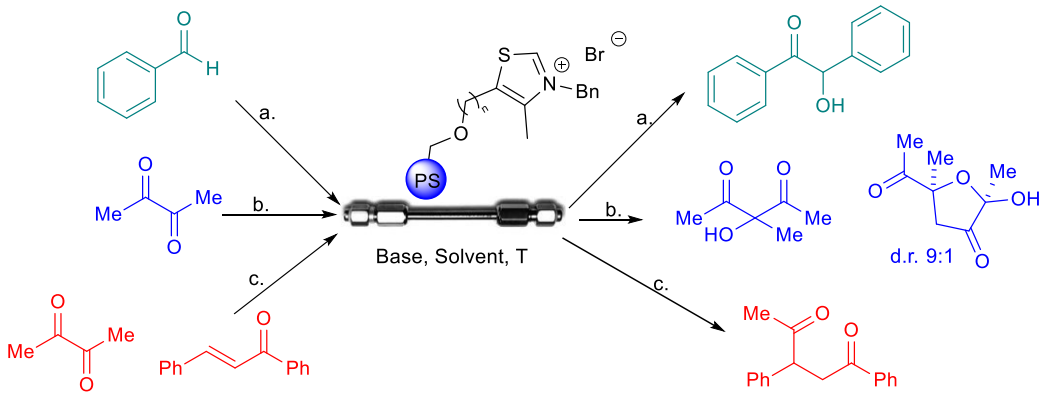

Scheme 18. a) benzoin condensation of benzaldehyde; b) acyloin-type condensation of biacetyl; c) Stetter reaction of biacetyl with trans-chalcone.

The same group also reported the only example in the literature of supported metal-free enantioselective NHC. A Rovis catalyst has been immobilized onto silica and polystyrene for the study of asymmetric intramolecular Stetter reaction to produce chromanones (Scheme 19).[56] Respect to the silica supported catalyst, the polystyrene one proved to be superior, probably because it is less sensitive to moisture. Batch experiments showed a recyclability up to 10 times with unaltered enantioselectivity and only a slight decrease of conversion. The monolithic version for the flow regime study was operated for 120 hours with constant excellent enantiomeric excess (*ee*) value during the whole process while the conversion decreased in a slow but steady manner. A TON of 132 was reached and a similar set-up was then used to prepare a library of chromanones **48** (81–95% *ee*).

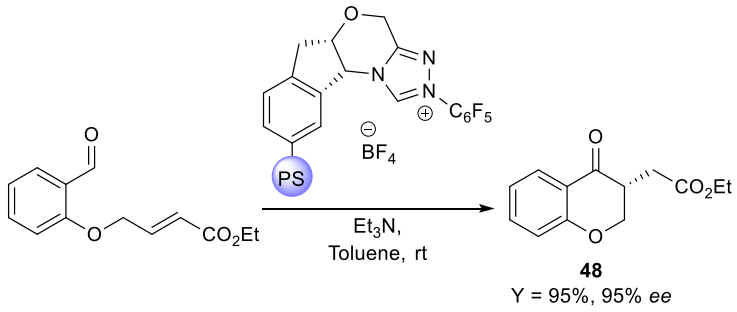

Scheme 19. Polystyrene supported triazolium pre-catalyst for asymmetric intramolecular Stetter reaction.

1.4.2 Heterogeneous catalysis promoted by isothioureas

In analogy to NHCs, in the last few years isothiourea organocatalysts have been used to perform heterogeneous reactions.[45b] Pericas,[57] reported the first example on the anchoring of an analogue of benzotetramisole (BTM) *via* azide-alkyne cycloaddition (Scheme 20). However, the immobilization strategy led to the introduction of a second stereocenter in the BTM scaffold **49** showing a profound effect in the diastereoselectivity with respect to the homogeneous process. The first application of **49** involved a domino Michael addition-cyclization between *in*

situ activated arylacetic acids and α,β-unsaturated sulfonylimines, giving dihydropyridinones in good yields and enantioselectivities (Scheme 20a). The recyclability of the catalyst **44** was tested for six consecutive runs, in which conversion and *ee* remained essentially constant. Finally, a flow-mode synthesis was also carried out. The procedure including both formation of the mixed anhydride and subsequent asymmetric reaction in a packed bed reactor containing **49**, was carried out for 11 hours. Furthermore, the performed system was used to expand the scope of the reaction, preparing a library of seven analogues in gram-scale and reaching a TON of 51. Later, the same catalyst has been used to promote a [4+2] annulation reactions with alkylidene pyrazolones and thiazolones. As in the former case, this supported catalyst showed much better diastereoselectivity than BTM for a broad substrate scope with good enantioselectivities (Scheme 20b). Additionally, the catalyst could be used for nine runs with two hours reaction time and for two runs for 24 hours reaction time with a slight decrease of conversion and *ee* (TON of 77). As in the previous study, a flow experiment was carried out thanks to the preparation of a packed bed reactor. The mixed anhydride was prepared and circulated through the reactor along with the heterocycle for 18 hours, providing more than 3 g of the desired compound as a single stereoisomer.[58] Later, a [8+2] process between activated arylacetic acids and azaheptafulvenes (Scheme 20c) has been studied. As for the previous cases, this cycloaddition gave the desired products with good yields and excellent diastereoselectivity and enantioselectivity. Likewise, the cycloadducts could be additionally derivatized by hydrogenation or Diels-Alder reaction.[59]

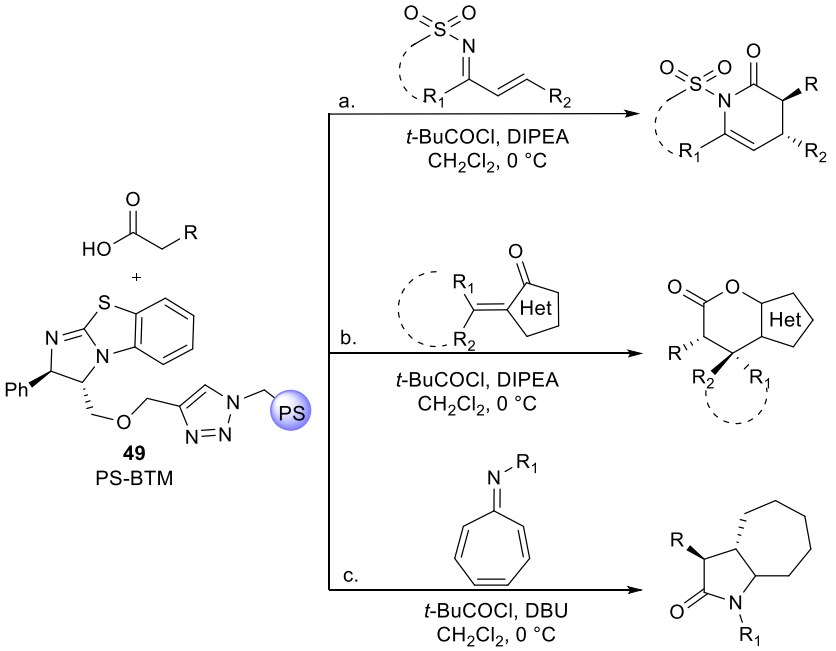

Scheme 20. Enantioselective solid-supported isothiourea catalysis for the a) generation of dihydropyridinones; b) [4+2] annulation of heterocyclic compounds and c) [8+2] formal cycloaddition of azaheptafulvenes.

Recently, a polystyrene-supported version of the isothiourea HyperBTM has been synthetized. This new supported catalyst **50** has been used for the kinetic resolution of alcohols in batch and flow (Scheme 21). A broad range of secondary alcohols with high selectivity (*s*) factors have been produced and the robustness of the catalyst has been tested for 15 consecutive runs showing retained catalytic activity. Additionally, a 24 h continuous flow process has also been conducted and the scope of the reaction has been finally extended in flow through the preparation of packed bed reactor.[60]

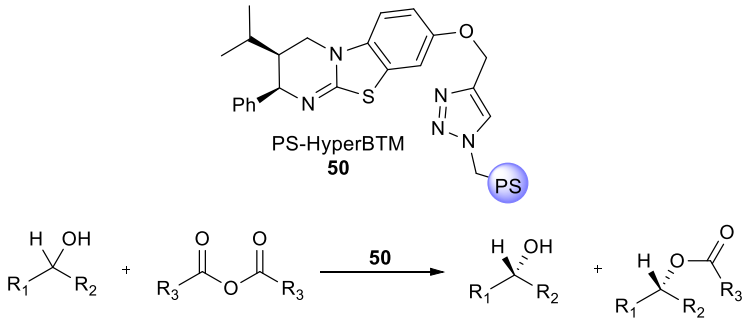

Scheme 21. Enantioselective solid-supported isothiourea catalysis for the kinetic resolution of alcohols.

1.5 Valorisation of biomass-derived platform molecules

It has been already underlined the success and the several applications of organocatalysts in the last two decades. However, apart from the aforementioned benefits, what have allowed them to gain this huge importance? Looking at the 12 principle of Green Chemistry[61] it becomes clear that organocatalysts are in the core of green chemistry. Their use permits to reduce the environmental impact of chemical processes avoiding the employment of precious metals and reduce the amount of waste occurring when stoichiometric reagents, mainly inorganic, are involved in organic synthesis.[62] Anyway, the high cost that often characterizes this kind of catalysts, along with their sensibility to air and moisture have limited their applications. Immobilization procedures enable to overcome these last problems, and, in most cases, catalytic enantioselective flow processes broaden the use of organocatalysts including the industrial field. The catalyst recyclability, in fact, plays an important role to overtake the high cost that often characterizes the use of organocatalysts. Other procedures aiming at making the organocatalyzed processes more sustainable focus on activation techniques such as microwave, mechanical activation, ultrasound, use of light or high pressure. Moreover, the use of greener reaction media like ionic liquids and deep eutectic solvents (DES), water, supercritical solvents or other green solvent alternatives represent the best choice to pursuit more sustainable synthesis.[63] Furthermore, the possibility to switch from non-renewable fossil

fuels to non-depleting and inexpensive feedstocks (e.g., biomass waste) is highly attractive and worth following. These materials can be used not only as reagent but also as catalysts support or as catalysts themselves. Recently, the European Committee in Standardization (CEN) clarified the term biomass as the material of biological origin excluding material embedded in geological formations and/or fossilised.[64] Moreover, the term bio-based platform molecule was introduced along with the former definition. Indeed, a bio-based (or bio-derived) platform molecule is a chemical compound whose constituent elements originated wholly from biomass, and that can be used as a building block for the production of other chemicals.[64] Thus, this interpretation underlies the use of small molecules, deriving from biomass, that could be employed as building blocks for the synthesis of higher value chemicals and materials.[65] Nowadays, a lot of efforts have been made in order to replace the fossil fuel-derived products with biomass-derived ones. In 2004, the US Department of Energy (US DOE) reported the compounds which can be considered as bio-based platform molecules.[66] Along with the first compounds reported, new ones have been added in the following years. Most of them become very important and are involved in organocatalytic processes leading to the formation of high added-value intermediates. Among them it is possible to count furaldehydes, glycerol and lactic acids.

1.5.1 Lewis base organocatalysts in biomass conversion and upgrading

Concerning the ever- growing desire to reduce to dependence on fossil fuels, Lewis base organocatalysts have played an emerging role in biomass conversion and upgrading. To date, the catalytic conversion of glucose, the valorisation of furaldehydes, and the organocatalytic polymerization of biomass feedstocks have been carried out through metal-free procedures.[67]

The first example involving the use of NHC-catalysis is the conversion of glucose to formaldehyde *via* retro-benzoin reaction. This process relies on the glucose equilibrium between its cyclic form (acetal) and acyclic form (aldehyde) in solution. Thus, the C-C bonds of glucose can be cut in the presence of NHC catalyst.[68] According to the proposed mechanism, the thiazolium carbene catalyst **51** attacks the aldehyde group of the glucose and forms the NHC-glucose complex **52**. The following proton transfer step leads to the cleavage of C1-C2 bond and hence acyclic C5 sugar is formed. Subsequently, the acyl anion **54** can be, for instance, utilized for a Stetter reaction with chalcone **55** to produce enone **56** (Scheme 22).

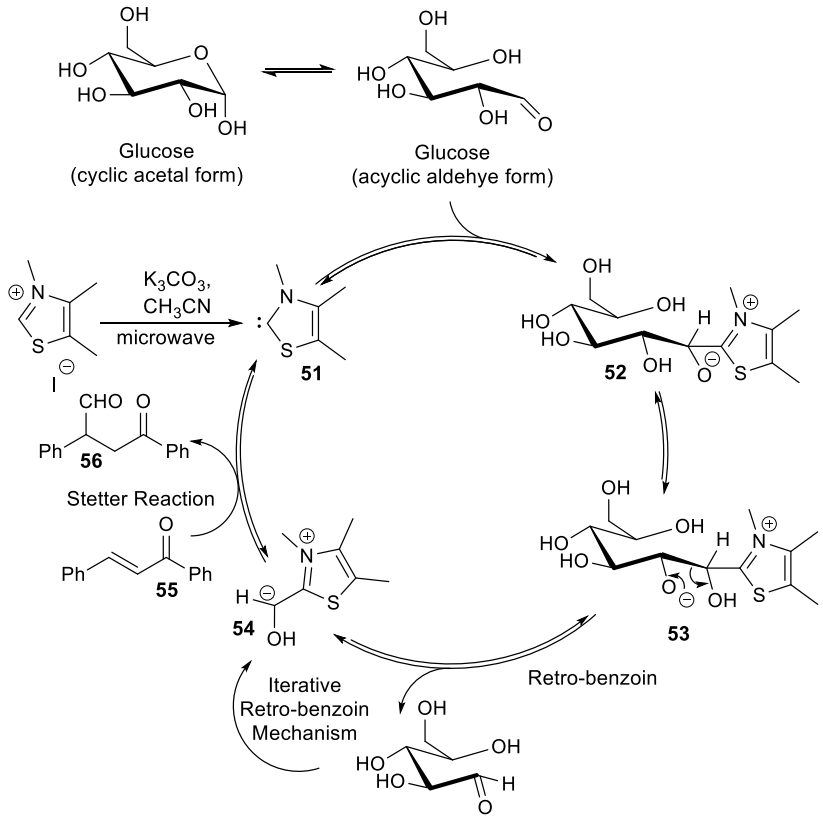

Scheme 22. Acyl anion formation from glucose through NHC-catalysed retro-benzoin.

The C5 sugar followed the analogous iterative retro-benzoin mechanism to form other five acyl anion intermediates **54**.

The upgrading of furfural leads, instead, to the formation of furoin in high to quantitative yield in analogy to the benzoin condensation.[69] As well as furfural, 5-hydroxymethylfurfural (HMF), which presents the -CH_2OH group at the 5-position, has been subjected to umpolung to give the 5,5'-di (hydroxymethyl)furoin (DHMF).[70] The process, promoted by [EMIM]OAc NHC pre-catalyst is reported in Scheme 23. The 1-ethyl-3-methylimidazolin-2-ylidene carbene catalyst **57**, after a nucleophilic addition to the aldehyde group of HMF, generates a zwitterionic tetrahedral intermediate, which is protonated to afford a 2-(5-hydroxymethyl-2-α-hydroxyfuranyl)imidazolium acetate salt **58**. This intermediate, at high temperature (80 °C) is deprotonated by the acetate anion to form the Breslow intermediate **59**. Subsequently, this acyl anion equivalent attacks the aldehyde group of a second HMF molecule to form another tetrahedral intermediate (**60**), thus leading to the formation of the product and the turnover of the catalyst **57**. Moreover, the DHMF product can be further modified through reactions such as etherification, esterification, and hydrogenation or to provide oxygenated biodiesel fuels.[67]

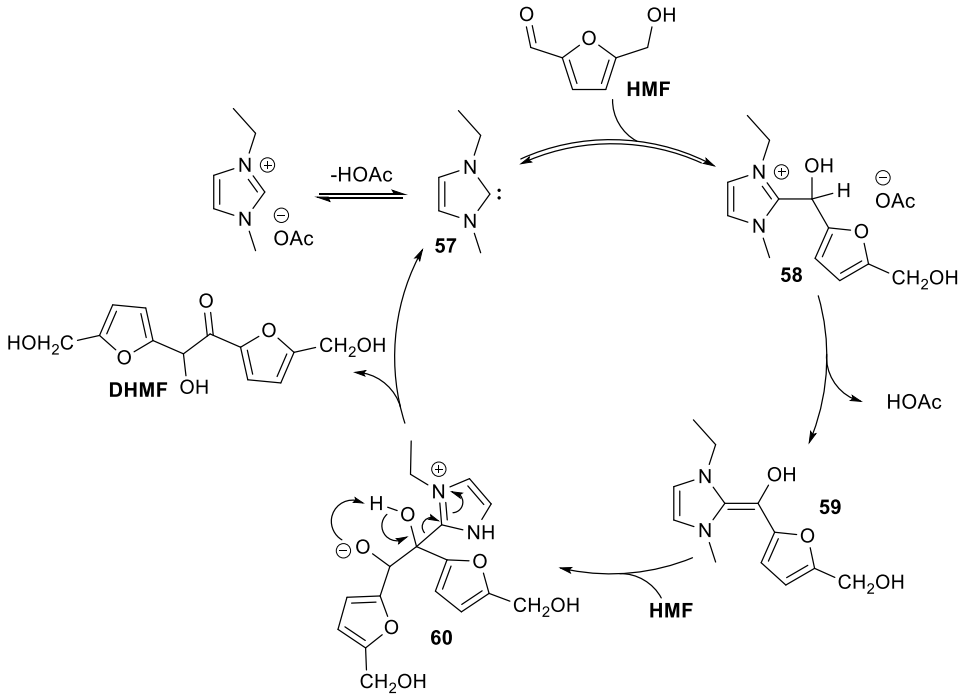

Scheme 23. Synthesis of DHMF through umpolung self-condensation of HMF.

Additionally, NHCs were also employed for the synthesis of polyurethanes. Taton and co-workers demonstrated that condensation polymerization of aliphatic diisocyanates and primary diols can be catalysed by I*t*Bu (Scheme 24).[71] According to the proposed mechanism, the isocyanate undergoes a nucleophilic attack by the activated alcohol **61** leading to the formation of the urethane bond. Anyway, the product shows a low molecular weight ranging from 2000 – 3000 g mol^{-1}.

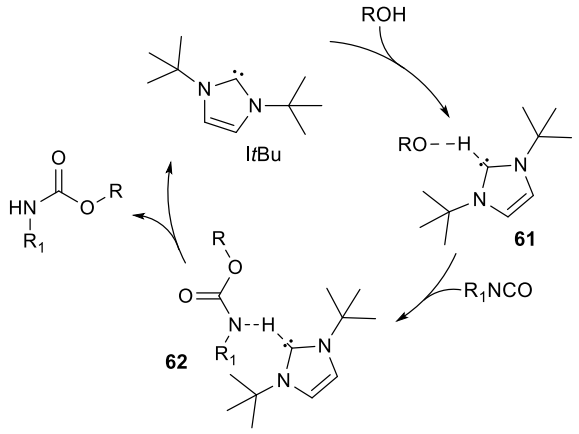

Scheme 24. Suggested mechanism of polyurethane formation through condensation polymerization catalysed by I*t*Bu.

Furthermore, in the field of organocatalytic valorisation of biomass through polymerization procedure, Waymouth and Hedrick have also reported the ring open polymerization (ROP) of lactide into poly(lactic acid) (PLA) through NHC-catalysis.[72] Generally, this polymerization can be labelled as a nucleophile-catalysed, alcohol-initiated reaction. The obtained linear PLA

presents alkoxide ester and hydroxyl functionalities as chain end groups (Scheme 25). The developed methods relies on *in situ* generated NHCs and the activity of a thiazolyl carbene **63** and imidazole-2-ylidene carbene **64** were compared.[72] The results showed that the imidazole-2-ylidene carbene **64** is significantly more active for the ROP of lactide respect to the thiazolyl carbene **63**. Benzyl alcohol was chosen as the initiator and using catalyst/initiator ratio of 1.5, PLA materials with Mn > 25000 g mol^{-1} can be produced in high yields (> 90%) in THF within 15 minutes at room temperature.

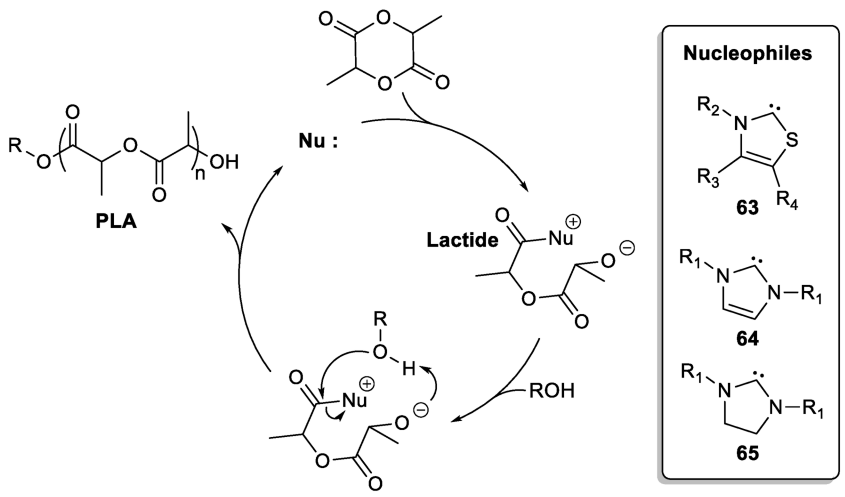

Scheme 25. Mechanism of the NHC-catalysed alcohol initiate ROP of lactide.

Lastly, NHCs have been used to promote the polymerization of α-methylene-γ-butyrolactone (MBL), and γ-methyl-α-methylene-γ-butyrolactone (γ-MMBL) in DMF at room temperature leading to medium or high molecular weight polymers in less than one minute.[73] The optimal results depend upon the strong nucleophilic character of I*t*Bu, which activates the α,β-unsaturated monomer that evolves to the final polymer through the zwitterionic intermediate **66** (propagation step), in agreement with the proposed mechanism (Scheme 26).

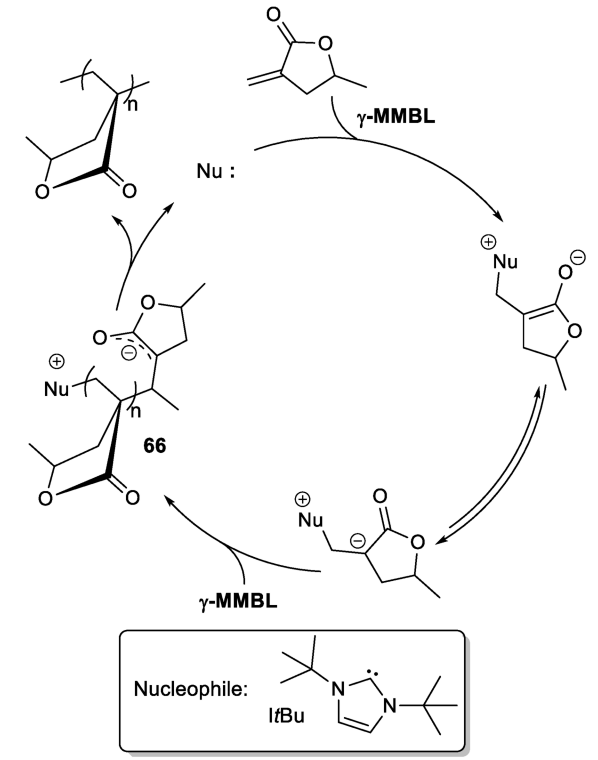

Scheme 26. Supposed mechanism for the polymerization of γ-MMBL.

1.6 References

1. D. W. C. MacMillan, *Nature,* **2008**, *455*, 304–308.
2. A. Berkessel, H. Groger, *Asymmetric organocatalysis-From Biomimetic Concepts to Applications in Asymmetric Synthesis. Acc. Che. res.,* **2004**, *37*, 8.
3. J. Seayad, B. List, *Org. Biomol. Chem*., **2005**, *3*, 719 –724.
4. A. J. Arduengo, R. L. Harlow, M. Kline, *J. Am. Chem. Soc.,* **1991**, *113*, 361–363.
5. a) S. Diez-Gonzalez, N. Marion, S. P. Nolan, *Chem. Rev.,* **2009**, *109*, 3612–3676. (b) F. E. Hahn, M. C. Jahnke, *Angew. Chem. Int. Ed.,* **2008**, *47*, 3122–3172. (c) S. Bellemin-Laponnaz, S. Dagorne, *Chem. Rev.,* **2014***, 114,* 8747–8774.
6. A. T. Biju, *N-Heterocyclic Carbenes in Organocatalysis*, Wiley-VCH Weinheim, **2019**
7. D. Seebach, E. J. Corey, *J. Org. Chem*. **1975**, *40*, 231; D. Seebach, *Angew. Chem. Int. Ed. Eng.,* **1979**, *18*, 239–258.
8. F. Wöhler, J. Liebig, *Ann. Pharm.* **1832**, *3*, 249−282.
9. A. J. Lapworth, *Chem. Soc.* **1903**, *83*, 995–1005.
10. T. Ugai, R. Tanaka, T. J. Dokawa, *Pharm. Soc. Jpn.*, **1943**, *6*, 296−300.
11. R. Breslow, *J. Am. Chem. Soc.*, **1958**, *80*, 3719−3726.
12. J. Sheehan, D. H. Hunneman, *J. Am. Chem. Soc.,* **1966**, *88*, 3666−3667.
13. S. W. Ragsdale, *Chem. Rev*., **2003**, 103, 2333 –2346; R. Kluger, K. Tittmann, *Chem. Rev*. **2008**, 108, 1797–1833.
14. S. De Sarkar, A. Biswas, R. C. Samanta, A. Studer, *Chem. Eur. J.*, **2013**, *19*, 4664.
15. a) E. J. Corey, N. W. Gilman, B. E. Ganem, *J.Am. Chem. Soc*., **1968**, *90*, 5616–5617; b) B. E. Maki, A. Chan, E. M. Phillips, K. A. Scheidt, *Org. Lett.*, **2007**, *9*, 371−374.
16. B. Maji, S. Vedachalan, X. Ge, S. Cai, X. Liu, *J. Org. Chem.*, **2011**, *76*, 3016−3023.
17. B. E. Maki, K. A. Scheidt, *Org. Lett.,* **2008**, *10*, 4331–4334; M. Rueping, H. Sundén, L. Hubener, E. Sugiono, *Chem. Commun*., **2012**, *48*, 2201–2203.
18. a) Y.-C. Xin, S.- H. Shi, D.-D. Xie, X.-P. Hui, P.-F. Xu, *Eur. J. Org. Chem*., **2011**, 6527–6531; b) L. Lin, Y. Li, W. Du, W.-P. Deng, *Tetrahedron Lett*., **2010**, *51*, 3571–3574; c) J. H. Park, S. V. Bhilare, S. W. Youn, *Org. Lett*., **2011**, *13*, 2228–2231; d) Y.-K. Liu, R. Li, L. Yue, B.-J. Li, Y.-C. Chen, Y. Wu, L.-S. Ding, *Org. Lett.*, **2006**, *8*, 1521–1524.
19. O. Bortolini, C. Chiappe, M. Fogagnolo, P. P. Giovannini, A. Massi, C. S. Pomelli, D. Ragno, *Chem. Commun.*, **2014**, *50*, 2008−2011.
20. J. Castells, H. Llitjos, M. Moreno-Manas, *Tetrahedron Lett.*, **1977**, *18*, 205−206.
21. M. D. Corbett, *Bioorg. Chem.*, **1974**, *3*, 361−365.
22. F. T. Wong, P. K. Patra, J. Seayad, Y. Zhang, J. Y. Ying, *Org. Lett.*, **2008**, *10*, 2333−2336.
23. S. Tam, L. Jimenez, F. Diederich, *J. Am. Chem. Soc.*, **1992**, *114*, 1503−1505.
24. C. Noonan, L. Baragwanath, S. J. Connon, *Tetrahedron Lett.*, **2008**, *49*, 4003–4006.
25. J. Guin, S. De Sarkar, S. Grimme, A. Studer, *Angew. Chem*., **2008**, *120*, 8855–8858; *Angew. Chem. Int. Ed.,* **2008**, *47*, 8727–8730.
26. S. De Sarkar, S. Grimme, A. Studer, *J. Am. Chem. Soc.*, **2010**, *132*, 1190−1991.
27. A. Axelsson, A. Antoine-Michard, H. Sundén, *Green Chem.*, **2017**, *19*, 2477−2481.
28. J. E. Taylor, S. D. Bull, J. M. J. Williams, *Chem. Soc. Rev.,* **2012**, *41*, 2109–2121.
29. V. B. Birman, X. Li, *Org. Lett*., **2006**, *8 (7)*, 1351–1354.
30. V. B. Birman, E. W. Uffman, H. Jiang, X. Li, C. J. Kilban, *J. Am. Chem. Soc,* **2004**, *126*, 12226–12227; V. B. Birman, H. Jiang, *Org. Lett.,* **2005**, *7*, 3445–3447.
31. For a review on chiral DMAP organocatalysis, see R. P. Wurz, *Chem. Rev.,* **2007**, *107*, 5570–5595.
32. a) M. Kobayashi, S. Okamoto, *Tetrahedron Lett.,* **2006**, *47*, 4347–4350; b) V. B. Birman, X. Li, *Org. Lett.,* **2008**, *10*, 1115–1118; c) C. Joannesse, C. P. Johnson, C. Concellon, C. Simal, D. Philp, A. D. Smith, *Angew. Chem. Int. Ed.,* **2009**, *48*, 8914–8918.
33. For a review on isothiourea organocatalysts, see J. Merad, J.-M. Pons, O. Chuzel, C. Bressy, *Eur. J. Org. Chem.,* **2016**, *34*, 5589–5610.

34. A. Spivey, S. Arseniyadis, *Angew. Chem. Int. Ed.,* **2004**, *43*, 5436–5441; *Angew. Chem.* **2004**, *116*, 5552−5557; S. Xu, I. Held, B. Kempf, H. Mayr, W. Steglich, H. Zipse, *Chem. Eur. J.,* **2005**, *11*, 4751–4757.
35. Selected papers: a) M. E. Abbasov, B. M. Hudson, D. J. Tantillo, D. Romo, *J. Am. Chem. Soc.,* **2014**, *136*, 4492; b) V. B. Birman, X. Li, Z. Han, Org.Lett. **2007**, *9*, 37– 40; c) T. H.West, D. M. Walden, J. E. Taylor, A. C. Brueckner, R. C. Johnson, P. H.-Y. Cheong, G. C. Lloyd-Jones, A. D. Smith, *J. Am. Chem. Soc.*, **2017**, *139*, 4366–4375; d) M. D. Greenhalgh, S. M. Smith, D. M. Walden, J. E. Taylor, Z. Brice, E. R. T. Robinson, C. Fallan, D. B. Cordes, A. M. Z. Slawin, H. C. Richardson, M. A. Grove, P. H.-Y. Cheong, A. D. Smith, *Angew. Chem. Int. Ed.*, **2018**, *57*, 3200–3206; *Angew. Chem.,* **2018**, *130*, 3254–3260; e) C. M. Young, A. Elmi, D. J. Pascoe, R. K. Morris, C. McLaughlin, A. M. Woods, A. B. Frost, A. de la Houpliere, K. B. Ling, T. K. Smith, A. M. Z. Slawin, P. H. Willoughby, S. L. Cockroft, A. D. Smith, *Angew. Chem. Int. Ed.,* **2020**, *59*, 3705–3710.
36. L. Brammer, *Faraday Discuss*., **2017**, *203*, 485–507.
37. For reviews in this area, see: a) K. T. Mahmudov, M. N. Kopylovich, M. F. C. G. da Silva, A. J. L. Pombeiro, *Dalton Trans*., **2017**, *46*, 10121–10138; b) S. Benz, A. I. Poblador-Bahamonde, N. Low-Ders, S. Matile, *Angew. Chem. Int. Ed*., **2018**, *57*, 5408–5412; *Angew. Chem*., **2018**, *130*, 5506–5510; c) L. Vogel, P. Wonner, S. M. Huber, *Angew. Chem. Int. Ed.*, **2019**, *58*, 1880–1891; *Angew. Chem.* **2019**, *131*, 1896–1907.
38. a) D. J. Pascoe, K. B. Ling, S. L. Cockroft, *J. Am. Chem. Soc*., **2017**, *139*, 15160–15167; b) G. R. Desiraju, P. S. Ho, L. Kloo, A. C. Legon, R. Marquardt, P. Metrangolo, P. Politzer, G. Resnati, K. Rissanen, *Pure Appl. Chem.*, **2013**, *85*, 1711–1713.
39. V. Lutz, J. Glatthaar, C. Würtele, M. Serafin, M. Hausmann, P. R. Schreiner, *Chem. Eur. J.,* **2009**, *15*, 8548–8557.
40. C. Mateo, J.M. Palomo, G. Fernandez-Lorente, J.M. Guisan, R. Fernandez-Lafuente, *Enzyme Microb.Technol.,* **2007***, 40:* 1451−1463.
41. M. Benaglia, A. Puglisi*, Catalyst Immobilization*, Wiley-VCH, **2020**.
42. J. Regalbuto, *Catalyst Preparation: Science and Engineering*. Boca Raton, FL: CRC Press, Taylor & Francis Group, **2007**; C. Freire, C. Pereira, S. Rebelo, *Catalysis,* **2012***, 24*, 116–203.
43. a) B. Altava, M. I. Burguete, E. García-Verdugo, S. V. Luis, *Chem.Soc. Rev.,* **2018***, 47*: 2722–2771; b) M. R. Buchmeiser, M.R., *Polymeric Materials in Organic Synthesis and Catalysis*. Wiley-VCH Weinheim, **2005**; c) Lu, J. and Toy, P.H. (2009). *Chem. Rev.,* **2009***, 109*: 815−838; d) C. Li, and Y. Liu, *Bridging Heterogeneous and Homogeneous Catalysis: Concepts, Strategies, and Applications*. Weinheim: Wiley-VCH, **2014**.
44. L. M. Rossi, N. J. S. Costa, F. P. Silva, R. Wojcieszak, *Green Chem.,* **2014***, 16*, 2906–2933.
45. M. Colella, C. Carlucci, R. Luisi, *Topics in Current Chemistry*, **2018**, *376,* 46.
46. a) R. Zhong, A. C. Lindhorst, F. J. Groche, F. E. Kühn, *Chem. Rev*., **2017,** *117 (3)*, 1970–2058; b) C. De Risi, O. Bortolini, A. Brandolese, G. Di Carmine, D. Ragno, A. Massi, *React. Chem. Eng*. **2020**, *5*, 1017−1052.
47. A. V. Zhukhovitskiy, M. J. MacLeod, J. A. Johnson, *Chem. Rev*., **2015**, *115 (20)*, 11503−11532.
48. K. V. S. Ranganath, A. H. Schäfer, F. Glorius, *Chem. Cat. Chem.,* **2011**, *3*, 1889−1891.
49. (a) S. Köytepe, T. Seçkin, S. Yaşar, I. Özdemir, *Des. Monomers Polym*., **2008**, *11 (5)*, 409−422; (b) M-X. Tan, Y. Zhang, J. Y. Ying, *Adv. Synth. Catal*., **2009**, *351*, 1390−1394; (c) J. Beier, W. Knolle, A. Prager-Duschke, M. R. Buchmeiser, *Macromol. Rapid Commun.,* **2008**, *29 (11)*, 904−909; (d) A. Monge-Marcet, R. Pleixats, X. Cattoen, M. Wong Chi Man, *Tetrahedron,* **2013**, *69*, 341−348; (e) G. Lázaro, M. Iglesias, F. J. Fernandez-Alvarez, P. J. S. Miguel, J. J. Perez-Torrente, L. A. Oro, *Chem. Cat. Chem,* **2013**, *5* (*5*), 1133−1141.

50. (a) A. G. Barrett, A. C. Love, L. Tedeschi, *Org. Lett,* **2004**, *619*, 3377−3380; (b) J. M. Storey, C. Williamson, *Tetrahedron Lett*., **2005**, *46*, 7337−7339; (c) K. Zietler, I. Mager, *Adv.Synth. Catal*., **2007**, *349*, 1851–1857.
51. M. B. Plutschack, B. Pieber, K. Gilmore, P. H. Seeberger, *Chem. Rev.,* **2017**, *117*, 11796−11893.
52. L. Di Marco, M. Hans, L. Delaude, J. M. Monbaliu, *Chem. Eur. J.,* **2016**, *22*, 4508–4514.
53. a) R. A. Green, D. Pletcher, S. G. Leach, R. C. D. Brown, *Org. Lett.* **2015**, *17,* 3290–3293; b) R. A. Green, D. Pletcher, S. G. Leach, R. C. D. Brown, *Org. Lett.* **2016**, *18,* 1198–1201.
54. M. Asadi, J. F. Hooper, D. W. Lupton, *Tetrahedron,* **2016**, *72,* 3729–3733.
55. O. Bortolini, A. Cavazzini, P. Dambruoso, P. P. Giovannini, L. Caciolli, A. Massi, S. Pacifico, D. Ragno, *Green Chem*., **2013**, *15*, 2981–2992.
56. D. Ragno, G. Di Carmine, A. Brandolese, O. Bortolini, P.P. Giovannini, A. Massi, *ACS Catal.,* **2017**, *7*, 6365–6375.
57. J. Izquierdo, M. A. Pericàs, *ACS Catal.,***2016***, 6*, 348–356.
58. S. Wang, J. Izquierdo, C. Rodriguez-Escrich, M. A. Pericàs, *ACS Catal.,* **2017***, 7*, 2780–2785.
59. S. Wang, C. Rodriguez-Escrich, M. A. Pericàs, *Angew. Chem. Int. Ed.,* **2017***, 56,* 15068–15072.
60. R. M. Neyyappadath, R. Chisholm, M. D. Greenhalgh, C. Rodríguez-Escrich, M. A. Pericàs, G. Hähner, A. D. Smith, *ACS Catal.,* **2018***, 8*: 1067–1075.
61. P. Anastas, J. C. Warner in *Green Chemistry: Theory and Practice*; Oxford University Press: Oxford, U.K., **1998**.
62. S. Menino, *ChemSusChem,* **2020**, *13*, 439−468.
63. D. Kristofikova, V. Modrocká, M. Mečiarová, R. Sebesta, *ChemSusChem*, **2020**, *13*, 2828−2858.
64. J. Clark, F. Deswarte, *Introduction to Chemicals from Biomass,* (Eds.: J. Clark, F. Deswarte) John Wiley & Sons, Ltd, **2015**.
65. P. F. Levy, J. E. Sanderson, R. G. Kispert, D. L. Wise, *Enzyme and Microbial Technology*, **1981**, *3* (*3*), 207–215; E. S. Lipinsky, (1978) *Science*, **1978**, *199* (*4329*), 644–651.
66. T. Werpy, G. Pedersen, *Top Value-Added Chemicals From Biomass*, US Department of Energy, Oak Ridge, USA., **2005**.
67. D. J. Liu, E. Y.-X. Chen, *Green Chem.*, **2014**, *16*, 964−981.
68. J. Zhang, C. Xing, B. Tiwari and Y. R. Chi, *J. Am. Chem. Soc.*, **2013**, *135*, 8113−8116.
69. a) H. Stetter, R. Y. Raemsch, H. Kuhlmann, *Synthesis*, **1976**, 733−735.; b) C. K. Lee, M. S. Kim, J. S. Gong, I.-S. H. Lee, *J. Heterocycl. Chem.*, **1992**, *29*, 149−153; c) D. Enders, U. Kallfass, *Angew. Chem. Int. Ed.*, **2002**, *41*, 1743−1745; d) A. S. K. Hashmi, M. Wölfle, J. H. Teles, W. Frey, *Synlett.*, **2007**, 1747−1752.
70. D. Liu, Y. Zhang, E. Y.-X. Chen, *Green Chem.*, **2012**, *14*, 2738−2746.
71. O. Coutelier, M. E. Ezzi, M. Destarac, F. Bonnette, T. Kato, A. Baceiredo, G. Sivasankarapillai, Y. Gnanou, D. Taton, *Polym. Chem.*, **2012**, *3*, 605−608.
72. G. W. Nyce, T. Glauser, E. F. Connor, A. Möck, R. M. Waymouth, J. L. Hedrick, *J. Am. Chem. Soc.*, **2003**, *125*, 3046−3056.
73. Y. Zhang, E. Y.-X. Chen, *Angew. Chem., Int. Ed. Engl.,* **2012**, 51, 2465–2469.

2. Aims and objectives

As stated in the Introduction, the use of organocatalysts along with their immobilization represents a challenging method towards the development of more sustainable synthetic processes. Moreover, the transition from batch to flow-mode studies increases the advantages derived from this new way of making synthesis. Indeed, as recently reported from the Government Accountability Office[1] of the USA on sustainable chemistry, three categories of technology can make chemical production more sustainable: catalysts, solvents (derived from renewable and less hazardous materials), and continuous processing (rather than batch processing of chemicals). Consequently, the doctoral studies conducted in the last three years were focused on the valorisation of the organocatalytic processes promoted by Lewis base catalysts through the development of both new methodologies and procedures for the synthesis of molecules with interesting biological, pharmaceutical and material applications. Additionally, the parallel immobilization of catalysts and investigations conducted with a flow apparatus emerged as useful tool towards the valorisation of bio-based products and to enhance the productivities of the performed studies.
The aims of the studies that were conducted during the PhD are summarised below.

Firstly, with the purpose to synthetise a novel library of fully bio-based monoacylglycerols (MAGs), the monoesterification of glycerol and solketal was investigated (Figure 1). At the same time, the study was focused on the preparation of a heterogeneous NHCs pre-catalysts (immobilized onto silica and polystyrene) able to work under oxidative conditions due to the presence of either the Kharasch oxidant or air (Chapter 3).

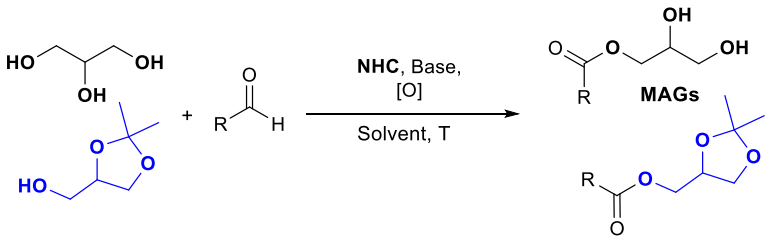

Figure 1. Novel synthetic methodology of glycerol and solketal esterification promoted by NHC-catalysis under oxidative conditions.

At this point of the work, it was also interesting to investigate whether this oxidative system could be further extended to the selective conversion of the bio-based 5-hydroxymethylfurfural (HMF) into the added-value 5-hydroxymethyl-2-furancarboxylic acid (Figure 2). As proof of concept, the disclosed oxidative system would also be applied for the

direct conversion of HMF and furfuraldehyde into their corresponding ester, amide, and thioester derivatives (Chapter 4).

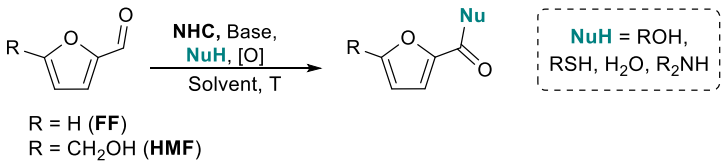

Figure 2. Proposed aerobic oxidation of 5-hydroxymethylfurfural and furfural into the corresponding carboxylic acid and derivatives through NHC-catalysis.

Later, driving by the everyday increasing attractiveness towards novel synthetic strategies to access bio-based polymer or to find new alternative routes for the synthesis of a novel class of polymer, the PhD work was further aimed to the use of NHC for the synthesis of polyesters and polyamides (Chapters 5 and 6; Figure 3).

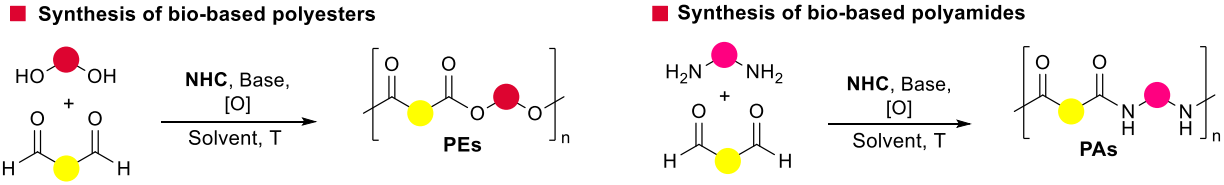

Figure 3. Proposed synthetic methodologies of bio-based polyesters and polyamide synthesis promoted by oxidative NHC-catalysis.

Guided by the studies on NHC-promoted amide formation under oxidative conditions, a new N-acylation procedure promoted by Lewis base organocatalysts were considered as additional aim (Figure 4). This investigation would be applied for the oxidative N-acylation reaction of 3,4-dihydropyrimidin-2-(1H)-ones (DHPMs) with enals designed to obtain pharmaceutically relevant N3-acylated products (Chapter 7).

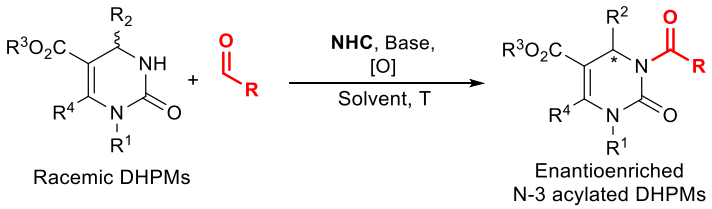

Figure 4. Novel strategy on N-acylation of DHPMs promoted by NHC-catalysis.

Lastly, building on the ever-increasing interest on the use of supported catalyst, the potential of immobilized Lewis base isothiourea organocatalyst was examined (Figure 5). Therefore, a sequantial kinetic resolution (DoCKR) of (±)-*syn*-1,2-diols and (±)-*anti*-1,3-diols kinetic resolution in flow-mode was chosen as benchmark reactions. This approach takes

advantage of an additive Horeau's amplification[2] and would provide access to highly enantioenriched compounds applying a highly practical protocol (Chapter 8).

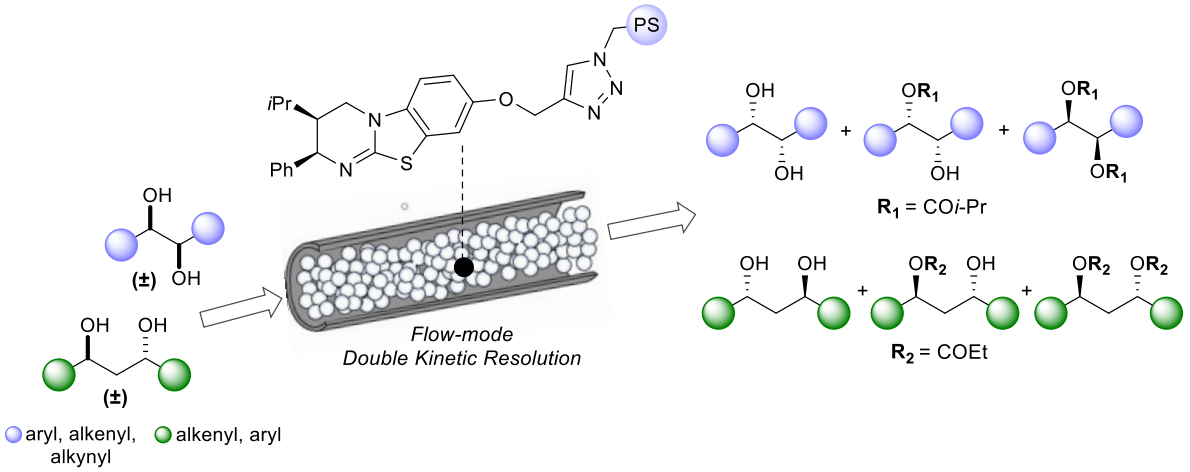

Figure 5. Sequential kinetic resolution of diols in flow-mode conditions.

2.1 References

1. Government accountability Office (GAO 18-307, February 2018).
2. J.-P. Vigneron, M. Dhaenes, A. Horeau, *Tetrahedron* **1973**, *29*, 1055−1059.

3. Esterification of glycerol and solketal by oxidative NHC-catalysis under heterogeneous batch and flow conditions

The work described in this chapter has formed the basis of the following peer reviewed publication: D. Ragno, A. Brandolese, D. Urbani, G. Di Carmine, C. De Risi, O. Bortolini, P. P. Giovannini, A. Massi, *React. Chem. Eng.*, **2018**, *3*, 816−825.

3.1 Introduction

N-heterocyclic carbene (NHCs) organocatalysts have proved to be useful for the upgrading of biomass-derived building blocks into added-value chemicals.[1,2] As robust, environmentally benign, and highly selective catalysts they have been employed in different synthetic area from medicinal to material ones. Their applications ranging from the umpolung reactivity to NHC-catalysed oxidation, C-C, C-N bond forming reactions, and chain-extension couplings.[3,4] This plethora of reactions allowed the synthesis of useful biofuels, polymeric materials, and pharmaceutical intermediates from the sugar-derived furfural (FF) and 5-hydroxymethylfurfural (HMF).[2,5] Likewise, the inexpensive glycerol, available in large amounts as by-product of biodiesel production,[6] has been exploited in synthetic programs. However, the ones promoted by NHC-catalysis were mainly focused on the synthesis of glycerol carbonate.[7,8] Indeed, Sundèn reported the first acylation of glycerol through oxidative NHC-catalysed telescoped protocol with aldehydes as the coupling substrates and air as the terminal oxidant.[7] In a batch approach, Bruijnincx[8] and co-workers developed, instead, a process in which glycerol carbonate has been synthetized using a silica-supported hydrogen carbonated-masked imidazolium pre-catalyst, which could be recycled if properly reactivated by anion-exchange procedure (Figure 1a).

However, the well-known low stability of soluble NHCs to air and moisture has often limited their industrial application to produce new bio-based chemicals, justifying the few reported examples. On the other hand, the recently implemented organocatalyst immobilization strategies and flow-mode synthesis[9,10] represent important improvements in terms of increasing catalyst stability, productivity scalability, and sustainability of the whole synthetic procedure.[11,12] Yet, despite these advantages, the application of the umpolung reactivity in flow for the upgrading of bio-based molecules has been nowadays scarcely investigated. The development of new catalytic methods for the derivatization of biomass-derived building blocks into added-value chemicals using inexpensive reagents and simple reaction conditions therefore

remains an important area of research. Herein, the oxidative monoesterification of glycerol and its derivative solketal has been developed (Figure 1b). The procedure has been performed in batch and continuous-flow through the design and synthesis of a set of triazolium salt pre-catalyst immobilized on silica and polystyrene supports. The study allowed the synthesis of monoacylglycerols (MAGs), interesting bio-based derivatives, used in energy, polymer, pharmaceutical, and cosmetic fields.[13,14] In the past, heterogeneous organocatalytic approaches have been established for the selective synthesis of MAGs using strong supported Brønsted base and acid catalysts.[15] The presented protocol, not only involved the use of immobilized NHC Lewis base catalysts, but also exploited the synthesis of fully bio-based MAGs, starting from the biomass-derived aldehydes FF and HMF, and from the biogenic citronellal and vanillin.

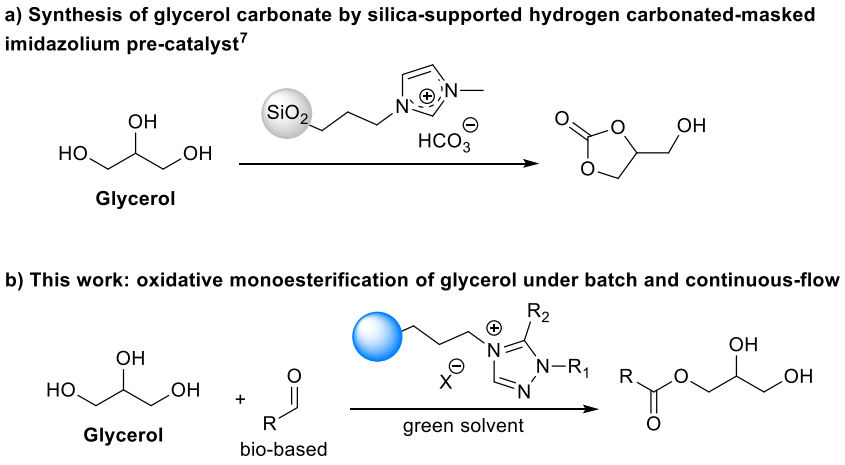

Figure 1. Glycerol upgrading through NHC-catalysis.

3.2 Results and discussion

The model monoesterification of glycerol **1** with 1-napthaldehyde **2a** was performed under oxidative homogeneous conditions to identify the optimal class of azolium salt pre-catalysts for their further immobilization on inert supports (Table 1). In initial investigations, the triazolylidene catalyst proved to be more effective in the **1/2a** coupling compared to imidazolylidene, imidazolylidene, and thiazolylidene carbenes as observed by Sundèn and co-workers.[7] Thus, the followed experiments were conducted using triazolium salts **A**−**C** with an equimolar amount of the Kharasch oxidant **6** and DBU as the base (20 mol%) in THF under degassed conditions (entries 1−3). The degassed conditions turned out to be very important for limiting the formation of 1-naphtoic acid **5a**. Indeed, the carboxylic acid could be produced by a side oxygenative pathway promoted by NHCs in the presence of residual oxygen.[16–18]

The most effective bicyclic pentafluorophenyl pre-catalyst **C** provided a 66:34 mixture of MAG **3a** and diacylglycerol (DAG) **4a** with almost full conversion of stoichiometric reagents in one hour at room temperature without any evidence of formation of the by-product **5a** (entry 3). Later, different soluble organic bases were tested (entries 4−6); NEt_3 afforded the best result with a mono/diester ratio of 73:27 (entry 6). Additionally, this kind of base turned out to be suitable for the subsequent development of a flow-mode process.

Table 1. Screening of reaction conditions with soluble triazolium pre-catalysts **A**−**C**.[a]

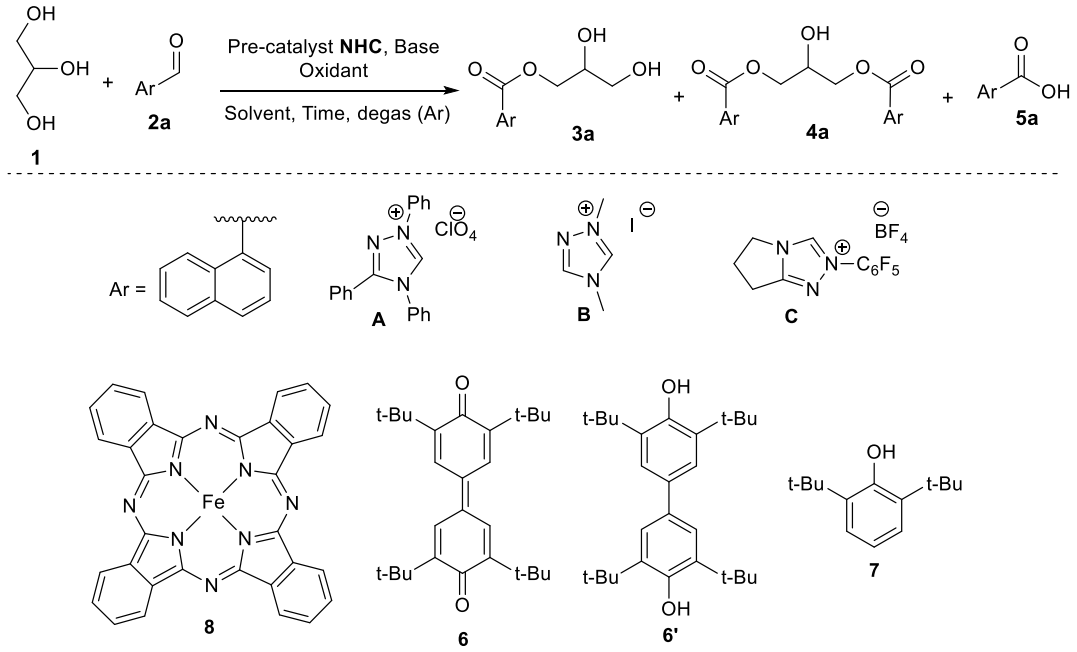

Entry	Pre-Catalyst (mol%)	Base (mol%)	Time (h)	**3a**+**4a** (%)[b]	**3a**:**4a**[b]	**5a** (%)[b]	Oxidant (mol%)
1	**A** (10)	DBU (20)	24	22	88:12	/	**6** (100)
2	**B** (10)	DBU (20)	24	82	71:29	/	**6** (100)
3	**C** (10)	DBU (20)	1	>95%	66:34	/	**6** (100)
4	**C** (10)	KHMDS (20)	1	>95%	63:37	/	**6** (100)
5	**C** (10)	DIPEA (20)	1	>95%	67:33	/	**6** (100)
6	**C** (10)	NEt_3 (20)	1	>95%	73:27	/	**6** (100)
7	**C** (2.5)	NEt_3 (2.5)	1	>95%	71:29	/	**6** (100)
8[c]	**C** (2.5)	NEt_3 (2.5)	1	>95%	84:16	/	**6** (100)
9[d]	**C (2.5)**	**NEt_3 (2.5)**	**1**	**>95%**	**91:9**	/	**6 (100)**
10	**C** (2.5)	NEt_3 (2.5)	4	39	>95:5	/	TEMPO (150)
11	**C** (2.5)	NEt_3 (50)	24	59	82:18	/	MnO_2 (500)
12	**C** (2.5)	NEt_3 (5)	24	10	>95:5	59	O_2
13[e]	**C** (2.5)	NEt_3 (50)	24	81	80:20	10	Air, **7/8**
14[d,e]	**C (2.5)**	**NEt_3 (50)**	**24**	**95**	**90:10**	**5**	**Air, 7/8**
15[d,e,f]	**C** (2.5)	NEt_3 (50)	24	67	94:6	19	Air, **7/8**

[a]**1** (0.12 mmol), **2a** (0.12 mmol), THF (1.0 mL), room temperature. [b]Yield and selectivity detected by ^1H NMR of the crude reaction mixture with durene as an internal standard. [c]**1** (2 equiv., 0.24 mmol). [d]**1** (3 equiv., 0.36 mmol). [e]ETM/ETM' system: **7** (20 mol%), **8** (5 mol%). [f]T = 50 °C.

The high catalytic activity of the catalyst **C** has been confirmed by lowering the catalyst amount to 2.5 mol% which left almost unchanged the reaction outcome (entry 7). Increasing the quantity of glycerol showed a better selectivity (entries 8−9) detecting the highest value (**3a**:**4a** = 91:9) with 3 equivalents of **1** (entry 9). Later, alternatives to the Kharasch oxidant **6** were considered (entries 10−13). A lower conversion of glycerol was detected with the stable radical TEMPO (entry 10), while MnO_2 determined a substantial increase of the reaction time (entry 11). The direct use of oxygen was also investigated through balloon technique (1 bar), and only a small amount of MAG **3a** was detected due to the preferential formation of **5a** (59%; entry 12). The formation of the carboxylic acid is due to the oxygenative pathway which is in competition with the oxidative one (see Scheme 7). Subsequently, an electron transfer mediator system (ETMs) was tested in agreement with Sundèn's works[7,19] based on Backvall's group[20] studies. Indeed, the inexpensive precursor **7** was used along with a catalytic amount of iron (II) phthalocyanine **8** (ETM') and atmospheric oxygen as the terminal oxidant. Under these conditions the reaction is expected to proceed through the oxidative pathway (as explained in Scheme 7) thus reducing the formation of the carboxylic acid **5a**. Hence, equimolar **1** and **2a** reacted in THF in the presence of **C** (2.5 mol%) and NEt_3 (50 mol%) affording **3a** and **4a** in 81% yield and 80:20 ratio after 24 hours (entry 13). By increasing the excess of glycerol (3 equiv.; entry 14), a higher selectivity was recorded (**3a**:**4a** = 90:10) along with the reduction of acid **5a** formation (5%). Lastly, the effect of the temperature was investigated. However, a lower conversion was observed along with higher amount (19%) of acid **5a** (entry 15).

Once the optimal reaction conditions for the synthesis of MAG derivatives of type **3** in homogeneous phase have been defined, the further immobilization strategy of the most promising pre-catalysts **B**−**C** was investigated. Considering the previous studies on organocatalyst fixation by click reactions[21−23] and the seminal works of Rovis and co-workers on the synthesis of soluble bicyclic triazolium pre-catalysts,[4,24] the preparation of the silica-supported version of most active triazolium salt **C** was attempted starting from the readily available 4-azidopyrrolidin-2-one **9**[25] (Scheme 1). The crude hydrazinium tetrafluoroborate salt **10** has been isolated with 95% overall yield after two steps composed of the standard amidate formation with the Meerwein's salt, followed by treatment with pentafluorophenyl hydrazine. However, the later thermal ring closure in presence of triethyl orthoformate and chlorobenzene at 120 °C afforded a very complex reaction mixture. Thus, after a long investigation, the use of neat trimethyl orthoformate and microwave heating (102 °C; 3 h) turned out to be the best conditions to obtain the full conversion of **10** with formation of a cleaner reaction mixture. The azido tetrafluoroborate triazolium salt **11**, recovered in 48% yield after crystallization, has been immobilized through the Ruthenium-catalysed Azide Alkyne Cycloaddition (RuAAC)[26] of **11**

and the alkyne-functionalized silica **12**. The latter compound was readily prepared from 3-aminopropyl-silica and 4-pentynoic acid according to a known process.[27] The use of RuAAC strategy instead of the more common Cu-catalysed procedure[22,23] was driven by the need to avoid a basic medium, detrimental for the triazolium salt **11** stability. Therefore, the **11/12** coupling proceeded smoothly in DMF at 50 °C in the presence of the Cp*RuCl(COD) catalyst (10 mol%) affording the target silica-supported triazolium salt **D** with good conversion as determined by elemental analysis (*f*: 0.71 mmol g^{-1}).

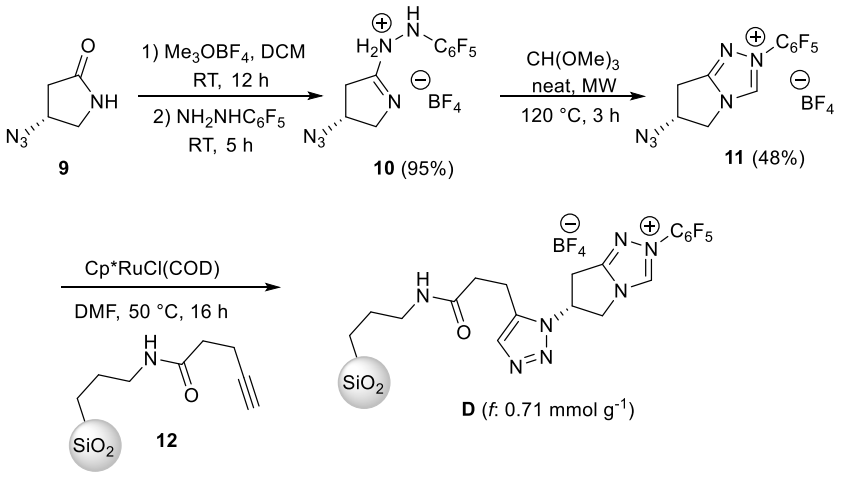

Scheme 1. Synthesis of silica-supported triazolium pre-catalyst **D**.

The silica- and polystyrene-supported analogues of the triazolium salt **B** were prepared by N-alkylation of the commercially available 1-methyl-1*H*-1,2,4-triazole **13**. Inspired by the preparation of an analogous homogenous catalyst,[28a] the heterogeneous pre-catalyst **E** was obtained with the satisfactory loading of 0.66 mmol g^{-1} using a 3-chloropropyl silica gel **14**[28b] (CH_3CN, 90 °C, 16 h; Scheme 2). Being aware of the influence of the support hydrophilicity on the catalytic performance (activity and selectivity) of solid promoters in glycerol esterifications,[15] the polystyrene-supported version **F** was instead synthetized from the commercially available Merrifield resin **15** with a comparable level of efficiency (Scheme 2).

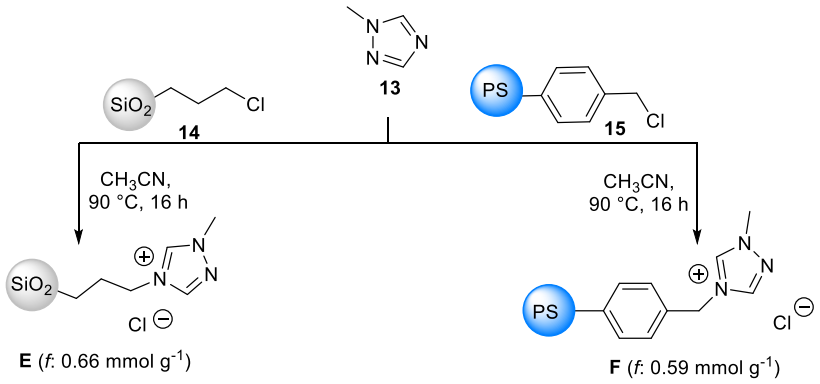

Scheme 2. Synthesis of silica- and polystyrene-supported pre-catalysts **E** and **F**.

Once the heterogeneous catalysts **D**−**F** were obtained their catalytic activity and recyclability for the model reaction were deeply investigated (Table 2). Thus, the pre-catalyst **D** was initially tested under the conditions previously optimized for its homogeneous counterpart **C** (Table 1, entry 14), for a direct comparison. Disappointingly, the aerobic esterification of glycerol **1** (3 equiv.) with **2a** promoted by **D** (10 mol%) in the presence of NEt_3 (50 mol%) and ETMs in THF resulted in a substantial decrease of reaction conversion (41% vs. 95%; entry 1). This behaviour was attributed to the residual acidity of the silica support. Indeed, the replacing of NEt_3 with the stronger DBU base led to satisfactory results (**3a**+**4a** = 82%, **3a**:**4a** = 91:9; entry 2). Subsequently, the enantioselectivity of the process was also investigated but, the presence of the remote stereocenter in the pyrrolidine framework of pre-catalyst **D** had little effect on the outcome of the monoesterification process (**3a**: 21% *ee*; see the Experimental section for further details). Moreover, the followed brief solvent screening with DCM and toluene (entries 3, 4) assessed that the reaction results could not be improved. Therefore, no further investigations were conducted on the asymmetric process. At this point of the study, the silica-supported pre-catalyst **E** was tested under different reaction conditions (entry 5, selected example) however, just a modest reactivity was detected. On the other hand, the polystyrene-supported analogue **F** worked properly yielding the target MAG **3a** with almost the same level of efficiency as **D** (entry 6). The latter catalyst was thus chosen for the further optimization of the monoesterification procedure due to its simple one-step preparation. Focusing on enhanced sustainable process the screening of environmentally benign solvents was carried out (entries 7−11). Successfully, the use of biomass derived 2-methyltetrahydrofuran (Me-THF)[29] provided a substantial improvement of the reaction output in terms of both conversion (**3a**+**4a** = 92%) and selectivity (**3a**:**4a** > 95:5; entry 7). Ethyl lactate and γ-valerolactone were fewer effective solvents (entries 8−9), whereas the deep eutectic mixture of glycerol and choline chloride[30] totally inhibited the catalytic process (entry 10). Lastly, the 1:1 THF:H_2O mixture was used with the aim to take advantage of favourable interactions between the catalytic sites and the polystyrene support of **F**.[31] However, this condition turned out to be unsuccessful leading to the preferential formation of the carboxylic acid **5a** (entry 11).

The best performing Me-THF solvent was thus used for additional optimization studies. An excellent MAG/DAG selectivity was detected both at room temperature and 50 °C (> 95:5; entries 12−13) along with a drop of conversion when 2 equivalents of glycerol were used. A control experiment confirmed that no leaching of the active triazolium catalyst occurred during the process. Indeed, filtering **F** at 40% of the conversion and letting the filtrate to react under the optimal conditions of entry 7 led no further conversion of glycerol, thus excluding the activity of any soluble species in the esterification process (entry 14). Later, the catalytic activity

of heterogenous **F** was evaluated under degassed conditions in the presence of the Kharasch oxidant **6** detecting a bit lower conversion compared to the experiment conducted with air and the mediators (84%, entry 15). Lastly, catalyst recyclability performed through a simple filtration, washing, and drying of the resin was explored over five and ten recycles. Both terminal oxidants, air (entries 16−17) and **6** (entries 18−19), showed an unaltered selectivity (**3a**:**4a** > 95:5) with only a moderate decrease (ca. 5%) of conversion after each recycle. Globally, the catalyst showed an accumulated turnover number (TON) of 66 with air and of 56 with the Kharasch oxidant **6**, confirming the high stability of the catalyst **F**.

Table 2. Screening of reaction conditions with supported triazolium pre-catalysts **D**−**F**.[a]

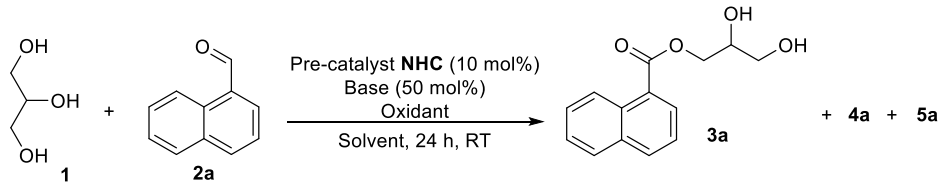

Entry	Pre-catalyst	Solvent	Base	**3a+4a** (%)[b]	**3a**:**4a**[b]	**5a** (%)[b]	Oxidant
1	**D**	THF	NEt_3	41	>95:5	/	Air, **7/8**
2	**D**	THF	DBU	82[c]	91:9	/	Air, **7/8**
3	**D**	DCM	DBU	22	>95:5	8	Air, **7/8**
4	**D**	Toluene	DBU	33	91:8	11	Air, **7/8**
5	**E**	THF	DBU	48	>95:5	8	Air, **7/8**
6	**F**	THF	DBU	83	92:8	/	Air, **7/8**
7	**F**	**Me-THF**	**DBU**	**90**	**>95:5**	**/**	**Air, 7/8**
8	**F**	Ethyl Lactate	DBU	34	>95:5	/	Air, **7/8**
9	**F**	γ-valerolactone	DBU	35	>95:5	12	Air, **7/8**
10	**F**	Ch-Cl:Gly[d]	DBU	/	/	/	Air, **7/8**
11	**F**	THF/H_2O (1:1)	DBU	16	>95:5	34	Air, **7/8**
12[e]	**F**	Me-THF	DBU	73	>95:5	5	Air, **7/8**
13[e,f]	**F**	Me-THF	DBU	70	>95:5	7	Air, **7/8**
14[g]	**F**	Me-THF	DBU	40	>95:5	/	Air, 7/8
15[h]	**F**	**Me-THF**	**DBU**	**84**	**>95:5**	**/**	**6 (100 mol%)**
16[i]	**F**	Me-THF	DBU	68	>95:5	/	Air**, 7/8**
17[j]	**F**	Me-THF	DBU	41	>95:5	/	Air, **7/8**
18[h,i]	**F**	Me-THF	DBU	55	>95:5	**/**	**6** (100 mol%)
19[h,j]	**F**	Me-THF	DBU	37	>95:5	**/**	**6** (100 mol%)

[a]**1** (0.36 mmol), **2a** (0.12 mmol), **NHC** (10 mol%), base (50 mol%), ETM/ETM' system: **7** (20 mol%), **8** (5 mol%), solvent (1.0 mL), reaction time 24 h. [b]Yields and selectivity detected by ^1H NMR on the crude reaction mixture with durene as an internal standard. [c]**3a**: 21% ee as determined by chiral HPLC (see the experimental section). [d]1:2 molar ratio eutectic mixture (Choline Cl-Glycerol). [e]**1** (2 equiv., 0.25 mmol). [f]T = 50 °C. [g]Catalyst **F** filtered off at 40% conversion; DBU (20 mol%). [h]Degassed conditions (Ar). [i]Fifth recycle. [j]Tenth recycle.

The scope of the monoesterification of glycerol **1** with representative classes of aldehydes **2** was later explored (Scheme 3) under the optimized heterogeneous procedure (Table 2, entry 7). As expected on the basis of previous observations,[17] the electron poor 4-bromobenzaldehyde gave the corresponding ester **3b** in lower isolated yield (60%) compared to 1-naphthaldehyde

2a due to the occurrence of the competitive homo-benzoin reaction. The α-β unsaturated cinnamaldehyde, instead, afforded MAG **3c** in good yield (83%), but also the long chain aliphatic aldehydes proved to be suitable substrates giving the corresponding esters **3d**–**e** in satisfactory yields. The substrate scope was similarly extended to bio-mass derived and biogenic aldehydes to access a new class of fully bio-based MAGs. For this purpose, citronellal and vanillin were used, furnishing the corresponding monoester **3f** and **3g** in reasonable yield without any evidence of formation of DAG derivatives.

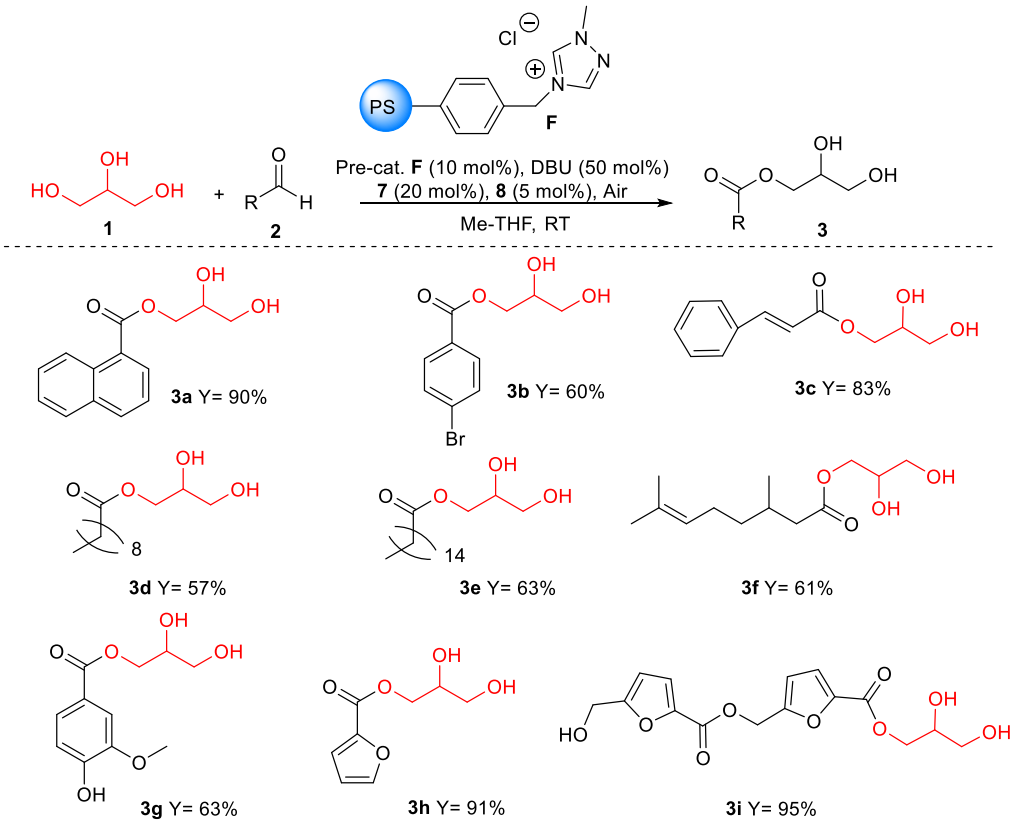

Conditions: **1** (0.75 mmol), aldehyde **2** (0.25 mmol), **F** (0.025 mmol), DBU (0.13 mmol), **7** (0.05 mmol), **8** (0.012 mmol), Me-THF (2.0 mL). All the reported yields (Y) are for the isolated compounds **3**.

Scheme 3. Reaction scope with **F** and glycerol **1** under batch conditions.

Furfural was also tested, proving to be the most active substrate (**3h**, 91% yield). Differently, HMF produced the notable diester **3i** in almost quantitative yield. Fairly, compound **3i** was formed by monoesterification of glycerol with a first molecule of unprotected HMF **2i**, followed by subsequent esterification of the resulting primary alcohol intermediate (not shown) with a second molecule of **2i**. However, the selectivity towards the formation of product **3i** with two molecules of HMF in place of three or four has not been explored further.

The heterogeneous batch procedure was additionally applied to the esterification of 1,2-isopropylideneglycerol **16** known as solketal (Scheme 4). Thanks to the absence of selectivity issues, a lower excess (1.5 equiv.) of alcohol **16** was used, leading to the corresponding esters

17a–i in good yield (52–92%). Of note, the coupling of solketal **16** with HMF produced the solely monoester derivative **17i** with 79% yield. This change in selectivity with respect to the use of glycerol could not be easily explained. However no further investigations have been conducted in this regards.

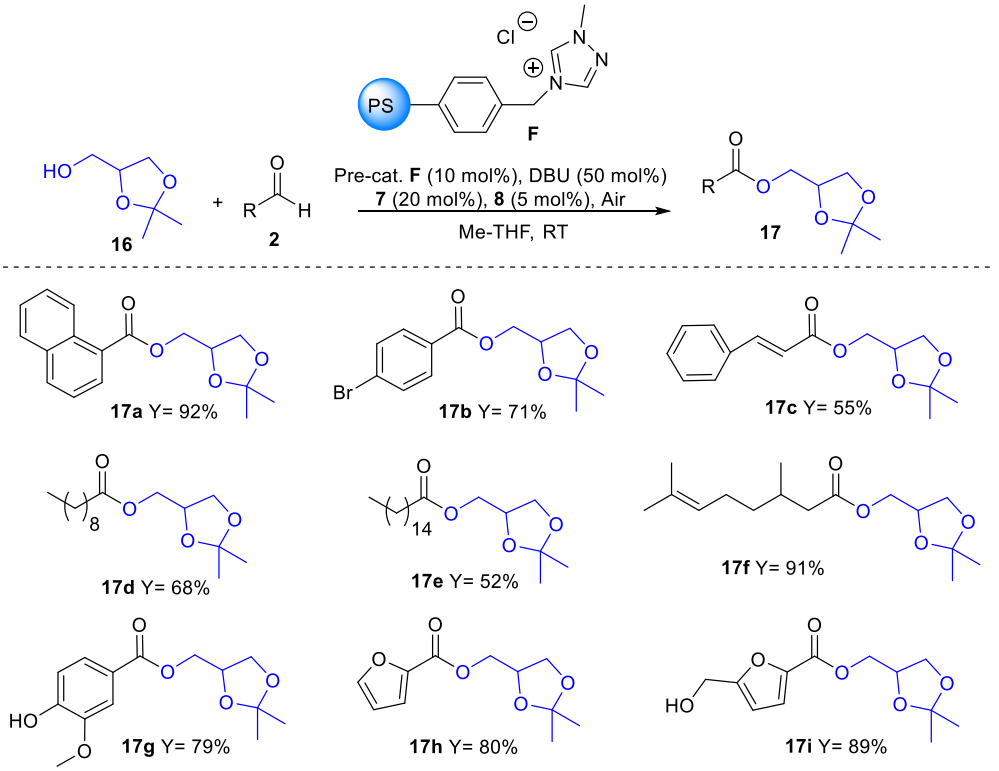

Conditions: **16** (0.38 mmol), aldehyde **2** (0.25 mmol), **F** (0.025 mmol), DBU (0.13 mmol), **7** (0.05 mmol), **8** (0.012 mmol), Me-THF (2.0 mL). All the reported yields (Y) are for the isolated compounds **17**.

Scheme 4. Reaction scope with **F** and solketal **16** under batch conditions.

Globally, it is important to point out that the developed batch procedure considerably diminishes the environmental impact of the monoesterification process. Indeed, the simplicity of catalyst recycle compared to previously reported procedures,[8,15] the use of air as the terminal oxidant, and the possibility of re-use the biomass-derived Me-THF and the excess of glycerol remarkably improve the sustainability of the approach.

A further aim of the work was the definition of an effective flow procedure for the valorisation of renewable chemicals such as glycerol and solketal. Thus, a packed-bed microreactor **R1** (Table 3) was prepared using the active polystyrene triazolium salt precatalyst **F**. Accordingly, a pressure-resistant stainless-steel column (length 10 cm, 0.46 cm internal diameter) was filled with the Me-THF swelled resin **F** by the slurry packing technique. Pycnometry measurements allowed to determine the hold-up (dead) volume (Vo) and the total porosity (ε_{tot}) of **R1** for calculation of the residence time at different flow rates.

Table 3. Main features of packed-bed microreactor **R1**.

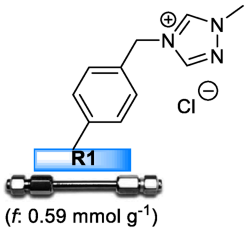

Loaded **F** [g][a]	V_G [mL][b]	V_o [mL][c]	Total porosity[d]	Time [min][e]	Pressure [bar][f]
0.75	1.66	0.78	0.47	39	2

[a]Calculated by difference with catalyst amount in the residual slurry solution. [b]Geometric volume (V_G) of the stainless-steel column. [c] Void volume (V_0) determined by pycnometry. [d] Total porosity ε_{tot}= V_0/V_G. [e] Residence time calculated at 20 μLmin^{-1}. [f] Backpressure measured at 20 μLmin^{-1} (RT, Me-THF).

The esterification of glycerol **1** with 1-napthaldehyde **2a** was used as benchmark reaction to understand the activity of the prepared microreactor **R1**. Continuous-flow experiments were conducted with the two-pump, three-way valve apparatus depicted in Scheme 5; however, due to the flow set-up it was no possible to use the ETMs **7/8** and air as the terminal oxidant. Attempts to take advantage of dissolved oxygen in the liquid phase inside the reactor, in fact, led to poor levels of conversion toward MAG **3a** (ca. 15%, detected by ^{1}H NMR analysis of the outlet stream). Consequently, an effective flow procedure was optimized using the air-recyclable oxidant **6**, instead of employing an air flow by means of a mass flow controller (MFC).[32]

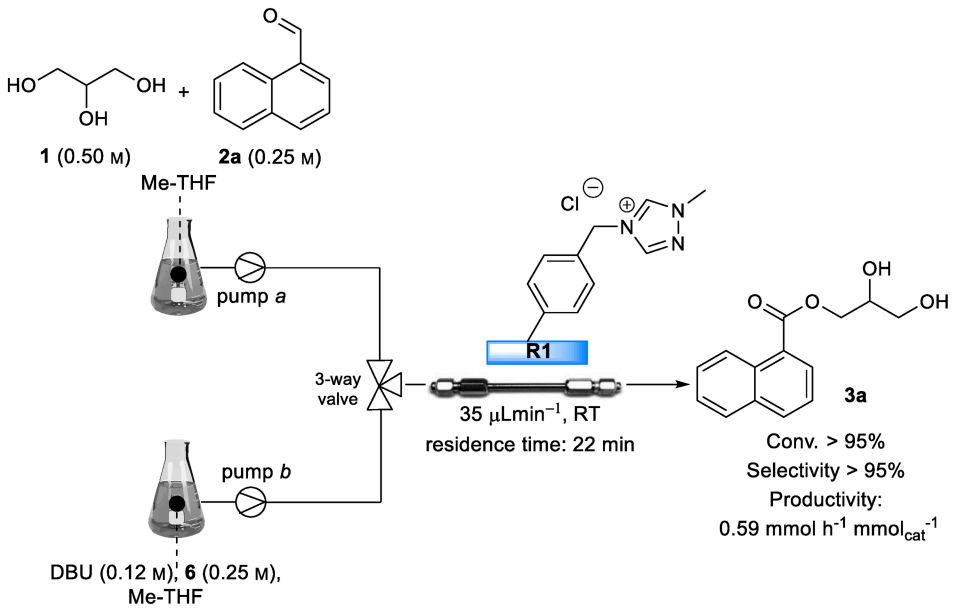

Scheme 5. Set-up for the continuous-flow experiments.

Hence, the pre-activated microreactor **R1** was independently fed at 35 μLmin^{-1} with continuously degassed mixtures of glycerol **1** (0.50 M)/**2a** (0.25 M) and DBU (0.12 M)/**6** (0.25 M). Under these optimized conditions, the steady-state regime was achieved after one hour yielding the ester **3a** with full conversion and complete selectivity. The unaltered output, maintained for 120 h led to a TON of 71, with a moderate but progressive loss of conversion efficiency after that time (Figure 2). Further control experiment of the catalyst performance confirmed a partial erosion of the catalytic activity in term of conversion with preservation of

selectivity (**3a**: 45%) when the packed pre-catalyst **F** (200 h operation) was recycled and tested in the model batch conditions (Table 2, entry 15). Unfortunately, the efficiency of the packing material of **R1** could not be regenerated even after acidic treatment (HCl 37%) for the conversion of the *in situ* generated carbene into the azolium salt pre-catalyst **F**. At this stage of the study, it was not possible to firmly suggest the mechanism of degradation of catalyst **R1**. Therefore, dedicated FT-IR and MAS-NMR analyses could be carried out in the future in order to furnish more information on catalyst deactivation. Nevertheless, the use of the flow set up led to an increase of productivity as previously observed in other studies on continuous flow NHC-catalysis[31,33] due to the continuous exclusion of trace impurities and moisture from the active carbene species. Additionally, it was also possible to avoid the over esterification of **3a** using a lower excess of glycerol **1** compared to the batch process (2 equiv. *vs* 3 equiv.) by checking the residence time (22 min) of the reactants within the reactor.

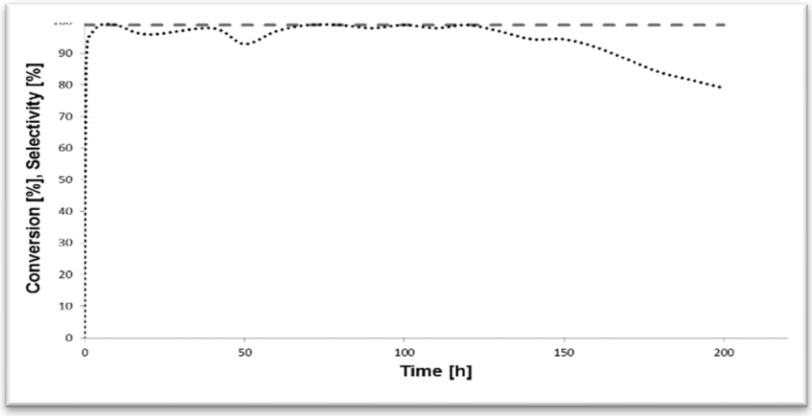

Figure 2. Long-term stability of the packed-bed microreactor **R1** in the flow synthesis of **3a**. Conversion [%], dotted line; selectivity [%], dashed line.

Lastly, a brief scope in continuous flow was carried out by adjusting the flow rates with the aim to reach high conversion (> 90%) for the simple downstream purification of **3f–i** and **17f–i** and for the recovery of the reduced alcohol **6'**. Overall, the target MAGs **3** and **17** were obtained with good productivities (ca. 0.5 $mmol h^{-1} mmol_{cat}^{-1}$) and complete selectivity (Scheme 6).

The quite complex procedure for the oxidation of hydroquinone **6'** to the expensive oxidant **6** reported in literature,[34] which used dioxygen in the presence of catalytic amounts of nitrogen dioxide, was replaced with a new one for our purposes. Indeed, the Kharasch oxidant **6** has been recovered through the quantitative oxidation of **6'**, easily achieved with air (1 atm balloon) and catalytic iron(II) phthalocyanine **8** (10 mol%, THF, RT).

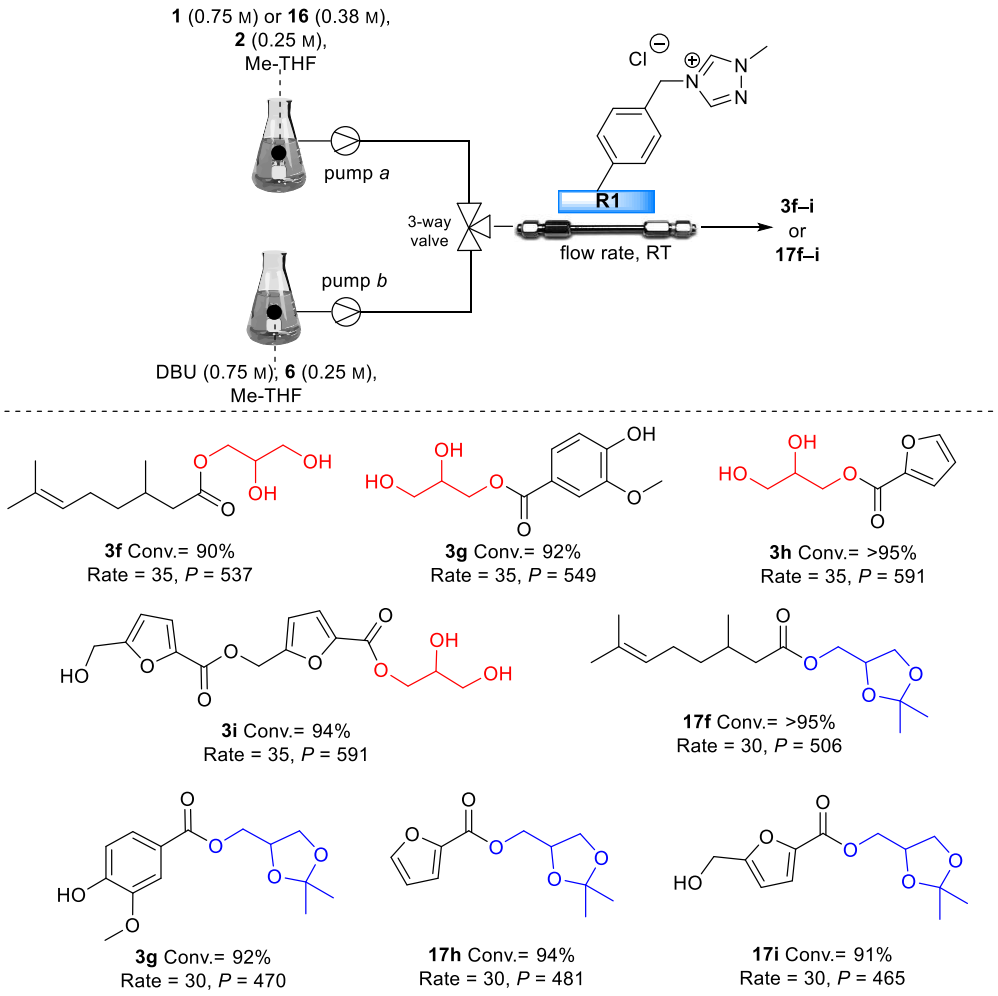

See the Experimental Section for a description of the flow apparatus. The conversion are reported as instant conversion in the steady-state regime as established by ^{1}H NMR analysis. Flow rate are measured in μLmin^{-1}; productivities (*P*) are measured in mmol$_{product}$ h^{-1} mmol$_{cat}^{-1}$.

Scheme 6. Continuous-flow production of selected monoesters **3** and **17** with microreactor **R1**.

A suggested mechanism explaining the role of the biomimetic system of electron transfer mediators has also been proposed on the basis of previous works.[7,19,20] While the formation of the carboxylic acid is mainly associated to the oxygenative pathway[17,18] (the presence of trace of water which act as nucleophile cannot be excluded) for the conversion of the Breslow intermediate (Scheme 7), the formation of the product is connected to the oxidative one. The role of the ETMs system lies in the *in situ* formation of a catalytic amount of the Kharasch oxidant **6** from the inexpensive precursor **7** under basic conditions. After electron transfer with the Breslow intermediate, the acyl azolium species is obtained along with the reduce alcohol **6'**. The latter could be re-oxidized to **6** in the presence of catalytic iron(II) phthalocyanine **8** (ETM') and atmospheric oxygen which act as the terminal oxidant (Scheme 7).

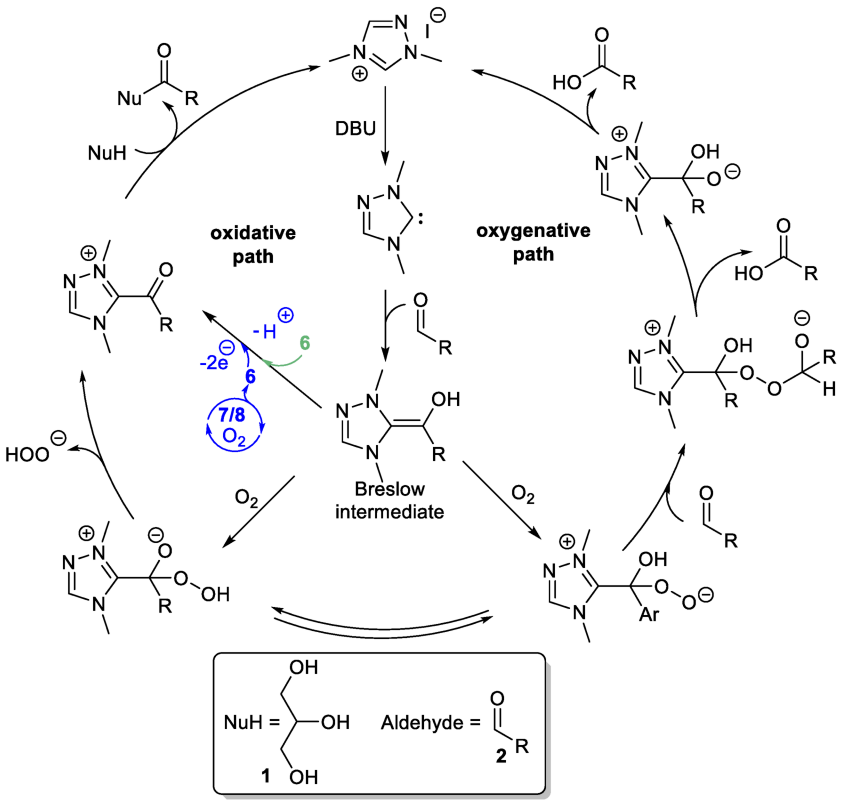

Scheme 7. Proposed mechanisms for the oxidative esterification of glycerol **1** with aldehyde **2**.

3.3 Conclusion

To sum up, a new procedure for the oxidative esterification of glycerol has been proposed using aldehydes in the presence of both homogeneous and heterogeneous NHCs catalysts. New oxidation systems have been performed as well.

The optimization study under homogenous conditions led to the immobilization on silica and polystyrene support of the best performing triazolium pre-catalysts. After a further optimization procedure under heterogeneous conditions the polystyrene-supported triazolium pre-catalyst **F** has been chosen to investigate the scope of the reaction. This promoter has been able to catalyse the environmentally benign synthesis of a novel class of MAG derivatives starting from bio-based aldehydes (furfural, hydroxymethylfurfural, citronellal, vanillin) with high conversions and selectivity in batch and flow-mode approaches using the green solvent Me-THF. A further investigation on the oxidative esterification of solketal led to the formation of corresponding esters with comparable level of efficiency. Lastly, the study was extended to continuous flow-mode synthesis leading to an increased productivity towards the corresponding MAGs.

3.4 Experimental section

General procedure

All moisture-sensitive reactions were performed under an argon atmosphere using oven-dried glassware. Solvents were dried over a standard drying agent and freshly distilled prior to use. Reactions were monitored by TLC on silica gel 60 F_{254} with detection by charring with potassium permanganate and/or phosphomolybdic acid. Flash column chromatography was performed on silica gel 60 (230−400 mesh). ^{1}H (300 MHz), ^{13}C (101 MHz) and ^{19}F (376 MHz) NMR spectra were recorded in $CDCl_3$ or acetone-d_6 solutions at room temperature. The chemical shifts in ^{1}H and ^{13}C NMR spectra were referenced to trimethylsilane (TMS). The chemical shifts in ^{19}F NMR spectra were referenced to $CFCl_3$. Peak assignments were aided by ^{1}H-^{1}H COSY and gradient-HMQC experiments. FT-IR analyses were performed using the Bruker Instrument Vertex 70. Elemental analyses were performed using a FLASH 2000 Series CHNS/O analyser (ThermoFisher Scientific). Optical rotations were measured at 25 ± 2 °C in the stated solvent; $[\alpha]_D$ values are given in 10^{-1}deg cm^{2}g^{-1} (concentration *c* given as g/100 mL). For high resolution mass spectrometry (HRMS) the compounds were analysed in positive ion mode using an Agilent 6520 HPLC-Chip Q/ TOF-MS (nanospray) with a quadrupole, a hexapole, and a time of flight unit to produce the spectra. The capillary source voltage was set at 1700 V; the gas temperature and drying gas were kept at 350 °C and 5 L min^{-1}, respectively. The MS analyser was externally calibrated with ESI-L low concentration tuning mix from *m/z* 118 to 2700 to yield accuracy below 5 ppm. Accurate mass data were collected by directly infusing samples in 40:60 H_2O:ACN 0.1% TFA into the system at a flow rate of 0.4 μLmin^{-1}. All commercially available reagents were used as received without further purification, unless otherwise stated. Catalyst **A** was synthetized according to a literature procedure.[35] Aldehyde **2d** was synthesized from the corresponding alcohol *via* PCC oxidation. (*R*)-4-Azidopyrrolidin-2-one **9**,[25] the alkyne-functionalized silica **12**,[27] and 3-chloropropyl silica gel **14**[28] were prepared as described. Liquid aldehydes and bases (DBU, TEA) were freshly distilled before their utilization.

Screening of reaction conditions with soluble triazolium pre-catalysts A−C (Table 1)

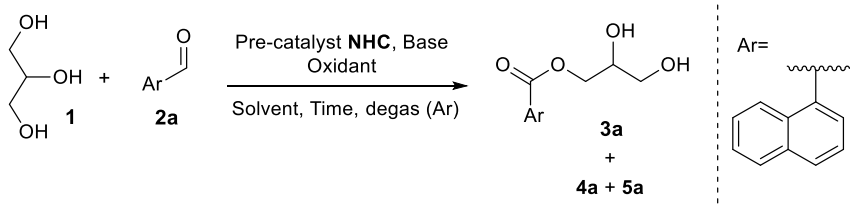

The following reaction conditions explain the operative optimization procedure. In all experiments, yield and selectivity were evaluated by ^{1}H NMR analysis of the reaction mixture (durene as internal standard).

Entries 1−3. A stirred mixture of glycerol **1** (11 mg, 0.12 mmol), 1-naphtaldehyde **2a** (16 μL, 0.12 mmol), oxidant **6** (49 mg, 0.12 mmol), durene (16 mg, 0.12 mmol) and the stated pre-catalyst (0.012 mmol) in anhydrous THF (1.0 mL) was degassed under vacuum and saturated with argon (by an Ar-filled balloon) three times. Then, DBU was added (3.6 μL, 0.024 mmol), and the reaction was stirred at room temperature for the stated time.

Entries 4−6. A stirred mixture of glycerol **1** (11 mg, 0.12 mmol), 1-naphtaldehyde **2a** (16 μL, 0.12 mmol), oxidant **6** (49 mg, 0.12 mmol), durene (16 mg, 0.12 mmol) and pre-catalyst **C** (4.4 mg, 0.012 mmol) in anhydrous THF (1.0 mL) was degassed under vacuum and saturated with argon (by an Ar-filled balloon) three times. Then, the stated base was added (0.024 mmol), and the reaction was stirred at room temperature for 1 h.

Entry 7. A stirred mixture of glycerol **1** (11 mg, 0.12 mmol), 1-naphtaldehyde **2a** (16 μL, 0.12 mmol), oxidant **6** (49 mg, 0.12 mmol), durene (16 mg, 0.12 mmol) and pre-catalyst **C** (1.2 mg, 0.003 mmol) in anhydrous THF (1.0 mL) was degassed under vacuum and saturated with argon (by an Ar-filled balloon) three times. Then, NEt_3 was added (20 μL of a 0.15 M solution in THF, 0.003 mmol), and the reaction was stirred at room temperature for 1 h.

Entries 8−9. A stirred mixture of glycerol **1** (stated amount), 1-naphtaldehyde **2a** (16 μL, 0.12 mmol), oxidant **6** (49 mg, 0.12 mmol), durene (16. mg, 0.12 mmol) and pre-catalyst **C** (1.2 mg, 0.003 mmol) in anhydrous THF (1.0 mL) was degassed under vacuum and saturated with argon (by an Ar-filled balloon) three times. Then, NEt_3 was added (20 μL of a 0.15 M solution in THF, 0.003 mmol), and the reaction was stirred at room temperature for 1 h.

Entry 10. A stirred mixture of glycerol **1** (11 mg, 0.12 mmol), 1-naphtaldehyde **2a** (16 μL, 0.12 mmol), TEMPO (28 mg, 0.18 mmol), durene (16. mg, 0.12 mmol) and pre-catalyst **C** (1.2 mg, 0.003 mmol) in anhydrous THF (1.0 mL) was degassed under vacuum and saturated with argon (by an Ar-filled balloon) three times. Then, NEt_3 was added (20 μL of a 0.15 M solution in THF, 0.003 mmol), and the reaction was stirred at room temperature for 4 h.

Entry 11. A stirred mixture of glycerol **1** (11 mg, 0.12 mmol), 1-naphtaldehyde **2a** (16 μL, 0.12 mmol), MnO_2 (52 mg, 0.6 mmol), durene (16. mg, 0.12 mmol) and pre-catalyst **C** (1.2 mg, 0.003 mmol) in anhydrous THF (1.0 mL) was degassed under vacuum and saturated with argon (by an Ar-filled balloon) three times. Then, NEt_3 was added (8.4 μL, 0.06 mmol), and the reaction was stirred at room temperature for 24 h.

Entry 12. A stirred mixture of glycerol **1** (11 mg, 0.12 mmol), 1-naphtaldehyde **2a** (16 μL, 0.12 mmol), durene (16 mg, 0.12 mmol) and pre-catalyst **C** (1.2 mg, 0.003 mmol) in anhydrous THF

(1.0 mL) was stirred under O_2 atmosphere (by an O_2-filled balloon). Then, NEt_3 was added (40 μL of a 0.15 M solution in THF, 0.006 mmol), and the reaction was stirred at room temperature for 24 h.

Entries 13−14. A stirred mixture of glycerol **1** (stated amount), 1-naphtaldehyde **2a** (16 μL, 0.12 mmol), **7** (5 mg, 0.024 mmol), **8** (3.4 mg, 0.006 mmol), durene (16 mg, 0.12 mmol) and pre-catalyst **C** (1.2 mg, 0.003 mmol) in anhydrous THF (1.0 mL) was stirred under an air atmosphere (by a compressed air-filled balloon). Then, NEt_3 was added (8.3 μL, 0.06 mmol), and the reaction was stirred at room temperature for 24 h.

Entry 15. A stirred mixture of glycerol **1** (11 mg, 0.12 mmol), 1-naphtaldehyde **2a** (16 μL, 0.12 mmol), **7** (5 mg, 0.024 mmol), **8** (3.4 mg, 0.006 mmol), durene (16 mg, 0.12 mmol) and pre-catalyst **C** (1.2 mg, 0.003 mmol) in anhydrous THF (1.0 mL) was stirred under an air atmosphere (by a compressed air-filled balloon). Then, NEt_3 was added (8.3 μL, 0.06 mmol), and the reaction was stirred at 50 °C for 24 h.

Synthesis of (*R*)-6-Azido-2-(perfluorophenyl)-6,7-dihydro-5H-pyrrolo[2,1-c][1,2,4]triazol-2-ium tetrafluoroborate (11)

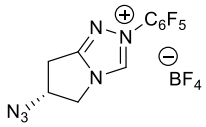

(*R*)-4-Azidopyrrolidin-2-one **9**[25] (0.50 g, 3.96 mmol) was dissolved in anhydrous CH_2Cl_2 (40 mL) loaded into a flame-dried 100 mL flask equipped with a magnetic stirrer. Next, the flask was evacuated and back-filled with Ar. Trimethyloxonium tetrafluoroborate (0.59 g, 3.96 mmol) was added to the solution in a single portion and the reaction mixture was then stirred under Ar atmosphere (by means of an Ar filled balloon) at room temperature for 16 h. Later, pentafluorophenyl hydrazine (0.78 g, 3.96 mmol) was added and the solution was then stirred for additional 5 h at room temperature, providing hydrazinium tetrafluoroborate **10** in 95% yield. The solvent was evaporated under reduced pressure and the crude mixture was transferred into a 20 mL microwave vial, where trimethyl orthoformate (10 mL) and methanol (2.5 mL) were added; the mixture was then heated under microwave irradiation at 120 °C for 3 h. After that time ^{1}H NMR analysis of the crude mixture displayed the complete conversion of the starting **10**, so the solvent was removed under reduced pressure. Purification of the product was performed by crystallization (MeOH/Et_2O) obtaining the triazolium salt **11** (0.77 g, 48%) as brown amorphous solid. $[\alpha]_D^{25}$ −3.6 (*c* 0.5 in acetone). **^{1}H NMR** (300 MHz, acetone-d_6) δ = 10.45 (s, 1H, CH-3), 5.63−5.45 (m, 1H, CH-6), 5.16 (dd, *J* 13.4, 6.4 Hz, 1H, CH_2-5), 4.81 (dd, *J* 13.4, 3.0 Hz, 1H, CH_2-5), 3.98 (dd, *J* 18.0, 7.2 Hz, 1H, CH_2-7), 3.54 (dd, *J* 18.0, 3.1 Hz, 1H,

CH_2-7); **^{13}C NMR** (101 MHz, acetone-d_6) δ = 161.8(*C*), 143.8 (*C*H), 141.9 (Ar*C*), 141.5 (Ar*C*), 138.9 (2C, Ar*C*), 136.4 (2C, Ar*C*), 62.1 (*C*HN_3), 54.0 (-N*C*H_2CHN_3-), 29.2 (-*C*H_2CHN_3-); **^{19}F NMR** (376 MHz, acetone-d_6) δ = −147.1 (m, 2F), −149.9 (m, 1F), −152.0 (s, 4F), −162.0 (m, 2F); **HRMS** (ESI/QTOF) calcd. for $C_{11}H_6F_5N_6$ ([M−BF_4]$^+$): 317.0569; found: 317.0603.

Synthesis of pre-catalyst D

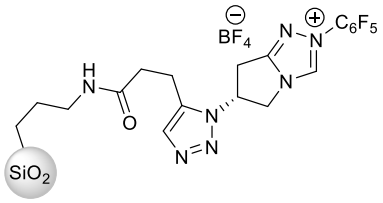

Triazolium salt **11** (0.30 g, 0.74 mmol) and silica **12**[27] (320 mg, 0.37 mmol, loading = 1.16 mmol g^{-1}, 230−400 mesh) were loaded into a 5 mL vial and suspended in dry DMF (3.0 mL). The stirred solution was degassed under vacuum and saturated with argon (by an Ar-filled balloon) three times and Cp*RuCl(COD) (14 mg, 0.037 mmol) was next added in one portion. The mixture was heated at 50 °C for 16 h and later cooled to room temperature. The crude was thus centrifuged with fresh portions of Et_2O (2 × 8 mL) and acetone (2 × 8 mL) and the resulting silica-supported triazolium salt **D** was finally dried (0.1 mbar, 40 °C, 6 h). **Elemental analysis** (%) found: N 5.9 (loading = 0.71 mmol g^{-1}). **FT-IR** (KBr): ν 3656, 2980, 1876, 1691, 1528, 1412, 1097 cm^{-1}.

Synthesis of pre-catalyst E

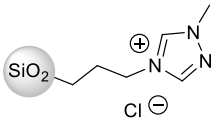

1-Methyl-1H-1,2,4-triazole **13** (0.18 mL, 2.40 mmol) and 3-chloropropyl silica gel **14**[28] (1.00 g, 0.80 mmol, loading Cl = 0.8 mmol g^{-1}, 230−400 mesh) were loaded into a 10 mL vial and dissolved in dry CH_3CN (4.0 mL) under argon atmosphere. The reaction mixture was next heated at 90 °C for 16 h and once cooled to room temperature it was centrifuged with fresh portions of CH_3CN (2 × 8 mL) and Et_2O (2 × 8 mL). The resulting silica-supported triazolium salt **E** was finally dried (0.1 mbar, 40 °C, 6 h). **Elemental analysis** (%) found: N 2.8 (loading = 0.66 mmol g^{-1}). **FT-IR** (KBr): ν 3654, 2962, 1992, 1873, 1659, 1523, 1446, 1100 cm^{-1}.

Synthesis of pre-catalyst F

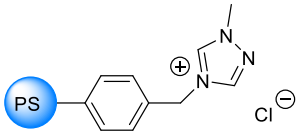

1-Methyl-1H-1,2,4-triazole **13** (0.46 mL, 6.10 mmol) and the Merrifield resin **15** (5.0 g, 17.5 mmol, loading Cl = 3.5 mmol g^{-1}, 200−400 mesh) were loaded into a 20 mL vial and dissolved in dry CH_3CN (10.0 mL) under argon atmosphere. The reaction mixture was next heated at 90 °C for 16 h and once cooled to room temperature it was centrifuged with fresh portions of CH_3CN (2 × 10 mL) and Et_2O (2 × 10 mL). The resulting silica-supported triazolium salt **F** was finally dried (0.1 mbar, 40 °C, 6 h). **Elemental analysis** (%) found: N 2.5 (loading = 0.59 mmol g^{-1}). **FT-IR** (KBr): ν 3646, 3002, 2915, 2817, 1908, 1874, 1671, 1512, 1587 cm^{-1}.

Screening of reaction conditions with supported triazolium pre-catalysts D−F (Table 2)

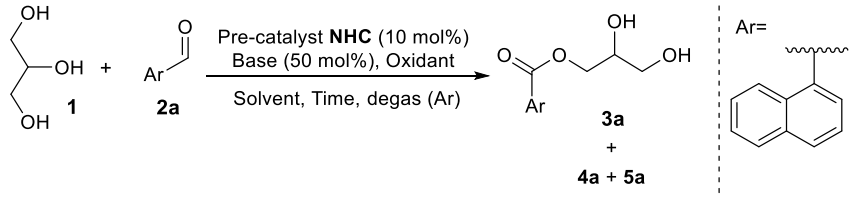

The following reaction conditions explain the operative optimization procedure. In all experiments, yield and selectivity were evaluated by ^1H NMR analysis of the reaction mixture (durene as internal standard).

Entries 1−2. A stirred mixture of glycerol **1** (33 mg, 0.36 mmol), 1-naphtaldehyde **2a** (16 μL, 0.12 mmol), **7** (5 mg, 0.024 mmol), **8** (3.4 mg, 0.006 mmol), durene (16 mg, 0.12 mmol), and pre-catalyst **D** (17 mg, 0.012 mmol, loading = 0.71 mmol g^{-1}) in anhydrous THF (1.0 mL) was stirred under an air atmosphere (by a compressed air-filled balloon). Then, the stated base was added (0.06 mmol), and the reaction was stirred at room temperature for 24 h.

Entries 3−4. A stirred mixture of glycerol **1** (33 mg, 0.36 mmol), 1-naphtaldehyde **2a** (16 μL, 0.12 mmol), **7** (5 mg, 0.024 mmol), **8** (3.4 mg, 0.006 mmol), durene (16 mg, 0.12 mmol), and pre-catalyst **D** (17 mg, 0.012 mmol, loading = 0.71 mmol g^{-1}) in the stated solvent (1.0 mL) was stirred under an air atmosphere (by a compressed air-filled balloon). Then, DBU was added (9 μL, 0.06 mmol), and the reaction was stirred at room temperature for 24 h.

Entry 5. A stirred mixture of glycerol **1** (33 mg, 0.36 mmol), 1-naphtaldehyde **2a** (16 μL, 0.12 mmol), **7** (5 mg, 0.024 mmol), **8** (3.4 mg, 0.006 mmol), durene (16 mg, 0.12 mmol), and pre-catalyst **E** (18 mg, 0.012 mmol, loading = 0.66 mmol g^{-1}) in anhydrous THF (1.0 mL) was stirred under an air atmosphere (by a compressed air-filled balloon). Then, DBU was added (9 μL, 0.06 mmol), and the reaction was stirred at room temperature for 24 h.

Entry 6. A stirred mixture of glycerol **1** (33 mg, 0.36 mmol), 1-naphtaldehyde **2a** (16 μL, 0.12 mmol), **7** (5 mg, 0.024 mmol), **8** (3.4 mg, 0.006 mmol), durene (16 mg, 0.12 mmol), and pre-catalyst **F** (20 mg, 0.012 mmol, loading = 0.59 mmol g^{-1}) in anhydrous THF (1.0 mL) was

stirred under an air atmosphere (by a compressed air-filled balloon). Then, DBU was added (9 µL, 0.06 mmol), and the reaction was stirred at room temperature for 24 h.

Entries 7-11. A stirred mixture of glycerol **1** (33 mg, 0.36 mmol), 1-naphtaldehyde **2a** (16 µL, 0.12 mmol), **7** (5 mg, 0.024 mmol), **8** (3.4 mg, 0.006 mmol), durene (16 mg, 0.12 mmol), and pre-catalyst **F** (20 mg, 0.012 mmol, loading = 0.59 mmol g^{-1}) in the stated solvent (1.0 mL) was stirred under an air atmosphere (by a compressed air-filled balloon). Then, DBU was added (9 µL, 0.06 mmol), and the reaction was stirred at room temperature for 24 h. For *entry 11*, the deep eutectic mixture (Choline Cl: Glycerol) was obtained from a vigorous stirred solution of glycerol (630 mg, 6.84 mmol) and Choline Cl (478 mg, 3.42 mmol) heated at 80 °C for 2 h under an argon atmosphere. After this period, the mixture was cooled to room temperature and used as the reaction solvent.

Entries 12−13. A stirred mixture of glycerol **1** (22 mg, 0.24 mmol), 1-naphtaldehyde **2a** (16 µL, 0.12 mmol), **7** (5 mg, 0.024 mmol), **8** (3.4 mg, 0.006 mmol), durene (16 mg, 0.12 mmol), and pre-catalyst **F** (20 mg, 0.012 mmol, loading = 0.59 mmol g^{-1}) in Me-THF (1.0 mL) was stirred under an air.

General procedure for the synthesis of monoacylglycerols 3a−i with pre-catalyst F

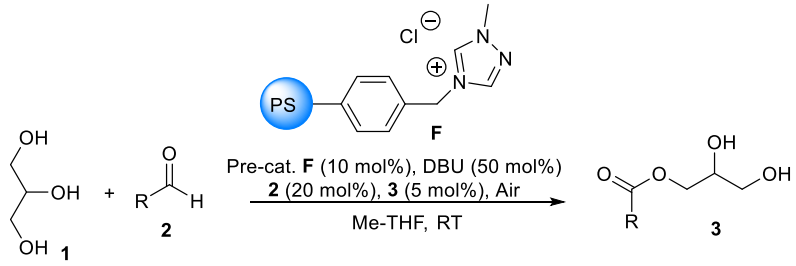

A stirred mixture of glycerol **1** (69 mg, 0.75 mmol), aldehyde **2a−i** (0.25 mmol), **8** (6.8 mg, 0.012 mmol), **7** (10.2 mg, 0.05 mmol), and pre-catalyst **F** (40 mg, 0.025 mmol, loading = 0.59 mmol g^{-1}) in Me-THF (2.0 mL) was stirred under an air atmosphere (by an air-filled balloon). Then, DBU was added (19.5 µL, 0.13 mmol), and the reaction was stirred at room temperature for 24 h. Filtration and washing (EtOAc) of the catalyst, concentration, and elution of the resulting crude mixture from a column of silica with the suitable elution system afforded the target product **3a−i**.

2,3-Dihydroxypropyl 1-naphthoate (3a)

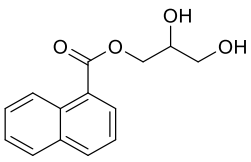

Column chromatography with 1:1 cyclohexane:EtOAc afforded **3a** (27 mg, 90%) as a colourless oil. **^{1}H NMR** (300 MHz, $CDCl_3$) δ = 8.88 (d, *J* 7.4 Hz, 1H, ArH), 8.19 (dd, *J* 7.4, 1.3

Hz, 1H, ArH), 8.03 (d, *J* 8.3 Hz, 1H, ArH), 7.88 (dd, *J* 8.3, 1.3 Hz, 1H, ArH), 7.64 − 7.58 (m, 1H, ArH), 7.57 − 7.42 (m, 2H, ArH), 4.58 − 4.42 (m, 2H, CH_2-1), 4.20 − 4.05 (m, 1H, CH-2), 3.77 (m, 2H, CH_2-3), 2.93 (d, *J* 5.0 Hz, 1H, OH-2), 2.47 (t, *J* 5.7 Hz, 1H, OH-3); **^{13}C NMR** (101 MHz, $CDCl_3$) δ = 167.8 (*C*O), 133.8 (2C, Ar*C*H), 131.3 (Ar*C*), 130.5 (Ar*C*H), 128.6 (Ar*C*H), 128.0 (Ar*C*H), 126.3 (2C, Ar*C*H), 125.6 (Ar*C*H), 124.4 (Ar*C*H), 70.4 (*C*H-2), 65.8 (*C*H_2-1), 63.5 (*C*H_2-3); **HRMS** (ESI/Q-TOF) calcd. for $C_{14}H_{15}O_4$ ([M + H]$^+$): 247.0965, found: 247.1003.

2-Hydroxypropane-1,3-diyl bis(1-naphthoate)(4a)

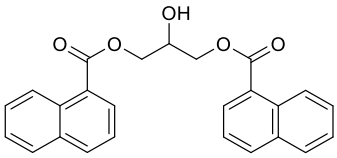

Column chromatography with 3:1 cyclohexane:EtOAc afforded **4a** (30 mg, 59%; Table 1, entry 12) as a colourless oil. **^{1}H NMR** (300 MHz, $CDCl_3$) δ = 8.92 (d, *J* 7.6 Hz, 2H, ArH), 8.23 (dd, *J* 7.6, 1.3 Hz, 2H, ArH), 8.04 (d, *J* 8.3 Hz, 2H, ArH), 7.88 (dd, *J* 8.3, 1.3 Hz, 2H, ArH), 7.61 (m, 3H, ArH), 7.55 − 7.34 (m, 3H, ArH), 4.77 − 4.55 (m, 4H, CH_2-1 and CH_2-3), 4.56 − 4.45 (m, 1H, CH-2), 2.79 (d, *J* 5.2 Hz, 1H, OH-2); **^{13}C NMR** (101 MHz, $CDCl_3$) δ = 167.5 (2C, *C*O), 133.8 (4C, Ar*C*H), 131.3 (2C, Ar*C*), 130.5 (2C, Ar*C*H), 128.6 (2C, Ar*C*H), 128.0 (2C, Ar*C*H), 126.3 (4C, Ar*C*H), 125.6 (2C, Ar*C*H), 124.5 (2C, Ar*C*H), 68.7 (*C*H-2), 66.0 (2C, *C*H_2-1 and *C*H_2-3); **HRMS** (ESI/Q-TOF) calcd. for $C_{25}H_{21}O_5$ ([M + H]$^+$): 401.1384; found: 401.1358.

2,3-Dihydroxypropyl 4-bromobenzoate (3b)

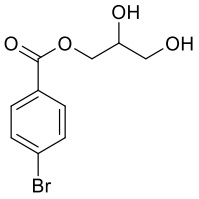

Column chromatography with 3:1 cyclohexane:EtOAc afforded **3b** (41 mg, 60%) as a pale-yellow oil. **^{1}H NMR** (300 MHz, $CDCl_3$) δ = 7.90 (d, *J* 8.9 Hz, 2H, ArH), 7.59 (d, *J* 8.9 Hz, 2H, ArH), 4.56 − 4.28 (m, 2H, CH_2-1), 4.07 (m, 1H, CH-2), 3.70 (m, 2H, CH_2-3), 2.65 (d, *J* 4.6 Hz, 1H, OH-2), 2.17 (t, *J* 5.7 Hz, 1H, OH-3); **^{13}C NMR** (101 MHz, $CDCl_3$) δ = 166.3 (*C*O), 131.9 (2C, Ar*C*H), 131.3 (2C, Ar*C*H), 128.6 (Ar*C*H), 128.5 (Ar*C*), 70.3 (*C*H-2), 66.0 (*C*H_2-1), 63.4 (*C*H_2-3); **HRMS** (ESI/Q-TOF) calcd. for $C_{10}H_{12}BrO_4$ ([M + H]$^+$): 274.9913; found: 274.9961.

2,3-Dihydroxypropyl cinnamate (3c)

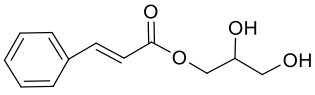

Column chromatography with gradient from 1:2 cyclohexane:EtOAc to 10:1 EtOAc:MeOH afforded **3c** (46 mg, 83%) as a colourless oil. **^{1}H NMR** (300 MHz, $CDCl_3$) δ = 7.74 (d, *J* 16.1 Hz, 1H, PhC*H*=CH), 7.58 − 7.49 (m, 2H, ArH), 7.46 − 7.31 (m, 3H, ArH), 6.49 (d, *J* 16.1 Hz, 1H, PhCH=C*H*), 4.40 − 4.25 (m, 2H, CH-1), 4.07 − 3.97 (m, 1H, CH-2), 3.80 − 3.62 (m, 2H, CH_2-3), 2.62 (bs, 1H, OH-2), 2.16 (bs, 1H, OH-3); **^{13}C NMR** (101 MHz, $CDCl_3$) δ = 167.4 (*C*O), 150.0 (Ph*C*H=CH), 134.1 (ArC), 130.6 (Ar*C*H), 128.9 (2C, Ar*C*H), 128.2 (2C, Ar*C*H), 117.1 (PhCH=*C*H), 70.3 (*C*H-2), 65.4 (CH_2-1), 63.3 (CH_2-3); **HRMS** (ESI/Q-TOF) calcd. for $C_{12}H_{15}O_4$ ([M + H]$^+$): 223.0965; found: 223.0916.

2,3-Dihydroxypropyl decanoate (3d)

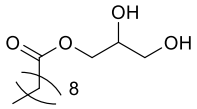

Column chromatography with gradient from 1:1 cyclohexane:EtOAc to EtOAc afforded **3d** (35 mg, 57%) as a colorless oil. **^{1}H NMR** (300 MHz, $CDCl_3$) δ = 4.27 − 4.08 (m, 2H, CH_2-1), 3.98 − 3.86 (m, 1H, CH-2), 3.76 − 3.51 (m, 2H, CH_2-3), 2.58 (bs, 1H, OH-2), 2.35 (t, *J* 7.5 Hz, 2H, $CH_{2(H\text{-}2dec)}$), 2.16 (bs, 1H, OH-3), 1.72 − 1.53 (m, 2H, $CH_{2(H\text{-}3dec)}$), 1.35 − 17 (m, 12H, $CH_{2(H\text{-}dec)}$), 0.87 (t, *J* 6.7 Hz, 3H, $CH_{3(H\text{-}10dec)}$); **^{13}C NMR** (101 MHz, $CDCl_3$) δ =174.5 (*C*O), 70.3 (*C*H-2), 65.3 (CH_2-1), 63.4 (CH_2-3), 34.2 ($CH_{2(H\text{-}dec)}$), 31.9 ($CH_{2(H\text{-}dec)}$), 29.5 ($CH_{2(H\text{-}dec)}$), 29.3 (2C, $CH_{2(H\text{-}dec)}$), 29.2 ($CH_{2(H\text{-}dec)}$), 25.0 ($CH_{2(H\text{-}dec)}$), 22.7 ($CH_{2(H\text{-}dec)}$), 14.2 ($CH_{3(H\text{-}10dec)}$); **HRMS** (ESI/Q-TOF) calcd. for $C_{13}H_{27}O_4$ ([M + H]$^+$): 247.1904; found: 247.1926.

2,3-Dihydroxypropyl palmitate (3e)

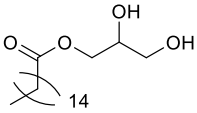

Column chromatography with gradient from 1:1 cyclohexane:EtOAc to EtOAc afforded **3e** (52 mg, 63%) as a colorless oil. **^{1}H NMR** (300 MHz, $CDCl_3$) δ = 4.25 − 4.10 (m, 2H, CH_2-1)), 4.00 − 3.89 (m, 1H, CH-2), 3.74 − 3.55 (m, 2H, CH_2-3), 2.56 (bs, 1H, OH-2), 2.35 (t, *J* 7.5 Hz, 2H, $CH_{2(H2\text{-}palm)}$), 2.13 (bs, 1H, OH-3), 1.69 − 1.55 (m, 2H, $CH_{2(H3\text{-}palm)}$), 1.38 − 1.17 (m, 24H, $CH_{2(H\text{-}palm)}$), 0.87 (t, *J* 6.6 Hz, 3H, $CH_{3(H16\text{-}palm)}$); **^{13}C NMR** (101 MHz, $CDCl_3$) δ = 174.5 (*C*O), 70.3 (*C*H-2), 65.2 (CH_2-1), 63.4 (CH_2-3), 34.2 ($CH_{2(H\text{-}palm)}$), 32.0 ($CH_{2(H\text{-}palm)}$), 29.8−29.5 (5C, $CH_{2(H\text{-}palm)}$), 29.7 ($CH_{2(H\text{-}palm)}$), 29.5 ($CH_{2(H\text{-}palm)}$), 29.4 ($CH_{2(H\text{-}palm)}$), 29.3 ($CH_{2(H\text{-}palm)}$), 29.2 ($CH_{2(H\text{-}palm)}$), 25.0 ($CH_{2(H\text{-}palm)}$), 22.8 ($CH_{2(H\text{-}palm)}$), 14.2 ($CH_{3(H16\text{-}palm)}$); **HRMS** (ESI/Q-TOF) calcd. for $C_{19}H_{39}O_4$ ([M + H]$^+$): 331.2843; found: 331.2802.

2,3-Dihydroxypropyl 3,7-dimethyloct-6-enoate (3f)

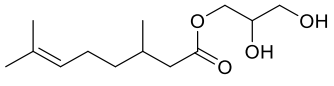

Column chromatography with 2:1 dichloromethane:EtOAc afforded **3f** (37 mg, 61%) as a colorless oil. **^{1}H NMR** (300 MHz, $CDCl_3$) δ = 5.08 (t, *J* 7.1Hz, 1H, C*H*=C$(CH_3)_2$), 4.26 − 4.09 (m, 2H, CH_2-1), 3.99 − 3.88 (m, 1H, CH-2), 3.76 − 3.53 (m, 2H, CH_2-3), 2.56 (bs, 1H, OH-2), 2.44 − 2.31 (m, 1H, $CH_{2(H2\text{-}oct)}$), 2.25 − 2.07 (m, 2H, $CH_{2(H2\text{-}oct)}$ and OH-3), 1.98 (m, 3H, $CH_{2(H5\text{-}oct)}$+$CH_{(H3\text{-}oct)}$), 1.68 (s, 3H, $CH_{3(H8\text{-}oct)}$), 1.60 (s, 3H, $CH_{3(H8\text{-}oct)}$), 1.44 − 1.13 (m, 2H, $CH_{2(H4\text{-}oct)}$), 0.97 (d, *J* 6.8, 3H, $CH_{3(H3\text{-}oct)}$); **^{13}C NMR** (101 MHz, $CDCl_3$) δ = 173.7 (*C*O), 131.5 (CH=*C*$(CH_3)_2$), 124.1 (*C*H=C$(CH_3)_2$, 70.3 (*C*H-2), 65.1 (*C*H_2-1), 63.3 (*C*H_2-3), 41.6 (*C*$H_{2(H2\text{-}oct)}$), 36.7 (*C*$H_{2(H4\text{-}oct)}$), 30.0 (*C*$H_{2(H5\text{-}oct)}$), 25.7 (*C*$H_{(H3\text{-}oct)}$), 25.3 (*C*$H_{3(H8\text{-}oct)}$), 19.6 (*C*$H_{2(H8\text{-}oct)}$), 17.6 (*C*$H_{3(H3\text{-}oct)}$); **HRMS** (ESI/Q-TOF) calcd. for $C_{13}H_{25}O_4$ ([M + H]$^+$) 245.1747; found: 245.1711.

2,3-Dihydroxypropyl 4-hydroxy-3-methoxybenzoate (3g)

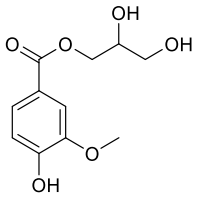

Column chromatography with gradient from 1:2 cyclohexane:EtOAc to 20:1 EtOAc:MeOH afforded **3g** (38 mg, 63%) as a colourless oil. **^{1}H NMR** (300 MHz, $CDCl_3$) δ = 7.65 (dd, *J* 8.3, 1.9 Hz, 1H, ArH), 7.54 (d, *J* 1.9 Hz, 1H, ArH), 6.95 (d, *J* 8.3 Hz, 1H, ArH), 6.10 (bs, 1H, OHAr), 4.53 − 4.31 (m, 2H, CH_2-1), 4.13 − 4.01 (m, 1H, CH-2), 3.95 (s, 3H, OCH_3), 3.78 − 3.59 (m, 2H, CH_2-3), 2.62 (bs, 1H, OH2), 2.22 (bs, 1H, OH-3); **^{13}C NMR** (101 MHz, $CDCl_3$) δ = 166.9 (*C*O), 150.4 (Ar*C*), 146.2 (Ar*C*), 124.4 (Ar*C*H), 121.5 (Ar*C*), 114.1 (Ar*C*H), 111.8 (Ar*C*H), 70.4 (*C*H-2), 65.6 (*C*H_2-1), 63.3 (*C*H_2-3), 56.1 (O*C*H_3); **HRMS** (ESI/Q-TOF) calcd. for $C_{11}H_{15}O_6$ ([M + H]$^+$): 243.0863; found: 243.0891.

2,3-Dihydroxypropyl furan-2-carboxylate (3h)

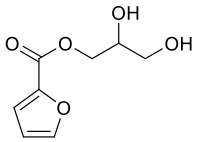

Column chromatography with 1:5 cyclohexane:EtOAc afforded **3h** (42 mg, 91%) as a pale-yellow oil. **^{1}H NMR** (300 MHz, $CDCl_3$) δ = 7.60 (dd, *J* 1.7, 0.7 Hz, 1H, ArH), 7.23 (dd, *J* 3.5, 0.7 Hz, 1H, ArH), 6.53 (dd, *J* 3.5, 1.7 Hz, 1H, ArH), 4.48 − 4.32 (m, 2H, CH_2-1), 4.11 − 3.99 (m, 1H, CH-2), 3.83 − 3.63 (m, 2H, CH_2-3), 2.74 (d, *J* 3.5 Hz, 1H, OH-2), 2.25 (bs, 1H, OH-3); **^{13}C NMR** (101 MHz, $CDCl_3$) δ = 159.0 (*C*O), 146.8 (Ar*C*H), 144.1 (Ar*C*), 118.9 (Ar*C*H), 112.1 (Ar*C*H), 70.2 (*C*H-2), 65.8 (*C*H_2-1), 63.3 (*C*H_2-3); **HRMS** (ESI/Q-TOF) calcd. for $C_8H_{11}O_5$ ([M + H]$^+$): 187.0601; found: 187.0615.

(5-((2,3-Dihydroxypropoxy)carbonyl)furan-2-yl)methyl 5-(hydroxymethyl)furan-2-carboxylate (3i)

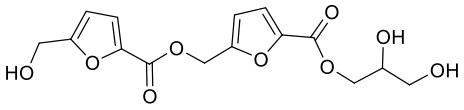

Column chromatography with gradient from EtOAc to 20:1 EtOAc:MeOH afforded **3i** (81 mg, 95%) as a pale yellow oil. **^{1}H NMR** (300 MHz, $CDCl_3$) δ = 7.23 − 7.08 (m, 2H, ArH), 6.67 − 6.52 (m, 1H, ArH), 6.52 − 6.38 (m, 1H, ArH), 5.31 (m, 2H, CH_2(OCO)), 4.68 (m, 2H, CH_2OH), 4.57 − 4.31 (m, 2H, CH_2-1), 4.14 − 3.99 (m, 1H, CH-2), 3.80 − 3.60 (m, 2H, CH_2-3), 2.62 (bs, 1H, OH-2), 2.17 (bs, 2H, OH-3 and OH_{furan}); **^{13}C NMR** (101 MHz, $CDCl_3$) δ = 158.8 (*C*O), 158.6 (*C*O), 158.0 (Ar*C*), 153.4 (Ar*C*), 144.3 (Ar*C*), 143.3 (Ar*C*), 119.8 (Ar*C*H), 119.4 (Ar*C*H), 112.9 (Ar*C*H), 109.6 (Ar*C*H), 70.1 (*C*H-2), 65.9 (*C*H_2-1), 63.3 (*C*H_2-3), 57.9 (*C*H_2(OCO)), 57.5 (*C*H_2OH); **HRMS** (ESI/Q-TOF) calcd. for $C_{15}H_{17}O_9$ ([M + H]$^+$): 341.0867; found: 341.0814.

General procedure for the synthesis of solketal derivatives 17a−i with pre-catalyst F

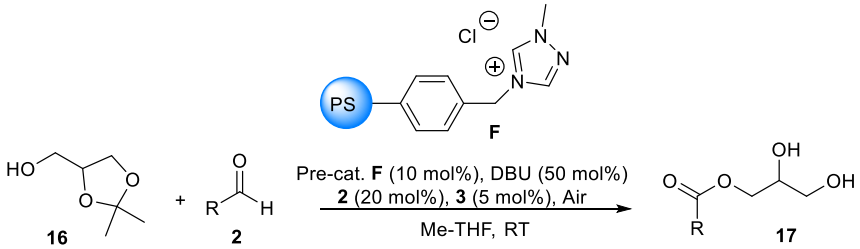

A stirred mixture of solketal **16** (34 mg, 0.38 mmol), aldehyde **2a−i** (0.25 mmol), **8** (6.8 mg, 0.012 mmol) ,**7** (10.2 mg, 0.05 mmol), and pre-catalyst **F** (40 mg, 0.025 mmol, loading = 0.59 mmol g^{-1}) in Me-THF (2.0 mL) was stirred under an air atmosphere (by an air-filled balloon). Then, DBU was added (19.5 µL, 0.13 mmol), and the reaction was stirred at room temperature for 24 h. Filtration and washing (EtOAc) of the catalyst, concentration, and elution of the resulting crude mixture from a column of silica with the suitable elution system afforded the target product **17a−i**.

(2,2-Dimethyl-1,3-dioxolan-4-yl)methyl 1-naphthoate (17a)

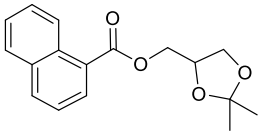

Column chromatography with 10:1 cyclohexane:EtOAc afforded **17a** (66 mg, 92%) as a colorless oil. **^{1}H NMR** (300 MHz, $CDCl_3$) δ = 8.92 (d, *J* 7.4 Hz, 1H, ArH), 8.23 (dd, *J* 7.4, 1.3 Hz, 1H, ArH), 8.04 (d, *J* 8.3 Hz, 1H, ArH), 7.89 (dd, *J* 8.3, 1.3 Hz, 1H, ArH), 7.66 − 7.58 (m, 1H, ArH), 7.58 − 7.46 (m, 2H, ArH), 4.58 − 4.40 (m, 3H, CH-4 and CH_2(OCO)), 4.19 (dd, *J* 8.5, 6.1 Hz, 1H, CH_2-5), 3.93 (dd, *J* 8.5, 5.6 Hz, 1H, CH_2-5), 1.48 (s, 3H, CH_3-3), 1.41 (s, 3H, CH_3-3); **^{13}C NMR** (101 MHz, $CDCl_3$) δ = 167.5 (*C*O), 134.2 (Ar*C*H), 134.0 (Ar*C*H), 131.7

(Ar*C*), 130.8 (Ar*C*H), 128.9 (Ar*C*H), 128.2 (Ar*C*H), 127.0 (Ar*C*H), 126.6 (Ar*C*H), 126.1 (Ar*C*H), 124.8 (Ar*C*H), 110.2 (*C*-2), 74.1 (*C*H-4), 66.8 (*C*H_2(OCO)), 65.4 (*C*H_2-5), 27.1 (*C*H_3-2), 25.7 (*C*H_3-2); **HRMS** (ESI/QTOF) calcd. for $C_{17}H_{18}NaO_4$ ([M + Na]$^+$): 309.1097; found: 309.1126.

(2,2-Dimethyl-1,3-dioxolan-4-yl)methyl 4-bromobenzoate (17b)

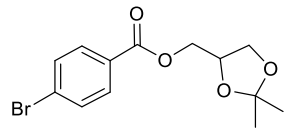

Column chromatography with 8:1 cyclohexane:EtOAc afforded **17b** (56 mg, 71%) as a pale-yellow oil. **^{1}H NMR** (300 MHz, $CDCl_3$) δ = 7.91 (d, *J* 8.9 Hz, 2H, ArH), 7.58 (d, *J* 8.9 Hz, 2H, ArH), 4.50 − 4.41 (m, 1H, CH-4), 4.41 − 4.28 (m, 2H, CH_2(OCO)), 4.14 (dd, *J* 8.5, 6.1 Hz, 1H, CH_2-5), 3.86 (dd, *J* 8.5, 5.6 Hz, 1H, CH_2-5), 1.45 (s, 3H, CH_3-2), 1.38 (s, 3H, CH_3-2); **^{13}C NMR** (101 MHz, $CDCl_3$) δ = 165.6 (*C*O), 131.8 (2C, Ar*C*H), 131.2 (2C, Ar*C*H), 128.6 (Ar*C*), 128.3 (Ar*C*), 109.9 (*C*-2), 73.6 (*C*H-4), 66.3 (*C*H_2(OCO)), 65.3 (*C*H_2-5), 26.7 (*C*H_3-2), 25.3 (*C*H_3-2); **HRMS** (ESI/Q-TOF) calcd. for $C_{13}H_{15}BrNaO_4$ ([M + Na]$^+$): 337.0046; found: 337.0011.

(2,2-Dimethyl-1,3-dioxolan-4-yl)methyl cinnamate (17c)

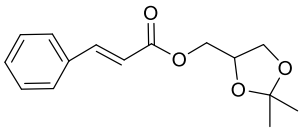

Column chromatography with 6:1 cyclohexane:EtOAc afforded **17c** (36 mg, 55%) as a pale-yellow oil. **^{1}H NMR** (300 MHz, $CDCl_3$) δ = 7.73 (d, *J* 16.1 Hz, 1H, CH-3), 7.57 − 7.47 (m, 2H, ArH), 7.44 − 7.35 (m, 3H, ArH), 6.48 (d, *J* 16.1 Hz, 1H, CH-2), 4.46 − 4.36 (m, 1H, CH-4), 4.36 − 4.17 (m, 2H, CH_2(OCO)), 4.13 (dd, *J* 8.5, 6.1 Hz, 1H, CH_2-5), 3.81 (dd, *J* 8.5, 5.6 Hz, 1H, CH_2-5), 1.47 (s, 3H, CH_3-2), 1.39 (s, 3H, CH_3-2); **^{13}C NMR** (101 MHz, $CDCl_3$) δ = 166.7 (*C*O), 145.5 (Ph*C*H=CH), 134.2 (Ar*C*), 130.4 (Ar*C*H), 128.9 (2C, Ar*C*H), 128.1 (2C, Ar*C*H), 117.4 (PhCH=*C*H), 109.9 (*C*-2), 73.7 (*C*H-4), 66.4 (*C*H_2(OCO)), 64.9 (*C*H_2-5), 26.7 (*C*H_3-2), 25.4 (*C*H_3-2); **HRMS** (ESI/Q-TOF) calcd. for $C_{15}H_{18}NaO_4$ ([M + Na]$^+$): 285.1097; found: 285.1146.

(2,2-Dimethyl-1,3-dioxolan-4-yl)methyl decanoate (17d)

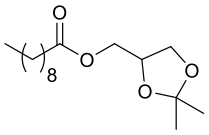

Column chromatography with 9:1 cyclohexane:EtOAc afforded **17d** (49 mg, 68%) as a colourless oil. **^{1}H NMR** (300 MHz, $CDCl_3$) δ = 4.36−4.26 (m, 1H, CH-4), 4.20 − 4.10 (m, 2H, CH_2(OCO)), 4.07 (dd, *J* 8.5, 6.1 Hz, 1H, CH_2-5), 3.73 (dd, *J* 8.5, 5.6 Hz, 1H, CH_2-5), 2.34 (t, *J*

7.6 Hz, 2H, CH_2-2), 1.67 − 1.58 (m, 2H, CH_2-3), 1.43 (s, 3H, CH_3-2), 1.37 (s, 3H, CH_3-2), 1.34 − 1.19 (m, 12H, $CH_{2(H\text{-}dec)}$), 0.87 (t, *J* 6.7 Hz, 3H, $CH_{3(H\text{-}10dec)}$); **^{13}C NMR** (101 MHz, $CDCl_3$) δ = 173.7 (*C*O), 109.8 (*C*-2), 73.6 (*C*H-4), 66.3 (CH_2(OCO)), 64.5 (CH_2-5), 34.1 ($CH_{2(H\text{-}dec)}$), 31.8 ($CH_{2(H\text{-}dec)}$), 29.4 ($CH_{2(H\text{-}dec)}$), 29.2 (2C, $CH_{2(H\text{-}dec)}$), 29.1 ($CH_{2(H\text{-}dec)}$), 26.7 (CH_3-2), 25.4 (CH_3-2), 24.9 ($CH_{2(H\text{-}dec)}$), 22.7 ($CH_{2(H\text{-}dec)}$), 14.1 ($CH_{3(H10\text{-}dec)}$); **HRMS** (ESI/Q-TOF) calcd. for $C_{16}H_{30}NaO_4$ ([M + Na]$^+$): 309.2036; found: 309.2076.

(2,2-Dimethyl-1,3-dioxolan-4-yl)methyl palmitate (17e)

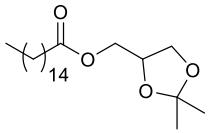

Column chromatography with 10:1 cyclohexane:EtOAc afforded **17e** (48 mg, 52%) as a colourless oil. **^{1}H NMR** (300 MHz, $CDCl_3$) δ = 4.37 − 4.26 (m, 1H, CH-4), 4.20 − 4.10 (m, 2H, CH_2(OCO)), 4.08 (dd, *J* 8.5, 6.1 Hz, 1H, CH_2-5), 3.74 (dd, *J* 8.5, 5.6 Hz, 1H, CH_2-5), 2.34 (t, *J* 7.6 Hz, 2H, CH_2-2), 1.68 − 1.58 (m, 2H, $CH_{2(H3\text{-}palm)}$), 1.43 (s, 3H, CH_3-2), 1.37 (s, 3H, CH_3-2), 1.34 − 1.18 (m, 24H, $CH_{2(H\text{-}palm)}$), 0.87 (t, *J* 6.7 Hz, 3H, $CH_{3(H16\text{-}palm)}$); **^{13}C NMR** (101 MHz, $CDCl_3$) δ = 173.7 (*C*O), 109.9 (*C*-2), 73.7 (*C*H-4), 66.4 (CH_2(OCO)), 64.6 (CH_2-5), 34.2 ($CH_{2(H\text{-}dec)}$), 32.0 ($CH_{2(H\text{-}dec)}$), 31.0 ($CH_{2(H\text{-}dec)}$), 29.7 − 29.5 (5C, $CH_{2(H\text{-}dec)}$), 29.5 ($CH_{2(H\text{-}dec)}$), 29.4 ($CH_{2(H\text{-}dec)}$), 29.3 ($CH_{2(H\text{-}dec)}$), 29.2 ($CH_{2(H\text{-}dec)}$), 26.8 (CH_3-2), 25.5 (CH_3-2), 25.0 ($CH_{2(H\text{-}dec)}$), 22.8 ($CH_{2(H\text{-}palm)}$), 14.2 ($CH_{3(H16\text{-}palm)}$); **HRMS** (ESI/Q-TOF) calcd. for $C_{22}H_{42}NaO_4$ ([M + Na]$^+$): 393.2975, found: 393.2949.

(2,2-Dimethyl-1,3-dioxolan-4-yl)methyl 3,7-dimethyloct-6-enoate (17f)

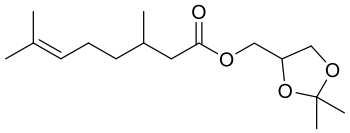

Column chromatography with 10:1 cyclohexane:EtOAc afforded **17f** (65 mg, 91%) as a colourless oil. **^{1}H NMR** (300 MHz, $CDCl_3$) δ = 5.08 (t, *J* 7.7, 6.2 Hz, 1H, C*H*=C$(CH_3)_2$), 4.38 − 4.25 (m, 1H, CH-4), 4.22 − 4.10 (m, 2H, CH_2(OCO)), 4.07 (dd, *J* 8.5, 6.1 Hz, 1H, CH_2-5), 3.73 (dd, *J* 8.5, 5.6 Hz, 1H, CH_2-5), 2.36 (dd, *J* 15.3, 5.9 Hz, 1H, $CH_{2(H2\text{-}oct)}$), 2.16 (dd, *J* 15.3, 7.9 Hz, 1H, $CH_{2(H2\text{-}oct)}$), 2.08 − 1.88 (m, 3H, $CH_{2(H5\text{-}oct)}$ and $CH_{(H3\text{-}oct)}$), 1.67 (s, 3H, $CH_{3(H8\text{-}oct)}$), 1.59 (s, 3H, $CH_{3(H8\text{-}oct)}$), 1.42 (s, 3H, CH_3-2), 1.37 (s, 3H, CH_3-2), 1.31 − 1.14 (m, 2H, $CH_{2(H4\text{-}oct)}$), 0.94 (d, *J* 6.8 Hz, 3H, $CH_{3(H3\text{-}oct)}$); **^{13}C NMR** (101 MHz, $CDCl_3$) δ = 173.0 (*C*O), 131.6 (CH=*C*$(CH_3)_2$), 124.2 (*C*H=C$(CH_3)_2$), 109.8 (*C*-2), 73.6 (*C*H-4), 66.4 (CH_2(OCO)), 64.4 (CH_2-5), 41.5 ($CH_{2(H2\text{-}oct)}$), 36.7 ($CH_{2(H4\text{-}oct)}$), 29.9 ($CH_{2(H5\text{-}oct)}$), 26.9 (CH_3-2), 26.7 ($CH_{(H3\text{-}oct)}$), 25.7 (CH_3-2), 25.4 ($CH_{3(H8\text{-}oct)}$), 19.6 ($CH_{3(H8\text{-}oct)}$), 17.6 ($CH_{3(H3\text{-}oct)}$); **HRMS** (ESI/Q-TOF) calcd. for $C_{16}H_{28}NaO_4$ ([M + Na]$^+$): 307.1880; found: 307.1845.

(2,2-Dimethyl-1,3-dioxolan-4-yl)methyl 4-hydroxy-3-methoxybenzoate (17g)

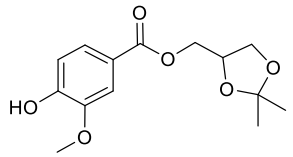

Column chromatography with 2:1 diethyl ether:cyclohexane afforded **17g** (56 mg, 80%) as a colourless oil. **^{1}H NMR** (300 MHz, $CDCl_3$) δ = 7.66 (dd, *J* 8.3, 1.9 Hz, 1H, Ar), 7.56 (d, *J* = 1.9 Hz, 1H, Ar), 6.94 (d, *J* 8.3 Hz, 1H, Ar), 6.05 (bs, 1H, OHAr), 4.50 − 4.39 (m, 1H CH(4)), 4.38 − 4.32 (m, 2H, CH_2(OCO)), 4.14 (dd, *J* 8.5, 6.1 Hz, 1H, CH_2(5)), 3.94 (s, 3H, OCH_3), 3.87 (dd, *J* 8.5, 5.6 Hz, 1H, CH_2(5)), 1.46 (s, 3H, CH_3(2)), 1.39 (s, 3H, CH_3(2)); **^{13}C NMR** (101 MHz, $CDCl_3$) δ = 166.2 (*C*O), 150.2 (Ar*C*), 146.1 (Ar*C*), 124.4 (Ar*C*H), 121.81 (Ar*C*), 114.1 (Ar*C*H), 111.8 (Ar*C*H), 109.8 (*C*-2), 73.7 (*C*H-4), 66.4 (*C*H_2(OCO)), 64.9 (*C*H_2-5), 56.1 (O*C*H_3), 26.7 (*C*H_3-2), 25.4 (*C*H_3-2); **HRMS** (ESI/Q-TOF) calcd. for $C_{14}H_{18}NaO_6$ ($[M + Na]^+$): 305.0996; found: 305.1014.

(2,2-Dimethyl-1,3-dioxolan-4-yl)methyl furan-2-carboxylate (17h)

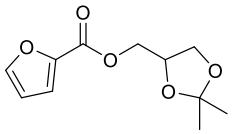

Column chromatography with dichloromethane afforded **17h** (50 mg, 89%) as a pale-yellow oil. **^{1}H NMR** (300 MHz, $CDCl_3$) δ = 7.59 (dd, *J* 1.7, 0.7 Hz, 1H, ArH), 7.22 (dd, *J* 3.5, 0.7 Hz, 1H, ArH), 6.51 (dd, *J* 3.5, 1.7 Hz, 1H, ArH), 4.48 − 4.38 (m, 1H, CH-4), 4.38 − 4.30 (m, 2H, CH_2(OCO)), 4.13 (dd, *J* 8.5, 6.1 Hz, 1H, CH_2-5), 3.84 (dd, *J* 8.5, 5.6 Hz, 1H, CH_2-5), 1.45 (s, 3H, CH_3-2), 1.38 (s, 3H, CH_3-2); **^{13}C NMR** (101 MHz, $CDCl_3$) δ = 158.4 (*C*O), 146.6 (Ar*C*H), 144.2 (Ar*C*), 118.4 (Ar*C*H), 111.9 (Ar*C*H), 109.9 (*C*-2), 73.5 (*C*H-4), 66.3 (*C*H_2(OCO)), 64.9 (*C*H_2-5), 26.7 (*C*H_3-2), 25.4 (*C*H_3-2); **HRMS** (ESI/QTOF) calcd. for $C_{11}H_{14}NaO_5$ ($[M + Na]^+$): 249.0733; found: 249.0760.

(2,2-Dimethyl-1,3-dioxolan-4-yl)methyl 5-(hydroxymethyl)furan-2-carboxylate (17i)

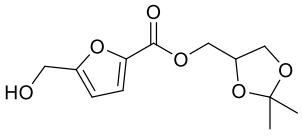

Column chromatography with 4:1 dichloromethane:EtOAc afforded **17i** (51 mg, 79%) as a pale-yellow oil. **^{1}H NMR** (300 MHz, $CDCl_3$) δ = 7.17 (d, *J* 3.5 Hz, 1H, ArH), 6.42 (d, *J* 3.5 Hz, 1H, ArH), 4.68 (d, *J* 6.4 Hz, 2H, CH_2OH), 4.47 − 4.37 (m, 1H CH-4), 4.37 − 4.31 (m, 2H, CH_2(OCO)), 4.13 (dd, *J* 8.5, 6.1 Hz, 1H, CH_2-5), 3.84 (dd, *J* 8.5, 5.6 Hz, 1H, CH_2-5), 1.99 (t, *J* 6.4 Hz, 1H, OH), 1.45 (s, 3H, CH_3-2), 1.38 (s, 3H, CH_3-2); **^{13}C NMR** (101 MHz, $CDCl_3$) δ = 158.9 (*C*O), 158.7 (Ar*C*), 144.1 (Ar*C*), 119.6 (Ar*C*H), 110.3 (Ar*C*H), 109.8 (*C*-2), 73.9 (*C*H-

4), 66.7 (CH_2(OCO)), 65.3 (CH_2-5), 58.0 (CH_2OH), 27.0 (CH_3-2), 25.7 (CH_3-2); **HRMS** (ESI/Q-TOF) calcd. for $C_{12}H_{16}NaO_6$ ([M + Na]$^+$): 279.0839; found: 279.0800.

Fabrication of Microreactor R1

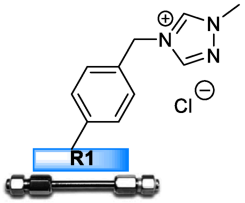

A slurry of the immobilized pre-catalyst **F** was prepared by suspending excess in weight of **F** in Me-THF. Slurry-packing was performed under constant pressure (300 bars, 30 min, Me-THF as solvent) by using an air driven liquid pump (by Haskel). The microreactor **R1** was fabricated by using a 10 × 0.46 cm stainless-steel column, which was filled with the swelled resin **F**. Microreactor void volume (V_0) was determined by pycnometry.[36] This method consists in filling the microreactor successively with two different solvents (solvent 1: water; solvent 2: *n*-hexane) and weighing the filled microreactors accurately. Mathematically $V_0 = (w_1-w_2)/(\delta_1-\delta_2)$, where w_1 and w_2 are the weights of the microreactor filled with solvents 1 and 2 and δ_1 and δ_2 the densities of the solvents.

Experimental set-up for the flow synthesis of esters 3f–i and 17f–i

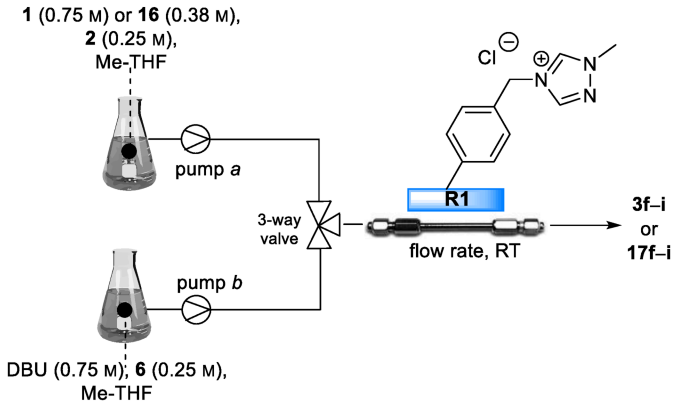

The continuous flow apparatus setup was composed by two binary pumps (Agilent 1100 and Agilent 1100 micro series). Channel-A was used to deliver a continuously degassed solution of **1** (0.50 M) or **16** (0.38 M) and aldehydes **2f–i** (0.25 M) in Me-THF. Channel-B delivered a continuously degassed solution of DBU (0.12 M) and **6** (0.25 M) in Me-THF. The feed solutions were pumped at the stated flow rate through the 3-way valve. Microreactor **R1** was initially activated by pumping (channel B, 50 μLmin^{-1}, 20 min) a degassed solution of DBU (0.75 M). The microreactor was operated for 6 h under steady state conditions and then the solution was collected and concentrated to afford a crude. Elution from a column of silica gel with the suitable elution system allow to recover first the alcohol **6'** and then the product **3f–i** or **17f–i**.

The quantitative oxidation of **6'** to the Kharasch oxidant **6** was performed with air (1 atm, balloon) and catalytic phthalocyanine **8** (10 mol%, THF, RT).

Long-term stability study

The long-term stability experiment was performed with the same flow setup above described, using aldehyde **2a** (0.25 M) and the microreactor **R1** which was operated at 25 °C with a flow rate of 35 μLmin^{-1} for ca. 200 h. After the achievement of the steady-state regime (ca. 1 h), >95% conversion of **2a** was maintained for 120 h, while a progressive loss of catalytic activity was observed after that time (TON = 71).

3.5 References and notes

1. H. Zang, K. Wang, M. Zhang, R. Xie, L. Wang, E. Y.-X. Chen, *Catal. Sci. Technol.*, **2018**, *8*, 1777–1798.
2. P. J. Deuss, K. Barta, J. G. de Vries, *Catal. Sci. Technol.*, **2014**, *4*, 1174–1196.
3. Q. Ren, M. Li, L. Yuan, J. Wang, *Org. Biomol. Chem.*, **2017**, 15, 4731–4749.
4. D. M. Flanigan, F. Romanov-Michailidis, N. A. White, T. Rovis, *Chem. Rev.*, **2015**, *115*, 9307–9387.
5. N. K. Gupta, A. Fukuoka, K. Nakajima, *ACS Sustainable Chem. Eng.*, **2018**, *6*, 3434–3442 and references therein.
6. S. Bagheri, N. M. Julkapli, W. A. Yehye, *Renewable Sustainable Energy Rev.*, **2015**, *41*, 113−127.
7. A. Axelsson, A. Antoine-Michard, H. Sunden, *Green Chem.*, **2017**, *19*, 2477−2481 and reference therein.
8 J. A. Stewart, R. Drexel, B. Arstad, E. Reubsaet, B. M. Weckhuysena, P. C. A. Bruijnincx, *Green Chem.*, **2016**, *18*, 1605–1618.
9. a) I. Atodiresei, C. Vila, M. Rueping, *ACS Catal.*, **2015**, *5*, 1972−1985; b) F. G. Finelli, L. S. M. Miranda, R. O. M. A. de Souza, *Chem. Commun.*, **2015**, *51*, 3708−3722.
10. C. Rodriguez-Escrich, M. A. Pericas, *Eur. J. Org. Chem.*, **2015**, 1173−1188.
11. M. B. Plutschack, B. Pieber, K. Gilmore, P. H. Seeberger, *Chem. Rev.*, **2017**, *117*, 11796−11893.
12. I. R. Baxendale, L. Brocken, C. J. Mallia, *Green Process. Synth.*, **2013**, *2*, 211–230.
13. P. U. Okoye, B. H. Hameed, *Renewable Sustainable Energy Rev.*, **2016**, *53*, 558−574.
14 C.-H. Zhou, J. N. Beltramini, Y.-X Fana, G. Q. Lu, *Chem. Soc. Rev.*, **2008**, *37,* 527−549.
15. F. Jerome, Y. Pouilloux, J. Barrault, *ChemSusChem*, **2008**, *1*, 586−613.
16. S. De Sarkar, A. Biswas, R. C. Samanta, A. Studer, *Chem. Eur. J.*, **2013**, *19*, 4664−4678.
17. O. Bortolini, C. Chiappe, M. Fogagnolo, P. P. Giovannini, A.; Massi, C. S. Pomelli, D. Ragno, *Chem. Commun.*, **2014**, *50*, 2008−2011.
18. O. Bortolini, C. Chiappe, M. Fogagnolo, A. Massi, C. S. Pomelli, *J. Org. Chem.*, **2017**, *82*, 302−312.
19. A. Axelsson, E. Hammarvid, L. Ta, H. Sunden, *Chem. Commun.*, **2016**, *52*, 11571−11574.
20. J. Piera, J.-E. Backvall, *Angew. Chem. Int. Ed.*, **2008**, *47*, 3506−3523.
21. O. Bortolini, L. Caciolli, A. Cavazzini, V. Costa, R. Greco, A. Massi, L. Pasti, *Green Chem.*, **2012**, *14*, 992−1000.
22 M. Meldal, C. W. Tornoe, *Chem. Rev.*, **2008**, *108*, 2952−3015.
23 E. Haldon, M. C. Nicasio, P. J. Perez, *Org. Biomol. Chem.*, **2015**, *13*, 9528−9550.
24. K. E. Ozboya, T. Rovis, *Synlett*, **2014**, *25*, 2665−2668.
25. K. E. Murphy-Benenato, P. R. Bhagunde, A. Chen, H. E. Davis,T. F. Durand-Reville, D. E. Ehmann, V. Gallulo, J. J. Harris, H. Hatoum-Mokdad, H. Jahic, A. Kim, M. R. Manjunatha, E. L. Manyak, J. Mueller, S. Patey, O. Quiroga, M. Rooney, L. Sha, A. B. Shapiro, M. Sylvester, B. Tan, A. S. Tasi, M. Uria-Nickelsen, Y. Wu, M. Zambrowski, S. X. Zhao, *J. Med. Chem.*, **2015**, *58*, 2195−2205.
26. J. R. Johansson, T. Beke-Somfai, A. S. Stalsmeden, N. Kann, *Chem. Rev.*, **2016**, *116*, 14726−14768.
27. L. Huang, S. Dolai, R. Krishnaswami, M. Kruk, *Langmuir*, **2010**, *26(4)*, 2688−2693.
28. a) E. G. Delany, C.-L. Fagan, S. Gundala, A. Mari, T. Broja, K. Zeitler S. J. Connon *Chem. Commun.,* 2013, **49**, 6510−6512; b) P. Li, L. Wang, Y. Zhang, G. Wang, *Tetrahedron*, **2008**, *64*, 7633−7638.
29. V. Pace, P. Hoyos, L. Castoldi, P. Dominguez de Maria, A. R. Alcantara, C*hemSusChem*, **2012**, *5*, 1369−1379.
30. C. Zeng, S. Qi, R. Xin, B. Yang, Y. Wang, *Bioprocess Biosyst Eng.*, **2015**, *38*, 2053−2061.

31. O. Bortolini, A. Cavazzini, P. Dambruoso, P. P. Giovannini, L. Caciolli, A. Massi, S. Pacifico, D. Ragno, *Green Chem.*, **2013**, *15*, 2981–2992.
32. T. S. A. Heugebaert, C. V. Stevens, C. O. Kappe, *ChemSusChem*, **2015**, *8*, 1648–1651 and references therein.
33. D. Ragno, G. Di Carmine, A. Brandolese, O. Bortolini, P. P. Giovannini, A. Massi, *ACS Catal.*, **2017**, *7*, 6365−6375 and references therein.
34. R. Rathore, E. Bosch, J. K. Kochi, *Tetrahedron Lett.*, **1994**, *35*, 1335-1338.
35. D. Enders, K. Breuer, U. Kallfass, T. Balensiefer, *Synthesis*, **2003**, 1292−1295.
36. R. M. McCormick and B. L. Karger, *Anal. Chem.*, **1980**, *52*, 2249−2257.

4. Aerobic oxidation of 5-hydroxymethylfurfural to 5-hydroxymethyl-2-furancarboxylic acid and derivatives by heterogeneous NHC-catalysis

The work described in this chapter has formed the basis of the following peer reviewed publication: A. Brandolese, D. Ragno, G. Di Carmine, T. Bernardi, O. Bortolini, P. P. Giovannini, O. G. Pandoli, A. Altomare, A. Massi, *Org. Biomol. Chem.*, **2018**, *16*, 8955−8964.

4.1 Introduction

The limited availability of fossil fuels destined to run out along with the desire to move towards more sustainable resources have recently led to a deep change in the chemical industry. Added-value products, polymers, fuels, and syngas could, in fact, alternatively be obtained from renewable carbon sources (agro-industrial waste and carbon dioxide).[1–4] Among them, an attracting role is played by furfural (FF) and 5-hydroxymethylfurfural (HMF) accessible from the dehydration of lignocellulosic sugars at the industrial scale.[5,6] Indeed, HMF belongs to the list of "Top 10+4" bio-based chemicals from the U.S. Department of Energy (DOE)[7] and its role as platform molecule is widely recognized. It can be upgraded into a variety of useful compounds by elaboration of the hydroxyl and formyl functionalities as well as of the furan ring.[8] In particular, oxidation reactions of HMF have led to the synthesis of new interesting products for polymer, pharmaceutical, and agrochemical industries. The full oxidation of HMF produces the 2,5-furandicarboxylic acid (FDCA), also included in the list of platform chemicals indicated by DOE.[7] FDCA has been mainly employed as a replacement of terephthalic, isophthalic, and adipic acids in manufacturing polyesters, polyamides, and polyurethanes.[9–11] The selective oxidation of the hydroxyl group instead leads to the formation of 2,5-diformylfuran (DFF), a valuable intermediate for the synthesis of fungicides,[12] furan-urea resins,[13,14] and functional materials.[15] Lastly, the synthesis of the corresponding carboxylic acid, 5-hydroxymethyl-2-furancarboxylic acid (HMFCA), has taken on importance due to the possibility to use this molecule as a novel monomer for the production of various polyesters,[16] and as a precursor of FDCA.[17] Moreover, HMFCA has proven to display anti-tumour activity[18] and it is also an intermediate in the synthesis of an interleukin inhibitor.[19] These potential industrial applications of HMFCA pushed several groups to propose new selective oxidizing procedures of the formyl functionality of HMF both in homogeneous and heterogeneous conditions (Scheme 1).[20] Overall, most of the developed researches focused on metal-catalysed HMFCA synthesis.[5,8,21–24] For instance, the ability of dioxomolybdenum (VI) complexes

immobilized on K-10 clay to activate molecular oxygen and to promote the formation of HMFCA has been investigated by Zhang, Deng and their co-workers.[25] Thanks to this procedure HMFCA could be obtained in good yield and complete selectivity in toluene at elevated temperature.[25] Mild oxidation conditions and inexpensive metal precursor have been instead employed by De La Rosa's group through a study on the catalytic activity of supported salen complexes of Fe(III) and Cu(II) for the production of HMFCA in aqueous medium with hydrogen peroxide as the oxidizing agent.[26] Lipases,[27] xanthine oxidases,[28] and whole-cell system,[29,30] have been similarly investigated as more environmental benign biocatalytic methods, showing high levels of selectivity and high loadings of HMF. A photocatalytic approach has been also described by the group of Son and Han, using Au nanocatalysts supported on TiO_2, and atmospheric air under UV and visible light irradiation in basic aqueous solution.[31] Lastly, an organocatalytic method using a soluble imidazolylidene N-heterocyclic carbene (NHC) catalyst and oxygen in DMSO[32] has been developed for the synthesis of HMFCA. However, as the procedure was optimized for furfural oxidation, the presence of the hydroxyl group in HMF induced a side reaction (the HMF oxidative esterification) that diminished the selectivity and the yield of HMFCA. Even if all these above reported methods globally displayed a high selectivity and yield towards HMFCA synthesis, they present some limitations as well. Thus, the search for highly selective, but also eco-friendly, and operationally simple synthesis of HMFCA still remains an interesting challenge. For this reason, a new organocatalyzed procedure has been developed, relying on the formation of HMF-based oligomers through oxidative esterifications, followed by oligomer hydrolysis with a basic resin in a one-pot two-step fashion (Scheme 2).

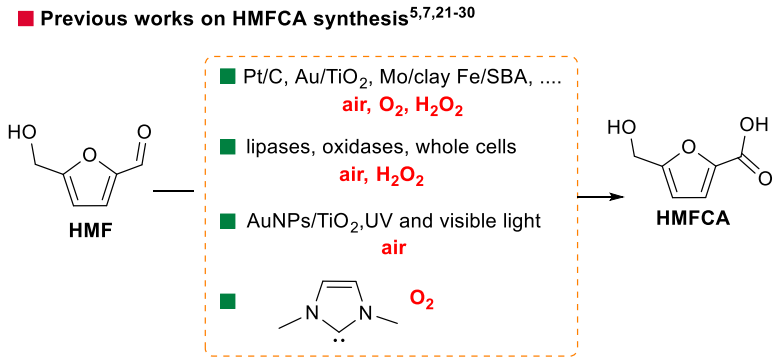

Scheme 1. Previously reported catalytic approaches to the synthesis of HMFCA.

The process, promoted by a heterogeneous NHC catalyst (triazolylidene), used air as the terminal oxidant. The purification of HMFCA was facilitated by the so called "catch and release" technique. The same supported NHC catalyst was applied to the synthesis of ester,

thioester, and amide derivatives of HMFCA under batch and continuous-flow conditions as well as to furfural oxidation to produce furoic acid and its derivatives.

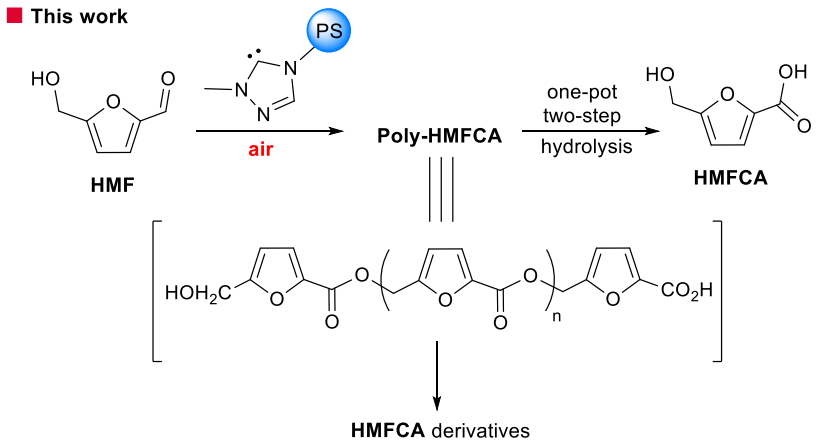

Scheme 2. Aerobic oxidation of 5-hydroxymethylfurfural (HMF) to 5-hydroxymethyl-2-furancarboxylic acid (HMFCA) and derivatives by heterogeneous NHC-catalysis.

4.2 Results and discussion

Starting from the previous results obtained on glycerol monoesterification[33] (see Chapter 3), a preliminary investigation on HMFCA synthesis by oxidative NHC-catalysis focused on the use of the polystyrene-supported triazolium pre-catalyst **A** (Table 1). Accordingly, the heterogeneous organocatalyst **A** (20 mol%) was tested using DBU (50 mol%) as the optimal base and air as the terminal oxidant in anhydrous THF (Table 1, entry 1). However, along with HMFCA (35%) that was the expected product of the oxygenative pathway[34–36] of HMF oxidation (see Scheme 4 for further details), other two products were detected, contributing to the almost complete conversion of HMF. These were an α-diketone compound, 5,5'-bihydroxymethyl furil (BHMF), formed by NHC-catalysed self-condensation of HMF followed by selective based-promoted oxidation of the hydroxyketone functionality of the benzoin intermediate[37] and a HMF-based polyester oligomers (poly-HMFCA) attributed to the sequential oxidative esterification involving the primary hydroxyl group of HMF as the nucleophile (NuH, see Scheme 4 for further details). Unfortunately, the addition of water in the reaction medium (2:1 THF:H_2O) with the aim to increase the formation of the target carboxylic acid did not lead to the desired outcome (entry 2). On the contrary, the use of the Kharasch oxidant **1** (1 equiv.) under degassed (Argon) anhydrous conditions yielded poly-HMFCA, underlying the occurrence of the sole oxidative pathway (entry 3). Thus, attempts to increase the yield of HMFCA under degassed environment by adding an excess of water in the reaction medium (which act as the nucleophile) did not provide the selective formation of target carboxylic acid (50%), which was instead detected along with poly-HMFCA (42%, entry 4).

As the side polycondensation of HMF could not be suppressed, the further investigations relayed on the use of poly-HMFCA as precursor of HMFCA by subsequent polyester hydrolysis.

Table 1. Screening of reaction conditions with supported triazolium pre-catalyst **A**.[a]

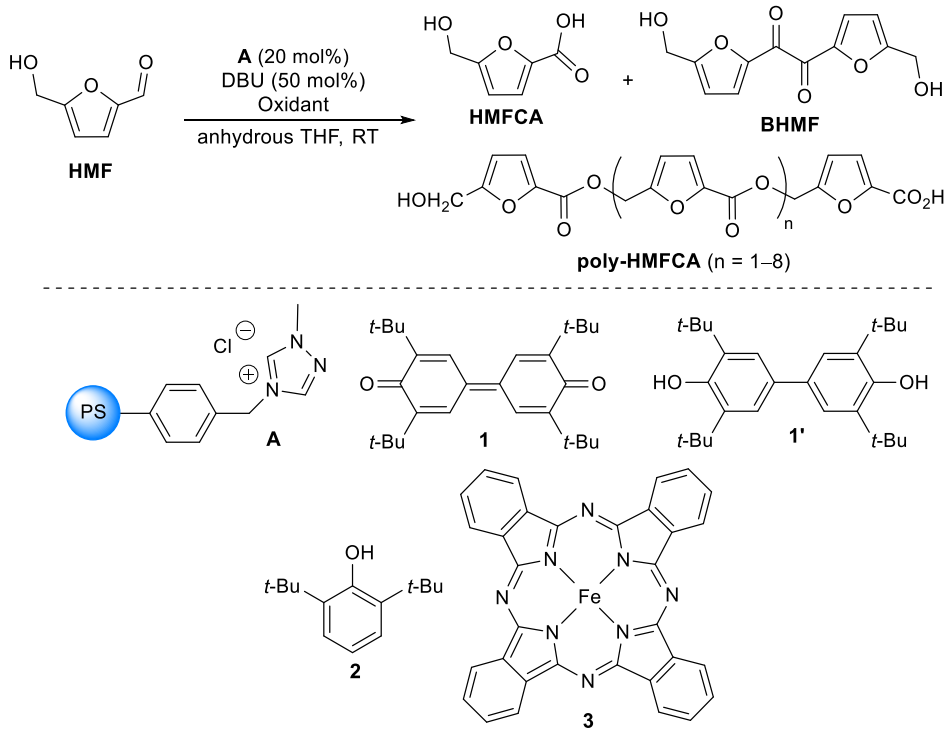

Entry	Oxidant (mol%)	**HMFCA** (%)[b]	**BHMF** (%)[b]	**poly-HMFCA** (%)[b]
1	Air	35	28	29
2[c]	Air	38	25	10
3[d]	**1** (100)	/	/	95
4[c,d]	**1** (100)	50	/	42
5	Air, **2** (20)/**3** (5)	5	/	92
6	Air, **3** (5)	5	/	92
7	Air, $FeCl_3$ (20)	8	35	5
8[e]	Air, **3** (5)	5	/	93
9[e,f]	Air, **3** (5)	5	/	91

[a]**HMF** (1 mmol), THF (4.0 mL), atmospheric air (balloon technique). [b]Yield detected by ^{1}H NMR of the crude reaction mixture after aqueous work-up with 1 M HCl (durene as an internal standard). [c] 2:1 THF:H_2O as the solvent. [d]Degassed conditions (Ar). [e]Anhydrous Me-THF as the solvent. [f]Reaction performed with recycled **A**.

An electron transfer mediator system was additionally tested using the inexpensive alcohol precursor **2** (20 mol%) in the presence of iron(II)phthalocyanine **3** (5 mol%) and with atmospheric oxygen as the terminal oxidant. Gratifyingly, these conditions led to the target poly-HMFCA with a 92% yield and only a slight formation of HMFCA (entry 5). Moreover, this outcome was kept unaltered even in the absence of the alcohol **2** (entry 6), indicating that

phthalocyanine **3** (E = +0.74 V vs. SCE)[38] is able to mediate the aerobic oxidative esterification of HMF with a low energy barrier and it reacts faster than oxygen with the Breslow intermediate (suppression of the oxygenative pathway; see Scheme 4 fur further details). On the other hand, the use of the previously reported catalytic oxidant $FeCl_3$[39] turned out to be less effective and selective in HMF oxidation (entry 7). Lastly, the process sustainability was further enhanced with the use of the biomass-derived methyltetrahydrofuran (Me-THF)[40] as solvent (entry 8), showing an unaltered selectivity.

With the optimal conditions defined (Table 1, entry 8), the collected reaction mixture was filtered, acidified with 1 M HCl solution, and extracted with ethyl acetate. Subsequently, the concentrated organic phase was dissolved in dichloromethane and diluted with cold methanol to give the poly-HMFCA species as a precipitate. The newly poly-HMFCA compound was therefore properly characterized by NMR and MS analyses. According to ^{1}H NMR analyses, a linear polyester oligomer was formed. The integration of signals at 5.30 ppm and 4.67 ppm corresponding to the internal and terminal methylene resonance, respectively, allowed to identify an average of repeated units (n) equal to 7.8 (Figure 1a). While the carbonyl carbon of the ester linkages was easily recognized at 158.1 ppm in the ^{13}C NMR spectrum, the carboxylic acid end-groups, instead, were not clearly identified from the background noise (Figure 1b). Anyway, the structure was confirmed through derivatization with diazomethane, observing the appearance of the diagnostic resonance of the methyl ester group at 3.80 ppm and 52.1 ppm in the ^{1}H NMR and ^{13}C NMR spectra, respectively (Figure 2).

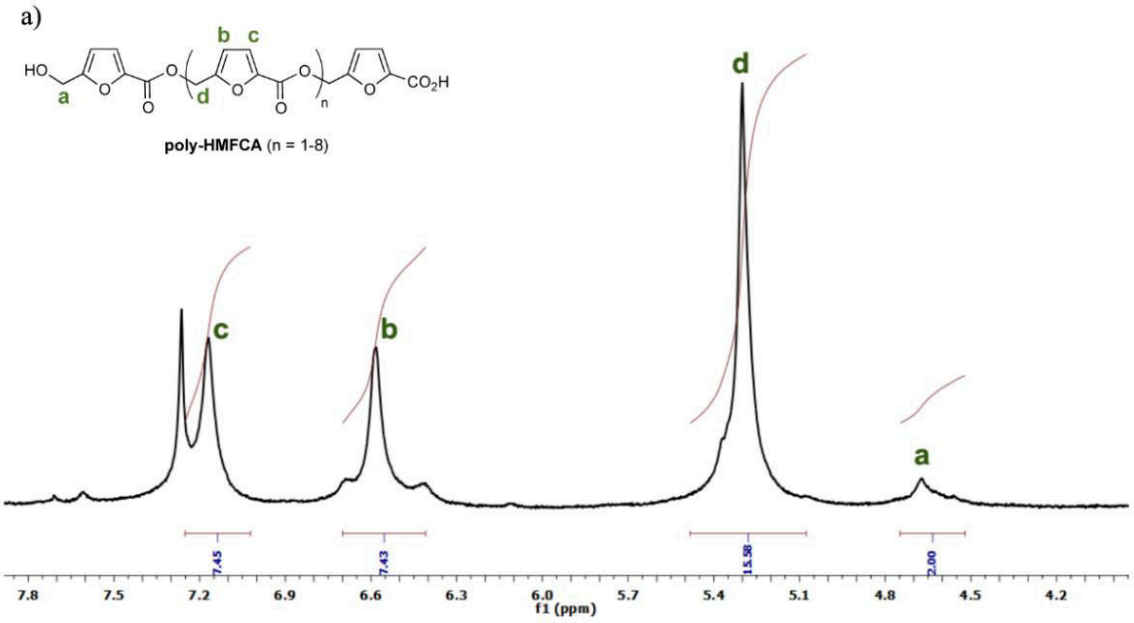

Figure 1. a) ^{1}H NMR spectra of poly-HMFCA in $CDCl_3$.

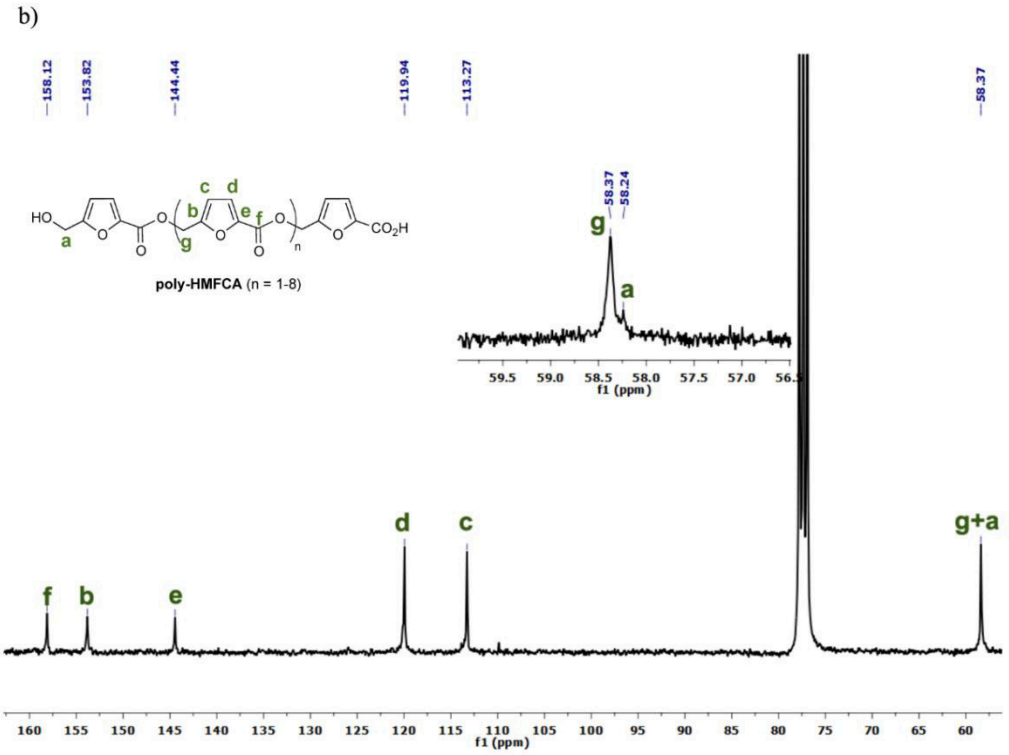

Figure 1 (continued). b) ^{13}C NMR spectra of poly-HMFCA in $CDCl_3$.

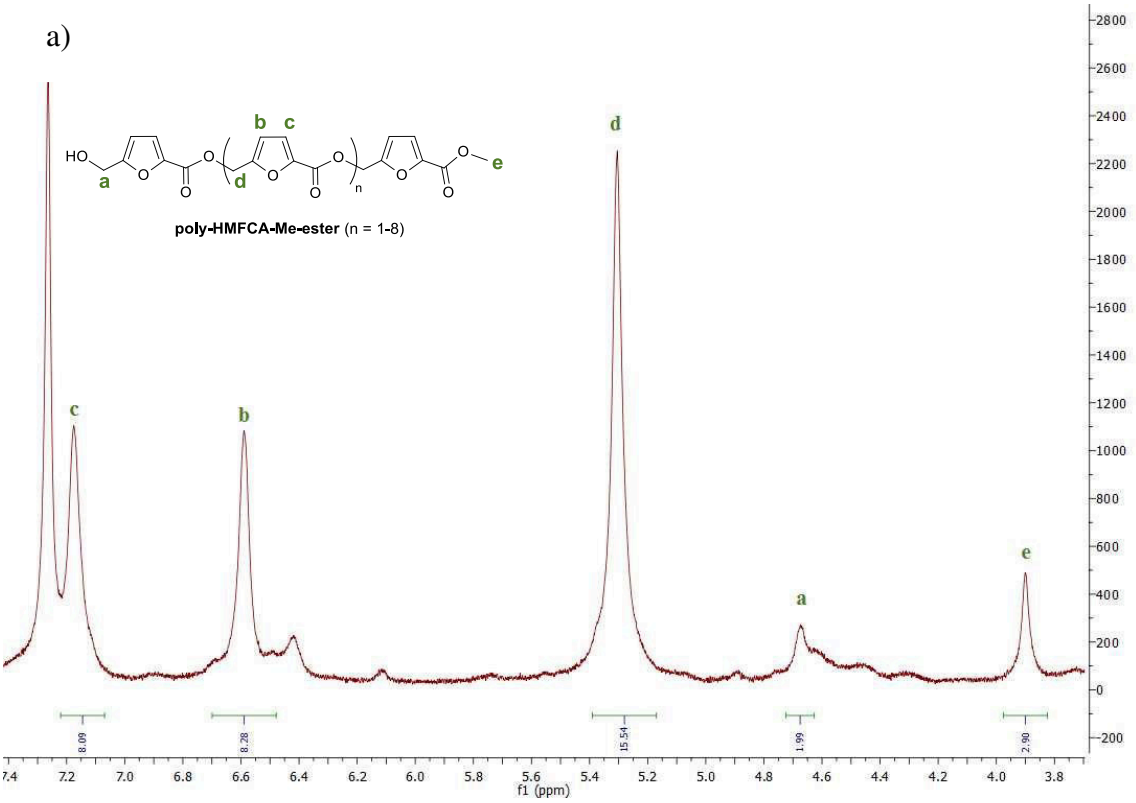

Figure 2. a) ^{1}H NMR spectra ($CDCl_3$) of poly-HMFCA-Me-ester.

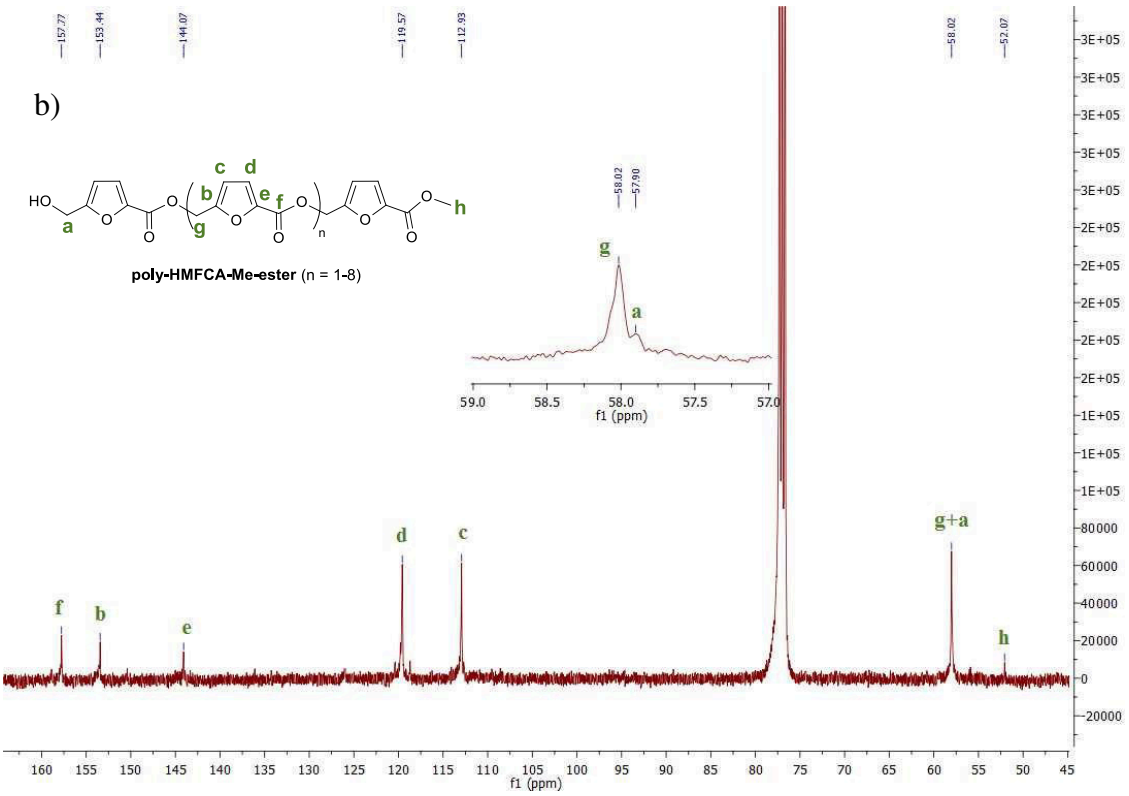

Figure 2 (continued). b) ^{13}C NMR spectra ($CDCl_3$) of poly-HMFCA-Me-ester.

The structure of the poly-HMFCA with the recurrence of methylfuran-2-carboxylate repeat unit was further confirmed by negative-ion mode ESI mass spectrum of poly-HMFCA (Figure 3a). Accordingly, a main series of ions, corresponding to deprotonated polyester oligomers (n= 1−8) with peak-to-peak mass increment of 124 Da were detected. Moreover, the calculated spectrum of poly-HMFCA (Figure 3b) and MS/MS analysis of the selected ionic species at *m/z* 885 (Figure 3c) further supported the proposed interpretation.

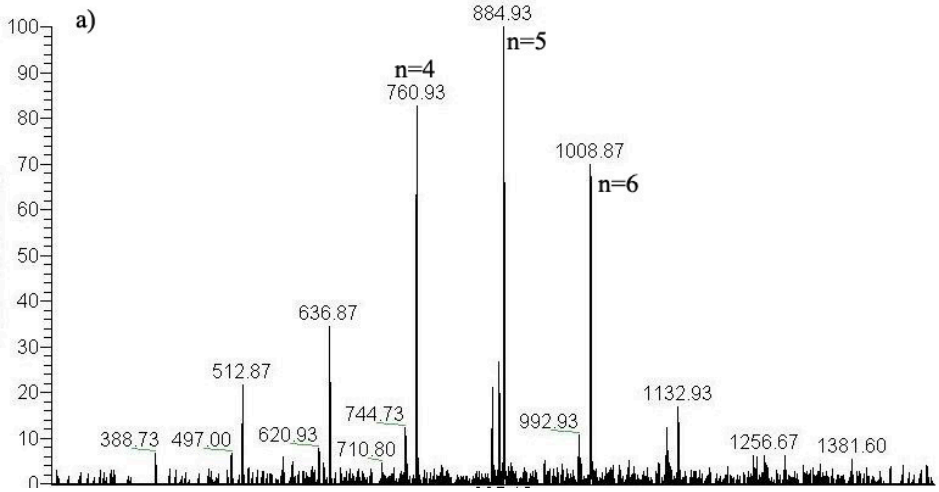

Figure 3. a) Experimental ESI-MS spectra (negative ion mode) of poly-HMFCA.

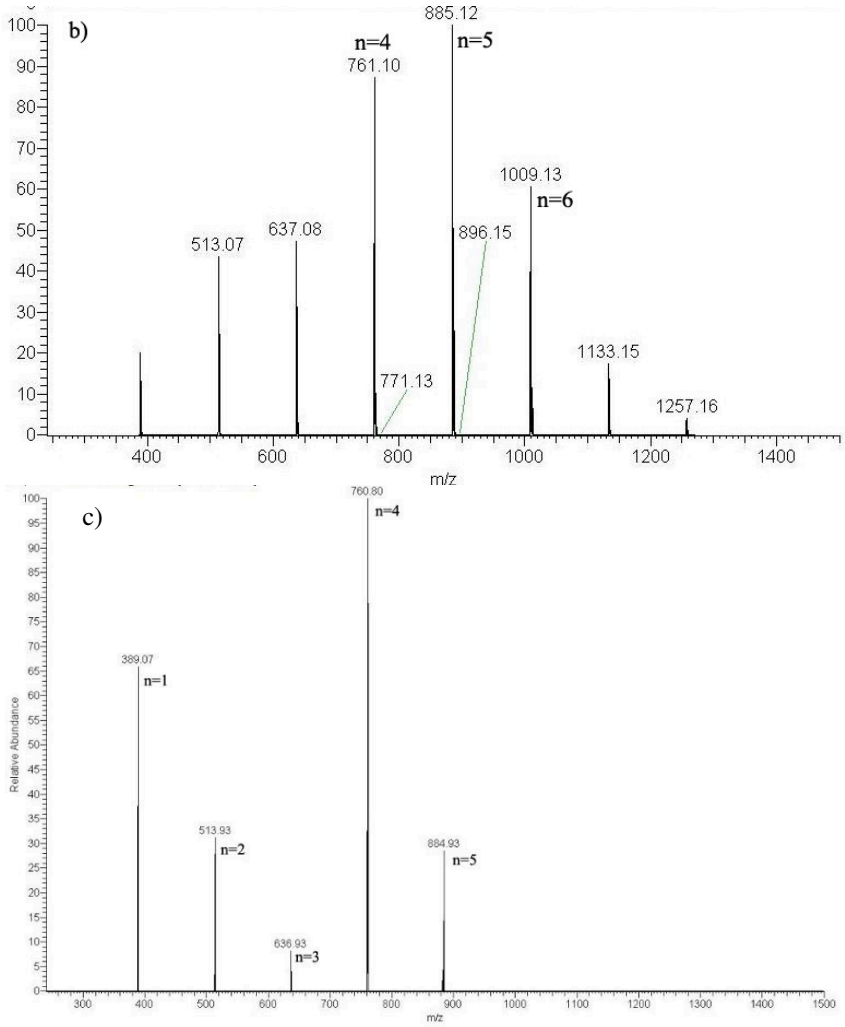

Figure 3 (continued). b) ESI-MS spectra (negative ion mode) of poly-HMFCA. c) poly-HMFCA MS/MS mass spectrum of selected ion at *m/z* 885.

At this point, the poly-HMFCA oligomers were subjected to derivatization for accessing different carboxylic acid derivatives (Scheme 3). A preliminary investigation under homogeneous conditions on the basic hydrolysis of the polyester for HMFCA synthesis was conducted (Scheme 3, *path a*) using an aqueous KOH solution. Subsequently, a set of ionic supported based (Amberlite IRN78, Amberlyst A26 OH form, Ambersep 900 OH) were screened with the aim to selectively catch the carboxylate ion of HMFCA on support for impurities removal and subsequently release the acid in solution by protonation. Therefore, through a "catch and release" technique, the target HMFCA was obtained in 87% overall yield (one-gram scale). Once the precatalyst **A** was recovered through filtration, the crude mixture of the oxidative esterification was diluted with water (20:1 Me-THF:H_2O) and treated at room temperature with Ambersep 900 OH. After filtration, the resin was suspended in acetic acid for one hour affording the target carboxylic acid.

The synthetic relevance of poly-HMFCA was additionally highlighted with the preparation of ester and amide derivatives of HMFCA. The target HMFCA methyl ester **4** was obtained in 90% overall yield, after column chromatography, when crude poly-HMFCA was treated with catalytic sodium methoxide (MeOH, 65 °C) (Scheme 3, *path b*). A similar one-pot two-step procedure was also investigated for the production of secondary amide **5** (88% yield) with butylamine as the nucleophile (2 equiv.) and catalytic DMAP (Me-THF, 70 °C; *path c*).

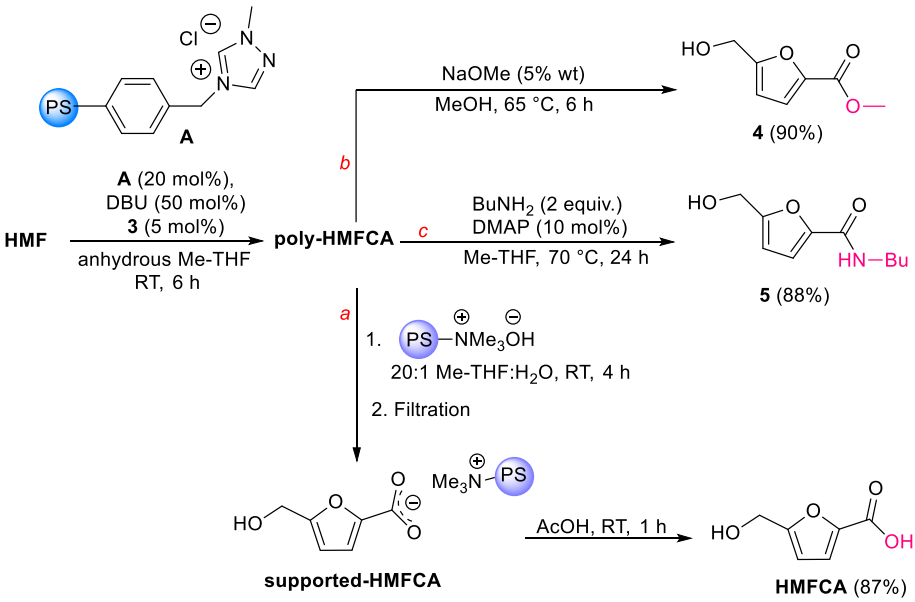

Scheme 3. One-pot two-step synthesis of ester **4** (*path a*), amide **5** (*path b*), and HMFCA through a "catch and release" technique (*path c*).

With the aim to compare the obtained results with the direct conversion of HMF into the corresponding ester, amide, and thioester derivatives, a parallel study with **A/3/**air system was also conducted (Table 2). To limit the side poly-condensation of HMFCA, an excess (5 equiv.) of nucleophile was used. The HMFCA methyl ester **4** and its higher homologue **6** were obtained in good yields; on the contrary, the synthesis of the secondary amide **5** (8%) produced unsatisfactory results, furnishing no strong evidences to clarify a probable NHC-catalysed aldehyde oxidative amidation mechanism.[41] Indeed, the preferential formation of HMF imine was instead observed. However, the use of the pyrrolidine secondary ammine reestablished the efficiency of the oxidative process generating the amide **7** in 61% isolated yield. The synthesis of a thioester derivative was also investigated and the target compound **8** was isolated in 48% yield despite the occurrence of competitive ethanethiol oxidation.[42]

The scope of the disclosed methodology was also extended to the synthesis of furoic acid and its derivatives. Indeed, the carboxylic acid **9**, which is a promising precursor of FDCA,[43] was obtained in 90% yield, a comparable result to that obtained with a soluble imidaziolium

promoter,[32] thus confirming the high catalytic activity of the supported pre-catalyst **A**. The carboxylic acid derivatives, ester **10**, amide **11**, and thioester **12**, were all obtained with higher efficiency compared to the HMF-based analogous thanks to the lack of polycondensation side reaction.

Table 2. Reaction scope of HMF and FF with pre-catalyst **A/3**/air oxidation system.

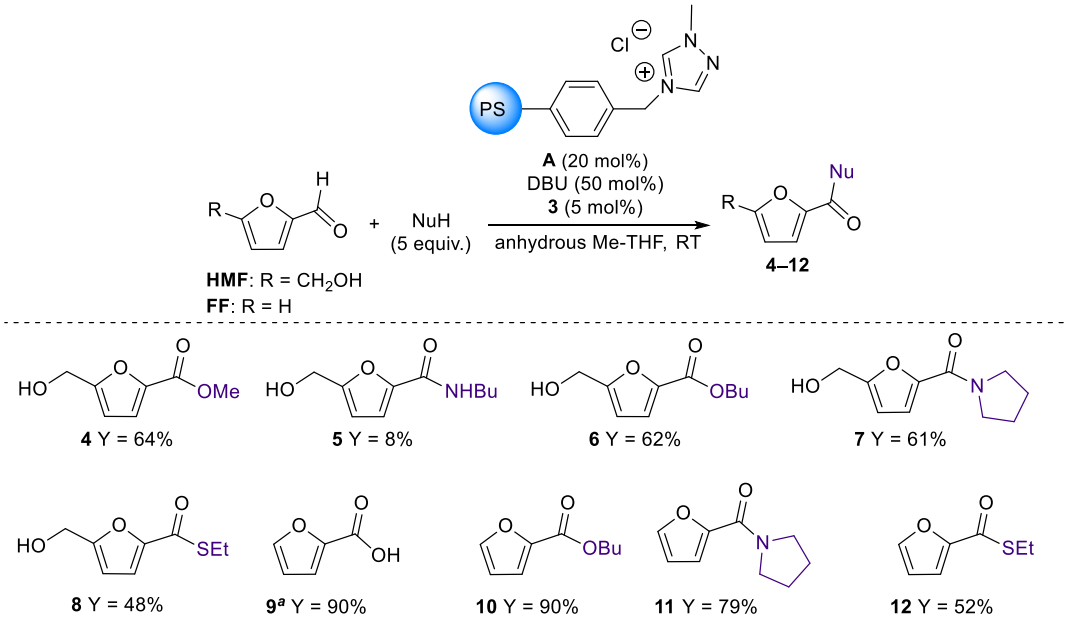

Conditions: HMF or **FF** (1 mmol), Me-THF (4.0 mL), atmospheric air (balloon technique). All the reported yield (Y) are for the isolated compounds **4–12**. [a] 2:1 THF:H_2O as the solvent.

Lastly, the set-up of a flow procedure for the continuous production of selected HMF and FF oxidation products was investigated (Table 3). As reported in Chapter 3, a stainless-steel column (length 10 cm, 0.46 cm internal diameter) fixed-bed microreactor **R1** was fabricated by slurry packing the pre-catalyst **A**. The microreactor **R1** was fully characterized and, as formerly observed,[33] the use of the **A/3**/air system was hampered by the low concentration of oxygen within the reactor. Hence, the Kharasch oxidant **1** was instead used and after a brief optimization procedure in flow, the scope of the reaction was explored. According to the information reported in Table 3, the flow experiments were conducted by independently pumping inside the pre-activated reactor degassed (Ar) solutions of aldehyde/NuH and DBU/**1**. Flow rates were adjusted to achieve high conversions (≥ 90%) for an easier downstream purification of the target products and for the recovery of alcohol **1'** for subsequent regeneration and recycle of the oxidant **1** (as explained in Chapter 3).

Table 3. Continuous-flow production of selected HMF and FF oxidation products.

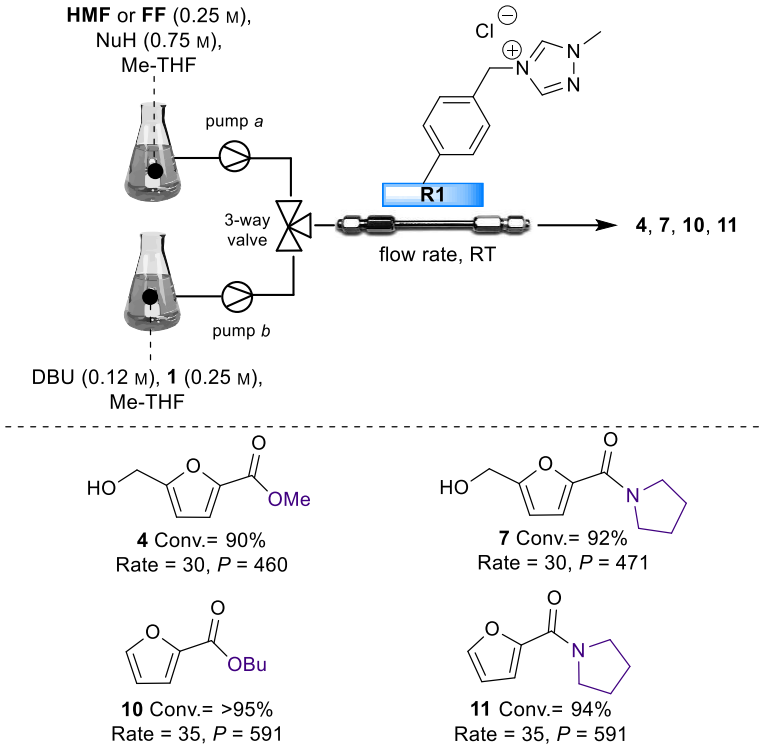

See the Experimental Section for a description of the flow apparatus. The conversion are reported as instant conversion in the steady-state regime as established by ^{1}H NMR analysis. Flow rates are measured in μLmin^{-1}; productivities (*P*) are measured in $mmol_{product}\ h^{-1}\ mmol_{cat}^{-1}$.

A mechanism which clarifies the formation of the carboxylic acid and its derivatives has also been proposed on the basis of previous works (see also Chapter 3, Scheme 7).[33,44,45] Indeed, catalytic Kharasch oxidant **1** could be generated *in situ* from the inexpensive precursor alcohol **2** in the presence of iron(II) phthalocyanine **3** and atmospheric oxygen as the terminal oxidant. After electron transfer from the Breslow intermediate to **1**, the acyl azolium species is formed along with the reduced alcohol **1'**, which in turn is re-oxidized to **1** by phthalocyanine **3** and oxygen (Scheme 4, red route). As already mentioned, the target carboxylic acids, HMFCA and **9**, are the expected products of the oxygenative pathway[35–37] of HMF and FF oxidation, respectively. The carboxylic acid derivatives as well as poly-HMFCA are instead the expected products of the oxidative pathway which is favored in the presence of an external oxidant.

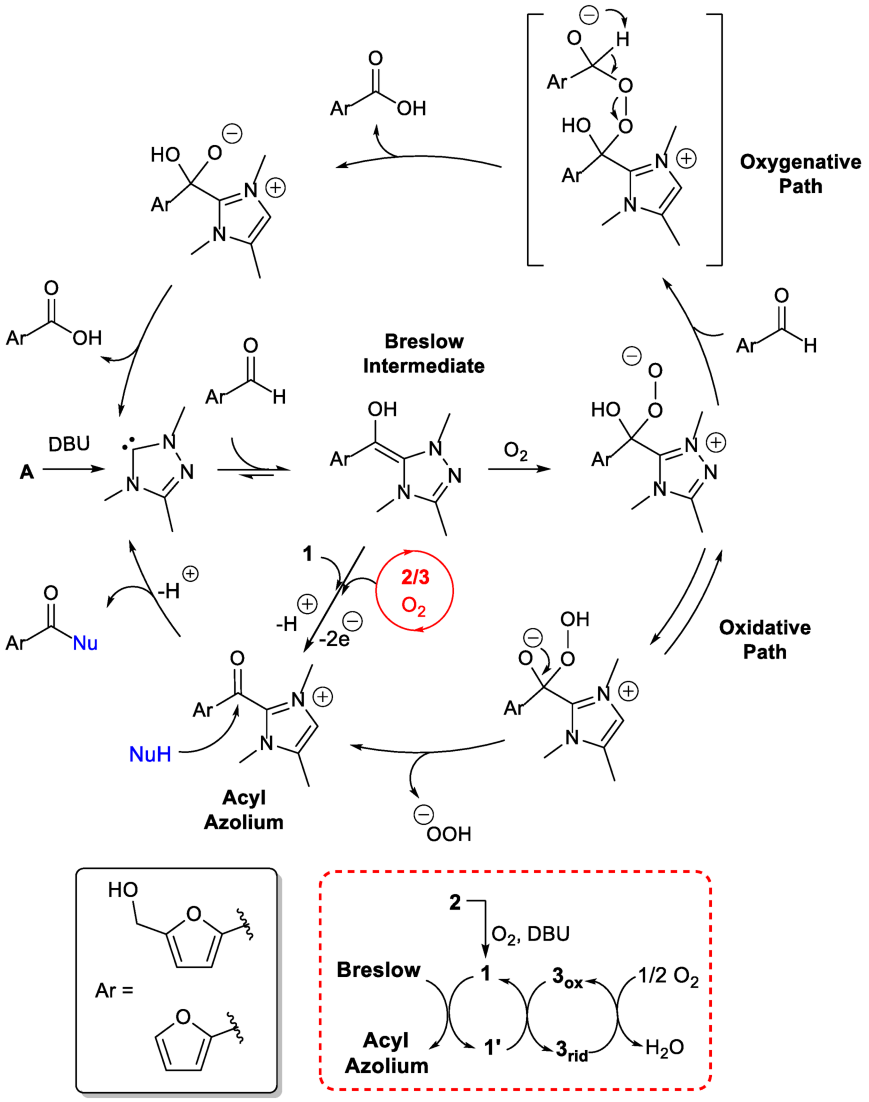

Scheme 4. Proposed mechanisms for oxidations of HMF and FF by NHC-catalysis.

4.3 Conclusion

To conclude, a novel catalytic procedure has been disclosed for the synthesis of value-added molecules from the bio-based HMF and FF. Through the utilization of polymer-supported triazolylidene and iron phthalocyanine catalysts with air as the terminal oxidant, an unprecedented poly-HMFCA has been synthetised. The latter has thus been used as precursor for the synthesis of valuable bio-based 5-hydroxymethyl-2-furancarboxylic acid (HMFCA) and other carboxylic acids derivatives. The direct conversion into carboxylic acids, ester, amide and thioesters, under batch and flow conditions, has been also investigated. Overall, the reported work emphasizes the role as HMF and FF as platform molecules and further demonstrates the potential of heterogeneous oxidative NHC-catalysis in the field of biomass valorisation.

4.4 Experimental section

General experimental procedure

Reactions were monitored by TLC on silica gel 60 F_{254} with detection by charring with potassium permanganate and/or phosphomolybdic acid. Flash column chromatography was performed on silica gel 60 (230−400 mesh). ^{1}H NMR (300 MHz) and ^{13}C NMR (101 MHz) spectra were recorded in $CDCl_3$ or acetone-d_6 solutions at room temperature. The chemical shifts in ^{1}H NMR and ^{13}C NMR spectra were referenced to trimethylsilane (TMS). Peak assignments were aided by ^{1}H-^{1}H COSY and gradient-HMQC experiments. For high resolution mass spectrometry (HRMS) the compounds were analysed using the LTQ-Orbitrap XL mass spectrometer (Thermo Scientific Inc., Milan, Italy) equipped with an electrospray ion source (Thermo Scientific Inc., Milan, Italy) set as follows: positive ion mode, spray voltage 5.5 kV, capillary temperature 275 °C, capillary voltage 16 V, tube lens offset 120 V. The MS analyser was externally calibrated with the LTQ ESI Positive Ion Calibration Solution (Thermo Fisher, Milan, Italy) to yield accuracy below 5 ppm. Accurate mass data were collected by directly infusing samples in 80:20 H_2O:ACN 0.1% Formic Acid into the system at a flow rate of 20 μL min^{-1}. Solvents were dried over a standard drying agent and freshly distilled prior to use. Pre-catalyst **A** was synthetized according to a literature procedure.[33] Kharasch oxidant **1**, 2,6-di-tert-butylphenol **2**, iron(II) phthalocyanine **3**, 5-hydroxymethylfurfural (HMF), furfural (FF), AMBERSEP 900 OH were commercially available and used as received. DBU was freshly distilled before its utilization. 5,5'-bihydroxymethyl furil (BHMF),[46] 5-hydroxymethyl-2-furancarboxylic acid (HMFCA),[47] **4**,[48] **9**,[49] **10**,[50] and **11**[41] are known compounds.

Screening of reaction conditions with pre-catalyst A (Table 1)

The following reaction conditions explain the operative optimization procedure. In all experiments, yield and selectivity were evaluated by ^{1}H NMR analysis of the reaction mixture (durene as internal standard).

Entries 1,2. A stirred mixture of HMF (98 μL, 1.00 mmol), durene (134 mg, 1.00 mmol) and pre-catalyst **A** (156 mg, 0.20 mmol, loading = 1.28 mmol g^{-1}) in the stated solvent (4.0 mL) was stirred under an air atmosphere (by an air-filled balloon). Then, DBU was added (75 μL, 0.50 mmol) and the reaction was stirred at room temperature for 16 h. Filtration, washing (MeOH) of the resin and concentration of the solution afforded the crude reaction mixture. Subsequently, the residue was dissolved in EtOAc (5.0 mL), acidified with 1 M HCl (5.0 mL), extracted with EtOAc (3 × 20 mL). The combined organic phases were dried over Na_2SO_4 and concentrated.

Entries 3,4. A stirred mixture of HMF (98 μL, 1.00 mmol), **1** (408 mg, 1.00 mmol), durene (134 mg, 1.00 mmol) and pre-catalyst **A** (156 mg, 0.20 mmol, loading = 1.28 mmol g^{-1}) in the stated solvent (4.0 mL) was degassed under vacuum and saturated with argon (by an Ar-filled balloon) three times. Then, DBU was added (75 μL, 0.50 mmol) and the reaction was stirred at room temperature for 16 h. Filtration, washing (MeOH) of the resin and concentration of the solution afforded the crude mixture of the reaction. Subsequently, the residue was dissolved in EtOAc (5.0 mL), acidified with 1 M HCl (5.0 mL), extracted with EtOAc (3 × 20 mL). The combined organic phases were dried over Na_2SO_4 and concentrated.

Entry 5. A stirred mixture of HMF (98 μL, 1.00 mmol), **2** (41 mg, 0.20 mmol), **3** (28 mg, 0.05 mmol), durene (134 mg, 1.00 mmol) and pre-catalyst **A** (156 mg, 0.20 mmol, loading = 1.28 mmol g^{-1}) in THF (4.0 mL) was stirred under an air atmosphere (by an air-filled balloon). Then, DBU was added (75 μL, 0.50 mmol) and the reaction was stirred at room temperature for 16 h. Filtration, washing (MeOH) of the resin and concentration of the solution afforded the crude mixture of the reaction. Subsequently, the residue was dissolved in EtOAc (5.0 mL), acidified with 1 M HCl (5.0 mL), extracted with EtOAc (3 × 20 mL). The combined organic phases were dried over Na_2SO_4, and concentrated.

Entry 6. A stirred mixture of HMF (98 μL, 1.00 mmol), **3** (28 mg, 0.05 mmol), durene (134 mg, 1.00 mmol) and pre-catalyst **A** (156 mg, 0.20 mmol, loading = 1.28 mmol g^{-1}) in THF (4.0 mL) was stirred under an air atmosphere (by an air-filled balloon). Then, DBU was added (75 μL, 0.50 mmol) and the reaction was stirred at room temperature for 16 h. Filtration, washing (MeOH) of the resin and concentration of the solution afforded the crude mixture of the reaction. Subsequently, the residue was dissolved in EtOAc (5 mL), acidified with 1 M HCl (5 mL), extracted with EtOAc (3 × 20 mL). The combined organic phases were dried over Na_2SO_4 and concentrated.

Entry 7. A stirred mixture of HMF (98 μL, 1.00 mmol), $FeCl_3$ (32 mg, 0.20 mmol), durene (134 mg, 1.00 mmol) and pre-catalyst **A** (156 mg, 0.20 mmol, loading = 1.28 mmol g^{-1}) in THF (4.0 mL) was stirred under an air atmosphere (by an air-filled balloon). Then, DBU was added (75 μL, 0.50 mmol), and the reaction was stirred at room temperature for 16 h. Filtration, washing (MeOH) of the resin and concentration of the solution afforded the crude mixture of the reaction. Subsequently, the residue was dissolved in EtOAc (5.0 mL), acidified with 1 M HCl (5.0 mL), extracted with EtOAc (3 × 20 mL). The combined organic phases were dried over Na_2SO_4 and concentrated.

Entry 8. A stirred mixture of HMF (98 μL, 1.00 mmol), **3** (28 mg, 0.05 mmol), durene (134 mg, 1.00 mmol) and pre-catalyst **A** (156 mg, 0.20 mmol, loading = 1.28 mmol g^{-1}) in Me-THF (4.0

mL) was stirred under an air atmosphere (by an air-filled balloon). Then, DBU was added (75 μL, 0.50 mmol) and the reaction was stirred at room temperature for 16 h. Filtration, washing (MeOH) of the resin and concentration of the solution afforded the crude mixture of the reaction. Subsequently, the residue was dissolved in EtOAc (5.0 mL), acidified with 1 M HCl (5.0 mL), extracted with EtOAc (3 × 20 mL). The combined organic phases were dried over Na_2SO_4 and concentrated.

Entry 9. Recycle of the pre-catalyst **A** was performed by simple filtration, washing (MeOH), and drying of the resin. The recycled **A** was used as described in entry 8.

DBU recycle

The aqueous phase collected from the work-up of the reaction mixture, was concentrated under vacuum and the resulting residue diluted with Me-THF (12 mL) and 1 M NaOH until alkaline pH. The resulting mixture was stirred for 2 h, partially concentrated, and extracted with EtOAc (3 × 20 mL). The combined organic phases were dried over Na_2SO_4 and concentrated to give DBU (195 mg, 1.29 mmol) at least 90% pure as judged by ^{1}H NMR analysis.

Poly-HMFCA

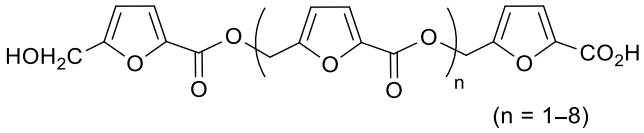

A stirred mixture of HMF (294 μL, 3.00 mmol), **3** (84 mg, 0.15 mmol) and pre-catalyst **A** (468 mg, 0.60 mmol, loading = 1.28 mmol g^{-1}) in Me-THF (12 mL) was stirred under an air atmosphere (by an air-filled balloon). Then, DBU was added (225 μL, 1.50 mmol) and the reaction was stirred at room temperature for 6 h. Filtration, washing (MeOH) of the resin and concentration of the solution afforded crude poly-HMFCA. Subsequently, the residue was dissolved in EtOAc (10 mL), acidified with 1 M HCl (10 mL), extracted with EtOAc (3 × 30 mL). The combined organic phases were dried over Na_2SO_4 and concentrated. Finally, the mixture was dissolved in dichloromethane (8 mL) and diluted with cold methanol (80 mL) to give poly-HMFCA (351 mg, 93%) as a precipitate. **^{1}H NMR** (300 MHz, $CDCl_3$) δ = 7.17 (s, 8H, Ar), 6.58 (s, 8H, Ar), 5.30 (s, 16H, $COOCH_2$), 4.67 (s, 2H, CH_2); **^{13}C NMR** (101 MHz, $CDCl_3$) δ = 158.1 (*C*O), 153.8 (Ar*C*, Furandimethylene), 144.4 (Ar*C,* Furandicarboxylate), 119.9 (Ar*C*H, Furandicarboxylate), 113.3 (Ar*C*H, Furandimethylene), 58.4 (COO*C*H_2). **ESI-MS** ($[M - H]^-$) found: 884.9, requires: 886.1 for n = 5.

Poly-HMFCA Me- ester

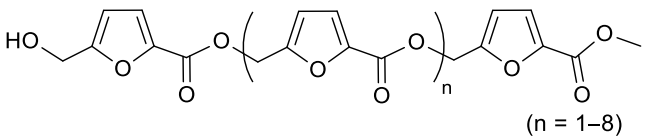

A stirred solution of poly-HMFCA (25 mg) in dichloromethane (1.0 mL) was cooled down at 0 °C. Thus, an ethereal solution of diazomethane was added dropwise and let the mixture stirred an additional 30 min. Then, it was warmed to room temperature, and evaporated to afford poly-HMFCA Me- ester. **^{1}H NMR** (300 MHz, $CDCl_3$) δ = 7.17 (s, 8H, Ar), 6.58 (s, 8H, Ar), 5.30 (s, 16H, $COOCH_2$), 4.67 (s, 2H, CH_2), 3.90 (s, 3H, $COOCH_3$); **^{13}C NMR** (101 MHz, $CDCl_3$) δ = 157.8 (*C*O), 153.4 (Ar*C*, Furandimethylene), 144.1 (Ar*C,* Furandicarboxylate), 119.6 (Ar*C*H, Furandicarboxylate), 112.9 (Ar*C*H, Furandimethylene), 58.0 (COO*C*H_2), 52.1 (O*C*H_3).

5-(Hydroxymethyl)furan-2-carboxylic acid (HMFCA)

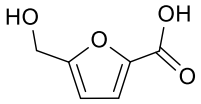

A mixture of HMF (784 µL, 8.00 mmol), **3** (224 mg, 0.40 mmol) and pre-catalyst **A** (1.25 g, 1.60 mmol, loading = 1.28 mmol g^{-1}) in Me-THF (30 mL) was stirred under an air atmosphere (by an air-filled balloon). Then, DBU was added (600 µL, 4.00 mmol) and the reaction was stirred at room temperature for 6 h. Filtration, washing (MeOH) of the resin and concentration of the solution afforded crude poly-HMFCA (1.45 g). The above crude poly-HMFCA (1.45 g) was dissolved in a Me-THF:H_2O mixture (20 mL Me-THF, 1.0 mL H_2O) and stirred in the presence of Ambersep 900 OH resin (4.00 g) at room temperature for 4 h. The resin was filtered off, thoroughly washed with EtOAc and suspended in acetic acid (10 mL) for 1 h. Subsequently, filtration, washing (EtOAc) of the resin and concentration of the solution afforded crude HMFCA. Purification by crystallization (EtOAc) afforded HMFCA (0.98 g, 87%) as a colourless solid with spectroscopic data in accordance with the literature.[47] **mp** 159−161 °C (EtOAc) {Lit.[51] 163−164 °C}; **^{1}H NMR** (300 MHz, acetone-d_6) δ = 7.14 (d, *J* 3.4 Hz, 1H, Ar), 6.46 (d, *J* 3.4 Hz, 1H, Ar), 4.58 (s, 2H, CH_2), 3.92 (bs, 1H, OH); **^{13}C NMR** (101 MHz, acetone-d_6) δ = 160.2 (*C*O), 159.1 (Ar*C*-2), 144.8 (Ar*C*-5), 118.7 (Ar*C*H-3), 108.9 (Ar*C*H-4), 56.8 (COO*C*H_2). **HRMS** (ESI/Q-TOF) calcd. for $C_6H_7O_4$ ([M + H]$^+$): 143.0339; found: 143.0336.

Methyl 5-(hydroxymethyl)furan-2-carboxylate (4)

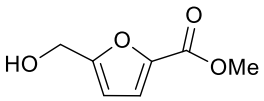

Procedure A: one-pot two step technique.

A stirred mixture of HMF (98 μL, 1.00 mmol), **3** (28 mg, 0.05 mmol) and pre-catalyst **A** (156 mg, 0.20 mmol, loading = 1.28 mmol g^{-1}) in Me-THF (4.0 mL) was stirred under an air atmosphere (by an air-filled balloon). Then, DBU was added (75 μL, 0.50 mmol) and the reaction was stirred at room temperature for 6 h. Filtration, washing (MeOH) of the resin and concentration of the solution afforded crude poly-HMFCA (190 mg). Later, a mixture of the above crude poly-HMFCA (190 mg), MeOH (5 mL) and a catalytic amount of sodium methoxide (6 mg, 5% wt) was stirred at 65 °C for 6 h. Subsequently, the reaction was cooled to room temperature, concentrated, and eluted from a column of silica gel with 1:1 cyclohexane:EtOAc to afford **4** (140 mg, 90%) as a colourless liquid with spectroscopic data in accordance with the literature.[48]

Procedure B: direct synthesis.

A mixture of HMF (98 μL, 1.00 mmol), MeOH (202 μL, 5.00 mmol), **3** (28 mg, 0.05 mmol) and pre-catalyst **A** (156 mg, 0.20 mmol, loading = 1.28 mmol g^{-1}) in Me-THF (4.0 mL) was stirred under an air atmosphere (by an air-filled balloon). Then, DBU was added (75 μL, 0.50 mmol), and the reaction mixture was stirred at room temperature for 16 h. Subsequently, the reaction was filtrated, and the resin was washed with EtOAc and MeOH. Concentration of the solution, and elution from a column of silica gel with 1:1 cyclohexane:EtOAc afforded **4** (100 mg, 64%) as a colourless liquid with spectroscopic data in accordance with the literature.[48]

^{1}H NMR (300 MHz, $CDCl_3$) δ = 7.14 (d, *J* 3.4 Hz, 1H, Ar), 6.42 (d, *J* 3.4 Hz, 1H, Ar), 4.68 (d, *J* 3.4 Hz, 2H, CH_2), 3.89 (s, 3H, OCH_3), 2.02 (t, *J* 3.4 Hz, 1H, OH); **^{13}C NMR** (101 MHz, $CDCl_3$) δ = 159.5 (*C*O), 158.6 (Ar*C*-2), 144.5 (Ar*C*-5), 119.2 (Ar*C*H-3), 109.8 (Ar*C*H-4), 57.9 (*C*H_2OH), 52.3 (O*C*H_3). **HRMS** (ESI/QTOF) calcd. for $C_7H_9O_4$ ([M + H]$^+$): 157.0495; found: 157.0491.

N-Butyl-5-(hydroxymethyl)furan-2-carboxamide (**5**)

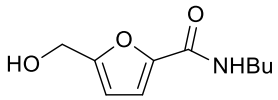

Procedure A: one-pot two step technique.

A stirred mixture of HMF (98 μL, 1.00 mmol), **3** (28 mg, 0.05 mmol) and pre-catalyst **A** (156 mg, 0.20 mmol, loading = 1.28 mmol g^{-1}) in Me-THF (4.0 mL) was stirred under an air atmosphere (by an air-filled balloon). Then, DBU was added (75 μL, 0.50 mmol) and the reaction was stirred at room temperature for 6 h. Filtration, washing (MeOH) of the resin and concentration of the solution afforded crude poly-HMFCA (190 mg). A mixture of the above

crude poly-HMFCA (190 mg), $BuNH_2$ (200 μL, 2.00 mmol) and DMAP (12 mg, 0.10 mmol) in Me-THF (4.0 mL) was stirred at 70 °C for 24 h. Subsequently, the reaction was cooled to room temperature, concentrated, and eluted from a column of silica gel with 1:2 cyclohexane:EtOAc to afford **5** (173 mg, 88%) as a colourless oil.

Procedure B: direct synthesis.

A mixture of HMF (98 μL, 1.00 mmol), $BuNH_2$ (500 μL, 5.00 mmol), **3** (28 mg, 0.05 mmol) and pre-catalyst **A** (156 mg, 0.20 mmol, loading = 1.28 mmol g^{-1}) in Me-THF (4.0 mL) was stirred under an air atmosphere (by an air-filled balloon). Then, DBU was added (75 μL, 0.50 mmol), and the reaction mixture was stirred at room temperature for 16 h. Subsequently, the reaction was filtrated, and the resin was washed with EtOAc and MeOH. Concentration of the solution, and elution from a column of silica gel with 1:2 cyclohexane:EtOAc afforded **5** (16 mg, 8%) as a colourless oil.

^{1}H NMR (300 MHz, $CDCl_3$) δ = 7.02 (d, *J* 3.4 Hz, 1H, Ar), 6.37 (d, *J* 3.4 Hz, 1H, Ar + bs, 1H, NH), 4.63 (s, 2H, OCH_2), 3.45 − 3.37 (m, 2H, $CH_{2(H\text{-}1butyl)}$), 1.81 (bs, 1H, OH), 1.63 − 1.52 (m, 2H, $CH_{2(H\text{-}2butyl)}$), 1.45 − 1.34 (m, 2H, $CH_{2(H\text{-}3butyl)}$), 0.95 (t, *J* 7.3 Hz, 3H, $CH_{3(butyl)}$); **^{13}C NMR** (101 MHz, $CDCl_3$) δ = 158.4 (*C*O), 155.5 (Ar*C*-2), 147.8 (Ar*C*-5), 114.6 (Ar*C*H-3), 110.0 (Ar*C*H-4), 57.4 (*C*H_2OH), 38.9 (*C*$H_{2(H\text{-}1butyl)}$), 31.7 (*C*$H_{2(H\text{-}2butyl)}$), 20.0 (*C*$H_{2(H\text{-}3butyl)}$), 13.7 $CH_{3(butyl)}$). **HRMS** (ESI/Q-TOF) calcd. for $C_{10}H_{16}NO_3$ ($[M + H]^+$): 198.1125; found: 198.1121.

General procedure for the oxidative esterification, thioesterification, and amidation of HMF or FF (Table 2)

A mixture of HMF (98 μL, 1.00 mmol) or FF (83 μL, 1.00 mmol), the stated nucleophile (5 equiv.), **3** (28 mg, 0.05 mmol) and precatalyst **A** (156 mg, 0.20 mmol, loading = 1.28 mmol g^{-1}) in Me-THF (4.0 mL) was stirred under an air atmosphere (by an airfilled balloon). Then, DBU was added (75 μL, 0.50 mmol), and the reaction was stirred at room temperature for 16 h. Filtration and washing (EtOAc and MeOH) of the resin, concentration, and elution of the resulting residue from a column of silica with the suitable elution system afforded the desired product.

Butyl 5-(hydroxymethyl)furan-2-carboxylate (6)

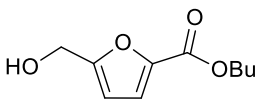

Column chromatography with 2:1 cyclohexane:EtOAc afforded **6** (123 mg, 62%) as a colorless liquid. **^{1}H NMR** (300 MHz, $CDCl_3$) δ = 7.12 (d, *J* 3.4 Hz, 1H, Ar), 6.41 (d, *J* 3.4 Hz, 1H, Ar),

4.68 (d, *J* 3.4 Hz, 2H, OCH_2), 4.30 (t, *J* 6.7 Hz, 2H, $CH_{2(H\text{-}1butyl)}$), 1.98 (t, *J* 3.4 Hz, 1H, OH), 1.78 − 1.66 (m, 2H, $CH_{2(H\text{-}2butyl)}$), 1.51 − 1.38 (m, 2H, $CH_{2(H\text{-}3butyl)}$), 0.96 (t, *J* 7.4 Hz, 3H, $CH_{3(butyl)}$); **^{13}C NMR** (101 MHz, $CDCl_3$) δ = 159.2 (*C*O), 158.5 (Ar*C*-2), 144.8 (Ar*C*-5), 118.9 (Ar*C*H-3), 109.7 (Ar*C*H-4), 65.2 ($CH_{2(H\text{-}1butyl)}$), 58.0 (CH_2OH), 31.1 ($CH_{2(H\text{-}2butyl)}$), 19.5 ($CH_{2(H\text{-}3butyl)}$), 14.0 ($CH_{3(butyl)}$). **HRMS** (ESI/Q-TOF) calcd. for $C_{10}H_{15}O_4$ ($[M + H]^+$): 199.0965; found: 199.0961.

(5-(Hydroxymethyl)furan-2-yl)(pyrrolidin-1-yl)methanone (7)

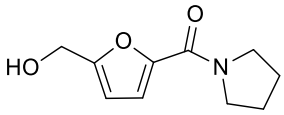

Column chromatography with 2:1 DCM:acetone afforded **7** (119 mg, 61%) as a colorless oil. **^{1}H NMR** (300 MHz, $CDCl_3$) δ = 6.96 (d, *J* 3.4 Hz, 1H, Ar), 6.37 (d, *J* 3.4 Hz, 1H, Ar), 4.65 (s, 2H, CH_2), 3.81 (t, *J* 6.7 Hz, 2H, $CH_{2(H\text{-}2pyrrolidin)}$), 3.64 (t, *J* 6.7 Hz, 2H, $CH_{2(H\text{-}5pyrrolidin)}$), 2.05 − 1.95 (m, 2H, $CH_{2(H\text{-}3pyrrolidin)}$), 1.95 − 1.84 (m, 2H, $CH_{2(H\text{-}4pyrrolidin)}$ + bs, 1H, OH); **^{13}C NMR** (101 MHz, $CDCl_3$) δ = 158.5 (*C*O), 156.3 (Ar*C*-2), 148.6 (Ar*C*-5), 116.7 (Ar*C*H-3), 109.4 (Ar*C*H-4), 58.0 (CH_2OH), 48.1 ($CH_{2(H\text{-}2pyrrolidin)}$), 47.3 ($CH_{2(H\text{-}5pyrrolidin)}$), 26.9 ($CH_{2(H\text{-}3pyrrolidin)}$), 24.1 ($CH_{2(H\text{-}4pyrrolidin)}$). **HRMS** (ESI/Q-TOF) calcd. for $C_{10}H_{14}NO_3$ ($[M + H]^+$): 196.0968; found: 196.0964.

S-Ethyl 5-(hydroxymethyl)furan-2-carbothioate (8)

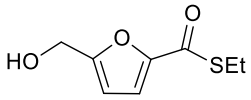

The reaction was conducted in the dark.[42] Column chromatography with DCM +2% acetone afforded **8** (89 mg, 48%) as a colorless oil. **^{1}H NMR** (300 MHz, $CDCl_3$) δ = 7.14 (d, *J* 3.5 Hz, 1H, Ar), 6.44 (d, *J* 3.5 Hz, 1H, Ar), 4.69 (s, 2H, OCH_2), 3.06 (q, *J* 7.4 Hz, 2H, $CH_{2(ethyl)}$), 1.98 (bs, 1H, OH), 1.34 (t, *J* 7.4 Hz, 3H, $CH_{3(ethyl)}$); **^{13}C NMR** (101 MHz, $CDCl_3$) δ = 180.9 (*C*O), 158.4 (Ar*C*-2), 150.9 (Ar*C*-5), 116.7 (Ar*C*H-3), 110.1 (Ar*C*H-4), 58.0 (CH_2OH), 23.0 ($CH_{2(ethyl)}$), 15.2 ($CH_{3(ethyl)}$). **HRMS** (ESI/Q-TOF) calcd. for $C_8H_{11}O_3S$ ($[M + H]^+$): 187.0423; found: 187.0420.

Butyl furan-2-carboxylate (10)

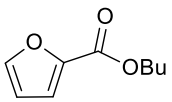

Column chromatography with 13:1 cyclohexane:EtOAc afforded **10** (152 mg, 90%) as a colorless oil with spectroscopic data in accordance with the literature.[50] **^{1}H NMR** (300 MHz, $CDCl_3$) δ = 7.57 (dd, *J* 1.7, 0.8 Hz, 1H, Ar), 7.17 (dd, *J* 3.5, 0.8 Hz, 1H, Ar), 6.50 (dd, *J* 3.5, 1.7 Hz, 1H, Ar), 4.31 (t, *J* 6.7 Hz, 2H, $CH_{2(H\text{-}1butyl)}$), 1.78 – 1.68 (m, 2H, $CH_{2(H\text{-}2butyl)}$), 1.51–1.39 (m, 2H, $CH_{2(H\text{-}3butyl)}$), 0.97 (t, *J* 7.4 Hz, 3H, $CH_{3(H\text{-}4butyl)}$); **^{13}C NMR** (101 MHz, $CDCl_3$) δ = 158.9 (*C*O), 146.1 (Ar*C*-2), 144.9 (Ar*C*H-5), 117.6 (Ar*C*H-3), 111.7 (Ar*C*H-4), 64.8 ($CH_{2(H\text{-}1butyl)}$), 30.7 ($CH_{2(H\text{-}2butyl)}$), 19.1 ($CH_{2(H\text{-}3butyl)}$), 13.7 ($CH_{3(H\text{-}4butyl)}$). **HRMS** (ESI/Q-TOF) calcd. for $C_9H_{13}O_3$ ($[M + H]^+$): 169.0859; found: 169.0855.

Furan-2-yl(pyrrolidin-1-yl)methanone (11)

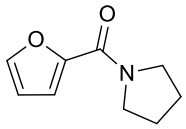

Column chromatography with 8:1 cyclohexane:EtOAc afforded **11** (132 mg, 79%) as a yellow oil with spectroscopic data in accordance with the literature.[41] **^{1}H NMR** (300 MHz, $CDCl_3$) δ = 7.49 (dd, *J* 1.7, 0.8 Hz, 1H, Ar), 7.05 (dd, *J* 3.4, 0.8 Hz, 1H, Ar), 6.48 (dd, *J* 3.4, 1.7 Hz, 1H, Ar), 3.83 (t, *J* 6.7 Hz, 2H, $CH_{2(H\text{-}2pyrrolidin)}$), 3.65 (t, *J* 6.7 Hz, 2H, $CH_{2(H\text{-}5pyrrolidin)}$), 2.05 – 1.93 (m, 2H, $CH_{2(H\text{-}3pyrrolidin)}$), 1.93 – 1.86 (m, 2H, $CH_{2(H\text{-}4pyrrolidin)}$); **^{13}C NMR** (101 MHz, $CDCl_3$) δ = 158.1 (*C*O), 148.8 (Ar*C*-2), 143.9 (Ar*C*H-5), 115.7 (Ar*C*H-3), 111.3 (Ar*C*H-4), 47.8 ($CH_{2(H\text{-}2pyrrolidin)}$), 47.0 ($CH_{2(H\text{-}5pyrrolidin)}$), 26.6 ($CH_{2(H\text{-}3pyrrolidin)}$), 23.7 ($CH_{2(H\text{-}4pyrrolidin)}$). **HRMS** (ESI/Q-TOF) calcd. for $C_9H_{12}NO_2$ ($[M + H]^+$): 166.0863; found: 166.0857.

S-Ethyl furan-2-carbothioate (12)

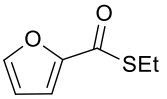

The reaction was conducted in the dark.[43] Column chromatography with 3:1 cyclohexane:DCM afforded **12** (82 mg, 52%) as a colorless oil. **^{1}H NMR** (300 MHz, $CDCl_3$) δ = 7.56 (dd, *J* 1.7, 0.7 Hz, 1H, Ar), 7.17 (dd, *J* 3.5, 0.7 Hz, 1H, Ar), 6.52 (dd, *J* 3.5, 1.7 Hz, 1H, Ar), 3.05 (q, *J* 7.3 Hz, 2H, $CH_{2(H\text{-}1ethyl)}$), 1.34 (t, *J* 7.3 Hz, 3H, $CH_{3(H\text{-}2ethyl)}$); **^{13}C NMR** (101 MHz, $CDCl_3$) δ = 180.7 (*C*O), 151.0 (Ar*C*-2), 145.9 (Ar*C*H-5), 115.2 (Ar*C*H-3), 112.1 (Ar*C*H-4), 22.6 ($CH_{2(ethyl)}$), 14.8 ($CH_{3(ethyl)}$). **HRMS** (ESI/Q-TOF) calcd. for $C_7H_9O_2S$ ($[M + H]^+$): 157.0318; found:157.0312.

Furoic acid (9)

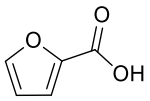

A mixture of FF (83 μL, 1.00 mmol), **3** (28 mg, 0.05 mmol) and pre-catalyst **A** (156 mg, 0.20 mmol, loading = 1.28 mmol g^{-1}) in 2:1 THF:H_2O (2.7 mL THF + 1.3 mL H_2O) was stirred under an air atmosphere (by an air-filled balloon). Then, DBU was added (75 μL, 0.50 mmol), and the reaction was stirred at room temperature for 16 h. Filtration, washing (EtOAc) of the resin and concentration of the solution afforded a residue that was diluted with EtOAc (5.0 mL) and 1 M HCl (5.0 mL). The aqueous phase was extracted with fresh portions of EtOAc (2 × 10 mL). The collected organic phases were washed with saturated $NaHCO_3$ solution (5.0 mL). Subsequently, the aqueous phase was acidified with 1 M HCl and extracted with EtOAc (2 × 10 mL). The combined organic phases were dried over Na_2SO_4 and concentrated to give furoic acid **9** (101 mg, 90%) at least 95% pure as judged by ^{1}H NMR analysis. Purification by crystallization (EtOH) afforded **9** as a gray solid with spectroscopic data in accordance with the literature.[49] **mp** 129−130 °C (EtOH) {Lit.[52] 130−132 °C}; **^{1}H NMR** (300 MHz, $CDCl_3$) δ = 10.22 (bs, 1H, OH), 7.64 (d, *J* 1.6 Hz, 1H, Ar), 7.33 (d, *J* 3.4 Hz, 1H, Ar), 6.55 (dd, *J* 3.4, 1.6 Hz, 1H, Ar); **^{13}C NMR** (101 MHz, $CDCl_3$) δ = 163.4 (*C*O), 147.4 (Ar*C*-2), 143.9 (Ar*C*H-5), 120.0 (Ar*C*H-3), 112.2 (Ar*C*H-4). **HRMS** (ESI/Q-TOF) calcd. for $C_5H_5O_3$ ($[M + H]^+$): 113.0233; found: 113.0229.

Continuous-flow production of selected HMF and FF oxidation products (Table 3)

The continuous flow apparatus setup was made of two binary pumps (Agilent 1100 and Agilent 1100 micro series) and the microreactor **R1** was fabricated by using a 10 × 0.46 cm stainless-steel column as described in reference 33. Channel-A was used to deliver a continuously degassed solution of HMF (0.25 M) [or FF (0.25 M)] and the nucleophile (0.75 M) dissolved in Me-THF. Channel-B, instead, delivered a continuously degassed solution of DBU (0.12 M) and **1** (0.25 M) in Me-THF. The feed solutions were pumped at the stated flow rate (reported in Table 3) through the 3-way valve. Microreactor **R1** was initially activated by pumping (channel B, 50 μL min^{-1} for 20 min) a degassed solution of DBU (0.75 M). The microreactor operated for 6 h under steady-state conditions. Later, the collected solution was concentrated, and eluted from a column of silica gel with the suitable elution system to recover first the alcohol **1'** and then give the products **4**, **7**, **10**, **11**. The quantitative oxidation of **1'** to the Kharasch oxidant **1** was performed with air (1 atm, balloon) and catalytic phthalocyanine **3** (10 mol%, THF, RT).[33]

4.5 References and notes

1. B. Kamm, *Angew. Chem., Int. Ed.,* **2007**, *46*, 5056−5058.
2. R. A. Sheldon, *Catal. Today*, **2011**, *167*, 3.
3. C. O. Tuck, E. Pérez, I. T. Horváth, R. A. Sheldon, M. Poliakoff, *Science*, **2012***, 337*, 695−699.
4. R. A. Sheldon, *Green Chem.,* **2014**, *16*, 950−963.
5. A. A. Rosatella, S. P. Simeonov, R. F. Frade, C. A. Afonso, *Green Chem.,* **2011**, *13*, 754−793.
6. X. Li, P. Jia, T. Wang, *ACS Catal.,* **2016**, *6*, 7621−7640.
7. J. J. Bozell, G. R. Petersen, *Green Chem.,* **2010**, *12*, 539−554.
8. R.-J. van Putten, J. C. van der Waals, E. de Jong, C. B. Rasrendra, H. J. Heeres and J. G. de Vries, *Chem. Rev.,* **2013**, *113*, 1499−1597.
9. C. Moreau, M. N. Belgacem, A. Gandini, *Top. Catal.,* **2004**, *27*, 11−30.
10. E. de Jong, M. A. Dam, L. Sipos, G. J. M. Gruter, *ACS Symp. Ser.,* **2012**, *1105*, 1−13.
11. A. F. Sousa, C. Vilela, A. C. Fonseca, M. Matos, C. S. R. Freire, G. J. M. Gruter, J. F. J. Coelho, A. J. D. Silvestre, *Polym. Chem.,* **2015**, *6*, 5961−5983.
12. D. T. Richter, T. D. Lash, *Tetrahedron Lett.,* **1999**, *40*, 6735−6738.
13. A. Gandini, M. N. Belgacem, *Prog. Polym. Sci.,* **1997**, *22*, 1203−1379.
14 A. S. Amarasekara, D. Green, L. D. Williams, *Eur. Polym. J.,* **2009**, *45*, 595−598.
15. J. Ma, Z. Du, J. Xu, Q. Chu, Y. Pang, *ChemSusChem,* **2011**, *4*, 51−54.
16. H. Hirai, *J. Macromol. Sci., Part A: Pure Appl. Chem.*, **1984**, *21*, 1165−1179.
17. S. E. Davis, L. R. Houk, E. C. Tamargo, A. K. Datye and R. J. Davis, *Catal. Today,* **2011**, *160*, 55−60.
18. M. Munekata, G. Tamura, *Agric. Biol. Chem.,* **1981**, *45*, 2149−2150.
19. A. C. Braisted, J. D. Oslob, W. L. Delano, J. Hyde, R. S. McDowell, N. Waal, C. Yu, M. R. Arkin, B. C. Raimundo, *J. Am. Chem. Soc.,* **2003**, *125*, 3714−3715.
20. The classical Cannizzaro reaction has also been described for the synthesis of HMFCA with the limit of the maximum theoretical selectivity (50%) due to the concomitant formation of equimolar 2,5-dihydroxymethylfurfural (DHMF): S. Subbiah, S. P. Simeonov, J. M. S. S. Esperanca, L. P. N. Rebelo, C. A. M. Afonso, *Green Chem.,* **2013**, *15*, 2849−2853.
21. O. Casanova, S. Iborra and A. Corma, *ChemSusChem,* 2009, **2**, 1138−1144.
22. Y. Y. Gorbanev, S. K. Klitgaard, J. M. Woodley, C. H. Christensen, A. Riisager, *ChemSusChem,* **2009**, *2*, 672−675.
23. S. E. Davis, B. N. Zope, R. J. Davis, *Green Chem.,* **2012**, *14*, 143−147.
24. S. E. Davis, A. D. Benavidez, R. W. Gosselink, J. H. Bitter, K. P. De Jong, A. K. Datye, R. J. Davis, *J. Mol. Catal. A: Chem.,* **2014**, *388*, 123−132.
25. Z. Zhang, B. Liu, K. Lv, J. Sun and K. Deng, *Green Chem.,* **2014**, *16*, 2762−2770.
26. D. X. Martínez-Vargas, J. R. De La Rosa, L. Sandoval-Rangel, J. L. Guzmán-Mar, M. A. Garza-Navarro, C. J. Lucio-Ortiz, D. A. De Haro-Del Río, *Appl. Catal., A,* **2017**, *547*, 132−145.
27. M. Krystof, M. Perez-Sanchez, P. Dominguez de Maria, *ChemSusChem,* **2013**, *6*, 826−830.
28. Y. Z. Qin, Y. M. Li, M. H. Zong, H. Wu, N. Li, *Green Chem.,* **2015**, *17*, 3718−3722.
29. K. Mitsukura, Y. Sato, T. Yoshida, T. Nagasawa, *Biotechnol. Lett.,* **2004**, *26*, 1643−1648.
30. X.-Y. Zhang, M.-H. Zong, N. Li, *Green Chem.,* **2017**, *19*, 4544−4551.
31. B. Zhou, J. Song, Z. Zhang, Z. Jiang, P. Zhang, B. Han, *Green Chem.,* **2017**, *19*, 1075−1081.
32. N. K. Gupta, A. Fukuoka, K. Nakajima, *ACS Sustainable Chem. Eng.,* **2018**, *6*, 3434−3442.
33. Ragno D., Brandolese A., Urbani D., Di Carmine G., De Risi C., Bortolini O., Giovannini P. P., Massi A., *React. Chem. Eng.*, **2018**, *3*, 816−825.
34. S. De Sarkar, A. Biswas, R. C. Samanta, A. Studer, *Chem.Eur. J.*, **2013**, *19*, 4664−4678.
35. O. Bortolini, C. Chiappe, M. Fogagnolo, P. P. Giovannini, A. Massi, C. S. Pomelli, D. Ragno, *Chem. Commun.*, **2014**, *50*, 2008−2011.

36. O. Bortolini, C. Chiappe, M. Fogagnolo, A. Massi, C. S. Pomelli, *J. Org. Chem.*, **2017**, *82*, 302−312.
37. E. G. Delany, C.-L. Fagan, S. Gundala, K. Zeitler, S. J. Connon, *Chem. Commun.,* **2013**, *49*, 6513−6515.
38. Y. Orihashi, M. Nishikawa, H. Ohno, E. Tsuchida, H. Matsuda, H. Nakanishi, M. Kato, *Bull. Chem. Soc. Jpn.,* **1987**, *60*, 3731−3738.
39. R. S. Reddy, J. N. Rosa, L. F. Veiros, S. Caddick, P. M. P. Gois, *Org. Biomol. Chem.,* **2011**, *9*, 3126−3129.
40. V. Pace, P. Hoyos, L. Castoldi, P. Domínguez de María, A. R. Alcántara, *ChemSusChem*, **2012**, *5*, 1369−379.
41. V. Kumar, S. J. Connon, *Chem. Commun.,* **2017**, *53*, 10212−10215.
42. This reaction was performed in the dark to prevent the photoinduced oxidation of ethanethiol promoted by phthalocyanine **3**: P. Kumar, G. Singh, D. Tripathi, S. L. Jain, *RSC Adv.,* **2014**, *4*, 50331−50337.
43. G. R. Dick, A. D. Frankhouser, A. Banerjee, M. W. Kanan, *Green Chem.,* **2017**, *19*, 2966−2972.
44. J. Piera, J.-E. Bäckvall, *Angew. Chem., Int. Ed.*, **2008**, *47*, 3506−3523.
45. A. Axelsson, A. Antoine-Michard, H. Sundén, *Green Chem.*, **2017**, *19*, 2477−2481 and reference therein.
46. Z. Mou, S. K. Feng, E. Y.-X. Chen, *Polym. Chem.,* **2016**, *7*, 1593−1602.
47. A. Dunbabin, F. Subrizi, J. M. Ward, T. D. Shepparda, H. C. Hailes, *Green Chem.,* **2017**, *19*, 397−404.
48. C. Schmuck, U. Machon, *Eur. J. Org. Chem.,* **2006**, 4385−4392.
49. V. Nair, V. Varghese, R. R. Paul, A. Jose, C. R. Sinu, R. S. Menon, *Org. Lett.,* **2010**, *12*, 2653−2655.
50. M. Pittelkow, F. S. Kamounah, U. Boas, B. Pedersen, J. B. Christensen, *Synthesis,* **2004**, 2485−2492.
51. S. Nielek, T. Leslak, *J. Prakt. Chem.,* **1988**, *330*, 825−829.
52. T.-L. Ho, *Synthesis,* **1972**, 560.

5. Oxidative NHC-catalysis as organocatalytic platform for the synthesis of polyester oligomers by step-growth polymerization

The work described in this chapter has formed the basis of the following peer reviewed publication: D. Ragno, G. Di Carmine, A. Brandolese, O. Bortolini, P. P. Giovannini, G. Fantin, M. Bertoldo, A. Massi, *Chem. Eur. J.*, **2019**, *25(64),* 14701−14710.

5.1 Introduction

In the past decade, organocatalyst applications have been hugely increased, including the macromolecular synthesis for polymer material productions. These new strategies, complementary to metal-catalysed approaches, avoid the presence of any metallic residues in the products and show to be useful in high-value applications in the areas of microelectronic and biomedical devices or food packaging.[1] Numerous organic activators, including Brønsted/Lewis acids or bases have been used as catalysts, both for chain-growth polymerizations and step-growth, and for depolymerization reactions as well. However, whereas organocatalytic chain-growth polymerizations have been deeply explored,[2] the use of organocatalysts for the synthesis of polyesters (PEs), polyurethanes (PUs), and polycarbonates (PCs) by step-growth polymerization is more restricted. Among all the types of polymers, polyester materials cover almost the 18% of the world plastic production, finding applications in food packaging, clothing, biomedical, and electronic devices.[3] These compounds can be easily accessed through three main strategies, which include ring-opening polymerization (ROP) of cyclic esters (chain-growth process), self-polycondensation of hydroxy acids and step-growth polymerization of diols and diacids or their derivatives (Figure 1).[4]

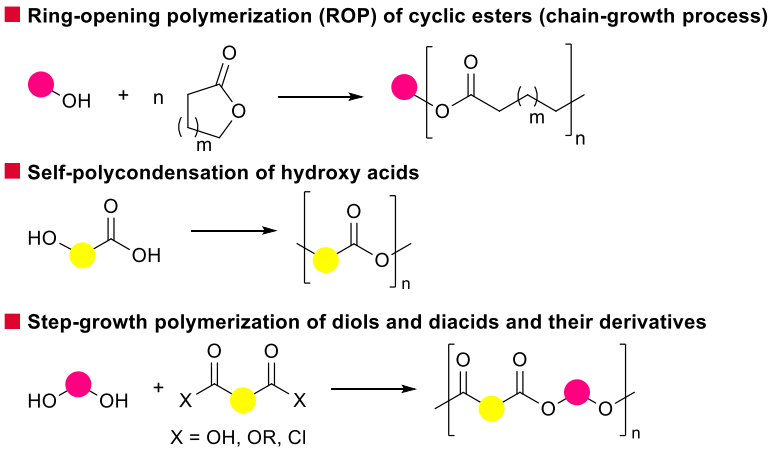

Figure 1. Main synthetic strategies for the synthesis of polyesters.

The latter, as already mentioned, has not been largely investigated yet, although the modularity and compatibility with functionalized monomers to access a wide range of polymers for diversified applications is easily feasible by this method.[5] On the contrary, the polycondensation of diols and activated carboxylic derivatives represents the favourite synthetic route for industry, although the ROP promises an accurate control of dispersity and molecular weight.[3,4] In this research field, N-heterocyclic carbenes (NHCs)[6] turned out to be interesting organocatalysts thanks to their peculiar features (Figure 2).

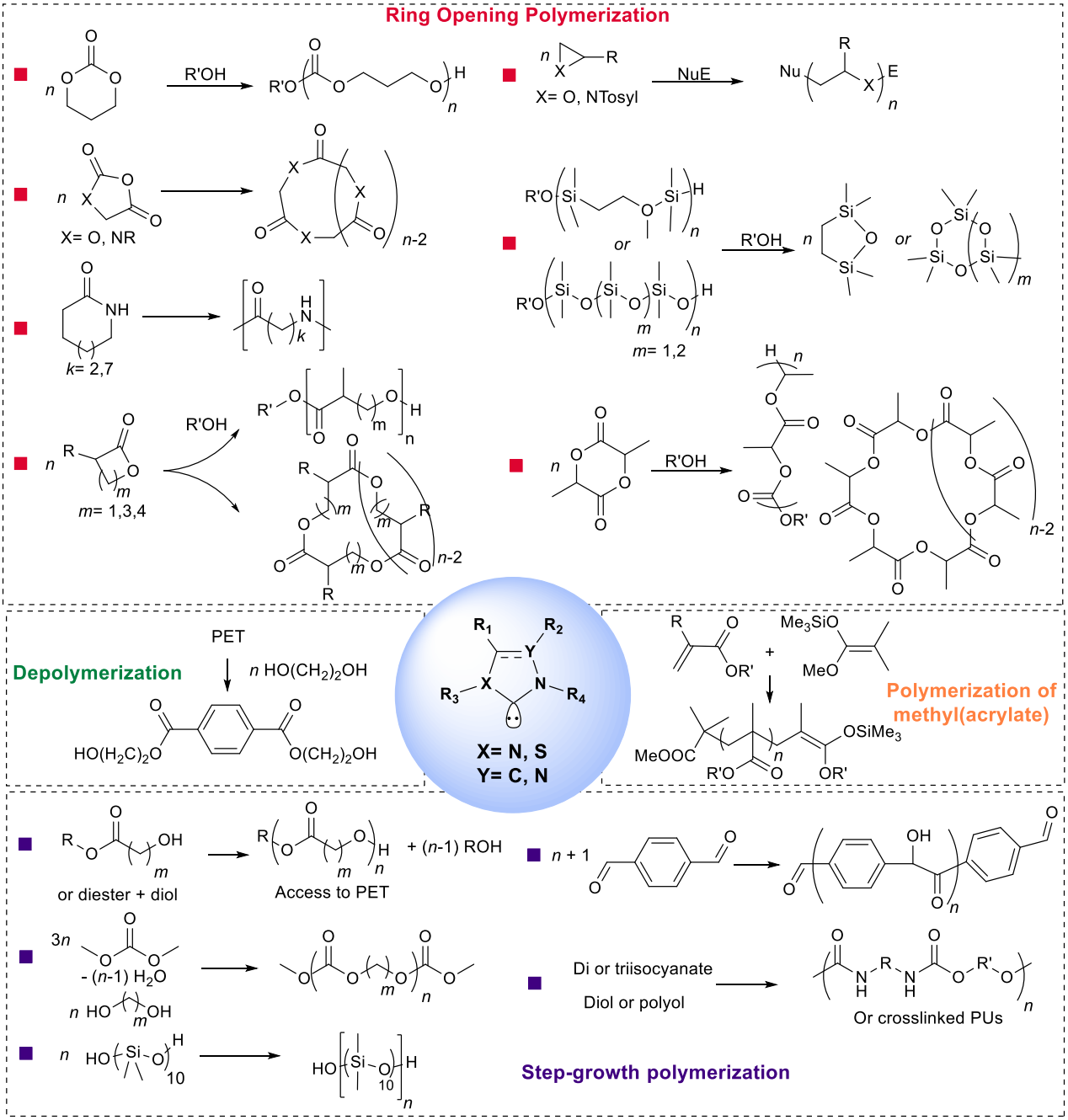

Figure 2. Scope of NHC-mediated polymerization reactions.

Indeed, they show ambiphilicity (σ-basicity and π-acidity), moderate nucleophilicity, and strong basicity[6] and for these reasons, all types of catalytic activation modes by NHCs have been conveniently exploited for the preparation of polymers. Numerous monomers such as lactones, anhydrides, carbonates, epoxides, lactams, siloxanes, acrylates, and aldehydes, have been employed under mainly ring opening and step-growth polymerization processes (Figure 2).[7,8]However, the applications in the step-growth polymerization to polyesters through NHCs catalysis remain scarcely explored, in fact, the sole poly-condensation of ethyl glycolate and the synthesis of polyethylene terephthalate (PET) by two-step strategy has been reported.[9] In particular, the ambiphilic character of NHCs has been used for the polybenzoin condensation of terephthalaldehyde[10] and the iterative Stetter reaction of dialdehydes and enones affording polymeric 1,4-diketones (Scheme 1a).[11] As well known, these procedures rely on the formation of the nucleophilic Breslow intermediate,[12] while oxidative protocols have not been reported yet. The formation of the acyl azolium intermediate, in fact, emerged as useful tools for the direct conversion of aldehydes into esters,[13,14] thus inspiring the rationalization of a new atom-economical synthetic route to polyester by step-growth polymerization technique (Scheme 1b).

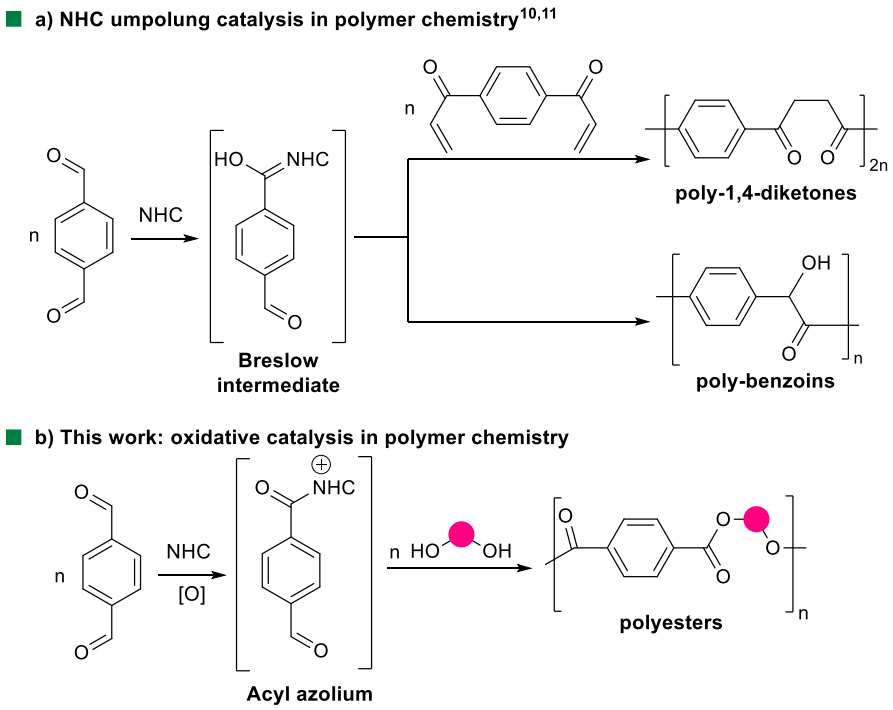

Scheme 1. NHC umpolung and oxidative catalysis in polymer chemistry.

This unprecedented polycondensation of dialdehydes and diols was initially applied for the synthesis of PET and subsequently for polyethylene isophthalate (PEI) oligomers. Furthermore, the potential of the revealed methodology for engineering polymers has been validated by the polycondensation of bio-based furanic monomers, glycerol, and isosorbide in order to access interesting polyester oligomers for the development of environmentally benign macromolecular

materials. Indeed, the union of environmental concerns and the desire to reduce the dependence on fossil fuels encouraged the investigation on the polymerization of monomers derived from renewable feedstocks.[12,15,16] Worth to note, oligoesters can be used not only to prepare thermoplastic polyesters through subsequent polycondensations but also as components in thermosetting resins and formulations along with isocyanates (polyurethane), urea (polyester-urea) or anhydrides (alkydic resins) to obtain high performance composites, adhesives, coatings or inks.

5.2 Results and discussion

Preliminary investigation on oxidative NHC-catalysed step-grow polymerization focused on the polycondensation of ethylene glycol **1a** and terephthalaldehyde **2a** in the presence of the inexpensive triazolium salt **A** and DBU as the base. According to the results reported in the Chapter 4, this precatalyst/base couple proved to be effective in the NHC-promoted esterification of aldehydes under different oxidative conditions.[17] Moreover, a slight excess of diol **1a** (1.1 equiv.) showed to be necessary in order to promote the formation of bis-hydroxyl-terminated polymers. To increase the process sustainability, initially the biomimetic system of electron transfer mediators (ETMs; **4**/**5**) was employed to verify the use of air as the terminal oxidant (Table 1, entry 1). Unfortunately, a low conversion of aldehyde was observed (20−22%) in anhydrous THF after 16 hours and the increase of the temperature to 60 °C did not improve the reaction outcome (entry 2). On the other hand, the use of stoichiometric amount of the Kharasch oxidant **6** turned out to be crucial both for the increase of the conversion (75%, 2 hours reaction time) and for the isolation of **3aa** (precipitation into excess of methanol) with a number-average molecular weight (*Mn*) as determined by ^{1}H NMR analysis of 4.2 kg mol^{-1} (entry 3). By extending the reaction time, an increasing of oligomer length (*Mn* = 6.5 kg mol^{-1}) was observed (entry 4). Further attempts to reduce the competitive nucleophilic attack by water through the addition of 4Å molecular sieves (MS) did not produce the desired outcome (entry 5). Neither heating of the reaction mixture (60 °C) nor the replacement of THF with anhydrous DCM or with the biomass-derived Me-THF showed enhancement of the polymer growth (entries 6−8). Lastly, the replacement of Kharasch oxidant **6** with azobenzene **7** (entry 9) or phenazine **8** (entry 10) produced unsatisfactory results as well. As no further increasing in the number-average molecular weight could be obtained, the gram-scale synthesis of **3aa** (1.69 g, 88% isolated yield) starting from 10 mmol of aldehyde **2a** (entry 11) was carried out.

Table 1. Optimization of the reaction conditions for the synthesis of PET oligomers **3aa**.[a]

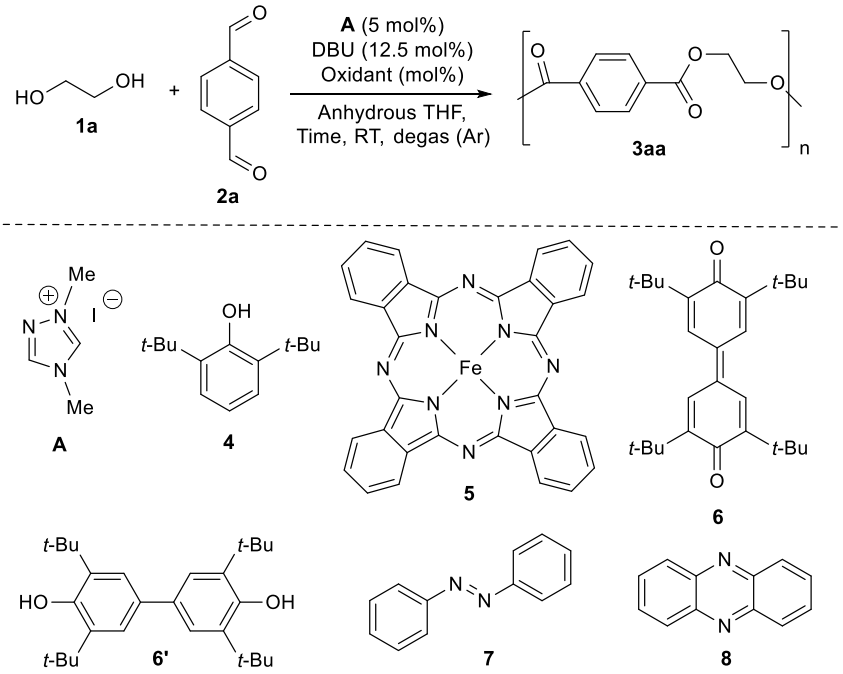

Entry	Oxidant	Time (h)	Conv. (%)[b]	**3aa** (%)[c]	M_n (kg mol^{-1})[d]
1	Air, **4** (10 mol%)/**5** (2.5 mol%)	16	20	10	n.d.
2[e]	Air, **4** (10 mol%)/**5** (2.5 mol%)	16	22	11	n.d.
3	**6** (100 mol%)	2	75	61	4.2
4	**6** (100 mol%)	**16**	**>95**	**82**	**6.5**
5[f]	**6** (100 mol%)	16	>95	80	6.5
6[e]	**6** (100 mol%)	16	>95	71	6.2
7[g]	**6** (100 mol%)	16	>95	80	6.3
8[h]	**6** (100 mol%)	16	>95	78	5.8
9	**7** (100 mol%)	2	-	-	-
10	**8** (100 mol%)	2	61	44	1.9
11[i]	**6** (100 mol%)	16	>95	88	6.5

[a]Conditions: **1a** (0.88 mmol), **2a** (0.80 mmol), **A** (0.08 mmol), DBU (0.20 mmol), THF (6.0 mL). [b]Detected by ^{1}H NMR of the crude reaction mixture (durene as internal standard). [c]Isolated yield *via* precipitation into excess methanol (see the Experimental section). [d]Calculated by ^{1}H NMR after precipitation of the polymer. [e]T = 60 °C. [f]Reaction run in presence of 4Å MS. [g]Anhydrous DCM as solvent. [h]Me-THF as solvent. [i]Conditions: **1a** (11.0 mmol), **2a** (10.0 mmol), **A** (1.00 mmol), **6** (20 mmol), DBU (2.5 mmol), THF (60 mL).

The synthesis of high molecular weight PET was further achieved through an NHC-promoted two-step procedure in analogy with the studies of Waymouth,[9] Hedrick,[9] Sardon,[18] and their co-workers (Scheme 2 and Table 2, entry 2). Therefore, isolated **3aa** (*Mn* = 6.5 kg mol^{-1}) was heated at 250 °C for 2 hours under vacuum in the presence of triazolium pre-catalyst **A** (5 mol%) and DBU (5 mol%) affording PET **3aa'** with high molecular weight, as evidenced by the disappearance of the end group signals in the ^{1}H NMR spectrum (it was not possible to determine the *Mn* through ^{1}H NMR analysis).

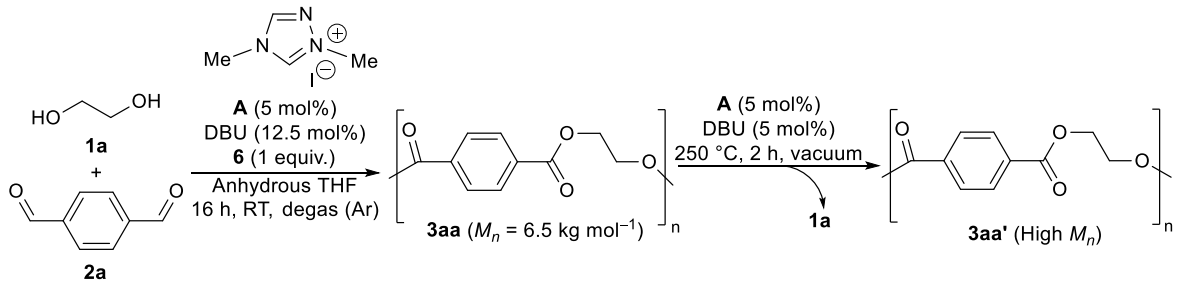

Scheme 2. NHC-promoted two-step procedure for the synthesis of high molecular weight PET **3aa'.**

The scope of this methodology was additionally proved with the preparation of isophthalate oligomers **3ab** (*Mn* = 6.5 kg mol^{-1}; 77% yield), readily obtained from diol **1a** and isomeric isophthalaldehyde **2b** (Table 2, entry 3). Extending the utility of the methodology was targeted through the use of renewable monomers, including the abundant and inexpensive glycerol for the synthesis of bio-based polymers. Indeed, polyesters derived from glycerol find important applications in pharmaceutical and biomedical fields as drug delivery agents,[19] surgical adhesives,[20] and tissue engineering scaffolds.[21] However, a controlled degree of acylation of glycerol PEs is highly desiderable[22,23] as the physical properties of polyglycerol esters strongly depend on the linear or branched microstructure of the glycerol unit.[24] The use of the optimized reaction conditions with terephthalaldehyde **2a** and glycerol **1b**, however, led to a rapid and quantitative formation of poly(glycerol terephthalate) (PGT) **3ba'** as a gel-like material, which was insoluble in common organic solvents (DCM, THF, DMSO, DMF) likely because of the high content of triacylglycerol units (Scheme 3a and Table 2, entry 4). Bearing in mind the challenge to propose an alternative metal-free procedure able to control the acylation of glycerol monomers, a screening of the reaction conditions conducted to the synthesis of linear PGT. Indeed, pre-catalyst **B** in combination with triethylamine in dilute solution emerged to be suitable to produce linear PGT oligomers **3ba** (*Mn* = 1.5 kg mol^{-1}) in 71% yield after precipitation (Scheme 3b and Table 2, entry 5). The catalyst screening suggested that the structural variation of NHC catalyst might allow the regioselective activation of the polyol substrate to produce polyesters with a well-defined architecture. Although the presented strategy did not permit to achieve high molecular weight linear PGT **3ba**, the maintenance of polyester microstructure was still observed, thanks to the mild reaction conditions that precluded acyl group migration during the polycondensation. Moreover, the detailed study by Slawko and Taylor on the characterization of glycerol-based PEs,[23] indicated that the formation of triacyl and 1,2-diacylglycerol motifs in **3ba** could be excluded by quantitative ^{13}C NMR analysis (DMSO-d_6) using chromium(III) acetylacetonate as relaxation agent.

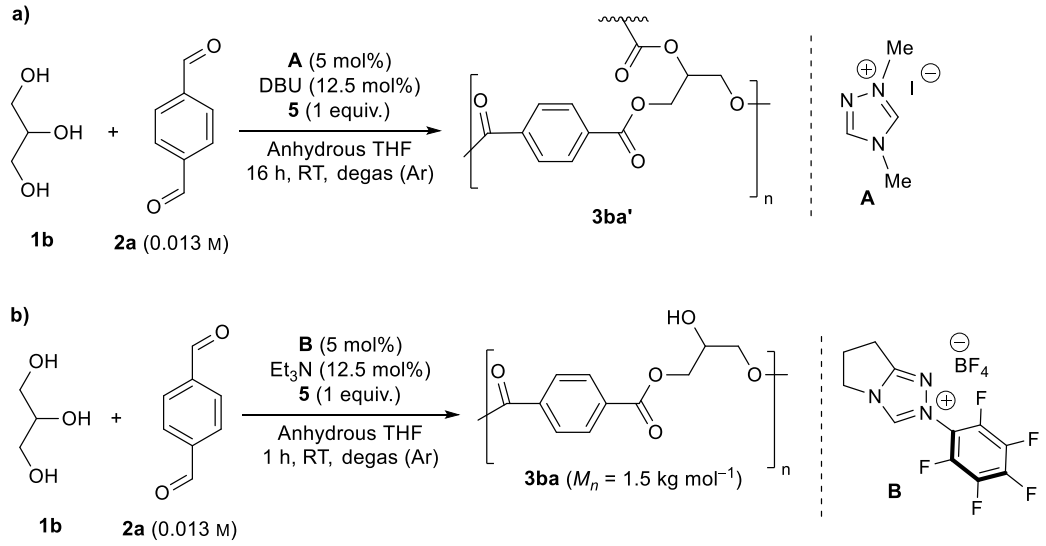

Scheme 3. Optimized conditions for the synthesis of (a) cross-linked **3ba'**and (b) linear **3ba** polyglycerol esters.

Table 2. Scope of the oxidative polycondensation of diols **1** and dialdehydes **2**.

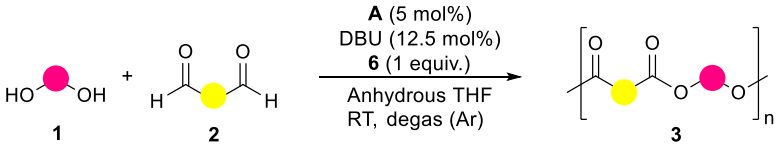

Entry	Diol	Dialdehyde	Polyester	M_n (kg/mol)[a]
1	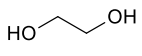 **1a**	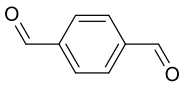 **2a**	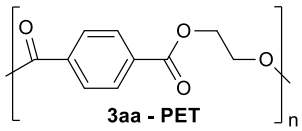 **3aa - PET** Y= 82%	6.5
2[b]	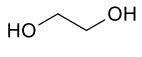 **1a**	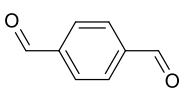 **2a**	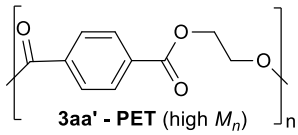 **3aa' - PET** (high M_n) Y= 78%	-
3	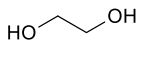 **1a**	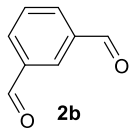 **2b**	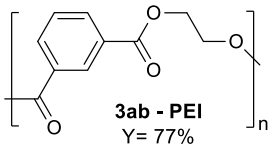 **3ab - PEI** Y= 77%	6.5
4	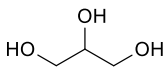 **1b**	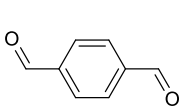 **2a**	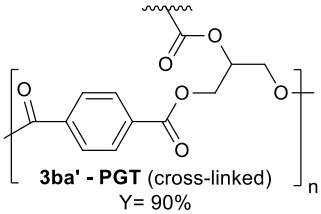 **3ba' - PGT** (cross-linked) Y= 90%	-
5[c]	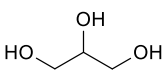 **1b**	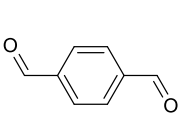 **2a**	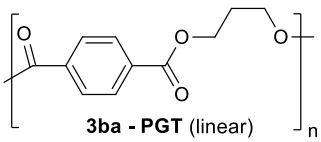 **3ba - PGT** (linear) Y= 71%	1.5

Conditions: **1** (0.88 mmol), **2** (0.80 mmol), **A** (0.08 mmol), DBU (0.20 mmol), **6** (1.60 mmol), THF (6.0 mL). All the reported yields are for the isolated product. [a]Calculated by ^{1}H NMR after precipitation of the polymer. [b]See Scheme 2 and the Experimental section for reaction conditions. [c]Performed with pre-catalyst **B** (0.08 mmol), Et_3N (0.20 mmol), THF (60 mL).

To expand the product diversity accessible through this method, the oxidative polycondensation protocol with other bio-based dialdehydes was investigated by the utilization of furan aldehydes derived from 5-hydroxymethyl furfural (HMF), namely 2,5-diformylfuran (DFF) **2c** and 5,5′-oxybis(methylene)bis-2-furaldehyde (OBFA) **2d** (Table 2). These two compounds have been recently used as monomers to prepare furan-urea resins and imine-based polymers,[25,26] and also as suitable precursors of the corresponding diacids, 2,5-furandicarboxylic acid (FDCA)[27] and 5,5′-oxybis(methylene)bis-2-furancarboxylic acid (OBFC).[28] In fact, the former is nowadays more and more used in place of terephthalic acid for the synthesis of PEs from renewable resources. The interesting mechanical and barrier properties showed by poly(ethylene furanoate)[29] has driven companies to create new building plants for industrial scale production. Likewise, the difuranic-diacid OBFC is under investigation for the synthesis of novel polyester-ether materials, including the promising poly(ethylene 5,5'-(oxybis(methylene)bis(2-furancarboxylate) (PEOBF).[28] Thus, using the optimized reaction conditions, PEF and PEOBF oligomers **3ac** (Mn = 1.5 kg mol^{-1}) and **3ad** (Mn = 3.5 kg mol^{-1}) were readily prepared starting from DFF and OBFA dialdehydes **2c** and **2d** in place of the corresponding acids FDCA and OBFC (Table 2, entries 6 and 7). The presence of a furan moiety was also studied by considering the use of 2,5-bis(hydroxymethyl)furan (BHMF) **1c**,[30] an HMF-derived diol widely employed to prepare PEs and PUs.[31] BHMF **1c** along with terephthalaldehyde **2a** produced poly(2,5-furandimethylene terephthalate)[32] (PBHMT) oligomers **3ca** (Mn = 3.1 kg mol^{-1}) with good efficiency (81% yield; Table 2, entry 8). The production of fully furan-based polyester was addressed through the replacement of **2a** with 2,5-diformylfuran **2c** yielding the poly(2,5-furandimethylene 2,5-furandicarboxylate) (PBHMF)[31] **3cc** with the highest molecular weight registered in this study (Mn = 7.8 kg mol^{-1}; Table 2, entry 9). It is worth noting that this mild polycondensation is compatible with the use of BHMF diol which showed low thermal stability in solution polymerizations.[31a] Variation of the diol was achieved through the use of isosorbide (IS) **1d**, which is a renewable compound (1,4:3,6-dianhydro-D-glucitol) available from glucose and cellulose. This secondary alcohol has recently gained a lot of attention in polymer chemistry in virtue of its rigid structure, chirality, and non-toxicity.[33] The polymers poly(isosorbide)terephthalate[31a,34] (PIT) and poly(isosorbide 2,5-furandicarboxylate)[35,36] (PIF) obtained with terephthalaldehyde and HMF, respectively, find applications as packaging materials owing to their excellent thermal and structural properties. Under the optimized oxidative conditions, PIT oligomers **3da** (Mn = 2.8 kg mol^{-1}) and PIF oligomers **3dc** (Mn = 2.7 kg mol^{-1}) were prepared in good yields (71−72%; entries 10, 11) even though the recorded Mn was too low for industrial applications. In these oligomers, the terminal isosorbide units were enchained through the more nucleophilic C5 hydroxyl group, as confirmed by ^{1}H NMR analysis

and through comparison with authentic samples of C2 and C5 benzoylated isosorbide derivatives (see the Experimental section for further details).

Table 2 (continued). Scope of the oxidative polycondensation of diols **1** and dialdehydes **2**.

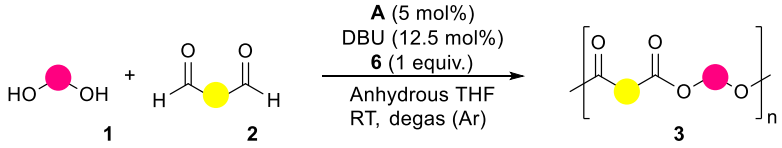

Entry	Diol	Dialdehyde	Polyester	M_n (kg/mol)[a]
6	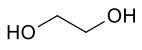 **1a**	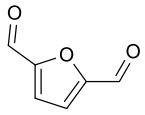 **2c** (DFF)	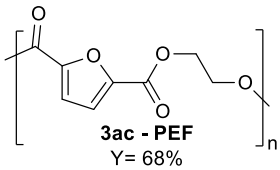 **3ac - PEF** Y= 68%	1.5
7	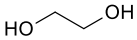 **1a**	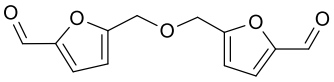 **2d** (OBFA)	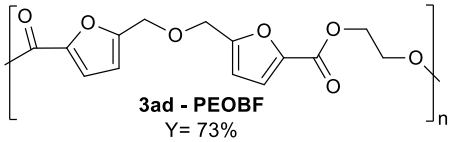 **3ad - PEOBF** Y= 73%	3.5
8	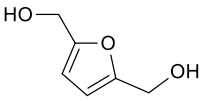 **1c** (BHMF)	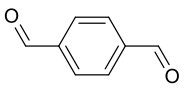 **2a**	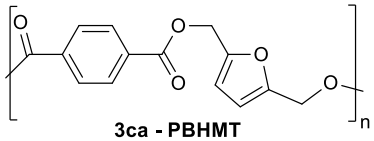 **3ca - PBHMT** Y= 81%	3.1
9	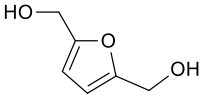 **1c** (BHMF)	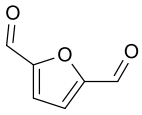 **2c** (DFF)	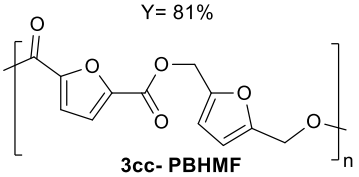 **3cc- PBHMF** Y= 78%	7.8
10	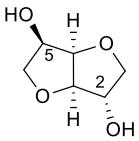 **1d** (IS)	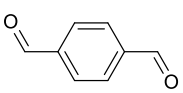 **2a**	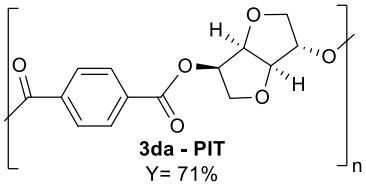 **3da - PIT** Y= 71%	2.8
11	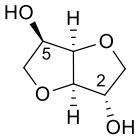 **1d** (IS)	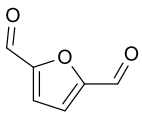 **2c** (DFF)	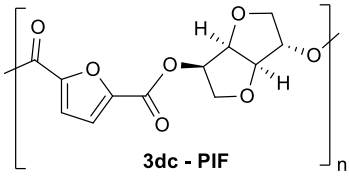 **3dc - PIF** Y= 72%	2.7

Conditions: **1** (0.88 mmol), **2** (0.80 mmol), **A** (0.08 mmol), DBU (0.20 mmol), **6** (1.60 mmol), THF (6.0 mL). All the reported yields are for the isolated product. [a]Calculated by ^{1}H NMR after precipitation of the polymer. [c]Performed with pre-catalyst **B** (0.08 mmol), Et_3N (0.20 mmol), THF (60 mL).

Scope and limitation of the disclosed procedure were further investigated by the screening of *ortho*-difunctionalized or trifunctionalized aromatic monomers as well as aromatic alcohols, which are known to be poorly reactive substrates in NHC promoted esterifications (Scheme 4).[13] As proved by NMR analysis, the polymerization of *o*-phthaldialdehyde **2e** with ethylene

glycol **1a** produced a complex mixture of compounds with no evidence of ester linkage formation (Scheme 4a). The target polyester **3af** was instead obtained in 79% yield after purification (Schema 4b) for the reaction of 1,3,5-tricarboxaldehyde **2f** with **1a**. However, due to the highly cross-linked structure, this polymer was insoluble in all common organic solvents. Gratefully, hydroquinone **1e** reacted efficiently with terephthalaldehyde **2a** furnishing the fully aromatic **3ea** in 88% yield but with low molecular weight (Mn = 0.4 kg mol^{-1}, Scheme 4c).[37] Lastly, aromatic triol 1,3,5-trihydroxybenzene (phloroglucinol) **1f** resulted to be unreactive in the polycondensation with **2a** under the disclosed polymerization conditions (Scheme 4d). The behaviour of aliphatic aldehydes was not explored as the basic reaction conditions would have led to competitive aldol reactions with a low conversion into the desired oligomers.

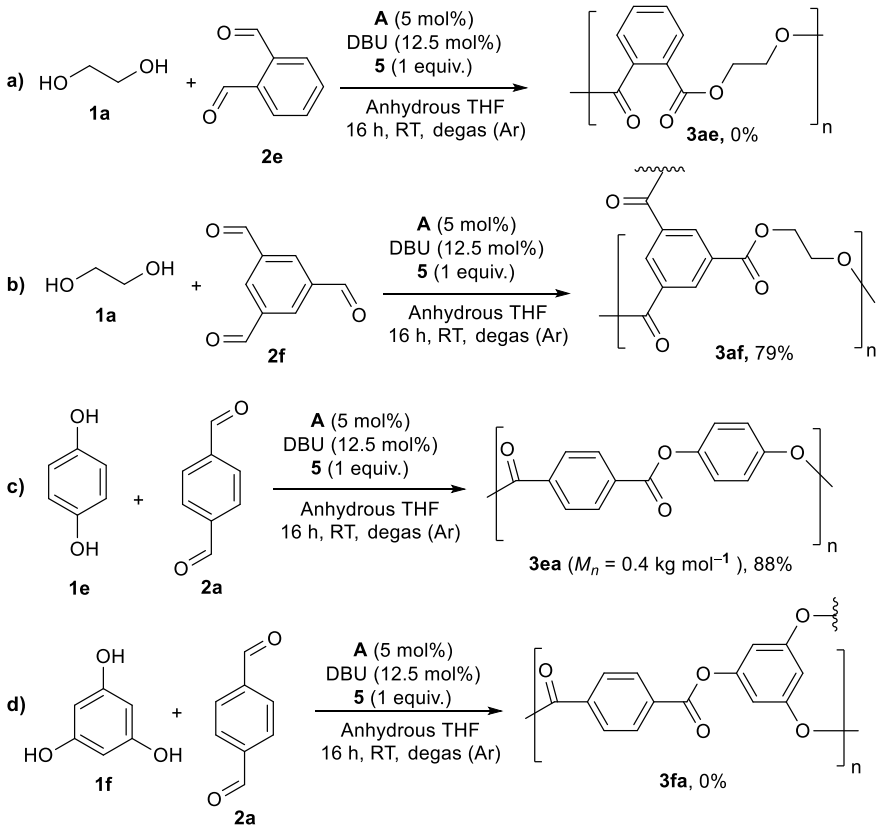

Scheme 4. Scope and limitation of the procedure with *o*-difunctionalized or trifunctionalized aromatic monomers and aromatic alcohols.

Furthermore, in parallel with the scope and optimisation studies, the recycling of both DBU and oxidant **6** was investigated for the development of a more sustainable polymerization procedure. Using the benchmark reaction for the preparation of polyester **3aa**, an operative protocol has been optimized. Accordingly, the reaction mixture containing **3aa** was concentrated and the resulting solid residue was triturated several times with Et_2O for the solubilization of DBU and alcohol **6'**, which was formed quantitatively at complete reaction

conversions. After washing with acidic aqueous solution, the protonated DBU and **6'** could be separated and alcohol **6'** quantitatively re-oxidized to quinone **6** with air in the presence of catalytic phthalocyanine **5** as depicted in the Experimental section.

Thermogravimetric analyses (TGA) were finally carried out (analyses conducted at ISOF-CNR, Bologna), recording the onset of thermal degradation (T_{di}), the temperature of maximum degradation rate (Td), and the residuum after degradation at 850 °C (Table 3). The degradation plot of the PET oligomer **3aa** reported in Figure 3 proved to be comparable to those reported for a commercial PET and for the same polymer prepared under different conditions.[37,38] The thermal stability of **3aa** was high with a T_{di} value of the main degradation process at 410 °C. The weight loss in between room temperature and 300 °C was minimum (3.1%) and mainly due to a step with onset temperature at 100 °C, which was attributed to the loss of moisture and to the dehydration of terminal hydroxyl groups.[37] This hypothesis was thus confirmed by the TGA analyses of **3aa**, which, after chain-elongation, does not show any dehydration reaction in agreement with its ^{1}H NMR spectrum displaying no detectable CH_2-OH groups. The DSC analysis instead displayed melting and crystallization peaks in the heating and cooling steps (Figures 4 and 5) for polyesters **3aa** and **3aa'**.

Table 3. Onset of thermal degradation (T_{di}), temperature of maximum degradation rate (T_d), and residuum after degradation (residuum) from TGA analyses; glass transition temperature (T_g), melting temperature (T_m), crystallization temperature (T_c), and melting enthalpy (ΔH_m) from DSC analyses of polyesters **3**.

	TGA			**DSC**			
	T_{di} (°C)	T_d[a] (°C)	Res.[b] (%)	T_g[c] (°C)	T_m[d] (°C)	T_c (°C)	ΔH_m (J/g)
3aa	410	444	5.3	65	242	209	53
3aa'	419	447	7.3	83	244	214	42
3ab	404	442	4.1	53	-	-	-
3ac	327	354	10.2	52	186	139	48
3ad	<200	342/392	25.6				
3af	<200	442	13.4	-	-	-	-
3ca	247	258/364	7.3	60	181	142	39
3ba	205	407	29.0	91	-	-	-
3ba'	212	422	1.1	176	-	-	-
3da	399	421	1.9	136	-	-	-
3cc	<200	333	6.9				
3dc	373	409	3.3	140	-	-	-
3ea	224	540	18.9	389	445[e]	-	84.6

[a]Temperature of the peak minimum in the DTGA plots. [b]Residuum at 850 °C. [c]Values at the midpoint. [d]Values at the peak maximum. [e] Maximum of the observed endothermic peak.

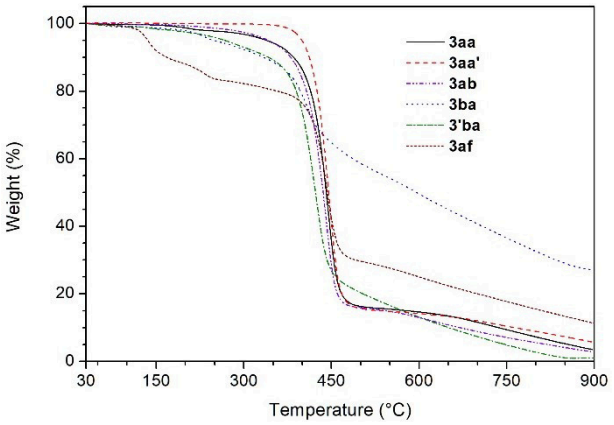

Figure 3. Comparison among the TGA curves of polyesters prepared from terephthalaldehyde/ isophthalaldehyde/benzene-1,3,5-tricarbaldehyde and ethylene glycol/glycerol (**3aa**, **3aa'**, **3ab**, **3ba**, **3ba'**, **3af**).

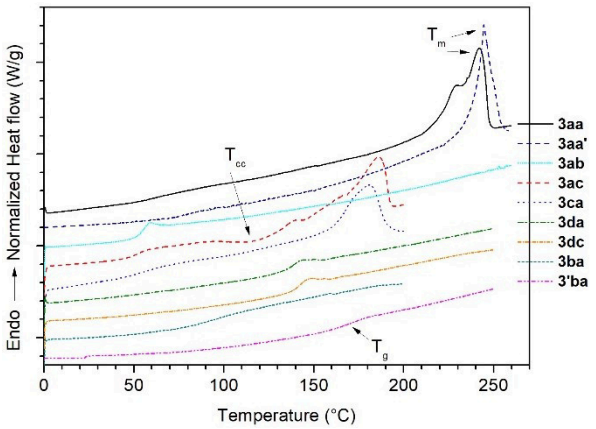

Figure 4. Second heating step in the DSC thermograms of polyesters **3** indicated in the legend. (Plots have been arbitrary shifted vertically for clarity and few significant transitions have been indicated as example.)

The presence of residuals or additives and the macromolecular features such as the molecular weight or the existence of defects, and the cooling protocol of a common PET influence the melting temperature.[39] Usually these values are between 245 °C and 265 °C when solid-state PET with regular sequence is analysed, confirming its semicrystalline nature. For the synthetized samples of **3aa** and **3aa'**, the melting peaks were observed at the minimum of the above-mentioned range (in accordance with the adopted measurement protocol). In particular, the melting peak of **3aa'** is shifted at little higher temperature as justified by a lower number of chain-ends and a higher molecular weight respect to **3aa** that on the contrary showed a shoulder toward low temperatures (Figure 4). The influence of more chain-ends on the melting point can be due to the occurrence of defect in polymer crystallization, affecting the kinetics and the thermodynamics of the process.[40] In fact, the glass transition temperature (T_g) of the low molecular weight oligomers **3aa** (65 °C) indicated a plasticization effect owing to the high number of chain-ends presented. On the contrary, **3aa'** showed a higher T_g (80 °C) in good agreement with the expected value for this polymer in the semi-crystalline form.[41] A lower ability to crystallize respect to PET is, instead, showed by poly(ethylene isophthalate) (PEI).[42] Indeed, PEI oligomers **3ab** displayed a T_g at 53 °C and thermal stability under nitrogen atmosphere similar to that of **3aa** (Figure 3) while no melting and crystallization peaks was detected by DSC analysis (Figures 4 and 5). These results are comparable with those reported by Lee and co-workers, who measured a T_g of 56 °C for a PEI with a molecular weight of 21000 kg mol^{-1} and residual crystallinity of only 2%.[43] TGA curve of the insoluble polymer **3af**, obtained from the polycondensation of ethylene glycol and the tricarboxaldehyde **2f**, displayed a thermal stability comparable to PET and PEI with the onset of the main degradation at 419

°C (Figure 3). The likely occurrence of impurities, which could not be efficiently removed from the rigid cross-linked structure, are identified in the additional weight loss step observed at low temperature ought to the degradation of the low molecular weight branches. In fact, the DSC analysis did not present any thermal transitions in the analysed range (up to 280 °C) suggesting a higher value of the glass transition due to the rigidity of the aromatic cross-linker (Figure 5). The introduction of glycerol as alcoholic moiety, along with terephthalaldehyde afforded the linear oligomer **3ba** which displayed lower thermal stability (Figure 3) compared to **3aa** in the region where the dehydration of hydroxyl groups is expected to occur (150 − 400 °C). Moreover, the analysis showed that this functional oligomer did not degrade completely in nitrogen atmosphere leaving a quite high residuum even at 900 °C (ca. 30%; Table 3), while the T_{di} of **3ba** was found at 205 °C.

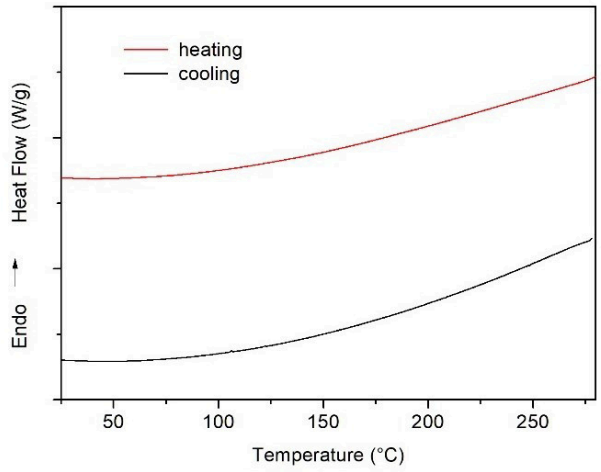

Figure 5. Cooling and second heating steps in the DSC thermograms of the cross-linked polyester **3af**.

Moving to the insoluble cross-linked analogue **3ba'** a plot more comparable to those of PET and PEI above 400 °C, with negligible residuum at 900 °C, was recorded, while a similar behaviour to **3ba** was displayed before 400 °C. Therefore, the occurrence of secondary free hydroxy groups in each repeating unit of the regular **3ba** could affect its degradation mechanism but additional investigation is needed to better explain this behaviour. Moreover, accordingly to a previous work,[23] cross-linked and linear poly(glycerol esters) **3ba'** and **3ba** were found to be amorphous exhibiting only a heat capacity jump while crossing the T_g during DSC analysis and no peaks in heating-cooling scan (Figures 4 and 6). The observed glass transition temperature of **3ba** was in fact lower by 85 °C respect to **3ba'**, thus disclosing a higher chain mobility in the oligomer **3ab** due to the presence of negligible number of crosslinks. The thermal stability of the oligoester **3da** from terephthalaldehyde and isosorbide was close to that of PET oligomer **3aa**, shifted of only 10 °C toward lower temperature (Figure 7). Accordingly, **3da** occurred also as amorphous solid with high T_g and good thermal stability, as previously

reported for the corresponding polymer prepared by polycondensation of isosorbide and terephthaloyl dichloride.[34a] Moreover, TGA plots indicate a lower thermal stability of the diformylfuran-based oligoesters **3ac** and **3dc** respect to those of terephthalaldehyde-based ones **3aa** and **3da** (Figure 7). This behavior is due to the higher instability of the furan moiety,[44] which can be overtaken using isosorbide instead of ethylene glycol. Indeed, the former led to the preparation of isosorbide-based oligoesters **3da** and **3dc** which showed higher thermal stability compared to ethylene glycol-derived oligoesters **3aa** and **3ac**. The different degradation mechanism is considered responsible for this behavior in place of chemical-physical differences. Note, moreover, that both isosorbide-based oligoesters **3da** and **3dc** are amorphous materials with very similar glass transition temperature values (Table 3) and both ethylene glycol-based oligoesters **3aa** and **3ac** are semicrystalline. Furthermore, the low molecular weight PEF **3ac** exhibited both melting and crystallization peaks in DSC analysis (Figures 4 and 6). In the literature, PEF has been described as a semicrystalline material with T_g = 70 − 90 °C, T_m = 200 − 215 °C, and Tc = 150 − 165 °C;[31a,35c, 44,45] however, the detected values for the synthetized oligoesters **3ac** and **3dc** were just below than those reported. Nevertheless, this decreasing trend with the reduction of molecular weight has been already observed for other polymers.[46]

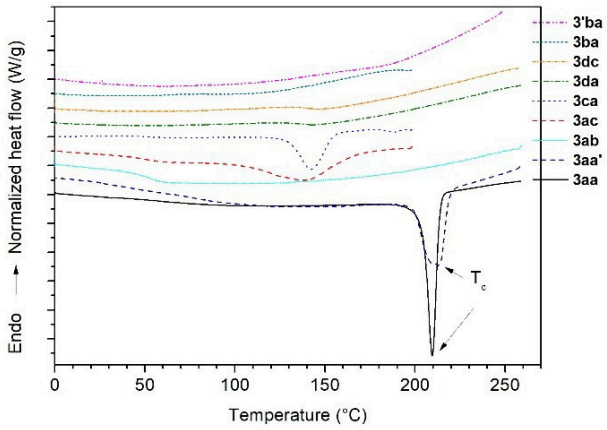

Figure 6. Cooling step in the DSC thermograms of polyesters **3** indicated in the legend. (Plots have been arbitrary shifted vertically for clarity. Two crystallization peaks have been indicated as examples.)

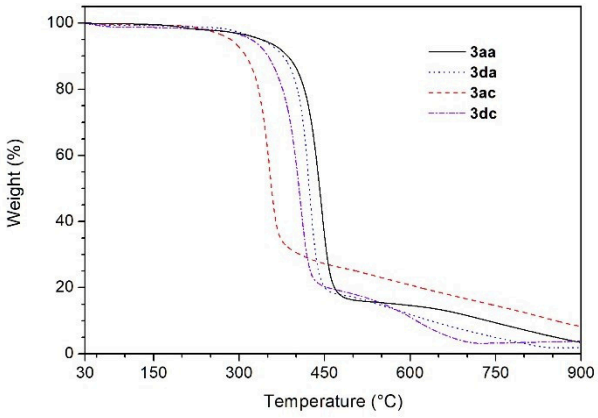

Figure 7. Comparison among the TGA curves of oligoesters prepared from diformylfuran/ terephthalaldehyde and ethylene glycol/isosorbide (**3aa**, **3da**, **3ac**, **3dc**).

Oligoesters presenting a 5-substituted furan-2-yl-moiety as a repeating unit, as **3cc**, **3ad** and **3ca**, displayed a lower thermal stability respect to PEF **3ac** (Figure 8). Among all, the oligoester **3ca**, derived from terephthalaldehyde, proved to be more stable and was found to be a semicrystalline polymer with T_g higher than room temperature (60 °C) and T_m of ca. 180 °C,

thus indicating this oligoester as a promising candidate to prepare transparent thermoplastic films. Despite its low molecular weight, the fully aromatic polyester **3ae** can be considered to show a good thermal stability, as the degradation process at low temperature can be ascribed to the loss of the chain-end groups. However, globally it showed a fairly complex process of degradation, composed by several steps, the largest one having onset temperature at 515 °C and the lowest at 225 °C (Figure 8). The DSC analysis of **3ea** showed a heat capacity jump at 390 °C and an endothermic peak with a maximum at 455 °C (Figure 9). This last peak can be attributed to a melting process even if the corresponding crystallization was not observed on cooling, while the first peak indicated a glass transition process. Note, however, that in this sample the first heating step was carried out up to 400 °C in order to remove any process responsible of the observed weight loss step in TGA, which occurred before this temperature. For this reason, the identification of the above-mentioned peak to any degradation process is unlikely since no weight loss processes were detected by TGA in this range. Finally, a little discrepancy of the measured characteristic temperature (T_g and T_m) of **3ea** with those reported in literature has been observed;[47] however, this can be explained by the difference of molecular weight and chain-end groups.

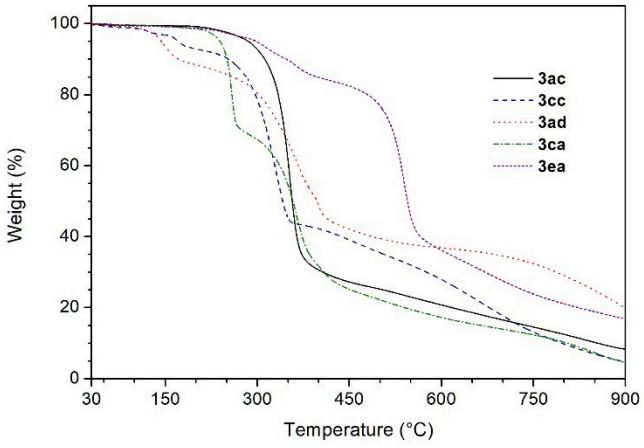

Figure 8. Comparison among the TGA curves of PEF oligomer **3ac**, oligoesters displaying the 5-substituted furan-2-yl-moity (**3cc**, **3ad**, **3ca**) and the fully aromatic oligoester **3ea**.

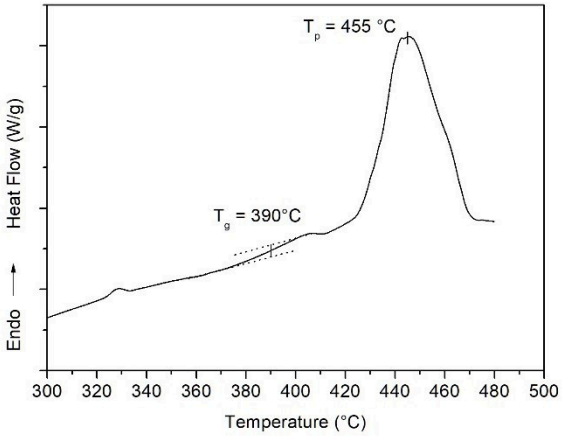

Figure 9. Second heating steps in the DSC thermogram of oligoester **3ea**.

5.3 Conclusion

To sum up, a new strategy for the synthesis of polyester (PEs) has been reported. The disclosed protocol focused on the polycondensation of diols and dialdehydes promoted by an N-heterocyclic carbene (NHC) catalyst in the presence of an external oxidant. This mild procedure was applied to the preparation of a series of synthetically relevant bio-based

polyesters from furanic monomers, glycerol, and isosorbide, though PEs of low molecular weight (Mn = 1.5 − 7.8 kg mol^{-1}) were obtained. Even if the relatively low molecular weight of these PEs hampers their industrial application these oligoester turned out to be compatible with subsequent NHC-catalysed chain-elongation step. Thus, PEs with higher molecular weight could be prepared by the latter strategy as exemplified by products **3aa'**. Lastly, the possibility of controlling the microstructure (linear or cross-linked) of polyglycerol esters by modulation of the steric hindrance of the NHC catalyst has been investigated as well.

5.4 Experimental section

General experimental procedure

All moisture-sensitive reactions were performed under an argon atmosphere using oven-dried glassware. Solvents were dried over a standard drying agent and freshly distilled prior to use. Reactions were monitored by TLC on silica gel 60 F_{254} with detection by UV lamp operating at 254 nm and 365 nm. Flash column chromatography was performed on silica gel 60 (230−400 mesh). ^{1}H (300 MHz) and ^{13}C (101 MHz) NMR spectra were recorded in $CDCl_3$, DMSO-d_6 solutions or $CDCl_3$:TFA mixtures at room temperature. The chemical shifts in ^{1}H and ^{13}C NMR spectra were referenced to trimethylsilane (TMS). Peak assignments were aided by ^{1}H-^{1}H COSY and gradient-HMQC experiments. FT-IR analyses were performed using the Bruker Instrument Vertex 70. For high resolution mass spectrometry (HRMS) the compounds were analysed in positive ion mode using an Agilent 6520 HPLC-Chip Q/ TOF-MS (nanospray) with a quadrupole, a hexapole, and a time of flight unit to produce the spectra. The capillary source voltage was set at 1700 V; the gas temperature and drying gas were kept at 350 °C and 5 L min^{-1}, respectively. The MS analyser was externally calibrated with ESI-L low concentration tuning mix from *m/z* 118 to 2700 to yield accuracy below 5 ppm. Accurate mass data were collected by directly infusing samples in 40:60 H_2O:ACN 0.1% TFA into the system at a flow rate of 0.4 μL min^{-1}. Thermogravimetric analysis (TGA) was performed from 30 to 900 °C under nitrogen atmosphere (30 mL min^{-1}) on a TGA 4000, PerkinElmer Inc., USA, instrument with Pyris software for data acquisition and analysis. Samples (5–10 mg) were analysed in an alumina pan at a heating rate of 10 °C min^{-1}. Differential scanning calorimetric analysis was performed on a DSC 8000, PerkinElmer Inc. USA instrument equipped with IntraCooler II cooling device and Pyris software for instrument control, data acquisition and analysis. Calorimetric measurements were performed using a PerkinElmer, USA DSC 8000 differential scanning calorimeter equipped with an Intracooler II as refrigeration system. The instrument was calibrated in temperature and energy with high-purity indium and zinc as standards. 3−10

mg of sample were analysed in aluminum pans under dry nitrogen atmosphere (30 mL min^{-1}). Samples were at first heated up to 200 °C (**3ac**, **3ca**, **3ba**) or 250 °C (**3da**, **3dc**, **3ba'**) or 260 °C (**3aa**, **3aa'**, **3ab**, **3af**) or 400 °C (**3ea**) to erase the thermal history and to remove any trapped volatile substance such as solvent residual from the synthesis, which are known to be frequently strongly trapped into furan-based polymers. Thus, samples were cooled down to 0 °C or below (cooling step) and finally heated up again (second heating step). Heating and cooling steps were all performed at 10 °C min^{-1} as scanning rate. Catalyst **A** was purchased from TCI, catalyst **B** was purchased from Sigma-Aldrich. Compounds **4−8** where purchased from TCI and used as received without further purification. All polyols and aldehydes are commercially available except for aldehyde **2d**, which was prepared by following a literature procedure.[48] Liquid aldehydes and bases (DBU, Et_3N) were freshly distilled before their utilization.

General procedure for the synthesis of polyesters 3

A mixture of diol **1** (0.88 mmol), aldehyde **2** (0.80 mmol), oxidant **6** (1.60 mmol) and pre-catalyst **A** (0.08 mmol) in anhydrous THF (6.0 mL) was degassed under vacuum and saturated with argon (by an Ar-filled balloon) three times. Then, DBU was added (0.20 mmol), and the reaction was stirred at room temperature for 16 h. The mixture was concentrated, and the resulting residue triturated with fresh portions of Et_2O or DCM (3 × 10 mL) and centrifugated. The organic solutions were collected for the recovery of DBU and oxidant **6**; the solid residue was dissolved in the minimum amount of appropriate solvent, and precipitated by dropwise addition into a poor solvent at 0 °C.

Poly(ethylene terephthalate) **(3aa, PET)**

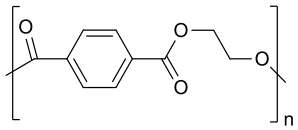

The reaction mixture was dissolved in a minimum amount of DCM and trifluoroacetic acid (TFA) (4:1, v/v) and precipitated from MeOH (10 volumes) at 0 °C. Filtration followed by washing with cold MeOH and drying under vacuum afforded the product **3aa** (126 mg, 82%, *Mn* = 6.5 kg mol^{-1}) as a pale yellow solid.

^{1}H NMR (300 MHz, 4:1 $CDCl_3$:TFA) δ = 8.15 (s, 4H, Ar), 4.80 (s, 4H, $COOCH_2$), 4.61 (bs, 4H, terminal $COOCH_2$), 4.20 (bs, 4H, terminal CH_2OH); **^{13}C NMR** (101 MHz, 4:1 $CDCl_3$:TFA) δ = 167.7 (CO), 133.4 (C, Ar), 130.1 (CH, Ar), 65.2 (terminal $COOCH_2$), 64.0 ($COOCH_2$), 63.2 (terminal CH_2OH); **FT-IR** (KBr) ν: 1714, 1243, 1095, 720 cm^{-1}.

Poly(ethylene isophthalate) **(3ab, PEI)**

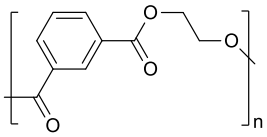

The reaction mixture was dissolved in a minimum amount of DCM and TFA (4:1, v/v) and precipitated from MeOH (10 volumes) at 0 °C. Filtration followed by washing with cold MeOH and drying under vacuum afforded the product **3ab** (118 mg, 77%, *Mn* = 6.4 kg mol^{-1}) as a pale yellow solid.

^{1}H NMR (300 MHz, 4:1 $CDCl_3$:TFA) δ = 8.71 (s, 1H, Ar), 8.31−8.19 (m, 2H, Ar), 7.63−7.50 (m, 1H, Ar), 4.80 (s, 4H, $COOCH_2$), 4.59 (bs, 4H, terminal $COOCH_2$), 4.17 (bs, 4H, terminal CH_2OH); **^{13}C NMR** (101 MHz, 4:1 $CDCl_3$:TFA) δ = 167.9 (CO), 135.3 (CH, Ar), 131.6 (C, Ar), 129.7 (CH, Ar), 129.6 (CH, Ar), 65.35 (terminal $COOCH_2$),64.1 ($COOCH_2$), 63.4 (terminal CH_2OH); **FT-IR** (KBr) ν: 1714, 1241, 1094, 724 cm^{-1}.

Poly(ethylene 2,5-furandicarboxylate) **(3ac, PEF)**

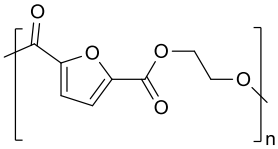

The reaction mixture was dissolved in a minimum amount of DCM and hexafluoroisopropanol (HFIP) (10:1, v/v) and precipitated from MeOH (10 volumes) at 0 °C. Filtration followed by washing with cold MeOH and drying under vacuum afforded the product **3ac** (99 mg, 68%, *Mn* = 1.4 kg mol^{-1}) as a pale yellow solid.

^{1}H NMR (300 MHz, DMSO-d_6) δ = 7.40 (s, 2H, Furan), 4.59 (s, 4H, $COOCH_2$), 4.27 (bs, 4H, terminal $COOCH_2$), 3.64 (bs, 4H, terminal CH_2OH); **^{13}C NMR** (101 MHz, DMSO-d_6) δ = 157.6 (CO), 146.4 (C, Furan), 119.9 (CH, Furan), 67.4 (terminal $COOCH_2$), 63.5 ($COOCH_2$), 59.2 (terminal CH_2OH); **FT-IR** (KBr) ν: 1714, 1239, 1095, 1017, 724 cm^{-1}.

Poly(ethylene 5,5′-(oxybis(methylene))bis(2-furancarboxylate)) **(3ad, PEOBF)**

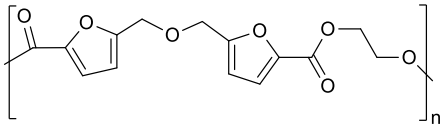

The mixture was dissolved in a minimum amount of DCM and TFA (4:1, v/v) and precipitated from MeOH (10 volumes) at 0 °C. Filtration followed by washing with cold MeOH and drying under vacuum afforded the product **3ad** (170 mg, 73% *Mn* = 3.5 kg mol^{-1}) as a brown solid.

^{1}H NMR (300 MHz, 4:1 $CDCl_3$:TFA) δ = 7.44 − 7.27 (m, 2H, H-3 Furan), 6.61 − 6.48 (m, 2H, H-4 Furan), 4.80−4.60 (m, 8H, Furan-CH_2O + $COOCH_2$), 4.54 (bs, 4H, terminal $COOCH_2$), 4.13 (bs, 4H, terminal CH_2OH), 4.00 (bs, 2H, OH); **^{13}C NMR** (101 MHz, 4:1 $CDCl_3$:TFA) δ = 161.3, 155.7 (C-5, Furan), 143.7 (C-2, Furan), 122.8 (terminal C-3, Furan), 121.4 (C-3, Furan), 113.3 (terminal C-4, Furan), 113.2 (C-4, Furan), 65.35 (terminal COO*C*H_2), 64.1 (COO*C*H_2), 63.8 (Furan-CH_2O), 63.2 (terminal CH_2OH); **FT-IR** (KBr) ν: 1714, 1240, 1095, 1017, 724 cm^{-1}.

Poly(2,5-furandimethylene terephthalate) **(3ca, PBHMT)**

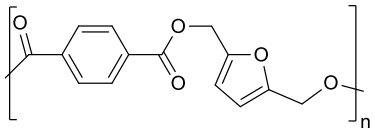

The reaction mixture was dissolved in a minimum amount of DCM and precipitated from MeOH (10 volumes) at 0 °C. Filtration followed by washing with cold MeOH and drying under vacuum afforded the product **3ca** (167 mg, 81%, *Mn* = 3.1 kg mol^{-1}) as a pale yellow solid.
^{1}H NMR (300 MHz, $CDCl_3$) δ = 8.08 (s, 4H, Ar), 6.50 (s, 2H, Furan), 6.45 (d, $J_{H3\text{-}H4}$ 3.1 Hz, 2H, terminal H-3 Furan), 6.29 (d, $J_{H4\text{-}H3}$ 3.1 Hz, 2H, terminal H-4 Furan), 5.36 − 5.26 (m, 4H, $COOCH_2$ and 4H, terminal $COOCH_2$), 4.62 (s, 4H, terminal CH_2OH); **^{13}C NMR** (101 MHz, $CDCl_3$) δ = 165.3 (CO), 150.0 (C, Furan), 133.7 (C, Ar), 129.7 (CH, Ar), 112.1 (CH, Furan), 58.9 (Furan-CH_2O); **FT-IR** (KBr) ν: 1715, 1243, 1091, 1016, 723 cm^{-1}.

Poly(2,5-furandimethylene 2,5-furandicarboxylate) **(3cc, PBHMF)**

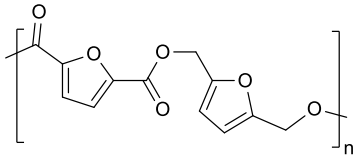

The reaction mixture was dissolved in a minimum amount of DCM and TFA (4:1, v/v) and precipitated from MeOH (10 volumes) at 0 °C. Filtration followed by washing with cold MeOH and drying under vacuum afforded the product **3cc** (154 mg, 78%, *Mn* = 7.8 kg mol^{-1}) as a pale brown solid.
^{1}H NMR (300 MHz, DMSO-d_6) δ = 7.42 (s, 2H, Furandicarboxylate), 6.65 (s, 2H, Furandimethylene), 6.52 (d, $J_{H3\text{-}H4}$ 3.1 Hz, 2H, terminal H-3 Furandimethylene), 6.27 (d, $J_{H4\text{-}H3}$ 3.1 Hz, 2H, terminal H-4 Furandimethylene), 5.39 (s, 4H, terminal $COOCH_2$), 5.31 (s, 4H, $COOCH_2$), 4.35 (s, 4H, terminal CH_2OH); **^{13}C NMR** (101 MHz, DMSO-d_6) δ = 157.3 (CO), 150.0 (C, Furandimethylene), 146.2 (C, Furandicarboxylate), 120.0 (CH, Furandicarboxylate),

113.2 (CH, Furandimethylene), 59.0 ($COOCH_2$). **FT-IR** (KBr): n 1717, 1581, 1270, 1120, 957, 769 cm^{-1}.

Poly(isosorbide terephthalate) **(3da, PIT)**

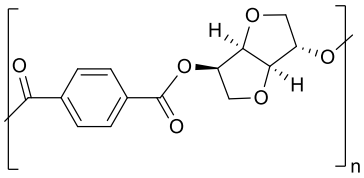

The reaction mixture was dissolved in a minimum amount of DCM and precipitated from MeOH (10 volumes) at 0 °C. Filtration followed by washing with cold MeOH and drying under vacuum afforded the product **3da** (157 mg, 71%, *Mn* = 2.8 kg mol^{-1}) as a white solid.

^{1}H NMR (300 MHz, $CDCl_3$) δ = 8.22 − 8.03 (m, 4H, Ar), 5.51 (s, 1H, H-2), 5.45 (m, 1H, H-5 and 2H, terminal H-5), 5.09 (m, 1H, H-4), 5.00 (m, 2H, terminal H-4), 4.70 (m, 1H, H-3), 4.46 (m, 2H, terminal H-3), 4.37 (bs, 2H; terminal H-2), 4.09 (m, 4H, H-1 and H-6), 4.00 (m, 4H, terminal H-6), 3.90 (m, 4H, terminal H-1); **^{13}C NMR** (101 MHz, $CDCl_3$) δ = 165.0 (CO), 164.6 (CO), 133.5 (C, Ar), 129.8 (CH, Ar), 88.4 (terminal C-3), 86.1 (C-3), 81.1 (C-4), 80.6 (terminal C-4), 78.8 (C-2), 76.2 (terminal C-2), 75.6 (terminal C-1), 74.9 (C-5), 73.4 (C-1 and terminal C-5), 70.8 (C-6 and terminal C-6); **FT-IR** (KBr) ν: 1716, 1409, 1246, 1093, 1017, 873, 724 cm^{-1}.

Poly(isosorbide 2,5-furandicarboxylate) **(3dc, PIF)**

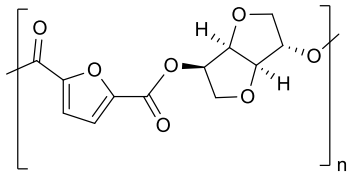

The mixture was dissolved in a minimum amount of DCM and TFA (4:1, v/v) and precipitated from MeOH (10 volumes) at 0 °C. Filtration followed by washing with cold MeOH and drying under vacuum afforded the product **3dc** (153 mg, 72%, *Mn* = 2.7 kg mol^{-1}) as a yellow solid.

^{1}H NMR (300 MHz, 4:1 $CDCl_3$:TFA) δ = 7.52−7.29 (m, 2H, Furan), 5.60 (bs, (2H, H-2 and H-5) and (2H, terminal H-5)), 5.28 (bs, 1H, H-4), 4.95 (bs, 2H, terminal H-4), 4.86 (bs, 1H, H-3), 4.77 (bs, 2H, terminal H-3), 4.70 (bs, 2H, terminal H-2), 4.27 (m, (4H, H-1 and H-6) + (4H, terminal H-6)), 3.88 (bs, 4H, terminal H-1); **^{13}C NMR** (101 MHz, 4:1 $CDCl_3$:TFA) δ = 158.9 (CO), 158.6 (CO), 146.3 (C, Furan), 120.8 (CH, Furan), 87.6 (terminal C-3), 85.9 (C-3), 81.5 (C-4), 81.0 (terminal C-4), 79.1 (C-2), 75.9 (terminal C-2), 75.5 (C-5), 75.3 (terminal C-1), 73.5

(C-1 and terminal C-5), 72.6 (terminal C-6), 70.9 (C-6); **FT-IR** (KBr) ν: 1716, 1580, 1384, 1269, 1222, 1117, 957, 873, 766 cm^{-1}.

Poly(1,4-phenylene terephthalate) **(3ea)**

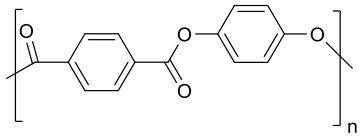

The mixture was dissolved in a minimum amount of DCM and TFA (4:1, v/v) and precipitated from MeOH (10 volumes) at 0 °C. Filtration followed by washing with cold MeOH and drying under vacuum afforded the product **3ea** (169 mg, 88%, *Mn* = 0.4 kg mol^{-1}) as a pale yellow solid.

^{1}H NMR (300 MHz, 4:1 $CDCl_3$:TFA) δ = 10.13 (s, 1H, terminal aldehyde), 8.52−8.38 (m, 4H, Ar), 8.38 − 8.28 (m, 2H, terminal $Ar_{othoCOOR}$), 8.18 (d, *J* 8.0 Hz, 2H, terminal $Ar_{othoCOH}$), 7.37 (s, 4H, Hydroquinone), 7.16 (d, *J* 8.5 Hz, 2H, terminal $Hydroquinone_{orthoOCOR}$), 7.01 (d, *J* 8.5 Hz, 2H, terminal $Hydroquinone_{orthoOH}$); **^{13}C NMR** (101 MHz, 4:1 $CDCl_3$:TFA) δ = 196.7 (COH), 166.9 (CO), 166.6 (terminal CO), 152.3 (C, terminal $Hydroquinone_{OH}$), 148.6 (C, Hydroquinone), 144.8 (C, terminal $Hydroquinone_{OCOR}$), 139.1 (C, terminal Ar_{COH}), 134.8 (C, terminal Ar_{COOR}), 133.5 (C, Ar), (131.3, 131.0, 130.9 (CH, terminal Ar_{COH} and CH, terminal Ar_{COOR} and CH, Ar)), 123.1 (CH, Hydroquinone), 122.8 (CH, terminal HydroquinoneorthoOCOR), 116.8 (CH, terminal $Hydroquinone_{orthoOH}$); **FT-IR** (KBr) ν: 1726, 1500, 1384, 1244, 1174, 1075, 1017, 872, 723 cm^{-1}.

Synthesis of high molecular weight PET 3aa'

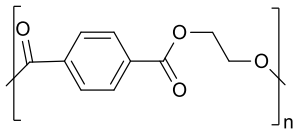

Isolated **3aa** (126 mg, 0.66 mmol of repeating unit, *Mn* = 6.5 kg mol^{-1}) was heated at 250 °C for 2 hours under vacuum along with triazolium pre-catalyst **A** (7.5 mg, 0.03 mmol) and DBU (4.5 μL, 0.03 mmol). After this period, the flask was cooled, the reaction mixture was triturated with DCM and centrifugated (3 × 10 mL). Final drying under vacuum afforded **3aa'** (120 mg, 88%) as a creamy solid with high molecular weight as confirmed by ^{1}H NMR analysis.

^{1}H NMR (300 MHz, 4:1 $CDCl_3$:TFA) δ = 8.15 (s, 4H, Ar), 4.80 (s, 4H, $COOCH_2$); **^{13}C NMR** (101 MHz, 4:1 $CDCl_3$:TFA) δ = 167.7 (CO), 133.4 (C, Ar), 130.1 (CH, Ar), 64.0 ($COOCH_2$); **FT-IR** (KBr) ν: 1716, 1245, 1096, 725 cm^{-1}.

Synthesis of cross-linked PGT 3ba'

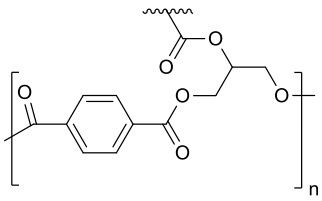

A mixture of glycerol **1b** (65 µL, 0.88 mmol), terephthalaldehyde **2a** (107 mg, 0.80 mmol), oxidant **6** (654 mg, 1.60 mmol) and pre-catalyst **A** (18 mg, 0.08 mmol) in anhydrous THF (6.0 mL) was degassed under vacuum and saturated with argon (by an Ar-filled balloon) three times. Then, DBU was added (30 µL, 0.20 mmol), and the reaction was stirred at room temperature for 16 h. Solvent removal under reduced pressure, trituration of the reaction mixture with DCM and subsequent centrifugation (3 × 10 mL) followed by drying under vacuum afforded **3ba'** (160 mg, 90%) as an off-white solid. The complete characterization was hampered as **3ba'** was insoluble in common organic solvents.

FT-IR (KBr) ν: 3128, 1716, 1274, 1117, 957, 764 cm^{-1}.

Synthesis of linear PGT 3ba

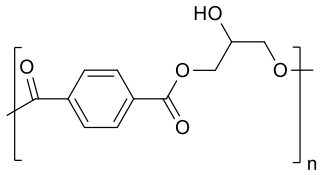

A mixture of glycerol **1b** (65 µL, 0.88 mmol), terephthalaldehyde **2a** (107 mg, 0.80 mmol), oxidant **6** (654 mg, 1.60 mmol) and pre-catalyst **B** (29 mg, 0.08 mmol) in anhydrous THF (60 mL) was degassed under vacuum and saturated with argon (by an Ar-filled balloon) three times. Then, Et_3N was added (28 µL, 0.20 mmol), and the reaction was stirred at room temperature for 1 h. After solvent removal under reduced pressure, trituration with DCM and subsequent centrifugation (3 × 10 mL), the resulting solid was dissolved in a minimum amount of DCM and MeOH (4:1, v/v) and precipitated from 2-propanol (10 volumes) at 0 °C. Filtration followed by washing with cold 2-propanol and drying under vacuum afforded **3ba** (126 mg, 71% *Mn* = 1.5 kg mol^{-1}) as an off white solid.

^{1}H NMR (300 MHz, DMSO-d_6) δ = 8.06 (m, 4H, Ar), 4.38 (bs, 4H, CH_2 and 4H, terminal $COOCH_2$), 4.21 (bs, 1H, CH + 2H, terminal CH)), 3.76 (bs, 4H, terminal CH_2OH); **^{13}C NMR** (101 MHz, DMSO-d_6) δ = 166.4 (terminal CO), 164.8 (CO), 133.4 (C, Ar), 133.0 (terminal C, Ar), 129.4 (CH, Ar + terminal CH,Ar), 69.1 (terminal CH), 66.7 (terminal $COOCH_2$), 66.1 (CH + $COOCH_2$), 62.4 (terminal CH_2OH); **FT-IR** (KBr) ν: 2964, 1714, 1244,1092, 1017, 872, 724 cm^{-1}.

Synthesis of polyester Poly(ethylene 1,3,5-benzenetricarboxylate) 3af

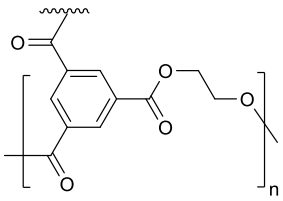

A mixture of diol **1a** (74 μL, 1.32 mmol), trialdehyde **2f** (130 mg, 0.80 mmol), oxidant **6** (981 mg, 2.40 mmol) and pre-catalyst **A** (18 mg, 0.08 mmol) in anhydrous THF (6.0 mL) was degassed under vacuum and saturated with argon (by an Ar-filled balloon) three times. Then, DBU was added (30 μL, 0.20 mmol), and the reaction was stirred at room temperature for 16 h. Solvent removal under reduced pressure, trituration of the reaction mixture with DCM and subsequent centrifugation (3 × 10 mL) followed by drying under vacuum afforded **3af** (158 mg, 79%) as a pale yellow solid. The complete characterization was hampered as **3af** was insoluble in common organic solvents.

FT-IR (KBr) ν: 3616, 2958, 1731, 1595, 1361, 1237,1090, 1041, 898 cm^{-1}.

Gram-scale synthesis of 3aa

A mixture of ethylene glycol **1a** (0.68 mL, 11.0 mmol), terephthalaldehyde **2a** (1.34 g, 10.0 mmol), oxidant **6** (8.17 g, 20.0 mmol) and pre-catalyst **A** (225 mg, 1.0 mmol) in anhydrous THF (60.0 mL) was degassed under vacuum and saturated with argon (by an Ar-filled balloon) three times. Then, DBU was added (374 μL, 2.5 mmol), and the reaction was stirred at room temperature for 16 h. The mixture was concentrated, and the resulting residue triturated with fresh portions of DCM (3 × 100 mL) and centrifugated. The organic solutions were collected for the recovery of DBU and oxidant **6** while the solid residue was dissolved in 50 mL of DCM and trifluoroacetic acid (TFA) (4:1, v/v) and precipitated from MeOH (500 mL) at 0 °C. Filtration followed by washing with cold MeOH and drying under vacuum afforded the product **3aa** (1.69 g, 88%, Mn = 6.5 kg mol^{-1}) as a pale yellow solid.

Procedure for DBU and oxidant 6 recycle

After trituration of the crude polycondensation mixture with DCM or Et_2O, the collected organic solutions (30 mL) were washed with 0.5 M HCl (2 × 10 mL).

*Oxidant **6** recycle*: the organic phase containing the alcohol **6'** was dried (Na_2SO_4), concentrated, and eluted from a short column of silica gel (4:1 cyclohexane:DCM) to give **6'** (578 mg) as a white amorphous solid. The quantitative oxidation to quinone **6** was performed stirring **6'** (578 mg, 1.41 mmol) with **6** (80 mg, 0.14 mmol) in THF (10 mL) under air

atmosphere (1 atm, balloon) for 16 h. Filtration over a celite pad and subsequent concentration under reduced pressure afforded **6** as a dark red amorphous solid (572 mg, 88%).

DBU recycle: the above aqueous phase was diluted with 2 M NaOH until alkaline pH and extracted with EtOAc (2 × 15 mL). The combined organic phases were dried (Na_2SO_4) and concentrated to give DBU (27 mg, 90%), at least 90% pure as determined by ^{1}H NMR analysis.

Synthesis of model benzoylated isosorbide derivatives

A mixture of isosorbide **1d** (146 mg, 1.00 mmol), benzaldehyde (102 µL, 1.00 mmol), oxidant **6** (408 mg, 1.0 mmol) and pre-catalyst **B** (36 mg, 0.10 mmol) in anhydrous THF (8.0 mL) was degassed under vacuum and saturated with argon (by an Ar-filled balloon) three times. Then, Et_3N was added (32 µL, 0.25 mmol) and the reaction was stirred at room temperature for 2 h. After solvent removal, DCM (10 mL) was added and the resulting organic solution was washed with water (3 × 3 mL). The organic layer was dried (Na_2SO_4), concentrated, and eluted from a column of silica gel (4:1 cyclohexane:EtOAc to 1:1 cyclohexane:EtOAc) to give, in order of elution, isosorbide dibenzoate, isosorbide 2-O-benzoate and isosorbide 5-O-benzoate.

Isosorbide dibenzoate

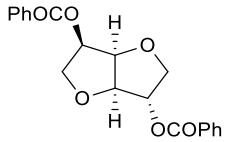

Column chromatography afforded the diester (63 mg, 18%) as a white solid with spectroscopic data in accordance with the literature.[49]

^{1}H NMR (300 MHz, $CDCl_3$) δ = 8.14 − 8.06 (m, 2H, Ar_{ortho}), 8.06−7.97 (m, 2H, Ar_{ortho}), 7.64 − 7.51 (m, 2H, Ar_{para}), 7.51 − 7.38 (m, 4H, Ar_{meta}), 5.49 (d, $J_{H2\text{-}H1a}$ 3.1 Hz, 1H, H-2), 5.43 (ddd, $J_{H5\text{-}H4} \approx J_{H5\text{-}H6a} \approx J_{H5\text{-}H6b} \approx$ 5.3 Hz, 1H, H-5), 5.07 (dd, $J_{H4\text{-}H3} \approx J_{H4\text{-}H5} \approx$ 5.0 Hz, 1H, H-4), 4.69 (d, $J_{H3\text{-}H4}$ 4.9 Hz, 1H, H-3), 4.17 − 4.00 (m, 4H, H-1 and H-6); **^{13}C NMR** (101 MHz, $CDCl_3$) δ = 165.9 (CO), 165.6 (CO), 133.4 (CH, Ar_{para}), 133.3 (CH, Ar_{para}), 129.8 (CH, Ar_{ortho}), 129.7 (CH, Ar_{ortho}), 129.5 (C, Ar), 129.4 (C, Ar), 128.5 (CH, Ar_{meta}), 128.4 (CH, Ar_{meta}), 86.2 (C-3), 81.1 (C-4), 78.5 (C-2), 74.5 (C-5), 73.5 (C-1), 70.7 (C-6); **HRMS** (ESI/Q-TOF) calcd. for $C_{20}H_{18}NaO_6$ ($[M + Na]^+$): 377.0996; found 377.0977.

Isosorbide 2-O-benzoate

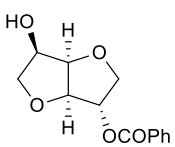

Column chromatography afforded the monoester (57 mg, 24%) as a white solid with spectroscopic data in accordance with the literature.[50]

^{1}H NMR (300 MHz, $CDCl_3$) δ = 8.07 − 7.98 (m, 2H, Ar_{ortho}), 7.63 − 7.54 (m, 1H, Ar_{para}), 7.50 − 7.40 (m, 2H, Ar_{meta}), 5.48 (d, $J_{H2\text{-}H1a}$ 3.4 Hz, 1H, H-2), 4.73 (dd, $J_{H4\text{-}H3} \approx J_{H4\text{-}H5} \approx$ 4.9 Hz, 1H, H-4), 4.64 (d, $J_{H3\text{-}H4}$ 4.9 Hz, 1H, H-3), 4.36 (ddd, $J_{H5\text{-}H4} \approx J_{H5\text{-}H6a} \approx J_{H5\text{-}H6b} \approx$ 5.5 Hz, 1H, H-5), 4.23 − 4.07 (m, 2H, H-1), 3.94 (dd, $J_{H6a\text{-}H6b}$ 9.5 Hz, $J_{H6a\text{-}H5}$ 6.0 Hz, 1H, H-6a), 3.62 (dd, $J_{H6b\text{-}H6a}$ 9.5 Hz, $J_{H6b\text{-}H5}$ 6.0 Hz, 1H, H-6b), 2.19 (bs, 1H, OH); **^{13}C NMR** (101 MHz, CDC_{l3}) δ = 165.6 (CO), 133.5 (CH, Ar_{para}), 129.8 (CH, Ar_{ortho}), 129.5 (C, Ar), 128.6 (CH, Ar_{meta}), 85.8 (C-3), 82.2 (C-4), 78.9 (C-2), 73.8 (C-1), 73.7 (C-6), 72.4 (C-5); **HRMS** (ESI/Q-TOF) calcd. for $C_{13}H_{14}NaO_5$ ($[M + Na]^+$): 273.0733; found 273.0716.

Isosorbide 5-O-benzoate

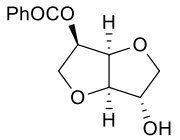

Column chromatography afforded the monoester (116 mg, 48%) as a white amorphous solid. **^{1}H NMR** (300 MHz, $CDCl_3$) δ = 8.11 − 8.03 (m, 2H, Ar_{ortho}), 7.62 − 7.53 (m, 1H, Ar_{para}), 7.50 − 7.40 (m, 2H, Ar_{meta}), 5.40 (ddd, $J_{H5\text{-}H4} \approx J_{H5\text{-}H6a} \approx J_{H5\text{-}H6b} \approx$ 5.3 Hz, 1H, H-5), 4.99 (dd, $J_{H4\text{-}H3} \approx J_{H4\text{-}H5} \approx$ 5.1 Hz, 1H, H-4), 4.46 (d, $J_{H3\text{-}H4}$ 5.1 Hz, 1H, H-3), 4.40 − 4.34 (m, 1H, H-2), 4.05 − 3.85 (m, 4H, H-1 and H-6), 1.76 (bs, OH); **^{13}C NMR** (101 MHz, $CDCl_3$) δ = 165.9 (CO), 133.2 (CH, Ar_{para}), 129.7 (CH, Ar_{ortho}), 129.5 (C, Ar), 128.4 (CH, Ar_{meta}), 88.4 (C-3), 80.7 (C-4), 76.3 (C-2), 75.6 (C-1), 74.5 (C-5), 70.8 (C-6); **HRMS** (ESI/Q-TOF) calcd. for $C_{13}H_{14}NaO_5$ ($[M + Na]^+$): 273.0733; found 273.0756.

5.5 References and notes

1. M. K. Kiesewetter, E. J. Shin, J. L. Hedrick, R M. Waymouth, *Macromolecules,* **2010**, *43*, 2093−2107.
2. W. N. Ottou, H. Sardon, D. Mecerreyes, J. Vignolle, D. Taton, *Prog. Polym. Sci.* **2016**, *56*, 64−115.
3. D. V. Rosato, *Plastic product material and process selection handbook*, Elsevier, New York, **2004**.
4. a) A. Fradet, M. Tessier, in *Synthetic methods in step-growth polymers*, (Eds. M. E. Rogers, T. E. Long), John Wiley & Sons Inc, New York, **2003**, p. 17−34; b) L. E. Elizalde, G. de los Santos-Villarreal, J. L. Santiago-Garcia, M. Aguilar-Vega, in *Handbook of polymer synthesis, characterization and processing*, (Eds. E. Saldivar-Guerra, E. Vivaldo-Lima), John Wiley & Sons Inc, New York, **2013**, p. 41−63.
5. A. Bossion, K. V. Heifferon, L Meabe, N. Zivic, D. Taton, J. L. Hedrick, T. E. Long, H. Sardon, *Prog. Polym. Sci.* **2019**, *90*, 164−210.
6. Selected recent reviews: a) S. J. Ryan, L. Candish, D. W. Lupton, *Chem. Soc. Rev.* **2013**, *42*, 4906−4917; b) M. N. Hopkinson, C. Richter, M. Schedler, F. Glorius, *Nature* **2014**, *510*, 485−496; c) D. M. Flanigan, F. Romanov-Michailidis, N. A. White, T. Rovis, *Chem. Rev.* **2015**, *115*, 9307−9387; d) X.-Y. Chen, Q. Liu, P. Chauhan, D. Enders, *Angew. Chem. Int. Ed.* **2018**, *57*, 3862−3873.
7. a) C. A. Smith, M. R. Narouz, P. A. Lummis, I. Singh, A. Nazemi, C.-H. Li, C. M. Crudden, *Chem. Rev.* **2019**, *119*, 4986−5056; b) S. Naumann, A. P Dove, *Polym. Int.* **2016**, *65*, 16−27; c) S. Naumann, A. P Dove, *Polym. Chem.* **2015**, *6*, 3185−3200; d) M. Fevre, J. Pinaud, Y. Gnanou, J. Vignolle, D. Taton, *Chem. Soc. Rev.* **2013**, *42*, 2142− 2172; d) T. K. H. Trinh, J.-P. Malval, F. Morlet-Savary, J. Pinaud, P. Lacroix-Desmazes, C. Reibel, V. Heroguez, A. Chemtob, *Chem. Eur.J.* **2019**, *25*, 9242−9252.
8. Akkattu T. Biju, *N-Heterocyclic Carbenes in Organocatalysis*, Wiley-VCH, **2019**.
9. G. W. Nyce, J. A. Lamboy, E. F. Connor, R. M. Waymouth, J. L.Hedrick, *Org. Lett.* **2002**, *4*, 3587−3590.
10. J. Pinaud, K. Vijayakrishna, D. Taton, Y. Gnanou, *Macromolecules* **2009**, *42*, 4932−4936.
11. a) R. A Jones, M. Karatza, T. N. Voro, P. U. Civir, A. Franck, O. Ozturk,J. P. Seaman, A. P. Whitmore, D. J. Williamson, *Tetrahedron* **1996**,*52*, 8707−8724; b) R. A Jones, P. U. Civir, *Tetrahedron* **1997**, *53*,11529−11540.
12. X. Zhang, M. Fevre, G. O. Jones, R. M. Waymouth, *Chem. Rev.* **2018**,*118*, 839−885.
13. a) C. E. I. Knappke, A. Imami, A. J. von Wangelin, *ChemCatChem* **2012**, *4*, 937−941; b) S. De Sarkar, A. Biswas, R. C. Samanta, A. Studer, *Chem. Eur. J.* **2013**, *19*, 4664−4678.
14. a) J. Mahatthananchai, J. W. Bode, *Acc. Chem. Res.* **2014**, *47*, 696−707; b) M. H. Wang, K.A. Scheidt, *Angew. Chem. Int. Ed.* **2016**, *55*, 14912−14922.
15. a) A. Gandini, T. M. Lacerda, A. J. Carvalho, E. Trovatti, *Chem. Rev.* **2016**, *116*, 1637−1669; b) J. A. Galbis, M. G. Garcia-Martin, M. V. de Paz, E. Galbis, *Chem. Rev.* **2016**, *116*, 1600−1636; c) F. A. Kucherov, L. V. Romashov, K. I. Galkin, V. P. Ananikov, *ACS Sustainable Chem.Eng.* **2018**, *6*, 8064−8092.
16. a) D. Liu, E. Y.-X. Chen, *Green Chem.* **2014**, *16*, 964−981; b) Z. Mou, E. Y.-X. Chen, *ACS Sustainable Chem. Eng.* **2016**, *4*, 7118−7129; c)Z. Mou, S. K. Feng, E. Y. X. Chen, *Polym. Chem.* **2016**, *7*, 1593−1602; d) J. Chen, J. Wu, J. Qi, H. Wang, *ACS Sustainable Chem. Eng.* **2019**, *7*, 1061−1071; e) J. F. Wilson, E. Y.-X. Chen, *ACS Sustainable Chem. Eng.* **2019**, *7*, 7035−7046; f) R. M. Cywar, L. Wang, E. Y.-X. Chen, *ACS Sustainable Chem. Eng.* **2019**, *7*, 1980−1988.
17. a) A. Brandolese, D. Ragno, G. Di Carmine, T. Bernardi, O. Bortolini, P. P. Giovannini, O. Ginoble Pandoli, A. Altomare, A. Massi, *Org. Biomol. Chem.* **2018**, *16*, 8955−8964; b) D. Ragno, A. Brandolese, D. Urbani, G. Di Carmine, C. De Risi, O. Bortolini, P. P. Giovannini, A. Massi, *React. Chem. Eng.* **2018**, *3*, 816−825.

18. I. Flores, J. Demarteau, A. J. Muller, A. Etxeberria, L. Irusta, F. Bergman, C. Koning, H. Sardon, *Eur. Polym. J.* **2018**, *104*, 170−176.
19. a) P. Kallinteri, S. Higgins, G. A. Hutcheon, C. B. S. Pourc, M. C.Garnett, *Biomacromolecules* **2005**, *6*, 1885−1894; b) V. M. Weiss, T. Naolou, G. Hause, J. Kuntsche, J. Kressler, K. Mader, *J. Controlled Release* **2012**, *158*, 156−164.
20. N. Lang, M. J. Pereira, Y. Lee, F. Ingeborg, N. V. Vasilyev, E. N. Feins, K. Ablasser, E. D. O'Cearbhaill, C. Xu, A. Fabozzo, R. Padera, S. Wasserman, F. Freudenthal, L. S. Ferreira, R. Langer, J. M. Karp, P. J. del Nido, *Sci. Transl. Med.* **2015**, *6*, 1−19.
21. a) Q. Chen, A. Bismarck, U. Hansen, S. Junaid, M. Q. Tran, S. E. Harding, N. N. Ali, A. R. Boccaccini, *Biomaterials* **2008**, *29*, 47−57; b) S. H. Zaky, K. Lee, J. Gao, A. Jensen, J. Close, Y. Wang, A. J. Almarza, C. Sfeir, *Tissue Eng., Part A* **2014**, *20*, 45−53.
22. a) B. J. Kline, E. J. Beckman, A. J. Russell, *J. Am. Chem. Soc.* **1998**,*120*, 9475−9480; b) H. Uyama, K. Inada, S. Kobayashi, *Macromol.Rapid Commun*. **1999**, *20*, 171−174; c) L. E. Iglesias, Y. Fukuyama, H. Nonami, R. Erra-Balsells, A. Baldessari, *Biotechnol. Tech.* **1999**, *13*, 923−926; d) H. Uyama, K. Inada, S. Kobayashi, *Macromol. Biosci.* **2001**, **1**, 40−44; e) A. Kumar, A. S. Kulshrestha, W. Gao, R. A. Gross, *Macromolecules* **2003**, *36*, 8219−8221; f) Z. You, H. Cao, J. Gao, P.H. Shin, B. W. Day, Y. Wang, *Biomaterials* **2010**, *31*, 3129−3138; g) Z. You, Y. Wang, *Adv. Funct. Mater.* **2012**, *22*, 2812−2820; h) O. Valerio, M. Misra, A. K. Mohanty, *ACS Sustainable Chem. Eng.* **2018**,*6*, 5681−5693.
23. For a recent synthesis of linear polyesters from glycerol with diarylborinic acid catalysts, see: E. Slavko, M. S. Taylor, *Chem. Sci.* **2017**, *8*, 7106−7111.
24. a) R. Rai, M. Tallawi, A. Grigore, A. R. Boccaccini, *Prog. Polym. Sci.* **2012**, *37*, 1051−1078; b) H. Zhang, M. W. Grinstaff, *Macromol. Rapid Commun*. **2014**, *35*, 1906−1924.
25. a) Z. Hui, A. Gandini, *Europ. Polym. J.* **1992**, *28*, 1461−1469; b) A. S. Amarasekara, D. Green, L. D. Williams, *Europ. Polym. J*. **2009**, *45*, 595−598.
26. a) H. Wang, Y. Wang, T. Deng, C. Chen, Y. Zhu, X. Hou, *Catal. Commun.* **2015**, *59*, 127−130; b) C. Moreau, M. N. Belgacem, A. Gandini, *Top. Catal.* **2004**, *27*, 11−30.
27. a) Z. H. Zhang, J. D. Zhen, B. Liu, K. L. Lv, K. J. Deng, *Green Chem.* **2015**, *17*, 1308−1317; b) X. Zuo, P. Venkitasubramanian, D. H. Busch, B. Subramaniam, *ACS Sustainable Chem. Eng.* **2016**, *4*, 3659−3668; c) M. Kim, Y. Su, T. Aoshima, A. Fukuoka, E. J. M. Hensen, K. Nakajima, *ACS Catal.* **2019**, *9*, 4277−4285.
28. A. S. Amarasekara, L. Nguyen, N. C. Okorie, S. Jamal, *Green Chem.* **2017***, 19,* 1570−1575.
29. a) A. Gandini, A. J. D. Silvestre, C. P. Neto, A. F. Sousa, M. Gomes, *J. Polym. Sci, Part A: Polym. Chem.* **2009**, *47*, 295−298; b) A. F. Sousa, M. Matos, C. S. R. Freire, A. J. D. Silvestre, J. F. J. Coelho, *Polymer* **2013**, *54*, 513−519; c) A. F. Sousa, C. Vilela, A. C. Fonseca, M. Matos, C. S. R. Freire, G.-J. M. Gruter, J. F. J Coelho, A. J. D. Silvestre, *Polym. Chem.* **2015**, *6*, 5961−5983.
30. a) M. Chatterjee, T. Ishizaka, H. Kawanami, *Green Chem*. **2014**, *16*, 4734−4739; b) W. Hao, W. Li, X. Tang, X. Zeng, Y. Sun, S. Liu, L. Lin, *Green Chem.* **2016**, *18*, 1080−1088.
31 a) M. Gomes, A. Gandini, A. J. D. Silvestre, B. Reis, *J. Polym. Sci., Part A: Polym. Chem.* **2011**, *49*, 3759−3768; b) C. Zeng, H. Seino, J. Ren, K. Hatanaka, N. Yoshie, *Macromolecules* **2013**, *46*, 1794−1802; c) Y. Jiang, A. J. Woortman, G. O. Alberda van Ekenstein, D. M. Petrovic, K. Loos, *Biomacromolecules* **2014**, *15*, 2482−2493.
32. For a partial characterization of poly(2,5-furandimethylene terephthalate), see the Chinese patent CN104277210A.
33. a) F. Fenouillot, A. Rousseaua, G. Colomines, R. Saint-Loupe, J.-P. Pascault, *Prog. Polym. Sci.* **2010**, *35*, 578−622; b) M. Rose, R. Palkovits, *ChemSusChem* **2012**, *5*, 167−176; c) J. Wu, P. Eduard, L. Jasinska-Walc, A. Rozanski, B. A. J. Noordover, D. S. van Es, C. E. Koning, *Macromolecules* **2013**, *46*, 384−394; c) Y. Chebbi, N. Kasmi, M. Majdoub, P. Cerruti, G. Scarinzi, M. Malinconico, G. Dal Poggetto, G. Z. Papageorgiou, D. N. Bikiaris, *ACS Sustainable Chem. Eng.***2019**, *7*, 5501−5514 and references therein.

34. a) R. Storbeck, M. Rehahn, M. Ballauff, *Makromol. Chem.* **1993**, *194*, 53−64; b) R. Storbeck, M. Ballauff, *J. Appl. Polym. Sci.* **1996**, *59*, 1199−202.
35. a) R. Storbeck, M. Ballauff, Polymer **1993**, *34*, 5003−5006; b) A. Gandini, D. Coelho, M. Gomes, B. Reis, A. Silvestre, *J. Mater. Chem.* **2009**, *19*, 8656−8664; c) P. Gopalakrishnan, S. Narayan-Sarathy, T. Ghosh, K. Mahajan, M. N. Belgacem, *J. Polym. Res.* **2014**, *21*, 340−348.
36. M. Yin, C. Li, G. Guan, D. Zhang, Y. Xiao, *J. Appl. Polym. Sci.* **2010**,*115*, 2470−2478.
37. ^{1}H and ^{13}C NMR analysis of **3ea** showed the presence of terminal hydroquinone and terephthalaldehyde units.
38. E. H. El-Gendy, I. A. El-Shanshour, *J. Appl. Polym. Sci.* **2004**, *92*, 3710−3720.
39. J. P. Jog, *J. Macromol. Sci. Part C: Polym. Rev.* **1995**, *35,* 531−53.
40. a) M. L. Di Lorenzo, C. Silvestre, *Prog. Polym. Sci.* **1999**, *24,* 917−950; b) G. Strobl, *Prog. Polym. Sci.* **2006**, *31*, 398−442.
41. B. Lepoittevin, P. Roger, in *Handbook of Engineering and Speciality Thermoplastics*, (Eds. S. Thomas, V. P. M.), John Wiley & Sons Inc, New York, **2011**, p. 97−126.
42. a) L. Finelli, M. Fiorini, V. Siracusa, N. Lotti, A. Munari, *J. Appl. Polym. Sci.* **2004,** *92*, 186−193; b) J. Ubach, A. Martınez de Ilarduya, R. Quintana, A. Alla, E. Rude, S. Munoz-Guerra, *J. Appl. Polym. Sci.* **2010**, *115*, 1823−1830.
43 S.W. Lee, M. Ree, C. E. Park, Y. K. Jung, C.-S. Park, Y. S. Jin, D. C.Bae, *Polymer,* **1999**, *40*, 7137−7146.
44. a) M. Jiang, Q. Liu, Q. Zhang, C. Ye, G. Zhou, *J. Polym. Sci. A Polym. Chem.* **2012**, *50,* 1026−1036; b) G. Z. Papageorgiou, V. Tsanaktsis, D. N. Bikiaris, *Phys. Chem. Chem. Phys.* **2014**, *16*, 7946−7958.
45 a) J. Ma, Y. Pang, M. Wang, J. Xu, H. Ma, X. Nie, *J. Mater. Chem.* **2012**, *22*, 3457−3461; b) R. J. I. Knoop, W. Vogelzang, J. van Haveren, D. S. van Es, *J. Polym. Sci. Part A: Polym. Chem.* **2013**, *51*, 4191−4199.
46. N. Kasmi, G. Z. Papageorgiou, D. S. Achilias, D. N. Bikiaris, *Polymers*, **2018**, *10*, 471−492.
47. a) M. Iqbal, B. Norder, E. Mendes, T. J. Dingemans, *J. Polym. Sci, Part A: Polym. Chem.* **2009**, *47*, 1368−1380; b) V. Frosini, G. Levita, *J. Polym. Sci. Polym. Phys. Ed.* **1977**, *15*, 239−245.
48. A. S. Amarasekara, L. Nguyen, N. C. Okorie, S. Jamal, *Green Chem.* **2017***, 19,* 1570−1575.
49. L. Ren, M. M. Yang, C. H. Tung, L. Z. Wu, H. Cong, *ACS Catal.* **2017**, *7*, 8134−8138.
50. N. Santschi, S. Wagner, C. Daniliuc, S. Hermann, M. Schafers, R. Gilmour, *ChemMedChem* **2015**, *10*, 1724−1732.

6. Exploring oxidative NHC-catalysis as organocatalytic polymerization strategy towards polyamide oligomers

The work described in this chapter has formed the basis of the following peer reviewed publication: D. Ragno, A. Brandolese, G. Di Carmine, S. Buoso, G. Belletti, C. Leonardi, O. Bortolini, M. Bertoldo, A. Massi, *Chem. Eur. J.* **2020**, *26*, 1–11.

6.1 Introduction

As discussed in the Chapter 5 for polyesters, polyamides (PAs) find a wide range of applications as fibers, films, and high-performance specialty materials in several industrial sectors,[1] becoming one of the most useful class of polymers. The possibility to form intermolecular hydrogen bonding interactions between the amide portions of polymeric chains, in fact, gives high chemical and heat resistance. The main strategies for the synthesis of PAs (Figure 1) include the polycondensation of diamines with diacids or their derivatives (acyl chlorides and esters), the self-polycondensation of ω-amino acid esters, and the ring-opening polymerization (ROP) of lactams or N-carboxyamino acid anhydrides through standard techniques (melt, interfacial, and solution polymerization).[2] Moreover, a catalytic polyamidation of diols and diamines through iterative dehydrogenation promoted by the Ru-based Milstein catalyst has also been reported.[3]

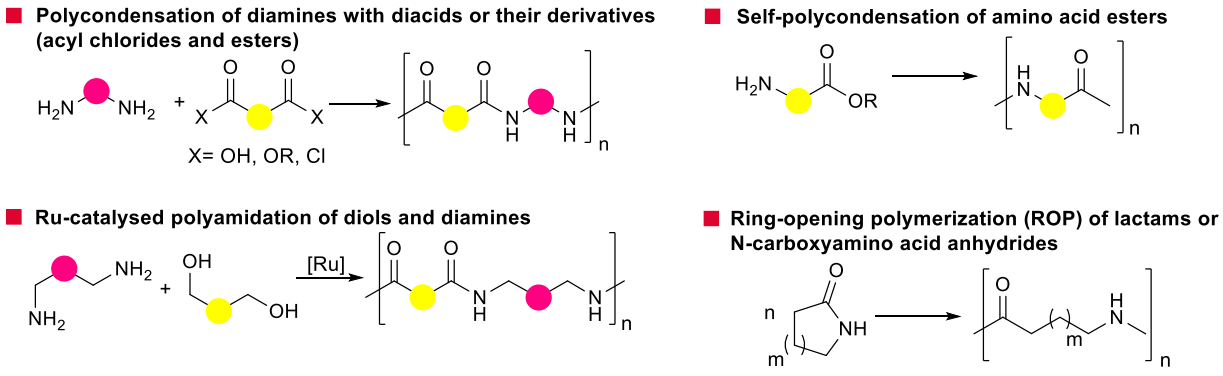

Figure 1. Main strategies for the synthesis of polyamides (PAs).

However, despite the benefits arising from the implementation of metal-free approaches, organocatalytic synthesis of PAs has seldom been investigated. This kind of procedure has already proved to be complementary to metal-catalysis methods in the production of polyesters (PEs), polyurethanes (PUs) and polycarbonates (PCs). Indeed, the catalyst stability and avoidance of contamination are among the advantages of this type of catalysis, thus playing an

important role for applications in the electronic and biomedical fields.[4] To date, the few reported examples focused on organocatalytic processes are limited to the use of guanidine (TBD) and phosphazene (*t*-BuP$_4$) Brønsted bases in the ROP of lactams.[5] Additionally, N-heterocyclic carbene (NHC) catalysts have been studied by DuPont in 2006 for the polymerization of ε-caprolactam[6] and later by Buchmeiser's group for the preparation of PA12 and PA6,12,[7] investigating their strong Brønsted base behaviour. As reported in the previous chapter, NHCs have been recently involved in the polymerization of different monomers such as epoxides, lactones, anhydrides, carbonates, acrylates, siloxanes, and also aldehydes.[9,10] Therefore, the unprecedent polycondensation of dialdehydes and diols promoted by NHCs under oxidative conditions to access PEs by the step-growth polymerization technique (Chapter 5)[11] driven the development of an analogous procedure for the synthesis of PAs (Scheme 1).

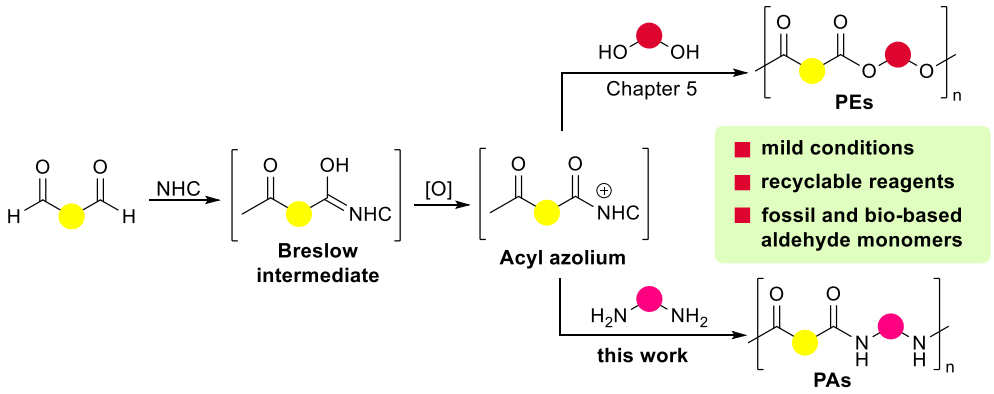

Scheme 1. NHC-based strategy to polyesters (PEs) and polyamides (PAs).

The definition of an NHC organocatalysed strategy to access PAs represents a challenging alternative route based on iterative NHC-catalysed aldehyde-to-amide conversion occurring under mild reaction conditions from readily available monomers. The previously reported methods, in fact, are characterized by some disadvantages such as elevated polycondensation temperatures and the need of reduced pressures in order to remove the condensate, along with the use of hazardous halogenating reagents (e.g., thionyl chloride) in case of more reactive diacyl chloride monomers. Moreover, the ROP procedure might require the multi-step synthesis of starting lactams, that is a time-consuming process especially if functional PAs are targeted.[5b,c] Additionally, the environmental sustainability of this new organocatalytic procedure has been further increased through the use bio-based aldehyde monomers in place of the fossil ones. There is, in fact, an ever-increasing interest in the use of renewable resources for the development of sustainable PAs due to their impact as high-performance materials involved, for instance, in the biomedical sector.[12,13]

6.2 Results and discussion

Preliminary investigation on the formation of PAs oligomers started choosing the polycondensation of ethylenediamine (EDA) **1a** with terephthalaldehyde **2a** as the benchmark reaction. A slight excess of diamine **1a** (1.1 equiv.) was used to promote the formation of the oligomeric poly(*p*-ethylene terephthalamide) (PETA)[14] **3aa** with terminal amine groups (Table 1). However, the direct application of the reaction condition previously optimized for the synthesis of PEs[11] (see Chapter 5 for further details) resulted in no formation of the target oligomer **3aa**, alternatively leading to a complex reaction mixture containing low molecular weight mixed aldehyde and imine derivatives of **2a** (mainly monomers and dimers), as judged by ESI-MS analysis (entry 1). These former conditions contemplated the use of the triazolium salt **C1** (5 mol%) as the pre-catalyst, 1,8-diazabicyclo[5.4.0]undec-7-ene (DBU, 12.5 mol%) as the base and quinone **4** (1 equiv.) as the external oxidant in anhydrous THF. Replacing the oxidant with phenazine **5** resulted in no change on the reaction outcome, producing the same results as the quinone **4** (entry 2). However, the application of direct oxidative N-acylation with aldehydes and primary amine,[15] as already reported in literature, might be precluded by the competing imine formation. The addition of nucleophiles as additives[15a,b,c,f] or the implementation of a two-step procedure with activated ester intermediates[15d,g] could overtake this issue. Consequently, driven by these previous investigations and in agreement with the studies conducted by Connon and co-workers[15m], the addition of the co-catalyst 1,2,4-triazole **6** (20 mol%) was explored. Accordingly, the formation of imine could be suppressed in an amidation of primary amines process; however, the presence of the co-catalyst, along with the couple **C1**/**5**, produced a mixture of mono- and bis-amide derivatives of **2a** without evidence of oligomeric species (detected through ^{1}H NMR and ESI-MS analyses; entry 3). Similarly, unsatisfactory results on the production of oligomers were obtained applying the oxidative amidation procedure of primary amines developed by the groups of Rovis[15b] and Bode.[15a] Indeed, the former method involved the use of **C2** (20 mol%) in combination with 1-hydroxy-7-azabenzotriazole (HOAt) **7** (20 mol%; entry 4), and of **C3** (20 mol%) with imidazole **8** (1.1 equiv.; entry 5), respectively. However in both cases oligomer **3aa** was no detected. Moving to the one-pot two-step amidation strategy *via* hexafluoroisopropyl esters, as reported by Studer and co-workers,[15d] encouraging results were instead recorded. Consequently, the mixture of aldehyde **2a**, **C1** (5 mol%), DBU (12.5 mol%), **4** (1 equiv.), and hexafluoro-2-propanol (HFIP) **9** (1.5 equiv.) in anhydrous THF was reacted for two hours. Afterwards, diamine **1a** (1.1 equiv.) was added and the mixture stirred under inert atmosphere (argon) for an additional 16 hours (entry 6). This procedure allowed the isolation of **3aa** (precipitation technique) in 90% yield

with a number-average molecular weight (M_n) of 1.9 kg mol^{-1} based on ^{1}H NMR spectroscopic analysis. Extending the reaction time (24 hours) did not increase the oligomer length (entry 7), while a shorter time (8 hours) afforded **3aa** with lower yield (70%) and M_n (1.2 kg mol^{-1}; entry 8). Regrettably, the addition of molecular sieves to avoid water nucleophilic attack onto acyl azolium (entry 9) or heating the reaction mixture to 50 °C (entry 10) did not allow to enhance the polymer growth.

Table 1. Optimization process for the synthesis of PETA oligomers **3aa**.[a]

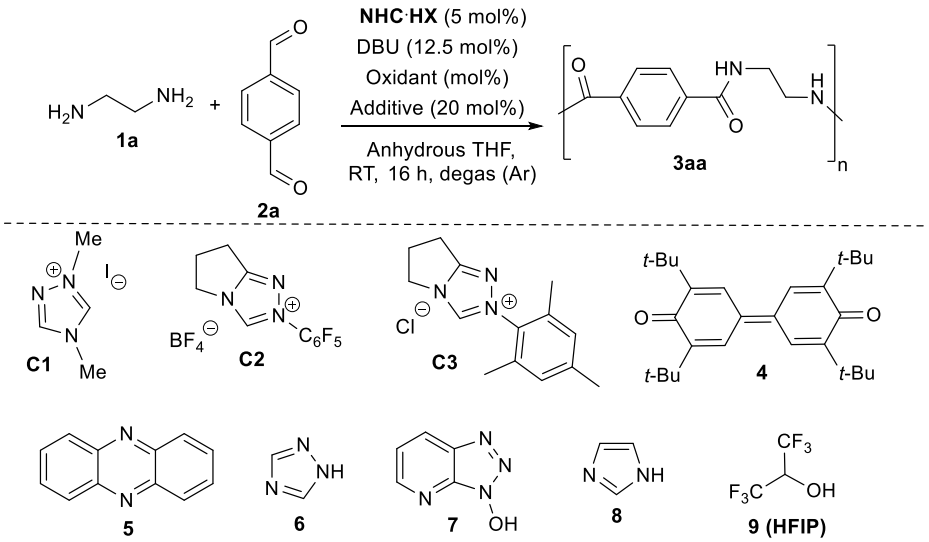

Entry	**NHC HX**	Oxidant	Additive	Conv. (%)[b]	**3aa** (%)[c]	M_n (kg mol^{-1})[d]
1	**C1**	**4**	**-**	>95	-	-
2	**C1**	**5**	**-**	88	-	-
3	**C1**	**5**	**6**	>95	-	-
4	**C2**	**4**	**7**	>95	-	-
5[e]	**C3**	**4**	**8**	>95	-	-
6[f]	**C1**	**4**	**9**	>95	90	1.9
7[f,g]	**C1**	**4**	**9**	>95	91	1.9
8[f,h]	**C1**	**4**	**9**	80	71	1.2
9[f,i]	**C1**	**4**	**9**	>95	86	1.9
10[f,j]	**C1**	**4**	**9**	>95	76	1.5
11[f,k]	**C1**	**4**	**9**	>95	82	1.1
12[l]	**C1**	**4**	**9**	>95	92	1.9

[a]Conditions: **1a** (0.88 mmol), **2a** (0.80 mmol), **NHC·HX** (0.08 mmol), DBU (0.20 mmol), oxidant (1.60 mmol), additive (0.32 mmol), THF (6.0 mL). [b]Detected by ^{1}H NMR of the crude reaction mixture (durene as internal standard). [c]Isolated yield *via* precipitation technique (see the Experimental section). [d]Calculated by ^{1}H NMR after precipitation of the polymer. [e]Imidazole **8**: 1.76 mmol. [f]HFIP **9**: 2.40 mmol. [g]Reaction time 24 h. [h]Reaction time 8 h. [i]Reaction run in the presence of 4Å molecular sieves. [j]Temperature: 50 °C. [k]Anhydrous DCM as solvent. [l]Conditions: **1a** (11.0 mmol), **2a** (10.0 mmol), **C1** (1.00 mmol), **4** (20 mmol), DBU (2.5 mmol), **9** (30.0 mmol), THF (60 mL).

Finally, the replacement of THF with anhydrous DCM showed no improvement likely because of the lower solubility of the growing polymer chain in this halogenated solvent (entry 11). With the optimized conditions in hand (entry 6), the gram-scale synthesis of **3aa** (1.75 g, 92% yield) was conducted using 10 mmol of **2a** (entry 12). As already mentioned in the previous chapters (see the Experimental section for further details), the disclosed procedure allowed the recycle of the quinone **4** (90% isolated yield) and HFIP **9** (up to 85% through evaporation).

The scope and limitations of the unveiled iterative N-acylation of diamines **1** with dialdehyde monomers **2** were further investigated focusing on the synthesis of other semi-aromatic and fully-aromatic PAs **3** of synthetic relevance (Table 2). For instance, oligomeric PETA **3aa** presents thermal stability and flame retardancy and it is often used as charring agent for the synthesis of halogen-free flame retardant polypropylene-based composites.[14c,d] This oligomer are commonly prepared by polycondensation of terephthaloyl acid or chloride with ethylenediamine. Similarly, it is possible to have access to the high molecular weight (HMW) poly(decamethylene terephthalamide, PA10T), which exhibits heat and mechanical resistance together with low water adsorption and good dimensional stability. Thanks to the highly attractive features of this polymer, its synthesis with the disclosed process was performed.

Table 2. Scope of the oxidative polyamidation of diamines **1** with dialdehydes **2**.

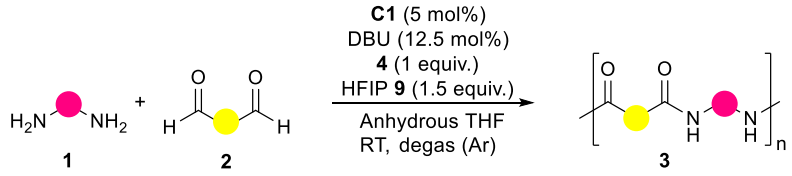

Entry	Diamine	Dialdehyde	Polyamide	M_n (kg mol^{-1})[a]
1	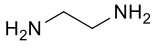 **1a** (EDA)	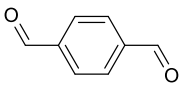 **2a**	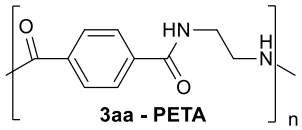 **3aa - PETA** Y= 90%	1.9
2	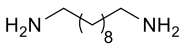 **1b** (1,10-DDA)	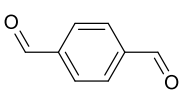 **2a**	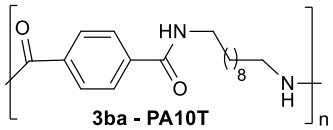 **3ba - PA10T** Y= 88%	2.6
3[b]	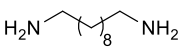 **1b** (1,10-DDA)	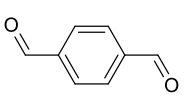 **2a**	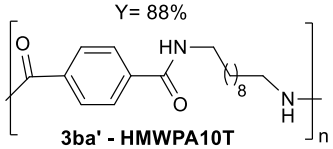 **3ba' - HMWPA10T** Y= 83%	62.8

Conditions: **1** (0.88 mmol), **2** (0.80 mmol), **C1** (0.08 mmol), DBU (0.20 mmol), **4** (1.60 mmol), HFIP **9** (2.40 mmol), THF (6.0 mL). All the reported yields are for the isolated product. [a]Calculated by ^{1}H NMR after precipitation of the polymer. [b]See Scheme 2 and the Experimental Section for reaction conditions.

Therefore, the 1,10-decanediamine (1,10-DDA) **1b**, easily accessible from renewable castor oil, reacted with terephthalaldehyde **2a** affording PA10T oligomers **3ba** in good yield (80%) and

satisfactory molecular weight (M_n = 2.6 kg mol^{-1}; Table 2, entry 2). Later, the oligomer **3ba** was employed as the prepolymer for the synthesis of HMW PA10T **3ba'** (Scheme 2 and Table 2, entry 3), mirroring the two-step polycondensation methodology used for the production of HMW PAs.[16a,c,d,17] Consequently, terephthaloyl chloride **10** was added to a mixture of isolated oligomers **3ba**, N,N-diisopropylethylamine (DIPEA) and LiCl in N,N-dimethylacetamide (DMA) at 0 °C and let it polymerize at room temperature for 48 hours affording **3ba'** (85%) with increased molecular weight (M_n = 62.8 kg mol^{-1}). This outcome was confirmed by the ^{1}H NMR analysis, which showed a fewer integral value of the end group signals at 3.04 ppm (1:1 $CDCl_3$: HFIP; Figure 2).

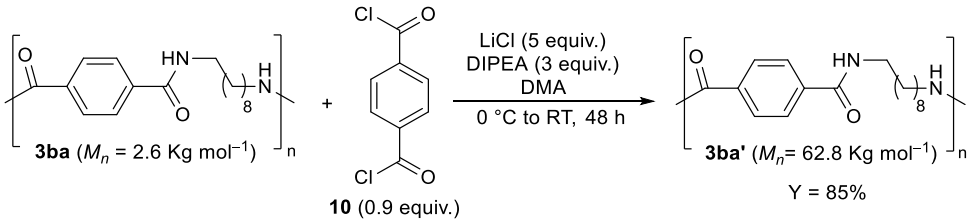

Scheme 2. Two-step procedure for the synthesis of high molecular weight (HMW) PA10T **3ba'**.

Figure 2. ^{1}H NMR spectra of oligomeric prepolymer PAT10 **3ba** and HMW PA10T **3ba'** (1:1 $CDCl_3$:HFIP).

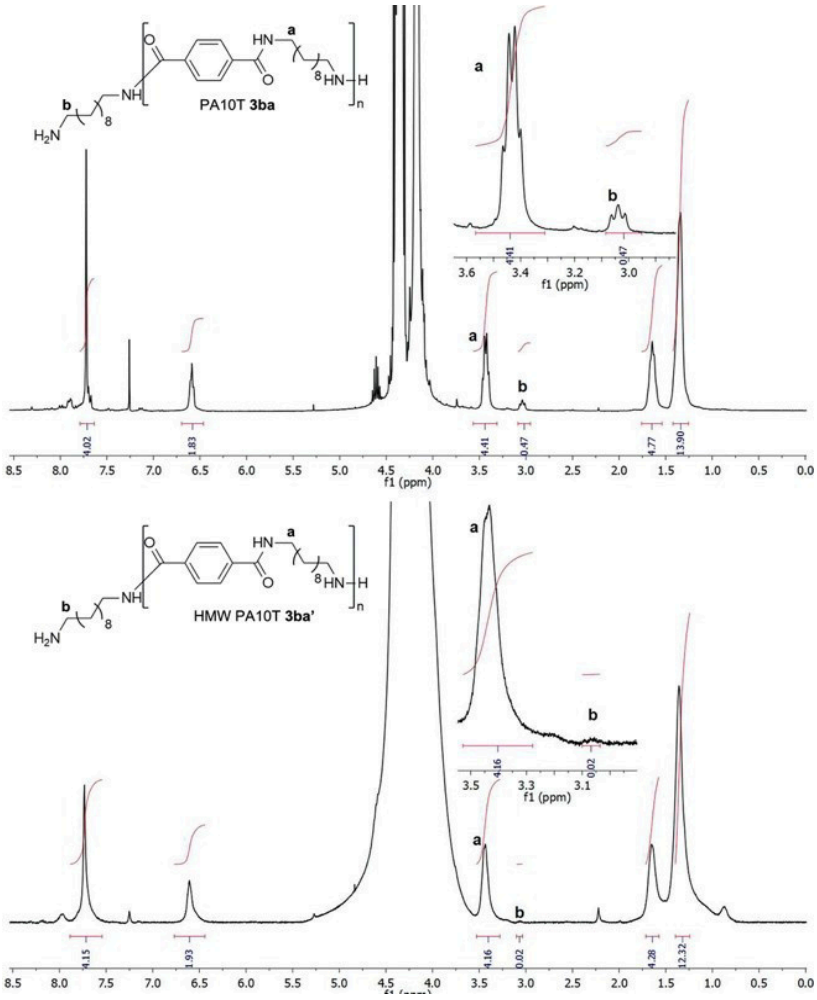

Generally, the most common used method for the determination of *Mn* is the size exclusion chromatography (SEC). However, the use of this technique for semi-aromatic PAs is complicated due to their low solubility in common organic solvents and thus required sophisticated equipment compatible with pure HFIP as eluent. Therefore, validation of the method for *Mn* determination by NMR analysis was performed for HMW PA10T by viscometry. In fact, viscometry is widely recognized as a reliable method for the determination of molecular weight for this class of polymers.[16e,18] In particular, Mathias and co-workers found a correlation between the number-average molecular weight estimated by NMR and the intrinsic viscosity ([η]) of a series of PAs[18a] with *Mn* in the range of ca. 2 − 25.2 kg mol^{-1}.[18] Based upon this correlation, the study started with the synthesis of an authentic sample of PA10T with a molecular weight to fall in the calibration range (**3ba''**, *Mn* = 20.2 kg mol^{-1}; see the Experimental section for further details). Then, **3ba''** was fully solubilized in sulfuric acid (96%) at a concentration of 0.5 g dL^{-1} (12 hours mixing). Single point intrinsic viscosity measurements were performed by means of an Ubbelohde viscometer in a 25 °C controlled water bath. Specific viscosity (η_{sp}) and relative viscosity (η_{rel}) were obtained from flow time data of sulfuric acid and **3ba''** (average of four values, ±0.2 s). Single point intrinsic viscosity ([η]) was then determined using the Solomon-Ciută equation 1[19] ([η] = 1.93). The number-average molecular weight of **3ba''** was estimated with the Mark-Houwink equation 2 considering $K = 5.58 \bullet 10^{-4}$ dL g^{-1} and α = 0.81. These constants were initially calculated for PA12T[18a] and subsequently adopted for PA10T due to the similar molecular structures of these polymers.[16e,18b] The resulting *Mn* for **3ba''** was 22.3 kg mol^{-1}, a value which was in good agreement with that determined by NMR analysis (*Mn* = 20.2 kg mol^{-1}).

$$[\eta] = \frac{\sqrt{2[\eta_{sp} - \ln(\eta_{rel})]}}{c} \qquad \text{(equation 1)}$$

$$Mn = \sqrt[a]{\frac{[\eta]}{K}} \qquad \text{(equation 2)}$$

The scope of the reaction was further extended to the use of 1,6-hexanediamine (1,6-HDA) which allowed the isolation of the oligomeric poly(hexamethylene terephthalamide) (PA6T)[16d] **3ca** (84% yield, M_n = 2.5 kg mol^{-1}) and poly(hexamethylene isophthalamide) (PA6I)[20] **3cb** (78% yield, M_n = 1.7 kg mol^{-1}) with terephthalaldehyde **2a** and isophthalaldehyde **2b**, respectively (Table 2, entries 4 and 5). The introduction of a furan-based moiety led to a special class of PAs characterized by higher solubility and processability respect to the polyphthalamides ones.[21,22] As matter of fact, these furan-based polyamides can be obtained by chemical and enzymatic methods using diamines and 2,5-furandicarboxylic acid (FDCA)[23] monomers (the effective equivalent of terephthalic acid). Thus, the synthesis of this PAs was

addressed using 2,5-diformylfuran (DFF)[24] **2c** as the dialdehyde monomer produced from the platform chemical 5-hydroxylmethyl furfural (HMF). Recently, DFF has found applications in the preparation of furan-urea resins,[25] imine-based polymers,[26] and polyesters.[11] Gratifyingly, the oligomeric polyamides, poly(decamethylene furanamide) (PA10F)[17,21] **3bc** and poly(hexamethylene furanamide) (PA6F)[17,21c,d,22] **3cc**, were obtained in good yield (**3bc** with 81% yield and M_n = 1.6 kg mol^{-1}; **3cc** with 72% yield and M_n = 1.6 kg mol^{-1}) through the unveiled complementary oxidative strategy using DFF **2c** as an alternative for the corresponding acid FDCA (Table 2, entries 6 and 7). In analogy with the synthesis of HMW PA10T **3ba'**, oligomeric **3bc** was utilized as the prepolymer to prepare chain-extended CE-PA10F **3bc'** (Table 2, entry 8). Accordingly, 2,5-furandicarbonyl dichloride **11** was added at 0 °C to a mixture of **3bc**, DIPEA and LiCl in DMA, and the polymerization let to proceed at room temperature for 48 hours affording **3bc'** (76%) with increased molecular weight (*Mn* = 6.5 kg mol^{-1}) as determined by NMR analysis (Scheme 3).

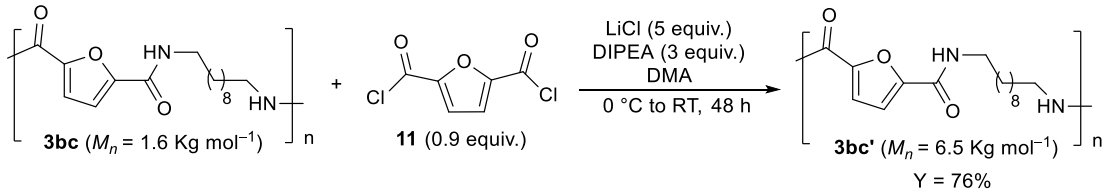

Scheme 3. Two-step procedure for the synthesis of CE-PA10F **3bc'**.

Unfortunately, *Mn* evaluation of **3bc'** by viscosity measurements was not possible due to the absence of known Mark-Houwink coefficients for PA10F and the degradation of the sample in concentrated sulfuric acid, likely because of instability of the furan ring under strong acidic conditions for the prolonged time necessary for viscosity analysis.

Additionally, the unprecedent polycondensation of 5,5'-[oxybis(methylene)]bis[2-furaldehyde] (OBFA)[27] **2d** with diamines **1b** and **1c** was also investigated, yielding the oligomers **3bd** (PA10FF; M_n = 3.2 kg mol^{-1}) and **3cd** (PA6FF; M_n = 3.6 kg mol^{-1}), which displayed the unusual polyamide-ether repeating unit (Table 2, entries 9 and 10). Lastly, the fully aromatic polyamide **3da** (86%; M_n = 1.9 kg mol^{-1}) with a potential enhanced thermal property, due to the stiffer backbone structure,[28] was addressed through the polyamidation of 2,5-bis(aminomethyl)furan (BAF)[29] **1d** with terephthalaldehyde **2a** (entry 11).

Table 2 (continued). Scope of the oxidative polyamidation of diamines **1** with dialdehydes **2**.

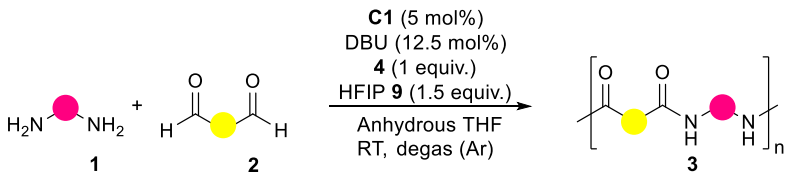

Entry	Diamine	Dialdehyde	Polyamide	M_n (kg mol^{-1})[a]
4	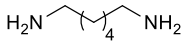 **1c** (1,6-HDA)	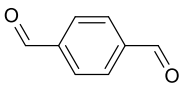 **2a**	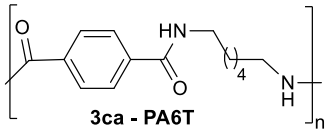 **3ca - PA6T** Y= 84%	2.5
5	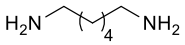 **1c** (1,6-HDA)	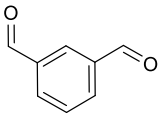 **2b**	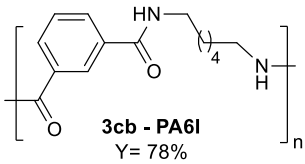 **3cb - PA6I** Y= 78%	1.7
6	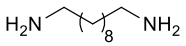 **1b** (1,10-DDA)	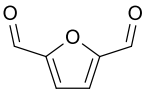 **2c** (DFF)	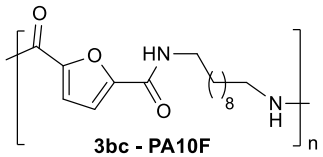 **3bc - PA10F** Y= 81%	1.6
7	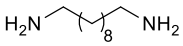 **1c** (1,6-HDA)	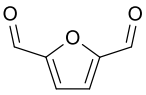 **2c** (DFF)	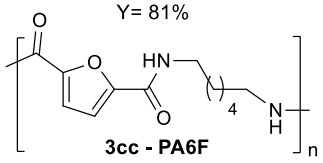 **3cc - PA6F** Y= 72%	1.7
8[b]	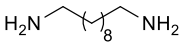 **1b** (1,10-DDA)	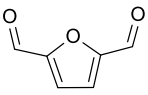 **2c** (DFF)	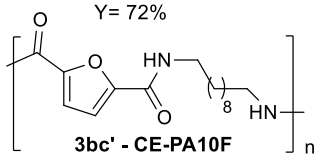 **3bc' - CE-PA10F** Y= 76%	6.5
9	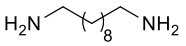 **1b** (1,10-DDA)	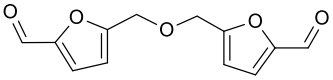 **2d** (OBFA)	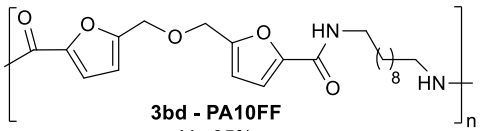 **3bd - PA10FF** Y= 95%	3.2
10	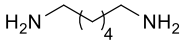 **1c** (1,6-HDA)	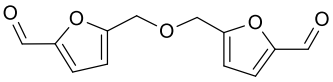 **2d** (OBFA)	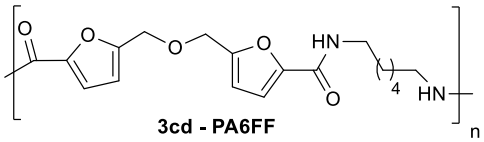 **3cd - PA6FF** Y= 90%	3.6
11	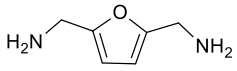 **1d** (BAF)	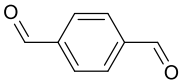 **2a**	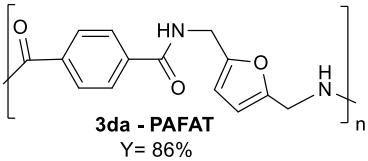 **3da - PAFAT** Y= 86%	1.9

Conditions: **1** (0.88 mmol), **2** (0.80 mmol), **C1** (0.08 mmol), DBU (0.20 mmol), **4** (1.60 mmol), HFIP **9** (2.40 mmol), THF (6.0 mL). All the reported yields are for the isolated product. [a]Calculated by ^{1}H NMR after precipitation of the polymer. [b]See Scheme 3 and the Experimental section for reaction conditions.

At this point of the study, thermogravimetric analysis was carried out to assess the thermal stability of the prepared PAs (Table 3; analyses conducted at ISOF-CNR, Bologna).

Table 3. Decomposition temperature at 5% weight loss ($T_{d,5\%}$), temperature of maximum degradation rate (T_d) and residuum after degradation (Res.) from TGA analyses; glass transition temperature (T_g), melting temperature (T_m), crystallization temperature (T_c) and melting enthalpy (ΔH_m) from DSC analyses of polyamides **3**.

	$T_{d,5\%}$ (°C)	T_d[a] (°C)	Res.[b] (%)	T_g[c] (°C)	T_m[d] (°C)	T_c (°C)	ΔH_m (J g^{-1})	M_n (kg mol^{-1})	ref.
PETA (3aa)	264	431	31.0±0.5	n.d.	n.d.	n.d.	n.d.	1.9.	
PETA (lit.)	250	450	n.a.	n.a.	n.a	n.a	n.a	4.2	31
	~420	~450	20-30	n.d.	n.d.	n.d.	n.d	>10	32
PA10T (3ba)	377	486	2.5±0.5	106	220	185	19	2.6	
PA10T (3ba'')	364	482	1.8±0.5	117	235	198	15.3	20.2	
HMW PA10T (3ba')	291	465	2.5±0.5	117	200, 287, 296	177, 273	3.2, 43.4[e]	62.8	
	n.a.	n.a.	n.a.	n.a.	304, 317	n.a.	90	4.2	16e[f]
	436	491	n.a.	132.3	302, 313	287.7	100	11	30b
PA10T (lit.)	n.a	n.a	n.a.		279	n.a.	n.a.	14	33
	420−440	479	< 5	132.6	313	276	n.a.	21	30a
	426	482	n.a.	113	290	n.a.	n.a.	26	33
PA6T (3ca)	355	472	6.5±0.5	146	277	217	16	2.5	
	>380	480−484	2.4−5.2	n.a.	374−379[f]	n.a.	108−146	3.8−3.9	34
PA6T (lit.)	245	471	n.a.	170	270	n.d..	n.d.	15.6	22a
	428	~450	~5	n.a.	368	n.d	n.d.	>10	32
PA6I (3cb)	176	475	3.6±0.5	105	n.d.	n.d.	n.d.	1.7	
PA6I (lit.)	409	455	n.a.	132	n.d.	n.d.	n.d.	15.7	22b
PA10F (3bc)	159	462	11.5±0.5	90	n.d.	n.d.	n.d.	1.6	
CE-PA10F (3bc')	310	455	21.8±0.5	132	n.d.	n.d.	n.d.	6.5	
PA10F (lit.)	n.a	350-450	n.a.	71	n.d.	n.d.	n.d.	5.3	21d
	366	473	n.a	98	135	n.a.	n.a..	13.4	21d
PA6F (3cc)	171	404	34.5±0.5	90−110	n.d.	n.d.	n.d.	1.7	
	380			95				2.4	22b
PA6F (lit.)	n.a	350−410	n.a.	110	n.d	n.d.	n.d.	5.2	21b
	322	460	n.a.	119	162	n.a	n.a	13.4	21d
	287−309	355−408	n.a.	86−64	n.d.	n.d.	n.d.	30−62	22a
PA10FF (3bd)	292	456	21.0±0.5	69	n.d.	n.d.	n.d.	3.2	
PA6FF (3cd)	225	357	28.0±0.5	73	n.d.	n.d.	n.d.	3.6	
PAFAT (3da)	157	349	19.5±0.5	n.d.	n.d.	n.d.	n.d.	1.9	

[a]Temperature of the peak minimum in the DTGA plots. [b]Residuum at 850 °C. [c]Values at the midpoint. [d]Values at the peak maximum. [e]Total area of the peaks with maximum at 287 °C and 296 °C; n.d. = not detected; n.a. = not available. [f]Data collected at 20 °C min^{-1} as scan rate.

Under standard conditions in nitrogen atmosphere, the PA10T oligomer **3ba** displayed a very good thermal stability, exhibiting a main degradation process with T_d at 486 °C (Figure 3). Surprisingly, samples of higher *Mn* (**3ba'** and **3ba''**), obtained by subsequent chain extension with terephthaloyl chloride, showed a lower value, and the stability decrease is highest for the polymer with the highest M_n. In any case, the values are comparable to those of PA10T obtained by other polymerization methods (Table 3 and references therein) and the differences lie within

the range often observed among similar samples prepared in different batches.[34] Moreover, the differences among the temperature at the maximum degradation rate reflect the differences among the temperature of 5% mass loss. The mass loss at low temperature is instead associated to the chain ends. The shift of the temperature which characterized polymers with high molecular weight can be ascribed to the increase of the polydispersity (PDI) in the second step process. Indeed, step growth polymerization is known to give polymers with PDI ≥ 2, depending on the reagent ratio. However, for a laboratory scale preparation the control over the reagent ratio can be difficult, while it can be usually overcome by scaling to industrial production where appropriate measure to reduce reagent volatilization can be implemented. The oligomer **3ca** presented a degradation temperature value between those detected for HMW PA10T **3ba'** and the oligomer **3ba** with an onset degradation temperature at 445 °C (Table 3). The detected values are comparable with those reported for PA6T obtained by solid-state polycondensation from salt precursors[16a] or by interfacial polycondensation.[30]

Later, DSC analysis (Table 3) was conducted showing high thermal stability for both PA6T **3ca** and PA10T **3ba** thus indicating a semicrystalline structure. Moreover, the temperature for the melting and crystallization peaks for PA6T turned out to be higher respect to those of PA10T as expected by the different length of the alkyl chain in agreement with literature.[35] As indicated in Figure 4, HMW PA10T **3ba'** exhibited a higher melting temperature and enthalpy than its precursor **3ba**. The melting and crystallization peaks observed in the extended chain polymer **3ba'** are also present in oligomer **3ba**, whereas the extra peak at higher temperature in HMW PA10T can be ascribed to crystals made of HMW chains (Figure 4). Low molecular weight (LMW) sample fractions or crystals including chain ends can instead be considered responsible for the low temperature peak. Indeed, as already mentioned polymers obtained by step-growth polymerization are known to have polydispersity index larger than 2 and the value is as much high as the reagent ratio in the feed differs from 1. This event may also occur if the two reagents have different volatility, therefore during the polymerization under vacuum the reagent ratio may change as in the case of the PA10T oligomeric precursor and terephthaloyl chloride. Lastly, the observed difference between the characteristic temperatures of the polymer prepared by the herein proposed method and by salt condensation supported the high polydispersity of the sample. Indeed, in the latter mentioned case, the characteristic temperature values are a little bit higher, thus supporting the lower polydispersity. The consistency of the presented data is corroborated by the intermediate characteristic temperatures observed for PA10T **3ba''** having intermediate molecular weight with respect to **3ba** and **3ba'**.

Additionally, chain extended PA10Ts showed glass transition temperature larger than the oligomer precursor, as expected, and the value is comparable to the one of PA10T exhibiting a similar melting value.[33] This last value is a little bit lower with respect to the other reported values, but this is strongly affected by the conditions adopted for sample isolation, as well as by the analysis conditions, such as heating rate, and isothermal steps.[16c] All others synthesized polymers **3** did not show any melting peaks in the analysed temperature range. This result is in accordance with the literature in the case of PA10F and PA6F as for both polymers, melting peaks were observed only for samples with molecular weight larger than the ones described in the present chapter (Table 3). In the case of PA10FF, PA6FF and PAFAT no data on the thermal behavior have been previously reported.

All the analysed polymers showed glass transition processes with temperature values ranging in between 69 °C and 146 °C, except for PETA **3aa** and PAFAT **3da** (Table 3). These values are in good accordance with previous reported data in the case of terephthalate polymers, when polymers with comparable molecular weight are considered (Table 3). Indeed, these polymers are made up of very rigid main-chain structure and their transitions temperature cannot be properly identified either because these transitions can be present at temperatures above the investigated range, or because they occur with a very low change in specific heats c_p. A further comparison among the thermal stability of terephthalaldehyde- and isophthalaldehyde-derived polyamides showed large differences between semicrystalline and amorphous PAs (Figure 3).

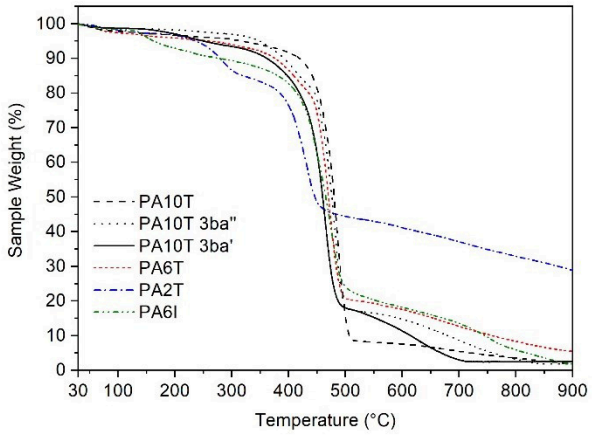

Figure 3. Comparison among the TGA curves of terephthalaldehyde- and isophthalaldehyde-derived polyamides.

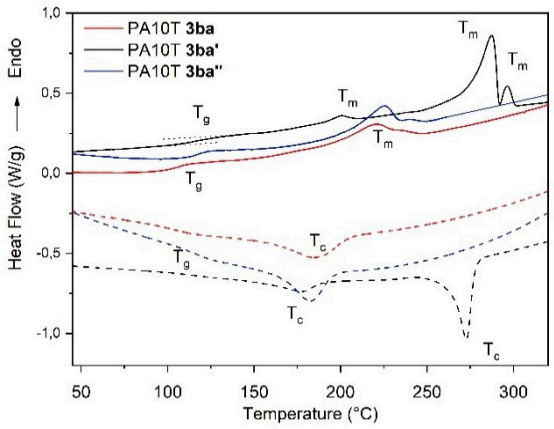

Figure 4. DSC analysis at 10 °C min^{-1} of PA10T oligomer (red lines), **3ba'** (black lines) and **3ba''** (blue lines). Dashed lines are cooling steps performed after pre-heating. Solid lines are 2nd heating steps accomplished after the cooling ones.

Indeed, a two-step process was observed for both PETA **3aa** and PA6I **3cb** with the first having onset temperature in the 200 − 300 °C temperature range, and the second at around 400 °C. The first step corresponded to the loss of low molecular weight fractions of the polymers.[32]

Additionally, degradation plots of PAs showed different residuum after thermal degradation, which is highest for PETA, medium for both PA6T and PA6I, and lowest for PA10T (Figure 3 and Table 3) in agreement with previous literature finding (Table 3 and references therein). As this difference depends on the N/C ratio, usually, the higher the ratio, the more this parameter increases. Apart from the oligomer of PA10F **3bc'** and PA10FF **3bd**, which is stable up to 310 °C, all the synthesised furan-based PAs displayed a general low thermal stability (Figure 5), starting to degrade in between 130 °C and 206 °C (Table 3). Although **3bd** did not show any crystallization and melting peaks during cooling and the subsequent heating (up to 250 °C) its higher thermal stability can be ascribed to the presence of some crystallinity phase with melting temperature above the degradation. However, at the present, this hypothesis cannot be confirmed without any additional investigation. For the same reason, the former hypothesis cannot support the data for PA10F **3dc'**, which is much more stable than the precursor **3bc**' at lower molecular weight. In fact, this polymer was previously reported to give crystallization with melting temperature at 138 °C, which is close to the glass transition. In any case, the still scarce data on these polymers do not allow to unambiguously explain the observed thermal behavior.

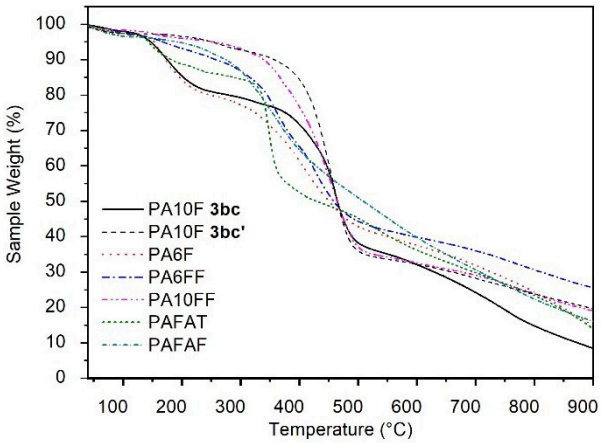

Figure 5. Comparison among the TGA curves of furan-based polyamides.

Lastly, a possible mechanism hypothesised for the NHC-promoted polyamidation relies on an ionic pathway in agreement with Studer proposal[15d] and the general mechanism of oxidative NHC-catalysis,[36] is reported in Scheme 4. Accordingly, the NHC **I** generated by deprotonation of triazolium salt **C1** reacts with aldehyde **2** to give the Breslow intermediate **II**, which in turn is oxidized to the acyl azolium **III** by the external oxidant **4**. Subsequently, the nucleophilic attack by HFIP **9** generates the hexafluoroisopropyl monoester **IV** along with the turnover of NHC catalyst. Later, the aldehyde functionality of monoester **IV** is then involved in a second catalytic cycle affording the hexafluoroisopropyl diester **V** (the concurrent oxidative

esterification of both aldehyde functionalities of **2** seems to be unlikely but it cannot be excluded). Diester **V** is, however, the key substrate of the subsequent amidation step as confirmed by NMR and IR analyses (see the Experimental section for details). At this point, substitution reaction with the amine **1** affords the amide **3** and release HFIP in an iterative manner yielding PAs **3**.

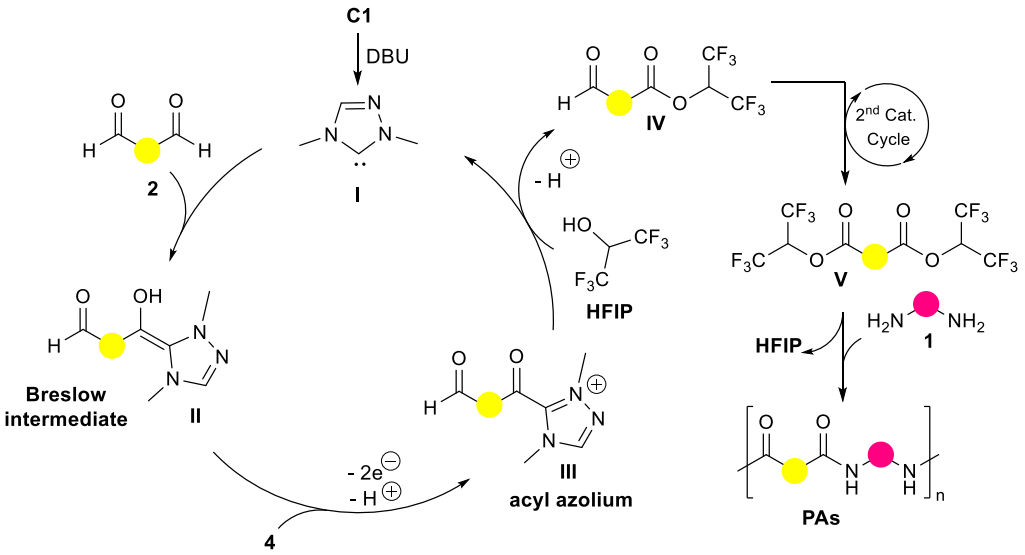

Scheme 4. Proposed catalytic cycles for NHC-catalysed amide bond formation.

6.3 Conclusion

In summary, a new strategy for the synthesis of oligomeric polyamides (PAs) has been developed. This methodology relied on the step-growth polycondensation of diamines and dialdehydes promoted by N-heterocyclic carbene (NHC) catalyst in oxidative conditions. The optimized procedure emerged as an eco-friendly alternative thanks to the mild conditions and the use of bio-based monomers, along with the possibility to recycle both the external oxidant **4** (90% isolated yield) and the hexafluoro-2-proponal (HFIP, up to 85% through evaporation). Indeed, the addition of HFIP as a nucleophilic additive proved to be essential to guarantee the oligomer growth, leading to PAs (M_n = 1.7 − 3.6 kg mol^{-1}) which are well-suited with a further chain-elongation step. A high molecular weight polyamide can thus be obtained as demonstrated by the synthesis of industrially relevant PA10T (with a M_n = 62.8 kg mol^{-1}) and PA10F (M_n = 6.5 kg mol^{-1}). Lastly, newly bio-based PAs have been synthetized as a further step for the development of environmentally benign macromolecular materials.

6.4 Experimental section

General experimental procedure

All moisture-sensitive reactions were performed under an argon atmosphere using oven-dried glassware. Solvents were dried over a standard drying agent and freshly distilled prior to use. Reactions were monitored by TLC on silica gel 60 F_{254} with detection by UV lamp operating at 254 nm and 365 nm. FT-IR analyses were performed using the Bruker Instrument Vertex 70. Flash column chromatography was performed on silica gel 60 (230−400 mesh). ^{1}H (300 MHz) and ^{13}C (101 MHz) NMR spectra were recorded in $CDCl_3$:HFIP mixtures or DMSO-d_6 solutions at room temperature. The chemical shifts in ^{1}H and ^{13}C NMR spectra were referenced to trimethylsilane (TMS). Peak assignments were aided by ^{1}H-^{1}H COSY and gradient-HMQC experiments. Bases (DBU, DIPEA) were freshly distilled before their utilization. All diamines and dialdehydes are commercially available except for aldehyde **2d**, which was prepared by following a literature procedure.[37] Catalyst **C1** was purchased from TCI, catalyst **C2** was purchased from ABCR and catalyst **C3** was purchased from Sigma-Aldrich. Compounds **4**−**11**, LiCl and iron(II) phthalocyanine were purchased from TCI and used as received without further purification. Thermogravimetric (TG) analysis was performed on a TGA 4000, PerkinElmer Inc., USA, instrument equipped with Pyris software for data acquisition and analysis. Samples (5–10 mg) in an alumina pans were analysed from 30 °C to 900 °C under nitrogen atmosphere (30 mL min^{-1}) at a heating rate of 10 °C min^{-1}. Calorimetric measurements (DSC) were performed using a PerkinElmer, USA DSC 8000 differential scanning calorimeter equipped with an Intracooler II as refrigeration system. The instrument was calibrated in temperature and energy with high-purity indium and zinc as standards. 5−10 mg of each sample was analysed in aluminum pans under dry nitrogen atmosphere (30 mL min^{-1}). Samples were at first heated up to a temperature T (see table below) to erase the thermal history and to remove any trapped volatile substance such as solvent residual from the synthesis. Then, they were cooled down to −10 °C and finally heated up again (2^{nd} heating step) up to at the temperature T (Table 4). Temperatures T was selected above the degradation temperature of polymers as determined by TGA. Heating and cooling steps were all performed at 10 °C min^{-1} as scanning rate.

Table 4. Maximum heating temperature in DSC analysis for the different samples.

Sample	Temperature T (°C)
PETA (3aa)	190
PA10T (3ba)	400
PA10T (3ba' and 3ba'')	340
PA6T (3ca)	350
PA6I (3cb)	140
PA10F (3bc)	140
CE-PA10F (3bc')	300
PA6F (3cc)	140
PA10FF (3bd)	250
PA6FF (3cd)	140
PAFAT (3da)	140

General procedure for the synthesis of polyamides 3

A mixture of pre-catalyst **C1** (0.08 mmol) and hexafluoro-2-propanol (HFIP) (2.40 mmol) in anhydrous THF (6.0 mL) was degassed under vacuum and saturated with argon (by an Ar-filled balloon) three times. Then, DBU was added (0.20 mmol), and the reaction was stirred at room temperature for 5 minutes. Later, oxidant **4** (1.60 mmol) and aldehyde **2** (0.80 mmol) were added, and the reaction mixture was stirred at room temperature for 2 h. After complete consumption of aldehyde (verified by ^{1}H NMR analysis), diamine **1** (0.88 mmol) was added and the reaction was stirred for 16 h at the same temperature. After this period, the mixture was concentrated, and the resulting residue triturated with fresh portions of Et_2O (3 × 10 mL) and centrifuged. The organic solutions were collected for the recovery of DBU and oxidant **4** while the solid precipitate was dissolved in the minimum amount of appropriate solvent, and precipitated by dropwise addition into a poor solvent at 0 °C.

Poly(ethylene terephthalamide) **(3aa, PETA)**

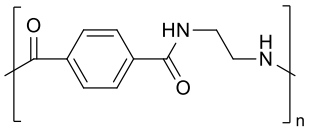

The reaction mixture was dissolved in a minimum amount of DCM and hexafluoroisopropanol (HFIP) (1:1, v/v) and precipitated from Et_2O (10 volumes) at 0 °C. Filtration followed by washing with cold Et_2O and drying under vacuum at 100 °C afforded the product **3aa** (137 mg, 90%, M_n = 1.9 kg mol^{-1}) as a pale yellow solid. **^{1}H NMR** (300 MHz, 1:1 $CDCl_3$:HFIP) δ = 7.74 (s, 4H, Ar), 7.47 − 7.29 (m, 2H, -CONH-), 3.70 (s, 4H, -C*H*$_2$NHCOR), 3.24 (s, 4H, terminal

-C*H*$_2$NH$_2$); **^{13}C NMR** (101 MHz, 1:1 CDCl$_3$:HFIP) δ = 170.6 (CO), 136.6 (C, Ar), 129.6 (periferic CH, Ar), 127.6 (CH, Ar), 41.2 (terminal -CH$_2$NH$_2$), 40.3 (-*C*H$_2$NHCOR); **FT-IR** (KBr) ν: 3289, 3060, 2920, 1630, 1536, 1284 cm^{-1}.

Poly(decamethylene terephthalamide) **(3ba, PA10T)**

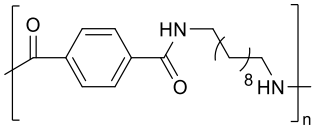

The reaction mixture was dissolved in a minimum amount of DCM and hexafluoroisopropanol (HFIP) (1:1, v/v) and precipitated from Et$_2$O (10 volumes) at 0 °C. Filtration followed by washing with cold Et$_2$O and drying under vacuum at 100 °C afforded the product **3ba** (213 mg, 88%, M_n = 2.6 kg mol^{-1}) as a pale yellow solid. **^{1}H NMR** (300 MHz, 1:1 CDCl$_3$:HFIP) δ = 7.70 (s, 4H, Ar), 6.59 (s, 2H, -CONH-), 3.43 (s, 4H, -C*H*$_2$NHCOR), 3.04 (s, 4H, terminal -C*H*$_2$NH$_2$), 1.64 (s, 4H, -C*H*$_2$CH$_2$NHCOR), 1.34 (s, 12H, -C*H*$_2$C*H*$_2$C*H*$_2$CH$_2$CH$_2$NHCOR); **^{13}C NMR** (101 MHz, 1:1 CDCl$_3$:HFIP) δ = 169.8 (CO), 136.8 (C, Ar), 127.1 (CH, Ar), 41.2 (terminal -CH$_2$NH$_2$), 40.8 (-*C*H$_2$NHCOR), 29.0 (-*C*H$_2$CH$_2$NHCOR), 28.8 (-*C*H$_2$CH$_2$CH$_2$NHCOR), 28.6 (-*C*H$_2$CH$_2$CH$_2$CH$_2$NHCOR), 26.4 (-*C*H$_2$CH$_2$CH$_2$CH$_2$CH$_2$NHCOR); **FT-IR** (KBr) ν: 3312, 2922, 2852, 1626, 1538, 1291 cm^{-1}.

Poly(hexamethylene terephthalamide) **(3ca, PA6T)**

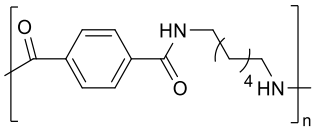

The reaction mixture was dissolved in a minimum amount of DCM and hexafluoroisopropanol (HFIP) (1:1, v/v) and precipitated from Et$_2$O (10 volumes) at 0 °C. Filtration followed by washing with cold Et$_2$O and drying under vacuum at 100 °C afforded the product **3ca** (165 mg, 84%, M_n = 2.5 kg mol^{-1}) as a pale yellow solid. **^{1}H NMR** (300 MHz, 1:1 CDCl$_3$:HFIP) δ = 7.72 (s, 4H, Ar), 6.64 (s, 2H, -CONH-), 3.46 (s, 4H, -C*H*$_2$NHCOR), 3.03 (s, 4H, terminal -C*H*$_2$NH$_2$), 1.66 (s, 4H, -C*H*$_2$CH$_2$NH COR), 1.44 (s, 4H, -C*H*$_2$CH$_2$CH$_2$NHCOR); **^{13}C NMR** (101 MHz, 1:1 CDCl$_3$:HFIP) δ = 170.3 (CO), 137.3 (C, Ar), 127.6 (CH, Ar), 41.1 (-*C*H$_2$NHCOR), 29.0 (-*C*H$_2$CH$_2$NHCOR), 26.5 (-*C*H$_2$CH$_2$CH$_2$NHCOR); **FT-IR** (KBr) ν: 3304, 2937, 2866, 1626, 1539, 1287 cm^{-1}.

Poly(hexamethylene isophthalamide) **(3cb, PA6I)**

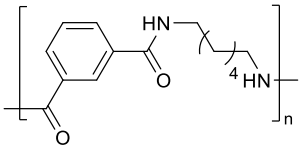

The reaction mixture was dissolved in a minimum amount of DCM and hexafluoroisopropanol (HFIP) (1:1, v/v) and precipitated from Et_2O (10 volumes) at 0 °C. Filtration followed by washing with cold Et_2O and drying under vacuum at 100 °C afforded the product **3cb** (153 mg, 78%, M_n = 1.7 kg mol^{-1}) as an off-white solid. **^{1}H NMR** (300 MHz, 1:1 $CDCl_3$:HFIP) δ = 7.95 (s, 1H, Ar), 7.88 − 7.76 (m, 2H, Ar), 7.69 − 7.47 (m, 1H, Ar), 6.92 − 6.59 (m, 2H, -CONH-), 3.44 (s, 4H, -C*H*$_2$NHCOR), 3.11 (s, 4H, terminal -C*H*$_2$NH$_2$), 1.67 (s, 4H, -C*H*$_2$CH$_2$NH COR), 1.45 (s, 4H, -C*H*$_2$CH$_2$CH$_2$NHCOR); **^{13}C NMR** (101 MHz, 1:1 $CDCl_3$:HFIP) δ = 170.0 (CO), 134.1 (CH, Ar), 132.1(C, Ar), 130.0 (CH, Ar), 129.7 (CH, Ar), 41.1 (terminal -CH_2NH_2), 40.6 (-*C*H$_2$NHCOR), 40.0 (terminal -*C*H$_2$NHCOR), 28.4 (-*C*H$_2$CH$_2$NHCOR), 28.2 (terminal -*C*H$_2$CH$_2$NHCOR), 26.8 (terminal -*C*H$_2$CH$_2$NH$_2$), 26.0 (-*C*H$_2$CH$_2$CH$_2$NHCOR), 25.2 (terminal -*C*H$_2$ CH$_2$CH$_2$NHCOR), 24.7 (terminal -*C*H$_2$CH$_2$CH$_2$NH$_2$); **FT-IR** (KBr) ν: 3277, 2932, 2855, 1737, 1635, 1532, 1373, 1282 cm^{-1}.

Poly(decamethylene 2,5-furandicarboxylamide) **(3bc, PA10F)**

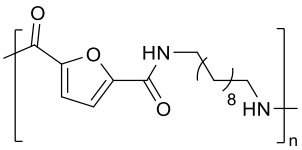

The reaction mixture was dissolved in a minimum amount of DCM and hexafluoroisopropanol (HFIP) (1:4, v/v) and precipitated from Et_2O (10 volumes) at 0 °C. Filtration followed by washing with cold Et_2O and drying under vacuum at 100 °C afforded the product **3bc** (189 mg, 81%, M_n = 1.6 kg mol^{-1}) as a creamy solid. **^{1}H NMR** (300 MHz, 1:4 $CDCl_3$:HFIP) δ = 7.18 (s, 2H, Furan), 3.46 (s, 4H, -C*H*$_2$NHCOR), 3.12 (s, 4H, terminal -C*H*$_2$NH$_2$), 1.66 (s, 4H, -C*H*$_2$CH$_2$NHCOR), 1.40 (s, 12H, -C*H*$_2$C*H*$_2$C*H*$_2$CH$_2$CH$_2$NHCOR); **^{13}C NMR** (101 MHz, 1:4 $CDCl_3$:HFIP) δ = 159.5 (CO), 147.6 (C, Furan), 115.4 (CH, Furan), 41.1 (terminal -CH_2NH_2), 40.1 (-*C*H$_2$NHCOR), 29.0 (-*C*H$_2$CH$_2$NHCOR), 28.8 (-*C*H$_2$CH$_2$CH$_2$NHCOR), 28.7 (-*C*H$_2$CH$_2$CH$_2$CH$_2$NHCOR), 26.4 (-*C*H$_2$CH$_2$CH$_2$CH$_2$CH$_2$NHCOR); **FT-IR** (KBr) ν: 3272, 2925, 2854, 1737, 1642, 1575, 1365, 1283, 1178 cm^{-1}.

Poly(hexamethylene 2,5-furandicarboxylamide) **(3cc, PA6F)**

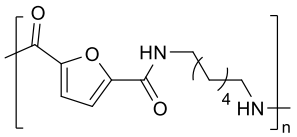

The reaction mixture was dissolved in a minimum amount of DCM and hexafluoroisopropanol (HFIP) (1:1, v/v) and precipitated from Et_2O (10 volumes) at 0 °C. Filtration followed by washing with cold Et_2O and drying under vacuum at 100 °C afforded the product **3cc** (136 mg, 72%, M_n = 1.7 kg mol^{-1}) as a creamy solid. **^{1}H NMR** (300 MHz, 1:1 $CDCl_3$:HFIP) δ = 7.07 (s, 2H, Furan), 3.41 (s, 4H, -C*H*$_2$NHCOR), 3.08 (s, 4H, terminal -C*H*$_2$NH$_2$), 1.63 (s, 4H, -C*H*$_2$CH$_2$NHCOR), 1.40 (s, 4H, -C*H*$_2$CH$_2$CH$_2$NHCOR); **^{13}C NMR** (101 MHz, 1:1 $CDCl_3$:HFIP) δ = 159.9 (CO), 147.9 (C, Furan), 115.9 (CH, Furan), 41.4 (terminal -CH$_2$NH$_2$), 40.1 (-*C*H$_2$NHCOR), 28.8 (-*C*H$_2$CH$_2$NHCOR), 26.1 (-*C*H$_2$CH$_2$CH$_2$NHCOR); **FT-IR** (KBr) ν: 3277, 2931, 2861, 1738, 1642, 1575, 1365, 1283, 1177 cm^{-1}.

Poly(decamethylene 5,5′-(oxybis(methylene))bis(2-furancarboxylamide)) **(3bd, PA10FF)**

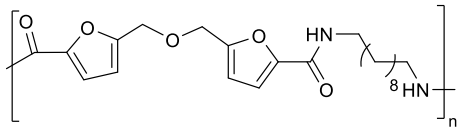

The reaction mixture was dissolved in a minimum amount of DCM and hexafluoroisopropanol (HFIP) (1:1, v/v) and precipitated from Et_2O (10 volumes) at 0 °C. Filtration followed by washing with cold Et_2O and drying under vacuum at 100 °C afforded the product **3bd** (306 mg, 95%, M_n = 3.2 kg mol^{-1}) as a pale yellow solid solid. **^{1}H NMR** (300 MHz, 1:1 $CDCl_3$:HFIP) δ = 7.06 (d, *J* 3.3 Hz, 2H, H-3, Furan), 6.87 (s, 2H, -CONH-), 6.52 (d, *J* 3.3 Hz, 2H, H-4, Furan), 4.53 (s, 4H, Furan-CH$_2$OR), 3.44−3.28 (m, 4H, -C*H*$_2$NHCOR), 3.09−2.91 (m, 4H, terminal -C*H*$_2$NH$_2$), 1.62 (s, 4H, -C*H*$_2$CH$_2$NHCOR), 1.33 (s, 12H, -C*H*$_2$C*H*$_2$C*H*$_2$CH$_2$CH$_2$NHCOR); **^{13}C NMR** (101 MHz, 1:1 $CDCl_3$:HFIP) δ = 160.2 (CO), 152.4 (C-5, Furan), 146.8 (C-2, Furan), 116.0 (C-3, Furan), 113.0 (C-4, Furan), 63.4 (Furan-CH$_2$OR), 39.8 (-*C*H$_2$NHCOR), 29.0 (-*C*H$_2$CH$_2$NHCOR), 28.8 (-*C*H$_2$CH$_2$CH$_2$NHCOR), 28.7 (-*C*H$_2$CH$_2$CH$_2$CH$_2$NHCOR), 26.4 (-*C*H$_2$CH$_2$CH$_2$CH$_2$CH$_2$NHCOR); **FT-IR** (KBr) ν: 3287, 2920, 2850, 1737, 1634, 1554, 1310, 1216 cm^{-1}.

Poly(hexamethylene 5,5'-(oxybis(methylene))bis(2-furancarboxylamide)) **(3cd, PA6FF)**

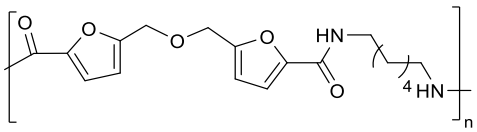

The reaction mixture was dissolved in a minimum amount of DCM and hexafluoroisopropanol (HFIP) (1:1, v/v) and precipitated from Et_2O (10 volumes) at 0 °C. Filtration followed by washing with cold Et_2O and drying under vacuum at 100 °C afforded the product **3cd** (249 mg, 90%, M_n = 3.6 kg mol^{-1}) as a pale yellow solid solid. **^{1}H NMR** (300 MHz, 1:1 $CDCl_3$:HFIP) δ = 7.08 (s, 2H, H-3, Furan), 6.94 (s, 2H, , -CONH-), 6.49 (s, 2H, H-4, Furan), 4.52 (s, 4H, Furan-CH_2OR), 3.41 (s, 4H, -C*H*$_2$NHCOR), 3.04 (s, 4H, terminal -C*H*$_2$NH$_2$), 1.70 (s, 4H, -C*H*$_2$CH$_2$NHCOR), 1.46 (m, 4H, -C*H*$_2$CH$_2$CH$_2$NHCOR); **^{13}C NMR** (101 MHz, 1:1 $CDCl_3$:HFIP) δ = 160.6 (CO), 152.8 (C-5, Furan), 147.1 (C-2, Furan), 116.4 (C-3, Furan), 113.3 (C-4, Furan), 63.8 (Furan-CH_2OR), 40.0 (-*C*H$_2$NHCOR), 29.0 (-*C*H$_2$CH$_2$NHCOR), 26.3 (-*C*H$_2$CH$_2$CH$_2$NHCOR); **FT-IR** (KBr) ν: 3283, 2930, 2861, 1738, 1639, 1552, 1365, 1301, 1216 cm^{-1}.

Poly(2,5-furandimethylene terephthalamide) **(3da, PAFAT)**

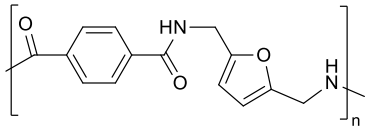

The reaction mixture was dissolved in a minimum amount of DCM and hexafluoroisopropanol (HFIP) (1:1, v/v) and precipitated from Et_2O (10 volumes) at 0 °C. Filtration followed by washing with cold Et_2O and drying under vacuum at 100 °C afforded the product **3da** (176 mg, 86%, M_n = 1.9 kg mol^{-1}) as a pale yellow solid. **^{1}H NMR** (300 MHz, DMSO-d_6) δ = 9.08 (s, 2H, -CONH-), 7.99 (s, 4H, Ar), 6.22 (s, 2H, Furan), 4.41 (s, 4H, Furan-C*H*$_2$NHCOR), 3.57 (s, 4H, terminal Furan-C*H*$_2$NH$_2$); **^{13}C NMR** (101 MHz, DMSO-d_6) δ = 166.0 (CO), 151.7 (C, Furan), 136.8 (C, Ar), 127.7 (CH, Ar), 108.3 (CH, Furan), 36.6 (-*C*H$_2$NHCOR); **FT-IR** (KBr) ν: 3284, 3040, 2940, 1737, 1640, 1538, 1376, 1287, 1191 cm^{-1}.

Synthesis of high molecular weight (HMW) PA10T 3ba'

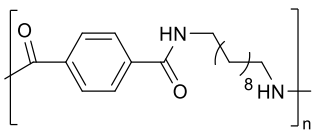

Oligomer **3ba** (200 mg, 0.077 mmol, M_n = 2.6 kg mol^{-1}), anhydrous N,N-dimethylacetamide (1 mL), lithium chloride (16 mg, 0.38 mmol) and N,N-diisopropylethylamine (40 µl, 0.23 mmol) were added in a 10 mL round bottom flask under Ar atmosphere. The resulting mixture was stirred at room temperature until most of the prepolymer was dissolved, then the mixture was cooled to 0 °C. In a different flask, terephthaloyl chloride **10** (15 mg, 0.073 mmol) was dissolved in 0.5 mL of anhydrous N,N-dimethylacetamide. The solution was transferred in an airtight syringe and injected in the prepolymer solution at 0 °C. After 10 minutes, the ice bath was removed, and the mixture was stirred at room temperature for 48 h. After this period, the solution was slowly added to water (15 mL). The resulting solid precipitate was filtered and washed with methanol (15 mL) and diethyl ether (15 mL). Finally, the polymer was dried in vacuum at 100 °C for 4 h to yield **3ba'** (183 mg, 85%, M_n = 62.8 kg mol^{-1}) as a pale yellow solid. **^{1}H NMR** (300 MHz, 1:1 $CDCl_3$:HFIP) δ = 7.72 (s, 4H, Ar), 6.59 (s, 2H, -CONH-), 3.44 (s, 4H, -CH_2NHCOR), 3.04 (s, 4H, terminal -CH_2NH$_2$), 1.64 (s, 4H, -CH_2CH$_2$NHCOR), 1.36 (s, 12H, -CH_2CH_2CH_2CH$_2$CH$_2$NHCOR); **^{13}C NMR** (101 MHz, 1:1 $CDCl_3$:HFIP) δ = 169.8 (CO), 136.8 (C, Ar), 127.1 (CH, Ar), 40.8 (-*C*H$_2$NHCOR), 29.0 (-*C*H$_2$CH$_2$NHCOR), 28.8 (-*C*H$_2$CH$_2$CH$_2$NHCOR), 28.6 (-*C*H$_2$CH$_2$CH$_2$CH$_2$NHCOR), 26.4 (-*C*H$_2$CH$_2$CH$_2$CH$_2$CH$_2$NHCOR); **FT-IR** (KBr) ν: 3312, 2920, 2850, 1625, 1538, 1291 cm^{-1}.

Poly(decamethylene terephthalamide) **(3ba'', PA10T)**

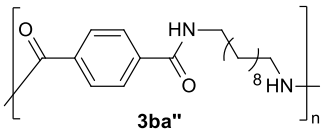

3ba''

The prodcuct was obtained as pale yellow solid (172 mg, 80% yield, NMR calculated *Mn* = 20.2 kg mol^{-1}, viscosimetry calculated *Mn* = 22.3 kg mol^{-1}). **^{1}H NMR** (300 MHz, 1:1 $CDCl_3$:HFIP) δ = 7.74 (s, 4H, Ar), 6.60 (s, 2H, -CONH-), 3.45 (s, 4H, -CH_2NHCOR), 3.07 (s, 4H, terminal -CH_2NH$_2$), 1.66 (s, 4H, -CH_2CH$_2$NHCOR), 1.37 (s, 12H, -CH_2CH_2CH_2CH$_2$CH$_2$NHCOR); **^{13}C NMR** (101 MHz, 1:1$CDCl_3$:HFIP) δ = 169.8 (CO), 136.8 (C, Ar), 127.1 (CH, Ar), 40.8 (-*C*H$_2$NHCOR), 29.0 (-*C*H$_2$CH$_2$NHCOR), 28.8 (-*C*H$_2$CH$_2$CH$_2$NHCOR), 28.6 (-*C*H$_2$CH$_2$CH$_2$CH$_2$NHCOR), 26.4 (-*C*H$_2$CH$_2$CH$_2$CH$_2$CH$_2$NHCOR). **FT-IR** (KBr): ν 3312, 2921, 2852, 1625, 1538, 1290 cm^{-1}.

Synthesis of chain-extended CE-PA10F 3bc'

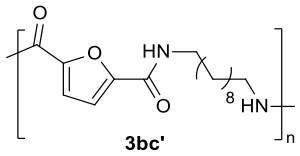

3bc'

Oligomer **3bc** (200 mg, 0.068 mmol, M_n = 1.6 kg mol^{-1}), anhydrous N,N-dimethylacetamide (1 mL), lithium chloride (14 mg, 0.34 mmol) and N,N-diisopropylethylamine (36 µl, 0.20 mmol) were added in 10 mL round bottom flask under Ar atmosphere. The resulting mixture was stirred at room temperature until most of the prepolymer was dissolved, then the mixture was cooled to 0 °C. In a different flask, 2,5-furandicarbonyl dichloride **11** (13 mg, 0.065 mmol) was dissolved in 0.5 mL of anhydrous N,N-dimethylacetamide. The solution was transferred in an air tight syringe and injected in the prepolymer solution at 0 °C. After 10 minutes, the ice bath was removed, and the mixture was stirred at room temperature for 48 h. After this period, the solution was slowly added to water (15 mL). The resulting solid precipitate was filtered and washed with methanol (15 mL) and diethyl ether (15 mL). Lastly, the polymer was dried in vacuum at 100 °C for 4 h to yield **3bc'** (162 mg, 76% yield, M_n = 6.5 kg mol^{-1}) as a creamy solid.

^{1}H NMR (300 MHz, 1:4 $CDCl_3$:HFIP) δ = 7.12 (s, 2H, Furan), 3.43 (s, 4H, -C*H*$_2$NHCOR), 3.10 (s, 4H, terminal -C*H*$_2$NH$_2$), 1.66 (s, 4H, -C*H*$_2$CH$_2$NHCOR), 1.38 (s, 12H, -C*H*$_2$C*H*$_2$C*H*$_2$CH$_2$CH$_2$NHCOR); **^{13}C NMR** (101 MHz, 1:4 $CDCl_3$:HFIP) δ = 159.6 (CO), 147.6 (C, Furan), 115.5 (CH, Furan), 40.1 (-*C*H$_2$NHCOR), 29.0 (-*C*H$_2$CH$_2$NHCOR), 28.7 (-*C*H$_2$CH$_2$CH$_2$NHCOR), 28.6 (-*C*H$_2$CH$_2$CH$_2$CH$_2$NHCOR), 26.4 (-*C*H$_2$CH$_2$CH$_2$CH$_2$CH$_2$NHCOR); **FT-IR** (KBr) ν: 3272, 2924, 2854, 1735, 1640, 1575, 1363, 1282, 1178 cm^{-1}.

Gram-scale synthesis of PETA 3aa

A mixture of pre-catalyst **C1** (225 mg, 1.0 mmol) and HFIP (3.16 mL, 30.0 mmol) in anhydrous THF (60.0 mL) was degassed under vacuum and saturated with argon (by an Ar-filled balloon) three times. Then, DBU was added (374 µL, 2.5 mmol), and the reaction was stirred at room temperature for 5 minutes. Later, oxidant **4** (8.17 g, 20.0 mmol) and terephthalaldehyde **2a** (1.34 g, 10.0 mmol) were added, and the reaction mixture was stirred at room temperature for 2 h. After complete consumption of aldehyde (verified by ^{1}H NMR analysis), diamine **1** (0.74 mL, 11.0 mmol) was added and reaction was stirred for 16 h at the same temperature. Thus, the mixture was transferred into a distillation unit to recover HFIP (bp 58 °C, up to 85% isolated

yield through evaporation) and remove THF. The resulting residue was triturated with fresh portions of Et_2O (3 × 100 mL) and centrifuged. The organic solutions were collected for the recovery of the oxidant **4** (90% isolated yield), while the solid residue was dissolved in 50 mL of DCM and HFIP (1:1, v/v) and precipitated from Et_2O (500 mL) at 0 °C. Filtration followed by washing with cold Et_2O and drying under vacuum at 100 °C afforded PETA **3aa** (1.75 g, 92%, M_n = 1.9 kg mol^{-1}) as a pale yellow solid.

Procedure for HFIP, DBU and oxidant 4 recycle

HFIP used for **3aa** purification was recovered by distillation as described before.

After trituration of the crude polycondensation mixture with Et_2O, the collected organic solutions (300 mL) were washed with 0.5 M HCl (2 × 50 mL).

*Oxidant **4** recycle*: the organic phase containing the corresponding reduced product *o,o′*-di-*tert*-butyl-*p*-bisphenol was dried (Na_2SO_4), concentrated, and eluted from a short column of silica gel (4:1 cyclohexane:DCM) to give *o,o′*-di-*tert*-butyl-*p*-bisphenol (7.98 g) as a white amorphous solid. The quantitative oxidation to quinone **4** was performed stirring the bisphenol (578 mg, 1.41 mmol) with iron(II) phthalocyanine (1.06 g, 1.87 mmol) in THF (80 mL) under air atmosphere (1 atm, balloon) for 16 h. Filtration over a pad of celite followed by concentration under reduced pressure afforded **4** as a dark red amorphous solid (7.61 g, 88%).

DBU recycle: 2 M NaOH was added to the above aqueous phase until alkaline pH. The resulting aqueous solution was then extracted with EtOAc (2 × 40 mL). The combined organic phases were dried (Na_2SO_4) and concentrated to give DBU (280 mg, 90%), at least 90% pure as determined by ^{1}H NMR analysis.

Synthesis of PA10T 3ba''

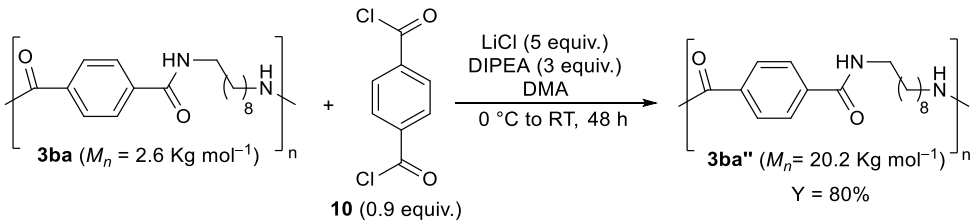

Oligomer **3ba** (200 mg, 0.077 mmol, M_n = 2.6 kg mol^{-1}), anhydrous N,N-dimethylacetamide (1 mL), lithium chloride (16 mg, 0.38 mmol) and N,N-diisopropylethylamine (40 µl, 0.23 mmol) were added to a 10 mL round bottom flask, under Ar atmosphere. The resulting mixture was stirred at room temperature until most of the prepolymer was dissolved, then the mixture was cooled to 0 °C. In a different round bottom flask, terephthaloyl chloride **10** (15 mg, 0.073

mmol) was dissolved in 0.5 mL of anhydrous N,N-dimethylacetamide. Thus, the solution was transferred in an airtight syringe and injected in the prepolymer solution at 0 °C. After 10 minutes, the ice bath was removed, and the mixture was stirred at room temperature for 24 h. After this period, the solution was slowly added to water (15 mL). The resulting solid precipitate was filtered and washed with methanol (15 mL) and diethyl ether (15 mL). Lastly, the polymer **3ba''** was dried in vacuum at 100 °C for 4 h (172 mg, 80% yield, NMR calculated M_n = 20.2 kg mol^{-1}). Molecular weight increase was confirmed by the diminished integral values of the end group signals at 3.04 ppm in the ^{1}H NMR spectrum (1:1 $CDCl_3$:HFIP, Figure 6).

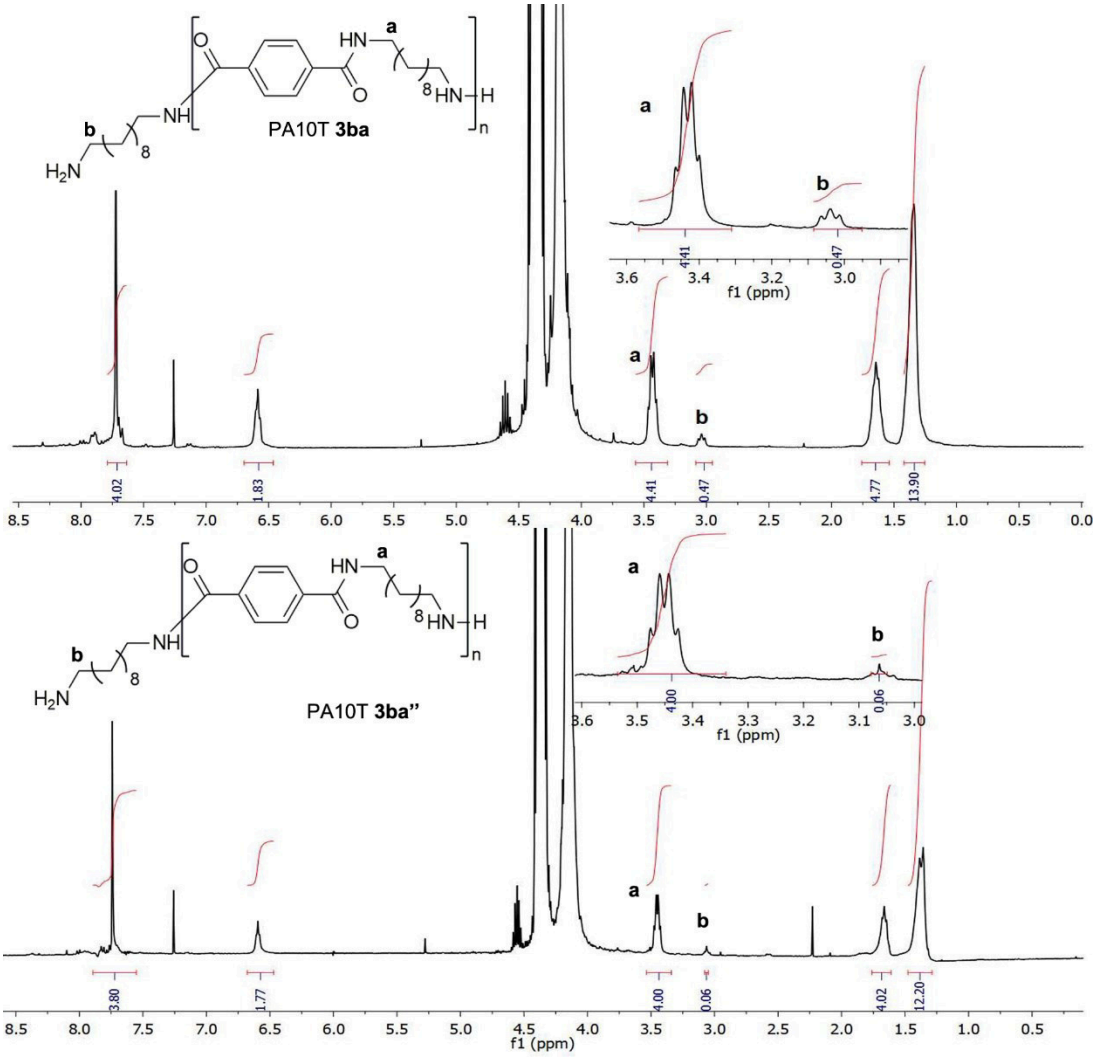

Figure 6. ^{1}H NMR spectra of oligomeric PA10T **3ba** and PA10T **3ba''** (1:1 $CDCl_3$:HFIP).

Viscosity analysis

A solution containing 0.5 g dL^{-1} of polymer in concentrated sulphuric acid (96%) was prepared as follows: 100 mg of **3ba''** were added to 20 mL of concentrated sulfuric acid into a 20 mL flask and stirred for 12 h. Later, the solution was filtered through a sintered glass filter and used

for analysis. Single-point intrinsic viscosity measurements were performed using an Ubbelohde viscometer in a 25 °C controlled water bath. Flow times were an average of four values that agreed within 0.2 s. Specific (η_{sp}) and relative (η_{rel}) viscosities were calculated from flow times data of sulphuric acid and polymer. Single point intrinsic viscosities were then determined using the Solomon-Ciută[19] equation, affording an intrinsic viscosity value [η] = 1.93. Number-average molecular weight for **PA10T 3ba''** was estimated from Mark-Houwink equation considering $K = 5.58 \bullet 10^{-4}$ dL g^{-1} and α = 0.81, previously calculated for **PA12T**[38] and adapted for **PA10T** affording $M_n = 22.3$ kg mol^{-1}.

Mechanistic studies

With the aim to understand the reaction mechanism, NMR and FT-IR investigations were performed.

NMR study: A mixture of pre-catalyst **C1** (10 µL, 0.03 mmol), hexafluoro-2-propanol **9** (HFIP) (85 µL, 0.80 mmol), oxidant **4** (221 mg, 0.53 mmol) and aldehyde **2a** (36 mg, 0.26 mmol) in anhydrous THF (2.0 mL) was degassed under vacuum and saturated with argon (by an Ar-filled balloon) three times. At this stage, 50 µL of the reaction mixture were withdrawn and added to $CDCl_3$ (0.8 mL) in a NMR tube. ^{1}HNMR spectra was recorded (Figure 7), showing the clear presence of the dialdehyde **2a** signals: 10.1 ppm (s, 2H, COH), 8.04 ppm (s, 4H, Ar). Then, DBU was added to the reaction mixture (10 µL, 0.67 mmol), and the reaction was stirred at room temperature for 2 h. After this period, 50 µL of the reaction mixture were withdrawn and added to $CDCl_3$ (0.8 mL) in a NMR tube. ^{1}HNMR spectra clearly (Figure 8), showed the complete disappearance of aldehyde **2a**, accompanied by the appearance of the signals related to the hexafluoroisopropyl diester: 8.22 ppm (s, 4H, Ar), 6.02 ppm (hept, 2H, CH). The comparison between the two spectra confirmed after 2 h the quantitative transformation of the starting aldehyde **2a** in the corresponding hexafluoroisopropyl diester, which represents the key highly reactive intermediate of the subsequent amidation step.

FT-IR study: FT-IR spectra of the starting aldehyde **2a** was recorded (Figure 9), showing a strong diagnostic band at 1683 cm^{-1}, corresponding to the C=O stretching. Next, a mixture of pre-catalyst **C1** (10 µL, 0.03 mmol), hexafluoro-2-propanol **9** (HFIP) (85 µL, 0.80 mmol), oxidant **4** (221 mg, 0.53 mmol) and aldehyde **2a** (36 mg, 0.26 mmol) in anhydrous THF (2.0 mL) was degassed under vacuum and saturated with argon (by an Ar-filled balloon) three times. At this stage, DBU was added to the reaction mixture (10 µL, 0.67 mmol), and the reaction was stirred at room temperature for 2 h. After this period, the reaction mixture was concentrated under reduced pressure. FT-IR measurement of the crude mixture was performed (Figure 10), showing the complete disappearance of the diagnostic aldehyde **2a** peak at 1683 cm^{-1}

accompanied by the appearance of a strong band at 1755 cm^{-1}, corresponding to the hexafluoroisopropyl diester C=O stretching. The superposition of the spectra clearly shows this behavior (Figure 11).

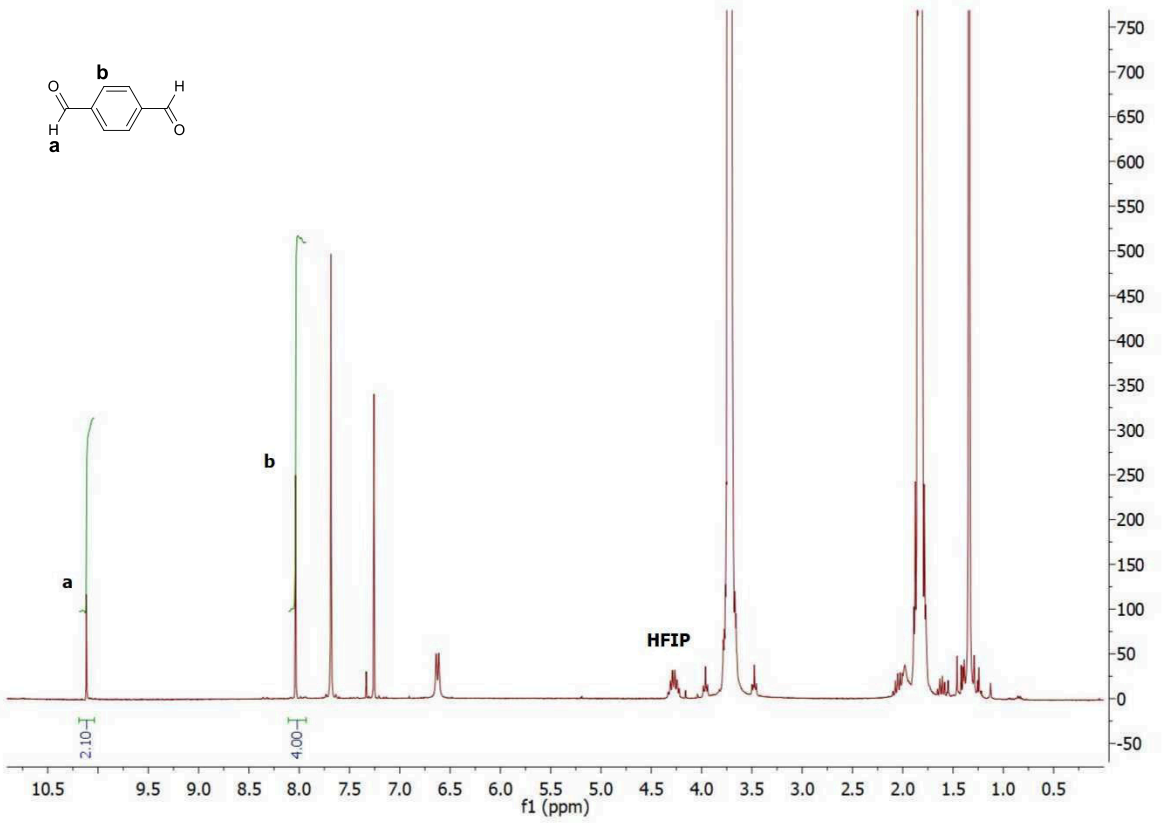

Figure 7. ^{1}H (300 MHz, $CDCl_3$) of the reaction mixture before DBU addition.

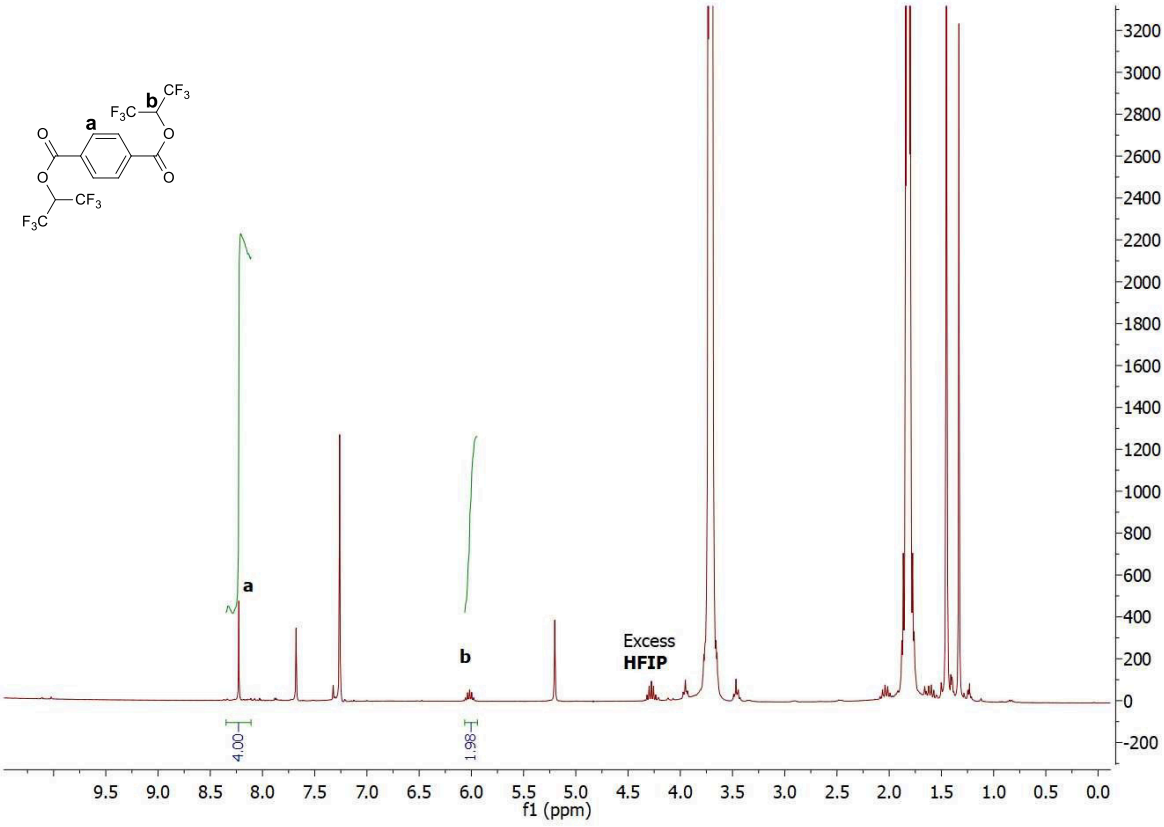

Figure 8. ^{1}H (300 MHz, $CDCl_3$) of the reaction mixture after DBU addition and 2 h stirring at room temperature.

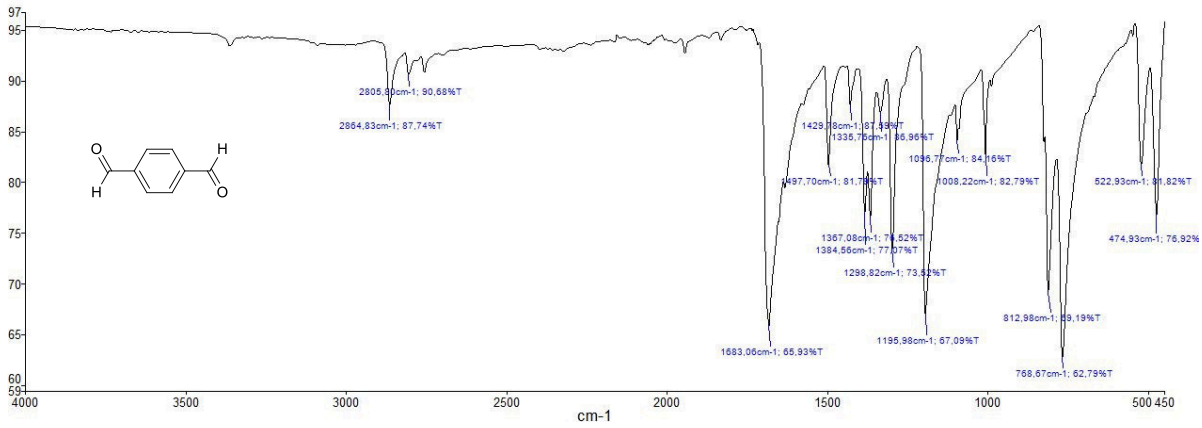

Figure 9. FT-IR spectra of terephthalaldehyde **2a**.

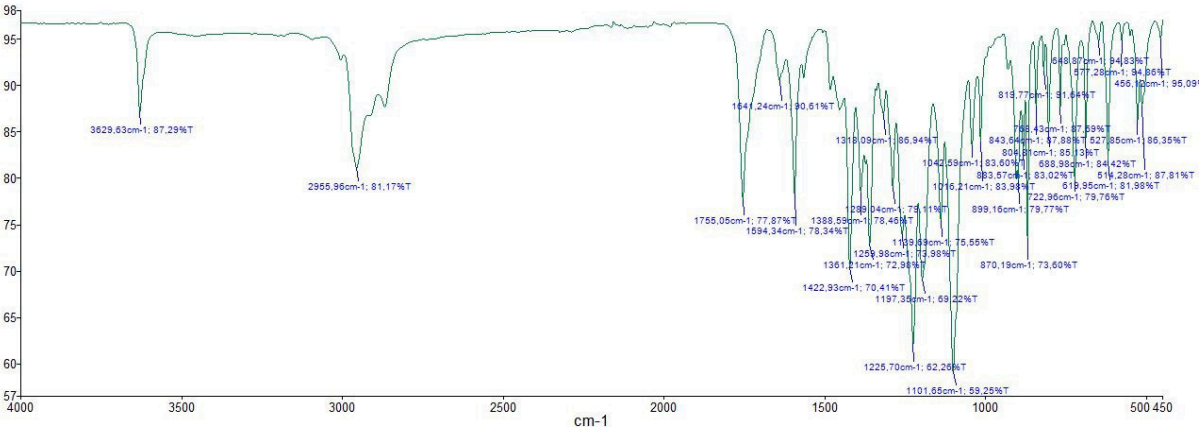

Figure 10. FT-IR spectra of the crude reaction mixture after 2 h stirring at room temperature.

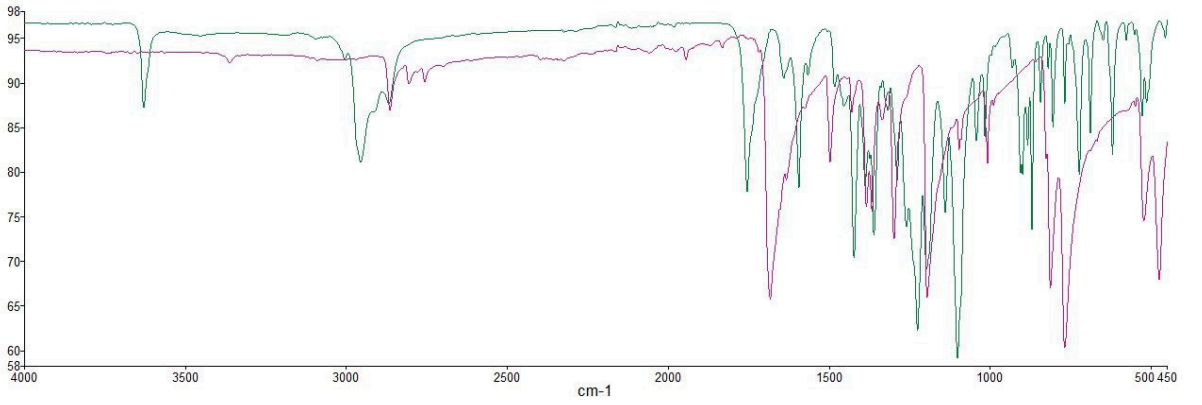

Figure 11. FT-IR spectra overlap of terephthalaldehyde **2a** (purple) and the crude reaction mixture after 2 h stirring at room temperature (green).

6.5 References and notes

1. a) R. Rulkens, C. Koning, Chemistry and Technology of Polyamides, in *Polymer Science: A Comprehensive Reference* (Eds.: K. Matyjaszewski, M. Möller), Elsevier B.V., Amsterdam, 1st Ed., **2012**, Vol. 5, pp 431−467; b) K. Marchildon, *Macromol. React. Eng.,* **2011**, *5*, 22−54.
2. R. J. Gaymans, Polyamides, in *Synthetic methods in step-growth polymers* (Eds. M. E. Rogers, T. E. Long) Wiley, New York, **2003**, pp. 135−195. For the ring-opening aminolysis-condensation (ROAC) of diamines and dilactones, see Refs. 5e,g.
3. a) H. Zeng, Z. Guan, *J. Am. Chem. Soc.,* **2011**, *133*, 1159−1161; b) C. Gunanathan, Y. Ben-David, D. Milstein, *Science,* **2007**, *317*, 790−792.
4. For reviews, see: a) M. K. Kiesewetter, E. J. Shin, J. L. Hedrick, R. M. Waymouth, *Macromolecules,* **2010**, *43*, 2093−2107; b) W. N. Ottou, H. Sardon, D. Mecerreyes, J. Vignolle, D. Taton, *Prog. Polym. Sci.,* **2016**, *56*, 64−115; c) S. Hua, J. Zhao, G. Zhang, H. Schlaad, *Prog. Polym. Sci.,* **2017**, *74*, 34−77; d) A. Bossion, K. V. Heifferon, L. Meabe, N. Zivic, D. Taton, J. L. Hedrick, T. E. Long, H. Sardon, *Prog. Polym. Sci.,* **2019**, *90*, 164−210.
5. Selected examples: a) N. Kolb, M. Winkler, C. Syldatk, M. A.R. Meier, *Eur. Polym. J.,* **2014**, *51*, 159−166; b) J. Chen, M. Li, W. He, Y. Tao, X. Wang, *Macromolecules,* **2017**, *50*, 9128−9134; c) W. He, Y. Tao, X. Wang, *Macromolecules* **2018**, *51*, 8248-8257; d) A. Basterretxea, E. Gabirondo, A. Sanchez-Sanchez, A. Etxeberria, O. Coulembier, D. Mecerreyes, H. Sardon, *Eur. Polym. J.,* **2017**, *95*, 650−659; e) G. Hua, K. Odelius, *Biomacromolecules,* **2018**, *19*, 1573−1581; f) Y. Liang, J.-L. Pan, L.-H. Sun, J.-M. Ma, H. Jiang, Z.-L. Li, *Macromol. Rapid Commun.,* **2019**, *40*, 1900435; g) C. Pronoitis, G. Hua, M. Hakkarainen, K. Odelius, *Macromolecules,* **2019**, *52*, 6181−6191.
6. W. Tam, D. T. Williamson, US0100365, **2006**.
7. a) S. Naumann, S. Epple, C. Bonten, M. R. Buchmeiser, *ACS Macro Lett.,* **2013**, *2*, 609−612; b) S. Naumann, F. G. Schmidt, M. Speiser, M. Böhl, S. Epple, C. Bonten, M. R. Buchmeiser, *Macromolecules,* **2013**, *46*, 8426−8433.
8. Selected recent reviews: a) S. J. Ryan, L. Candish, D. W. Lupton, *Chem. Soc. Rev.,* **2013**, *42*, 4906−4917; b) M. N. Hopkinson, C. Richter, M. Schedler, F. Glorius, *Nature,* **2014**, *510*, 485−496; c) D. M. Flanigan, F. Romanov-Michailidis, N. A. White, T. Rovis, *Chem. Rev.,* **2015**, *115*, 9307−9387; d) X.-Y. Chen, Q. Liu, P. Chauhan, D. Enders, *Angew. Chem. Int. Ed.,* **2018**, *57*, 3862−3873 and *Angew. Chem.,* **2018**, *130*, 3924−3935.
9. For reviews, see: a) M. Fèvre, J. Pinaud, Y. Gnanou, J. Vignolle, D. Taton, *Chem. Soc. Rev.,* **2013**, *42*, 2142−2172; b) S. Naumann, A. P. Dove, *Polym. Chem.,* **2015**, *6*, 3185−3200; c) S. Naumann, A. P. Dove, *Polym. Int.,* **2016**, *65*, 16−27; d) C. A. Smith, M. R. Narouz, P. A. Lummis, I. Singh, A. Nazemi, C.-H. Li, C. M. Crudden, *Chem. Rev.,* **2019**, *119*, 4986−5056.
10. For the precedent use of dialdehydes in NHC-catalysed polycondensations, see: a) R. Alan Jones, M. Karatza, T. N. Voro, P. U. Civir, A. Franck, O. Ozturk, J. P. Seaman, A. P. Whitmore, D. J. Williamson, *Tetrahedron,* **1996**, *52*, 8707−8724; b) R. A. Jones, P. U. Civir, *Tetrahedron,* **1997**, *53*, 11529−11540; d) J. Pinaud, K. Vijayakrishna, D. Taton, Y. Gnanou, *Macromolecules,* **2009**, *42*, 4932−4936.
11. D. Ragno, G. Di Carmine, A. Brandolese, O. Bortolini, P. P. Giovannini, G. Fantin, M. Bertoldo, A. Massi, *Chem. Eur. J.,* **2019**, *25*, 14701−14710.
12. a) I. Delidovich, P. J. C. Hausoul, L. Deng, R. Pfützenreuter, M. Rose, R. Palkovits, *Chem. Rev.,* **2016**, *116*, 1540−1599; b) M. Winnacker, B. Rieger, *Macromol. Rapid Commun.,* **2016**, *37*, 1391−1413.
13. a) Y. Jiang, K. Loos, *Polymers,* **2016**, *8*, 243−296; b) M. A. R. Meier, *Macromol. Rapid Commun.,* **2019**, *40*, 1800524; c) P. Radzik, A. Leszczyńska, K. Pielichowski, *Polym. Bull.,* **2020**, *77*, 501−528.
14. a) V. E. Shashoua, W. M. Eareckson III, *J. Polym. Sci.,* **1959**, *15*, 343−358; b) M. R. Hibbs, J. Holtzclaw, D. M. Collard, R. Y. F. Liu, A. Hiltner, E. Baer, D. A. Schiraldi, *J. Polym. Sci., Part A: Polym. Chem.,* **2004**, *42*, 1668−1681.

15. a) J. W. Bode, S. S. Sohn, *J. Am. Chem. Soc.,* **2007**, *129*, 13798−13799; b) H. U. Vora,T. Rovis, *J. Am. Chem. Soc.,* **2007**, *129*, 13796−13797; c) P.-C. Chiang, Y. Kim, J. W. Bode, *Chem. Commun.,* **2009**, 4566−4568; d) S. De Sarkar, A. Studer, *Org. Lett.,* **2010**, *12*, 1992−1995; e) M. Binanzer, S.-Y. Hsieh, J. W. Bode, *J. Am. Chem. Soc.,* **2011**, *133*, 19698−19701; f) S. Iwahana, H. Iida, E. Yashima, *Chem. Eur. J.,* **2011**, *17*, 8009−8013; g) B. Zhang, P. Feng, Y. Cui, N. Jiao, *Chem. Commun.,* **2012**, *48*, 7280−7282; h) P. Wheeler, H. U. Vora, T. Rovis, *Chem. Sci.,* **2013**, *4*, 1674−1679; i) C. A. Gondo, J. W. Bode, *Synlett,* **2013**, *24*, 1205−1210; j) R. W. M. Davidson, M. J. Fuchter, *Chem. Commun.,* **2016**, *52*, 11638−11641; k) R. A. Green, D. Pletcher, S. G. Leach, R. C. D. Brown, *Org. Lett.,* **2016**, *18*, 1198−1201; l) S. Premaletha, A. Ghosh, S. Joseph, S. R. Yetra, A. T. Biju, *Chem. Commun.,* **2017**, *53*, 1478−1481; m) V. Kumar, S. J. Connon, *Chem. Commun.,* **2017**, *53*, 10212−10215.
16. a) H. J. Liedloff, M. Schmid, US5708125A, **1998**; b) C. D. Papaspyrides, A. D. Porfyris, R. Rulkens, E. Grolman, A. J. Kolkman, *J. Polym. Sci., Part A: Polym. Chem.,* **2016**, *54*, 2493−2506; c) X. Sun, K. Mai, C. Zhang, M. Cao, Y. Zhang, X. Zhang, *J. Therm. Anal. Calorim.,* **2017**, *130*, 1021−1030; d) C. Zhang, M. Cao, S. Jiang, X. Huang, K. Mai, K. Yana, *Int. J. Polym. Anal. Charact.,* **2018**, *23*, 40−53; e) M. Li, J. *Polym. Sci., Part B: Polym. Phys.,* **2019**, *57*, 465−472.
17. D. Smith, J. Flores, R. Aberson, M. A. Dam, A. Duursma, G. Johannes, M. Gruter, WO2015059047A1, **2015**.
18. a) T. Novitsky, C. Lange, W. Jarrett, L. Mathias, S. Osborn, R. Ayotte, S. Manning, *J. Appl. Polym. Sci.* **2010**, *116*, 3388−3395; b) T. F. Novitsky, C. A. Lange, L. J. Mathias, S. Osborn, R. Ayotte, S. Manning, *Polymer* **2010**, *51*, 2417−2425.
19. O. Solomon, I. Ciută, *J. Appl. Polym. Sci.* **1962**, *6*, 683−686.
20. a) T. Cousin, J. Galy, J. Dupuy, *Polymer,* **2012**, *53*, 3203−3210; b) D. P. Gohari, M. R. Kalaee, A. Sharif, *J. Inorg. Organomet. Polym. Mater.,* **2019**, *29*, 1243−1251.
21. a) H. Hopff, A. Krieger, *Makromol. Chem.,* **1961**, *47*, 93−113; b) O. Grosshardt, U. Fehrenbacher, K. Kowollik, B. Tubke, N. Dingenouts, M. Wilhelm, *Chem. Ing. Tech.,* **2009**, *81*, 1829−1835; c) Y. Jiang, D. Maniar, A. J. J. Woortman, G. O. R. Alberda van Ekenstein, K. Loos, *Biomacromolecules,* **2015**, *16*, 3674−3685; d) Y. Jiang, D. Maniar, A. J. J. Woortman, K. Loos, *RSC Adv.,* **2016**, *6*, 67941−67953.
22. a) L. T. Cureton, E. Napadensky, C. Annunziato, J. J. La Scala T. *J. Appl. Polym. Sci.,* **2017**, *134*, 45514−45526; b) Cousin, J. Galy, A. Rousseau, J. Dupuy, *J. Appl. Polym. Sci.,* **2018**, *135*, 45901−459012.
23. a) Z. H. Zhang, J. D. Zhen, B. Liu, K. L. Lv, K. J. Deng, *Green Chem.,* **2015**, *17*, 1308−1317; b) X. Zuo, P. Venkitasubramanian, D. H. Busch, B. Subramaniam, *ACS Sustainable Chem. Eng.,* **2016**, *4*, 3659−3668; c) M. Kim, Y. Su, T. Aoshima, A. Fukuoka, E. J. M. Hensen, K. Nakajima, *ACS Catal.,* **2019**, *9*, 4277−4285.
24. J. Zhao, A. Jayakumar, Z.-T. Hu, Y. Yan, Y. Yang, J.-M. Lee, *ACS Sustain. Chem. Eng.,* **2018**, *6*, 284−291 and references therein.
25. a) Z. Hui, A. Gandini, *Eur. Polym. J.,* **1992**, *28*, 1461−1469; b) A. S. Amarasekara, D. Green, L. D. Williams, *Eur. Polym. J.,* **2009**, *45*, 595−598.
26. a) H. Wang, Y. Wang, T. Deng, C. Chen, Y. Zhu, X. Hou, *Catal. Commun.,* **2015**, *59*, 127−130; b) C. Moreau, M. N. Belgacem, A. Gandini, *Top. Catal.,* **2004**, *27*, 11−30.
27. A. S. Amarasekara, L. Nguyen, N. C. Okorie, S. Jamal, *Green Chem.,* **2017**,*19*, 1570−1575 and references therein.
28. a) A. Mitiakoudis, A. Gandini, *Macromolecules,* **1991**, *24*, 830−835; b) J. P. Klein, WO2015060827A1, **2015**.
29. Y. Xu, X. Jia, J. Ma, J. Gao, F. Xia, X. Li, J. Xu, *Green Chem.,* **2018**, *20*, 2697−2701 and references therein.

30. a) W. Wang, X. Wang, R. Li, B. Liu, E. Wang, Y. Zhang, *J. Appl. Polym. Sci*., **2009**, *114*, 2036−2042; b) W. Feng, P. Wang, G. Zou, Z. Ren, J. Ji, *Des. Monomers Polym*., **2018**, *21*, 33−42.
31. J. Liu, J. Xu, K. Li, Y. Chen, *Int. J. Polym. Sci.* **2013,** ID 616859.
32. L. Qu, S.-R. Long, M.-L. Zhang, G. Zhang, X.-J. Wang, J. Yang, *J. Macromol. Sci. A,* **2012,** *49*, 67−72.
33. W.-Z. Wang, Y.-H. Zhang, *eXPRESS Polym. Lett.* **2009,** *3* (8), 470−476.
34. A. D. Porfyris, C. D. Papaspyrides, R. Rulkens, E. Grolman, *J. Appl. Polym. Sci.* **2017**, *134*, 45080.
35. C. Zhang, *e-Polymers* **2018,** 18(5), 373−408.
36. Selected reviews on oxidative NHC-catalysis: a) C. E. I. Knappke, A. Imami, A. J. von Wangelin, *ChemCatChem* **2012**, *4*, 937−941; b) S. De Sarkar, A. Biswas, R. C. Samanta, A. Studer, *Chem. Eur. J.* **2013**, *19*, 4664−4678; c) J. Mahatthananchai, J. W. Bode, *Acc. Chem. Res.* **2014**, *47*, 696−707; d) M. H. Wang, K. A. Scheidt, *Angew. Chem. Int. Ed.* **2016**, *55*, 14912−14922; *Angew. Chem.* **2016**, *128*, 15134−15145.
37. A. S. Amarasekara, L. Nguyen, N. C. Okorie, S. Jamal, *Green Chem.,* **2017***, 19,* 1570−1575.
38. a) T. Novitsky, C. Lange, W. Jarrett, L. Mathias, S. Osborn, R. Ayotte, S. Manning, *J. Appl. Polym. Sci.* **2010**, *116*, 3388−3395; b) T. F. Novitsky, C. A. Lange, L. J. Mathias, S. Osborn, R. Ayotte, S. Manning, *Polymer* **2010**, *51*, 2417−2425; c) M. Li, J. *Polym. Sci., Part B: Polym. Phys.* **2019**, *57*, 465−472.

7. Enantioselective N-acylation of Biginelli dihydropyrimidines by oxidative NHC-catalysis

The work described in this chapter has formed the basis of the following peer reviewed publication: A. Brandolese; D. Ragno; C. Leonardi; C. De Risi; O. Bortolini; A. Massi, *Eur. J. Org. Chem.* **2020**, 2439–2447.

7.1 Introduction

Biginelli dihydropyrimidines (3,4-dihydropyrimidin-2-(1*H*)-ones, DHPMs)[1] are defined as "privileged" structures in medicinal chemistry displaying a plethora of pharmacological properties.[2] However, as it often occurs with molecules showing a pharmaceutical activity, optically active DHPMs typically exhibit different or even opposite biological action. Enantioenriched DHPMs have been addressed by chemical resolution, chromatography on chiral stationary phases, and by asymmetric multicomponent reaction through metal/organo/bio-catalytic approaches.[3] However, starting from racemic DHPM a facile access to optically active derivatives could also follow a kinetic resolution (KR) or a dynamic kinetic resolution (DKR) processes. The former is '*the achievement of partial or complete resolution by virtue of unequal rates of reaction of the enantiomers in a racemate with a chiral agent (reagent, catalyst, solvent, etc.)*' as established by IUPAC.[4] Therefore, KR relies upon differences in reactivity between enantiomers or enantiomeric complexes and it expected to provide no more than 50% yield. The efficiency of the process is assessed by the selectivity factor (*s*) which has been shown to be related to several parameters, such as the relative reaction rates of the two enantiomers, the reaction conversion (Conv.) and the enantiomeric excess (*ee*) of either the reaction product or the recovered starting material.[4] DKR processes instead are distinguished by the equilibration of a mixture of stereoisomers (enantiomers or diastereomers) through an in situ epimerization occurring prior to or during the KR.[4] Hence, DKR could theoretically convert 100% of the starting material into a single stereoisomer of the target product. While a previous example of enzymatic kinetic resolution has been employed through hydrolysis of activated ester derivatives of racemic DHPMs,[5] organocatalysed kinetic resolution processes have not been reported in literature yet.

The Biginelli compounds display a common functional group, the ureido moiety, often present in molecules with relevant synthetic and biological activity.[6] In fact, among all the several derivatizations on the DHPM core, of particular relevance is the N3-acylation, which leads to the synthesis of close structural analogues of pharmaceutically active Hantzsch 1,4-dihydropyridines. Noteworthy are the potent calcium channel blockers SQ-329266 and SQ-

32547[7] or the α_{1a} receptor antagonist agent L-771688 (Figure 1).[8] The substitution of DHPMs with carbonyl groups at the N3 position, in fact, often leads to an increase of their biological activity and stability.[9]

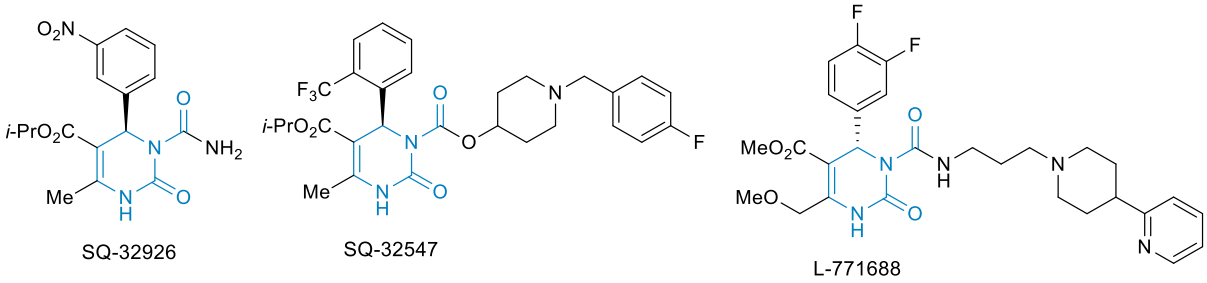

Figure 1. Biologically active N3-acylated DHPMs.

Generally, optically active N3-acylated DHPMs are obtained from the corresponding enantioenriched substrates by treatment with stoichiometric, highly reactive acid chlorides or anhydrides at elevated temperatures in the presence of a base.[9] Differently, the use of aldehyde agents, as in the reaction promoted by N-heterocyclic carbene (NHCs), to perform N-acylation reactions in place of carboxylic acids/derivatives has not been proposed yet. This strategy, in fact, shows some practical advantages such as mild reaction conditions, chemoselectivity and no need of coupling reagents. Moreover, synthetic routes are additionally expanded by the use of oxidative strategies (internal and external oxidation protocols)[10] leading to the formation of the acyl azolium intermediate. Consequently, acylation of oxygen-, sulfur-, and nitrogen-nucleophiles in challenging kinetic resolution (KR),[11] macrolactonization,[12] desymmetrization,[11,13] and polymerization[14] processes have been performed. This strategy has been applied for the functionalization of alkylamines,[15] anilines,[16] amides,[17] sulfoximines,[18] azomethine imines,[19] and several nitrogen-containing heterocycles (Scheme 1).[15c,15e,15i–21]
However, the direct oxidative N-acylation with aldehydes has been often hampered by the competing imine formation,[15] thus requiring the addition of oxygen nucleophiles as additives[15a,15b] or the execution of a two-step procedure with activated ester intermediates.[15d,15g] Herein, considering the valuable biological application of N3-acylated DHPMs, a challenging direct asymmetric N-acylation of racemic DHPMs promoted by oxidative NHC-catalysis has been developed. The reported method used aldehydes and substitutional variation around the DHPM scaffold has been investigated through catalytically generated acyl azolium intermediates (Scheme 1).

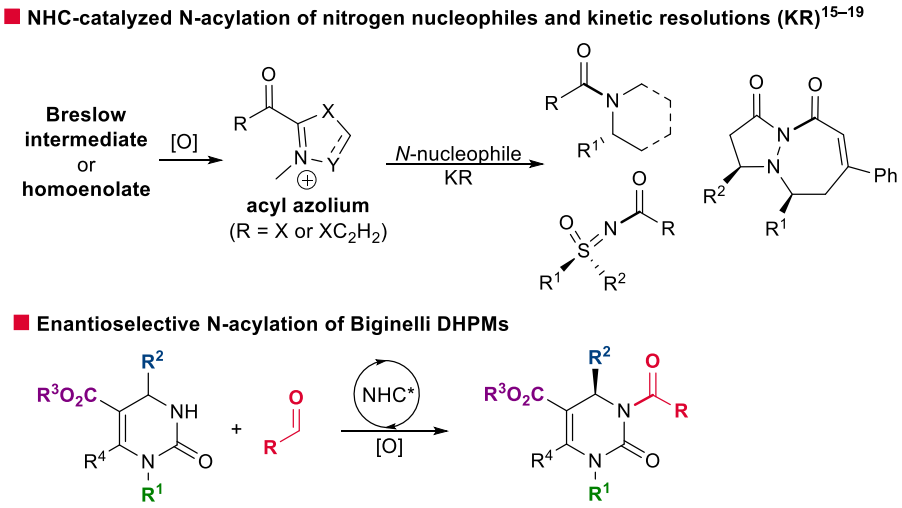

Scheme 1. NHC-catalysed N-acylation of nitrogen nucleophiles and kinetic resolutions; this work: enantioselective N-acylation of Biginelli DHPMs.

7.2 Results and discussion

Preliminary investigations on N-acylation of DHPM **1a** (Table 1) with the achiral triazolium pre-catalyst **C1** (10 mol%) started with the evaluation of the influence of the aldehyde reaction partner under oxidative condition due to the presence of quinone **8** (1 equiv.). Disappointingly, the use of equimolar cinnamaldehyde **2a** and DBU (2 equiv.) in anhydrous THF with 4Å molecular sieves, at room temperature resulted in no formation of the corresponding N3-acylated DHPM (±)-**5aa** (entry 1). This result can be justified as the DBU is not strong enough to activate the weak nucleophile (**1a**). However, the replacement of DBU with the stronger base NaH (2 equiv.) gave (±)-**5aa** in 41% yield after one hour, along with unreacted **1a** (48%; entry 2) and a detectable amount (15%) of cinnamic acid. Therefore, the use of a strong base which deprotonate the starting DHPM **1a** turned out to be fundamental for the positive outcome of the reaction. Only a moderate increase of yield (47−50%) was detected extending the reaction time to 24 h and along with the use of an excess of aldehyde **2a** (2 equiv.). In the last condition, in fact, the consumption of **2a** into the corresponding acid (entries 3 and 4) was instead observed. Replacing the α,β-unsaturated aldehyde **2a** with the aromatic 4-chlorobenzaldehyde **3a** resulted in marked decrease of reaction efficiency affording the acyl derivative (±)-**6aa** in poor yield (10%, entry 5). Finally, the use of the aliphatic *n*-butyraldehyde **4a** delivered a complex reaction mixture due to the competing aldol reaction with no evidence of product (±)-**7aa** formation (entry 6). At this point of the study, the use of 2 equivalents of DHPM **1a** turned out to promote the formation of the N3-acylated DHPM **5a** which was isolated in 74% yield (the yield of the process was calculated with respect to the cinnamaldehyde **2a** which was present as the limiting reagent; entry 7).

Table 1. Preliminary study on the achiral N-acylation of DHPM **1a** with model unsaturated, aromatic, and aliphatic aldehydes **2a**–**4a**.[a]

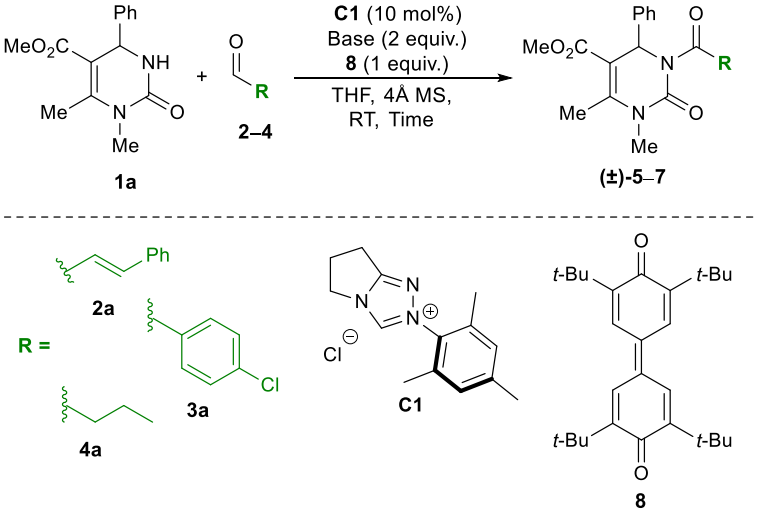

Entry	Aldehyde	Base	Time (h)	Product (%)[b]
1	**2a**	DBU	24	(±)-**5aa** (-)
2	**2a**	NaH	1	(±)-**5aa** (41)
3	**2a**	NaH	24	(±)-**5aa** (47)
4[c]	**2a**	NaH	24	(±)-**5aa** (50)
5	**3a**	NaH	24	(±)-**6aa** (10)
6	**4a**	NaH	24	(±)-**7aa** (-)
7[d]	**2a**	NaH	16	(±)-**5aa** (74)

[a]Conditions: **1a** (0.2 mmol), aldehyde (0.2 mmol), **C1** (10 mol%), base (0.4 mmol), **8** (0.2 mmol), anhydrous THF (2.0 mL), 4Å MS, RT. [b]Isolated yield. [c]Reaction run with 0.4 mmol of **2a**. [d]Reaction run with 0.4 mmol of **1a** and 0.46 mmol of NaH.

At this point, the screening of a set of chiral pre-catalysts **C2**−**C7** was carried out to perform the asymmetric version of the model N-acylation of DHPM **1a** in the presence of cinnamaldehyde **2a** as the limiting reagent (Table 2). Under the condition of the disclosed racemic process (Table 1, entry 7) the amino-indanol-derived triazolium salts **C2**−**C4** proved to be low effective even using a higher catalytic loading (20 mol%; Table 2, entries 1–3). However, the chiral catalyst **C3** promoted the formation of **5aa** in very low yield (8%) but with an encouraging enantiomeric ratio (*er* = 78:22; Table 2, entry 2). The pyrrole-derived triazolium pre-catalyst **C5** provided unsatisfactory results (Table 2, entry 4), while the analogue **C6** gave **5aa** in 50% isolated yield and 80:20 *er* after 16 h (entry 5). The lower efficiency observed with chiral catalyst could be attributed to the higher steric hindrance of the chiral pre-catalysts **C5**−**C6** compared to the achiral **C1**. A comparable yield of **5aa** (55%) accompanied, however, by a lower value of *er* (60:40) was detected with the morpholine-based triazolium salt **C7** (Table 2, entry 6).

Table 2. Screening of chiral triazolium salts.[a]

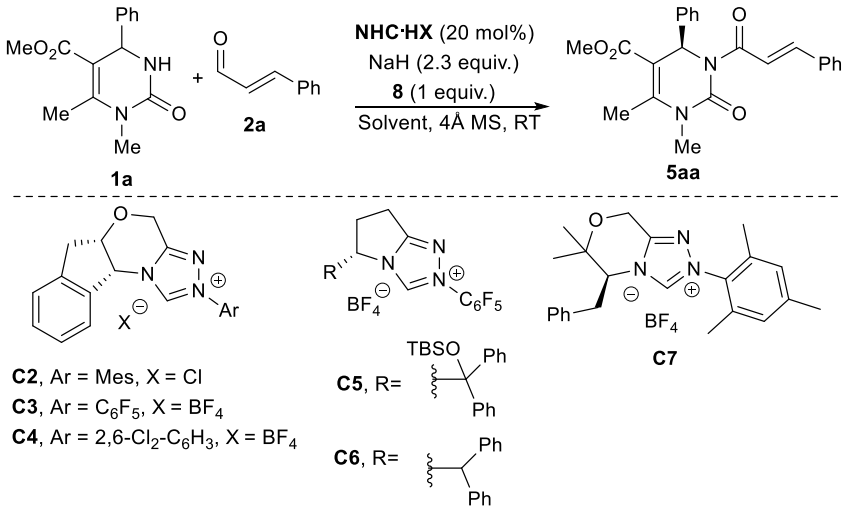

Entry	NHC·HX	Solvent	**5aa** (%)[b]	*er*[c]
1	**C2**	THF	-	-
2	**C3**	THF	8	78:22
3	**C4**	THF	-	-
4	**C5**	THF	-	-
5	**C6**	THF	50	80:20
6	**C7**	THF	55	60:40

[a]Conditions: **1a** (0.4 mmol), aldehyde (0.2 mmol), **NHC·HX** (0.04 mmol), base (0.46 mmol), oxidant (0.2 mmol), anhydrous THF (4.0 mL), 4Å MS, RT, 16 h. [b]Isolated yield. [c]Determined by chiral HPLC.

Later, the solvent screening with the optimal catalyst **C6** indicated THF as the optimal reaction medium (Table 3, entries 1−3). Therefore, further investigations were targeted through variation of the base employed (Table 3). However, the use of DIPEA and DBU produced unsatisfactory results (Table 3, entries 4 and 5); while the use of stronger organic and inorganic bases (Table 3, entries 6−9) indicating *n*-BuLi (2.3 equiv.) as the selected base, allowing to increase the yield (55%) and the enantioselectivity of the process (*er* = 83:17; Table 3, entry 9). At this point of the optimization step a further solvent screening with the optimal base *n*-BuLi was conducted, leading to disappointing values of both the reaction yield and enantioselectivity (Table 3, entries 10−13). The low yield detected for the reaction in DMF could be attributed to side reaction between DMF and the strong base *n*-BuLi, however no further investigations have been conducted in this regard.[22] The increasing of the temperature to 45 °C had a little effect on the reaction outcome, with a small improvement of the reaction yield (60%) together with a partial loss of enantioselectivity (*er* = 75:25; Table 3, entry 14). On the other hand, cooling the reaction mixture to 0 °C produced a drastic reduction of yield (25%) and only a little enhancement of *er* (85:15; Table 3, entry 15). According to the results obtained from the racemic process, the use of an excess (2 equiv.) of aldehyde **2a** resulted in a lower efficiency of the acylation procedure (Table 3, entry 16).

Table 3. Optimization study.[a]

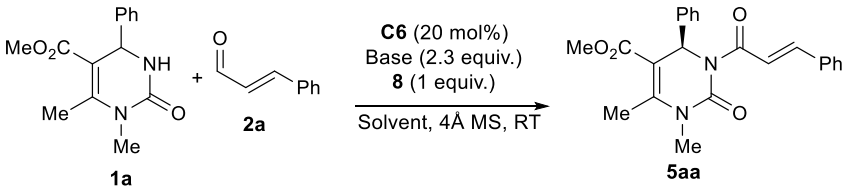

Entry	Solvent	Base	**5aa** (%)[b]	*er*[c]
1	THF	NaH	55	60:40
2	DCM	NaH	21	64:36
3	DMF	NaH	16	62:38
4	THF	DIPEA	-	-
5	THF	DBU	-	-
6	THF	KHMDS	20	61:39
7	THF	*t*-BuOK	18	63:37
8	THF	Cs_2CO_3	15	64:36
9	**THF**	***n*-BuLi**	**55**	**83:17**
10	DCM	*n*-BuLi	20	63:37
11	Toluene	*n*-BuLi	-	-
12	DMF	*n*-BuLi	18	65:35
13	NMP	*n*-BuLi	16	60:40
14[d]	THF	*n*-BuLi	60	75:25
15[e]	THF	*n*-BuLi	25	85:15
16[f]	THF	*n*-BuLi	32	82:18

[a]Conditions: **1a** (0.4 mmol), aldehyde (0.2 mmol), **C6** (0.04 mmol), base (0.46 mmol), **8** (0.2 mmol), anhydrous THF (4.0 mL), 4Å MS, RT, 16 h. [b]Isolated yield. [c]Determined by chiral HPLC. [d]Temperature: 45 °C. [e]Temperature: 0 °C, 32 h. [f]Conditions: **1a** (0.2 mmol), **2a** (0.4 mmol), **C6** (0.08 mmol), *n*-BuLi (0.25 mmol), **8** (0.4 mmol), 24 h.

During the optimization step no dedicated experiments were conducted with the aim to determine whether the DHPM **1a** goes through a KR or DKR process, differently the attention was focus on the use of the reaction conditions which allowed to obtain products with high enantioenrichment. Hence, the effect of a cooperative Lewis catalyst[23] was additionally explored; unfortunately, the addition of LiCl or $LiBF_4$ (25 mol%) left the enantiomeric ratio of **5aa** almost unchanged (Table 4, entries 1 and 2). Replacing the Kharasch oxidant **8** with different oxidants such as phenazine **9** and azobenzene **10** had a little effect both for the reaction yield (45−48%) and enantiomeric ratio (*er* = 80:20; Table 4, entries 3 and 4). Moreover, the possibility to use air as the terminal oxidant *via* biomimetic system of electron-transfer mediators (ETMs) developed by Bäckvall[24] and Sundeń[20,25] groups was also examined. Indeed, a catalytic amount (25 mol%) of quinone **8** (ETM') was employed in combination with iron(II) phthalocyanine **11** (5 mol%, ETM'') under air atmosphere affording **5aa** in poor yield (20%) and comparable enantioselectivity (*er* = 78:22; Table 4, entry 5). Lastly, control experiment to establish the possible racemization at C4 position of DHPM **5aa** confirmed that in presence of an excess of *n*-BuLi the stereochemical integrity of enantioenriched **5aa** is kept unaltered.

Promisingly, the configurational stability of the product was also tested under the full reaction conditions (in the presence of the oxidant and the base) detecting no relevant changes.

Table 4. Optimization study: additives and use of different oxidation systems.[a]

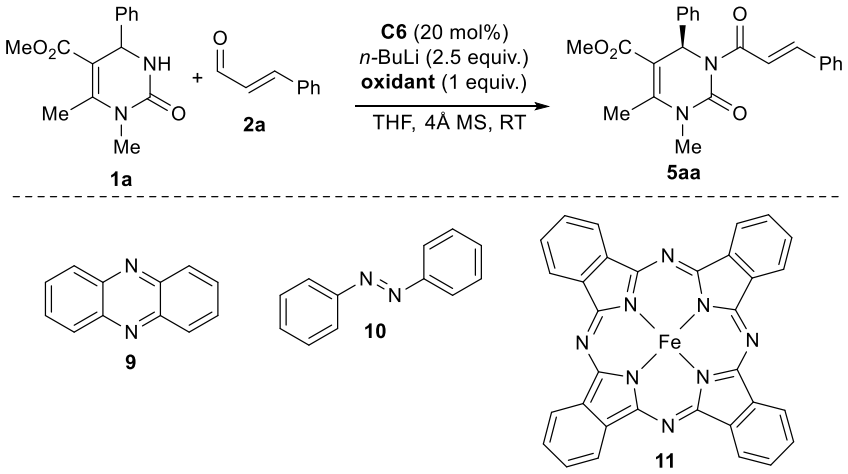

Entry	Oxidant	**5aa** (%)[b]	*er*[c]
1[d]	**8**	30	72:18
2[e]	**8**	42	80:20
3	**9**	45	80:20
4	**10**	48	80:20
5[f]	air	20	78:22

[a]Conditions: **1a** (0.4 mmol), aldehyde (0.2 mmol), **C6** (0.04 mmol), base (0.46 mmol), oxidant (0.2 mmol), anhydrous THF (4 mL), 4Å MS, RT, 16 h. [b]Isolated yield. [c]Determined by chiral HPLC. [d]Addition of LiCl (0.05 mmol). [e]Addition of $LiBF_4$ (0.05 mmol). [f]Addition of **8** (0.05 mmol) and **11** (0.01 mmol).

At this point, a further attempt aimed to enhance the enantioselectivity of the model N-acylation reaction was conducted. Inspired by the NHC/hydroxamic acid co-catalysis approach developed by Bode and co-workers for the KR of cyclic secondary amines,[15e] the achiral triazolium pre-catalyst **C1** (10 mol%) and the chiral hydroxamic acid co-catalyst **A** (10 mol%) were used for the benchmark reaction. Thus, equimolar ratio of DHPM **1a**, cinnamaldehyde **2a** and Kharasch oxidant **8** were employed in THF as the optimal solvent along with *n*-BuLi (1.5 equiv.) as the base. This synergistic catalysis relied on the generation of the key acylating agent **I** which is susceptible to nucleophilic attack by the deprotonated DHPM **1a** (Scheme 2). Unfortunately, the experimental outcome indicated that the likely competitive achiral pathway directly promoted by **C1** is predominant as the product **5aa** was obtained in higher yield (69%) but almost in racemic form (*er* = 53:47).

With optimized conditions in hand, the generality of this N-acylation protocol was investigated through variation of DHPMs scaffold (Table 5). Initially, the stereoelectronic properties of substituent in C4 position were tested through reaction with aldehyde **2a** under the developed

conditions (Table 3, entry 9). Notably, electron-withdrawing groups in *meta*- and *para*-position led to an increase of reactivity (**5ba**, 68%; **5ca**, 72%) with little effect on enantioselectivity compared to the model **5aa**. The *ortho*-chloro substituent, instead, determined a decrease of reactivity probably because of the steric hindrance around the C4 stereocenter affording the product **5da** with 41% yield without reducing the enantiomeric enrichment (*er* = 81:19). Differently, the presence of an electron-donating group in para-position of the C4 aromatic ring produced a little improvement in terms of *er* which was registered in DHPM **5ea** equal to 84:16. A much lower enantiomeric ratio was instead detected in the furyl-functionalized compound **5fa** (*er* = 62:38). Additional variations of the C5 ester group (**5ga**) and N1-substituent (**5ha**, **5ia**) in the DHPM core showed no appreciable modifications of reaction efficiency in comparison with model **5aa**, apart from the marked drop of enantiomeric ratio displayed by **5ha** (*er* = 57:43) bearing an aromatic N1 group. Furthermore, the introduction of an aliphatic chain at the C4 position resulted in a diminished enantioselectivity (**5ja**; *er* = 71:29) compared to **5ia** with the same substitution pattern (*er* = 78:22). The introduction of electron-withdrawing and electron-donating groups on cinnamaldehyde furnished the corresponding N3-acylated DHPMs **5ab** and **5ac** with low enantioselectivities, being **5ab** almost a racemic product (*er* = 53:47). Moving from the model DHPM **1a** to the thio-analogue **12** as the substrate led to a lack of enantiocontrol exerted by **C6** yielding the corresponding N3-acylated product **13** in good yield (79%) but negligible enantioselectivity (*er* = 58:42). This result suggests that this group might be important for stabilising the acylation transition state and thus dictating enantiodiscrimination.

To assign the absolute configuration of product **5**, a dedicated experiment was conducted, involving the known DHPM **1g** along with equimolar (in place of 2 equivalent as for the reaction scope) cinnamaldehyde **2a** (30% conversion). The recovered DHPM **1g** (*er* = 60:40) showed to be with (4*S*)-configuration (optical rotation analysis)[26] thus allowing to deduce the opposite (4*R*)-configuration for the acylated counterpart **5ga** (*er* = 77:23). This assignment was then extended to all DHPMs **5** by analogy.

Table 5. Reaction scope of the enantioselective N-acylation of DHPMs.

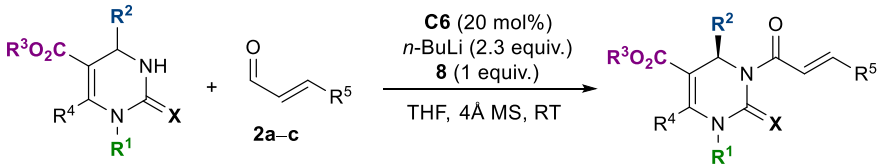

1a–j (X = O)
12 (X = S)

5 (X = O)
13 (X = S)

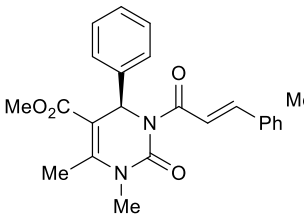

5aa, 55%, 83:17 *er*

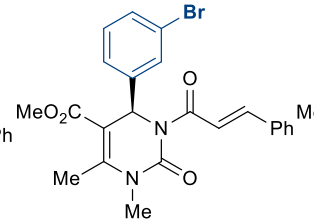

5ba, 68%, 72:28 *er*

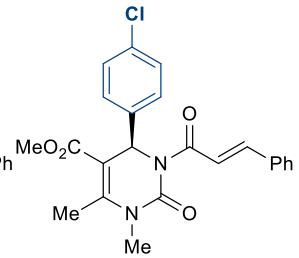

5ca, 72%, 73:27 *er*

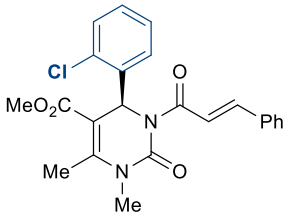

5da, 41%, 81:19 *er*

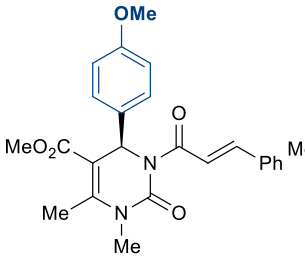

5ea, 50%, 84:16 *er*

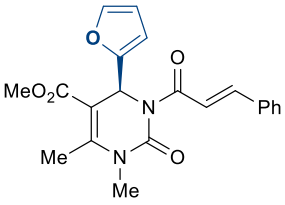

5fa, 52%, 62:38 *er*

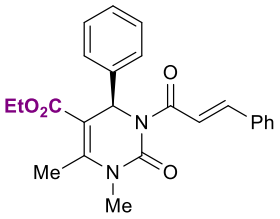

5ga, 57%, 77:23 *er*

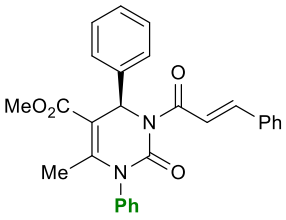

5ha, 58%, 57:43 *er*

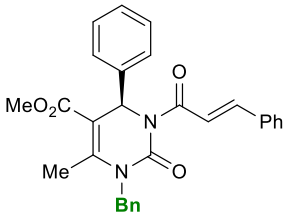

5ia, 62%, 78:22 *er*

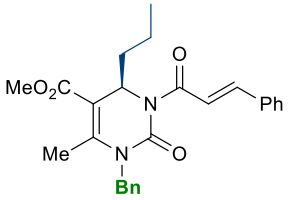

5ja, 58%, 71:29 *er*

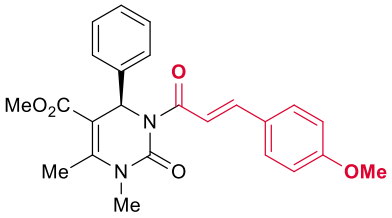

5ab, 60%, 53:47 *er*

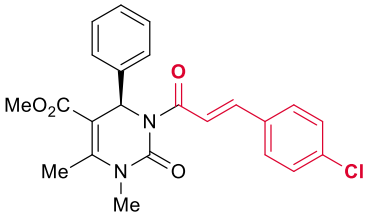

5ac, 55%, 63:37 *er*

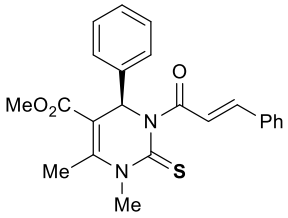

13, 79%, 58:42 *er*

Conditions: **1a** (0.4 mmol), aldehyde (0.2 mmol), **C6** (0.04 mmol), *n*-BuLi (0.46 mmol), **8** (0.2 mmol), anhydrous THF (4 mL), 4Å MS, RT, 16 h.

Finally, synthetic elaboration of the α,β-unsaturated functionality of the products **5** was investigated for the introduction of additional elements of diversity on the DHPM scaffold. As a proof of concept study, enantioenriched **5aa** (*er* = 83:17) was subjected to alkene hydroarylation[27] with benzene and triflic acid (TfOH) affording the diaryl derivative **14** in satisfactory yield (55%) and almost unchanged enantiomeric purity (*er* = 80:20; Scheme 3).

Noteworthy, the stoichiometric oxidant **8** could be easily regenerated with air and re-used in different runs (see previous Chapters and the Experimental section for further details).

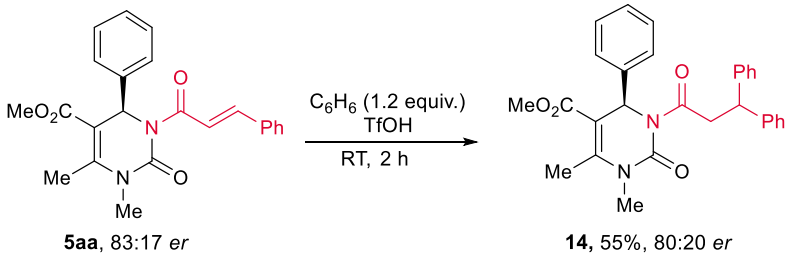

Scheme 3. Synthetic elaboration of enantioenriched DHPM **5aa**.

Lastly, a suggested mechanism for the disclosed asymmetric N-acylation of DHPMs is reported in Scheme 4. Accordingly, the deprotonation of triazolium salt **C6** generates the NHC **II** which reacts with aldehyde **2** to give the homoenolate intermediate **III**. Subsequent oxidation by the external oxidant **8** leads to the acyl azolium **IV** which is intercepted by the deprotonated DHPM **1'**. Later, the product **5** is obtained along with catalyst turnover through the intermediate **V**.

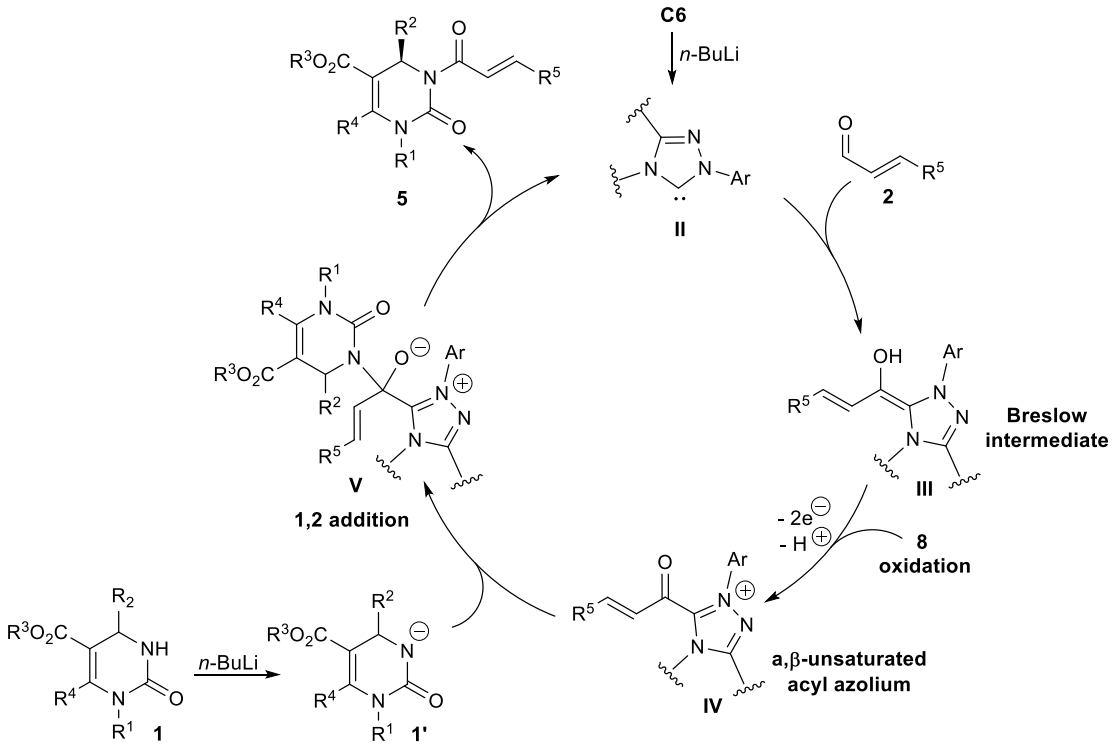

Scheme 4. Proposed reaction mechanism.

A suggested acylation transition state has been hypothesised as well (Figure 2). Building upon previous studies,[28] DHPMs display a boat-like conformation in which the aryl ring (at the C4 position) is positioned axially (in the (*R*)-enantiomer) and orthogonal to the dihydropyridine ring. An interaction among the C=O group and the positively charged acyl azolium intermediate

could be postulated as the responsible for the stabilization of the (*R*)-substrate. The (*S*)-substrate instead turned out to be more hindered thus limiting its reactivity. At this point of the study, more hypotheses could not be proposed as the collected data and the information already present in literature are not sufficient to explain the selectivity of the process. Indeed, although these models account for the sense of asymmetric induction in these kinetic resolutions, they are currently speculative as further investigations are ongoing to better understand the mechanism and the structure of the transition state.

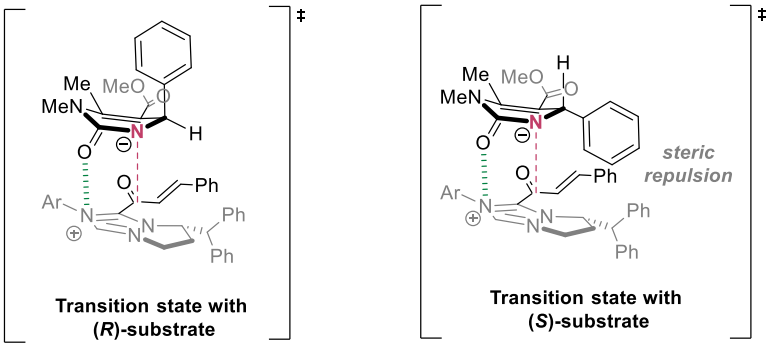

Figure 2. Suggested acylation TSs for the fast and slow reacting enantiomers.

7.3 Conclusion

To conclude, an asymmetric N-acylation strategy of DHPMs based on oxidative NHC-catalysis has been developed. The disclosed procedure allows access to a class of new pharmaceutically relevant N3-acylated DHPMs in enantioenriched form. The use of aldehydes as mild acylating agents globally emerged well suited for the (stereo)chemical decoration of molecules containing the ureido functionality. Scope and limitations of the direct N-acylation of DHPM nucleus were investigated and even though the process enantioselectivity was moderate, this work could be considered as a starting point for the development of further studies on the KR and DKR of amide-like substrates.

7.4 Experimental section

General procedure

^{1}H and ^{13}C NMR spectra were recorded on 300 and 400 MHz spectrometers in $CDCl_3$ at room temperature. ^{13}C NMR spectra were acquired with the ^{1}H broad-band decoupled mode, and chemical shifts (δ) are reported in ppm relative to residual solvents signals. Reactions were monitored by TLC on silica gel 60 F_{254} with detection by UV lamp operating at 254 nm and by spraying with vanillin-sulfuric acid reagent (6% vanillin [w/v] and 1% H_2SO_4 [v/v] in ethanol)

followed by a short, gentle heating. Flash column chromatography was performed on silica gel 60 (230–400 mesh). All reactions were performed in oven-dried (100 °C) glassware under an atmosphere of argon. Optical rotations were measured at 25 ± 2 °C in the stated solvent; $[\alpha]_D^{25}$ are given in 10^{-1} deg cm^2 g^{-1} (concentration *c* given as g/ 100 mL). The enantiomeric ratios were determined by chiral stationary phase HPLC (Daicel Chiralpak IA), using an UV detector operating at 254 nm. All HPLC traces of enantiomerically-enriched compounds were compared with authentic racemic spectra. Melting points were measured on an Electrothermal 9100 apparatus and are uncorrected. All commercially available reagents and compounds **3a**, **8–11** were purchased from TCI and used as received without further purification. Solvents were distilled from appropriate drying agents. Liquid aldehydes **2a**, **4a** and DBU base were freshly distilled before their utilization. Catalysts **C4**,[29a] **C5**,[29b] and **C6**[29c] were prepared by following literature procedure. Catalysts **A**, **C1**, **C2**, **C3** and **C7** were purchased from Sigma-Aldrich. Compounds **1** were prepared following a slightly modified literature procedure.[30] DHPMs **1e**,[31a] **1g**,[31b] **1i**[31c] are known compounds.

For the kinetic resolution, selectivity factors (*s*) was calculated according to Kagan's equation: $s = \ln((1\text{-Conv.})(1\text{-ee}_{rsm}))/\ln((1\text{-Conv.})(1+\text{ee}_{rsm})) = \ln(1\text{-Conv.}(1+\text{ee}_{prod}))/\ln(1\text{-Conv.}(1\text{-ee}_{prod}))$, wherein Conv. is conversion of the reaction, ee_{prod} is the enantiomeric excess of diester product and ee_{rsm} is the enantiomeric excess of the recovered monoester. Conversions (Conv.) were calculated by the following equation: $\text{Conv.} = \text{ee}_{rsm}/(\text{ee}_{prod}+\text{ee}_{rsm})$.[4]

General Procedure for the synthesis of 3,4-dihydropyrimidin-2(1*H*)-ones 1 and 12

A mixture of aldehyde (4 mmol), dicarbonyl compound (4 mmol), N-substituted urea/thiourea (6 mmol) and *p*-toluenesulfonic acid (100 mg) was refluxed in 5 mL of methanol for 16 h. Reaction progress was followed by TLC and after the completion, the reaction mixture was cooled down to 0 °C. In some cases, the products precipitated readily, otherwise nucleation was promoted by scratching the surface of the flask with a spatula. The solids were collected by filtration, washed with water and ice-cold methanol. In other cases, the organic mixture was concentrated and eluted from a column of silica gel with the suitable elution system to give the 3,4-dihydropyrimidin-2(1*H*)-one **1**.

Methyl 1,6-Dimethyl-2-oxo-4-phenyl-1,2,3,4-tetrahydropyrimidine-5-carboxylate (1a)

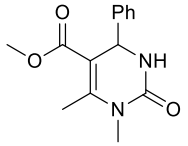

The product readily precipitated from MeOH cooled to 0 °C. Filtration, washing with cold MeOH and drying under vacuum afforded the product **1a** (0.93 g, 90%) as a white powder. **mp** 190–191 °C {Lit.[32] 190–192 °C}; **^{1}H NMR** (300 MHz, $CDCl_3$) δ = 7.40–7.14 (m, 5H, ArH), 5.44 (s, 1H, NH), 5.38 (d, *J* 3.3 Hz, 1H, H-4), 3.65 (s, 3H, CO_2CH_3), 3.23 (s, 3H, NCH_3-1), 2.52 (s, 3H, CH_3-6); **^{13}C NMR** (101 MHz, $CDCl_3$) δ = 166.6 (*C*O_2CH_3), 153.9 (-NCH_3*C*ONH-), 149.7 (*C*-6), 143.3 (Ar*C*), 128.8 (2C, Ar*C*H), 127.9 (Ar*C*H), 126.2 (2C, Ar*C*H), 104.1 (*C*-5), 54.0 (*C*H-4), 51.4 (O*C*H_3), 30.4 (N*C*H_3-1), 16.7 (*C*H_3-6); **HRMS**(ESI): calcd. for $C_{14}H_{17}N_2O_3^+$ ($[M + H]^+$): 261.1234; found: 261.1244.

Methyl 4-(3-Bromophenyl)-1,6-dimethyl-2-oxo-1,2,3,4-tetrahydropyrimidine-5-carboxylate (1b)

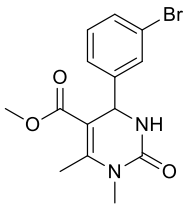

The product readily precipitated from MeOH cooled to 0 °C. Filtration, washing with cold MeOH and drying under vacuum afforded the product **1b** (1.08 g, 80%) as a yellowish powder. **mp** 138–140 °C; **^{1}H NMR** (300 MHz, $CDCl_3$) δ = 7.38 (s, 2H, ArH), 7.18 (d, *J* 5.0 Hz, 2H, ArH), 5.47 (s, 1H, NH), 5.36 (s, 1H, H-4), 3.67 (s, 3H, CO_2CH_3), 3.24 (s, 3H, NCH_3-1), 2.54 (s, 3H, CH_3-6); **^{13}C NMR** (101 MHz, $CDCl_3$) δ = 166.3 (*C*O_2CH_3), 153.6 (-NCH_3*C*ONH-), 150.2 (Ar*C*), 145.5 (*C*-6), 131.1 (Ar*C*H), 130.5 (Ar*C*H), 129.4 (Ar*C*H), 124.8 (Ar*C*H), 122.9 (Ar*C*), 103.3 (*C*-5), 53.6 (*C*H-4), 51.5 (O*C*H_3), 30.5 (N*C*H_3-1), 16.7 (*C*H_3-6); **HRMS**(ESI): calcd. for $C_{14}H_{16}BrN_2O_3^+$ ($[M + H]^+$): 339.0339; found: 339.0352.

Methyl 4-(4-Chlorophenyl)-1,6-dimethyl-2-oxo-1,2,3,4-tetrahydropyrimidine-5-carboxylate (1c)

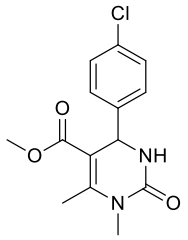

The product readily precipitated from MeOH cooled to 0 °C. Filtration, washing with cold MeOH and drying under vacuum afforded the product **1c** (1.00 g, 85%) as a yellow powder. **mp** 118–120 °C {Lit.[33] 117–119 °C}; **^{1}H NMR** (300 MHz, $CDCl_3$) δ = 7.28 (d, *J* 8.5 Hz, 2H, ArH), 7.18 (d, *J* 8.5 Hz, 2H, ArH), 5.45 (s, 1H, NH), 5.36 (s, 1H, H-4), 3.66 (s, 3H, CO_2CH_3),

3.24 (s, 3H, NCH_3-1), 2.52 (s, 3H, CH_3-6); **^{13}C NMR** (101 MHz, $CDCl_3$) δ = 166.4 (CO_2CH_3), 153.7 (-NCH_3CONH-), 149.9 (*C*-6), 141.8 (Ar*C*), 133.7 (Ar*C*), 129.0 (2C, Ar*C*H), 127.6 (2C, Ar*C*H), 103.7 (*C*-5), 53.4 (*C*H-4), 51.5 (OCH_3), 30.5 (NCH_3-1), 16.7 (CH_3-6); **HRMS**(ESI): calcd. for $C_{14}H_{16}ClN_2O_3^+$ ($[M + H]^+$): 295.0844; found: 295.0854.

Methyl 4-(2-Chlorophenyl)-1,6-dimethyl-2-oxo-1,2,3,4-tetrahydropyrimidine-5-carboxylate (1d)

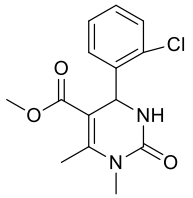

The product readily precipitated from MeOH cooled to 0 °C. Filtration, washing with cold MeOH and drying under vacuum afforded the product **1d** (0.95 g, 80%) as a yellowish powder. **mp** 115–117 °C; **^{1}H NMR** (300 MHz, $CDCl_3$) δ = 7.38 (dt, *J* 5.1, 2.8 Hz, 1H, ArH), 7.25 – 7.08 (m, 3H, ArH), 5.76 (s, 1H, NH), 5.72 (s, 1H, H-4), 3.58 (s, 3H, CO_2CH_3), 3.22 (s, 3H, NCH_3-1), 2.65 (s, 3H, CH_3-6); **^{13}C NMR** (101 MHz, $CDCl_3$) δ = 166.1 (CO_2CH_3), 153.3 (-NCH_3CONH-), 151.7 (*C*-6), 138.7 (Ar*C*), 132.9 (Ar*C*), 130.0 (Ar*C*H), 129.3 (Ar*C*H) , 127.4 (2C, Ar*C*H), 101.2 (*C*-5), 51.5 (*C*H-4), 50.7 (OCH_3), 30.3 (NCH_3-1), 16.5 (CH_3-6); **HRMS**(ESI): calcd. for $C_{14}H_{16}ClN_2O_3^+$ ($[M + H]^+$): 295.0844; found: 295.0856.

Methyl 4-(4-Methoxyphenyl)-1,6-dimethyl-2-oxo-1,2,3,4-tetrahydropyrimidine-5-carboxylate (1e)

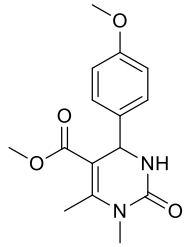

Column chromatography on silica gel with 1:1 cyclohexane:EtOAc afforded **1e** (0.81 g, 70%) as a yellowish powder with spectroscopic data in accordance with the literature.[30a]

mp 148–150 °C {Lit.[30a] 149–151 °C}; **^{1}H NMR** (300 MHz, $CDCl_3$) δ = 7.22–7.09 (m, 2H, ArH), 6.87 – 6.76 (m, 2H, ArH), 5.59 (s, 1H, NH), 5.32 (d, *J* 3.2 Hz, 1H, H-4), 3.78 (s, 3H, CO_2CH_3), 3.65 (s, 3H, ArOCH_3), 3.23 (s, 3H, NCH_3-1), 2.51 (s, 3H, CH_3-6); **^{13}C NMR** (101 MHz, $CDCl_3$) δ = 166.5 (CO_2CH_3), 159.1 (Ar*C*), 153.9 (-NCH_3CONH-), 149.2 (*C*-6), 135.5 (Ar*C*), 127.3 (2C, Ar*C*H), 114.0 (2C, Ar*C*H), 104.2 (*C*-5), 55.2 (ArOCH_3), 53.3 (*C*H-4), 51.3

(OCH_3), 30.3 (NCH_3-1), 16.6 (CH_3-6); **HRMS**(ESI): calcd. for $C_{15}H_{19}N_2O_4^+$ ($[M + H]^+$): 291.1339; found: 291.1328.

Methyl 4-(Furan-2-yl)-1,6-dimethyl-2-oxo-1,2,3,4-tetrahydropyrimidine-5-carboxylate (1f)

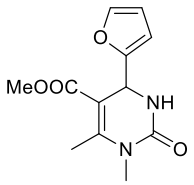

Column chromatography on silica gel with 1:1.5 cyclohexane:EtOAc afforded **1f** (0.70 g, 70%) as a white powder.

mp 155–157 °C; **^{1}H NMR** (300 MHz, $CDCl_3$) δ = 7.34 – 7.26 (m, 1H, ArH), 6.24 (dd, *J* 3.1, 1.8 Hz, 1H, ArH), 6.10 – 6.01 (m, 1H, ArH), 5.85 (s, 1H, NH), 5.41 (d, *J* 3.4 Hz, 1H, H-4), 3.68 (s, 3H, CO_2CH_3), 3.19 (s, 3H, NCH_3-1), 2.52 (s, 3H, CH_3-6); **^{13}C NMR** (101 MHz, $CDCl_3$) δ = 166.1 (CO_2CH_3), 154.6 (-NCH_3CONH-), 154.3 (Ar*C*), 151.2 (*C*-6), 142.3 (Ar*C*H), 110.1 (Ar*C*H), 105.6 (Ar*C*H), 101.2 (*C*-5), 51.4 (OCH_3), 47.5 (*C*H-4), 30.4 (NCH_3-1), 16.5 (CH_3-6); **HRMS**(ESI): calcd. for $C_{12}H_{15}N_2O_4^+$ ($[M + H]^+$): 251.1026; found: 251.1034.

Ethyl 1,6-Dimethyl-2-oxo-4-phenyl-1,2,3,4-tetrahydropyrimidine-5-carboxylate (1g)

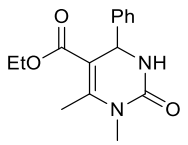

The product readily precipitated from MeOH cooled to 0 °C. Filtration, washing with cold MeOH and drying under vacuum afforded the product **1g** (0.98 g, 90%) as a white powder with spectroscopic data in accordance with the literature.[30b]

mp 181–183 °C {Lit.[30b] 180–182 °C}; **^{1}H NMR** (300 MHz, $CDCl_3$) δ = 7.42–7.21 (m, 5H, ArH), 5.66 (s, 1H, NH), 5.40 (s, 1H, H-4), 4.11 (q, *J* 7.1 Hz, 2H, $CO_2CH_2CH_3$), 3.24 (s, 3H, NCH_3-1), 2.52 (s, 3H, CH_3-6), 1.18 (t, *J* 7.1 Hz, 3H, $CO_2CH_2CH_3$); **^{13}C NMR** (101 MHz, $CDCl_3$) δ = 166.0 (CO_2CH_3), 154.0 (-NCH_3CONH-), 149.1 (*C*-6), 143.2 (Ar*C*), 128.8 (2C, Ar*C*H), 128.0 (Ar*C*H), 126.3 (2C, Ar*C*H), 104.5 (*C*-5), 60.3 ($CO_2CH_2CH_3$), 54.1 (*C*H-4), 30.4 (NCH_3-1), 16.6 (CH_3-6), 14.2 ($CO_2CH_2CH_3$); **HRMS**(ESI): calcd. for $C_{15}H_{19}N_2O_3^+$ ($[M + H]^+$): 275.1390; found: 275.1379.

Methyl 6-Methyl-2-oxo-1,4-diphenyl-1,2,3,4-tetrahydropyrimidine-5-carboxylate (1h)

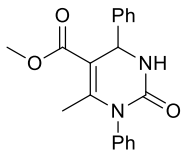

Column chromatography on silica gel with 2:1 cyclohexane:EtOAc afforded **1h** (0.97 g, 75%) as a white powder.

mp 140–142 °C; **^{1}H NMR** (300 MHz, $CDCl_3$) δ = 7.57–7.27 (m, 8H, NArH-1 and ArH-4), 7.24 (d, *J* 11.9 Hz, 2H, ArH-4), 5.54 (s, 1H, NH), 5.49 (d, *J* 3.0 Hz, 1H, H-4), 3.68 (s, 3H, CO_2CH_3), 2.11 (s, 3H, CH_3-6); **^{13}C NMR** (101 MHz, $CDCl_3$) δ = 166.5 (*C*O_2CH_3), 153.1 (-NPh*C*ONH-), 149.1 (*C*-6), 143.3 (Ar*C*), 137.6 (Ar*C*), 129.4 (2C, Ar*C*H), 129.0 (2C, Ar*C*H), 128.6 (2C, Ar*C*H), 128.1 (2C, Ar*C*H), 126.3 (2C, Ar*C*H), 104.8 (*C*-5), 54.5 (*C*H-4), 51.5(O*C*H_3), 18.7 (*C*H_3-6); **HRMS**(ESI): calcd. for $C_{19}H_{19}N_2O_3^+$([M + H]$^+$): 323.1390; found: 323.1403.

Methyl 1-Benzyl-6-methyl-2-oxo-4-phenyl-1,2,3,4-tetrahydropyrimidine-5-carboxylate (1i)

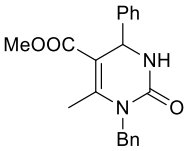

Column chromatography on silica gel with 2:1 cyclohexane:EtOAc afforded **1i** (0.99 g, 74%) as a white powder with spectroscopic data in accordance with the literature.[30c]

mp 139–140 °C {Lit.[30c] 136–137 °C}; **^{1}H NMR** (300 MHz, $CDCl_3$) δ = 7.33–7.15 (m, 8H, Ar-4 and NCH_2*ArH*-1), 7.10 (d, *J* 7.7 Hz, 2H, NCH_2*ArH*-1), 6.27 (s, 1H, NH), 5.44 (d, *J* 3.2 Hz, 1H, H-4), 5.21 (d, *J* 16.6 Hz, 1H, N*CH*$_2$Ar-1), 4.86 (d, *J* 16.6 Hz, 1H, N*CH*$_2$Ar-1), 3.63 (s, 3H, CO_2CH_3), 2.44 (s, 3H, CH_3-6); **^{13}C NMR** (101 MHz, $CDCl_3$) δ = 166.5 (*C*O_2CH_3), 154.1 (-NAr*C*ONH-), 149.4 (*C*-6), 143.0 (Ar*C*), 137.9 (Ar*C*), 128.7 (4C, Ar*C*H), 127.8 (Ar*C*H), 127.2 (Ar*C*H), 126.4 (2C, Ar*C*H), 126.3 (2C, Ar*C*H), 104.6 (*C*-5), 53.7 (*C*H-4), 51.4 (O*C*H_3), 45.9 (*C*H_2Ph), 16.5 (*C*H_3-6); **HRMS**(ESI): calcd. for $C_{20}H_{21}N_2O_3^+$ ([M + H]$^+$): 337.1547; found: 337.1559.

Methyl 1-Benzyl-6-methyl-2-oxo-4-propyl-1,2,3,4-tetrahydropyrimidine-5-carboxylate (1j)

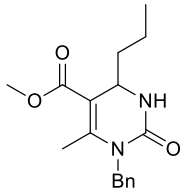

Column chromatography on silica gel with 3:1 cyclohexane:EtOAc afforded **1j** (0.43 g, 35%) as a white powder.

mp 131–133 °C; **^{1}H NMR** (300 MHz, $CDCl_3$) δ = 7.42 – 7.12 (m, 5H, ArH), 5.75 (s, 1H, NH), 5.14 (d, *J* 16.7 Hz, 1H, NCH_2Ar-1), 4.85 (d, *J* 16.6 Hz, 1H, NCH_2Ar-1), 4.28 (s, 1H, H-4), 3.72 (s, 3H, CO_2CH_3), 2.36 (s, 3H, CH_3-6), 1.59 – 1.23 (m, 4H, $CH_2CH_2CH_3$), 0.91 (t, *J* 7.1 Hz, 3H, $CH_2CH_2CH_3$); **^{13}C NMR** (101 MHz, $CDCl_3$) δ = 166.7 (*C*O_2CH_3), 154.8 (-NAr*C*ONH-), 149.2 (*C*-6), 138.3 (Ar*C*), 128.7 (2C, Ar*C*H), 127.1 (Ar*C*H), 126.3 (2C, Ar*C*H), 105.2 (*C*-5), 51.29 (*C*H-4), 50.1 (O*C*H_3), 45.9 (*C*H_2Ph), 39.2 (*C*$H_2CH_2CH_3$), 17.9 (CH_2*C*H_2CH_3), 16.4 (*C*H_3-6), 13.8 (CH_2*C*H_3); **HRMS**(ESI): calcd. for $C_{17}H_{23}N_2O_3^+$ ([M + H]$^+$): 303.1703; found: 303.1716.

Methyl 1,6-Dimethyl-4-phenyl-2-thioxo-1,2,3,4-tetrahydropyrimidine-5-carboxylate (12)

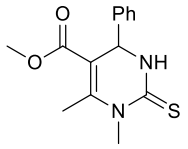

The product readily precipitated from MeOH cooled to 0 °C. Filtration, washing with cold MeOH and drying under vacuum afforded the product **12** (0.98 g, 89%) as a white powder.

mp 117–118 °C; **^{1}H NMR** (300 MHz, $CDCl_3$) δ = 7.54 – 6.95 (m, 6H, ArH and NH), 5.41 (s, 1H, H-4), 3.72 (s, 3H, CO_2CH_3), 3.62 (s, 3H, NCH_3-1), 2.52 (s, 3H, CH_3-6); **^{13}C NMR** (101 MHz, $CDCl_3$) δ = 179.7 (-NAr*C*SNH-), 166.0 (*C*O_2CH_3), 146.9 (*C*-6), 141.5 (Ar*C*), 128.9 (2C, Ar*C*H), 128.2 (Ar*C*H), 126.0 (2C, Ar*C*H), 107.4 (*C*-5), 53.7 (*C*H-4), 51.7 (O*C*H_3), 37.1 (N*C*H_3-1), 16.9 (*C*H_3-6); **HRMS**(ESI): calcd. for $C_{14}H_{17}N_2O_2S^+$ ([M + H]$^+$): 277.1005; found: 277.1014.

General procedure for the synthesis of racemic N3-Acylated DHPMs ((*rac*)-5,6)

A stirred mixture of **1a** (stated amount) and anhydrous THF (2.0 mL) was degassed under vacuum and saturated with argon (by an Ar-filled balloon) three times. Then the reaction mixture was cooled to 0 °C with an ice bath and NaH (stated amount) was added slowly. After 15 min at 0 °C, the ice bath was removed allowing the reaction to warm up till room temperature and the reaction mixture was stirred for an additional 15 min. Then, oxidant **8** (82 mg, 0.20

mmol), catalyst **C1** (6 mg, 0.02 mmol) and 4Å MS were added under an argon environment. Aldehyde **2**–**4** (0.20 mmol) was finally added, and the reaction was stirred at room temperature for the stated time (Table 1). The resulting solution was quenched with 0.5 M HCl (3.0 mL), partially concentrated under vacuum to reduce the amount of THF, extracted with DCM (3 × 15 mL), dried (anhydrous Na_2SO_4), and concentrated. Elution of the resulting residue from a column of silica with the suitable elution system afforded **(*rac*)-5,6**.

Methyl (*E*)-3-Cinnamoyl-1,6-dimethyl-2-oxo-4-phenyl-1,2,3,4-tetrahydropyrimidine-5-carboxylate ((*rac*)-5aa)

Column chromatography on silica gel with 3:1 cyclohexane:EtOAc afforded **(*rac*)-5aa** (58 mg, 74%) as a pale yellow oil. See below for full characterization.

Methyl (*E*)-3-(4-Chlorobenzoyl)-1,6-dimethyl-2-oxo-4-phenyl-1,2,3,4-tetrahydropyrimidine-5-carboxylate ((*rac*)-6aa)

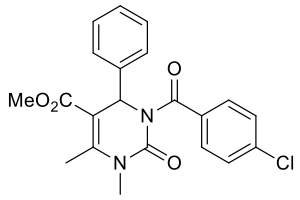

Column chromatography on silica gel with 3:1 cyclohexane:EtOAc afforded **(*rac*)-6aa** (8 mg, 10%) as a pale yellow oil. **^{1}H NMR** (300 MHz, $CDCl_3$) δ = 7.48 (d, *J* 8.4 Hz, 2H, COArH), 7.40–7.30 (m, 7H, COArH and ArH-4), 6.46 (s, 1H, H-4), 3.79 (s, 3H, CO_2CH_3), 3.15 (s, 3H, NCH_3-1), 2.63 (s, 3H, CH_3-6); **^{13}C NMR** (101 MHz, $CDCl_3$) δ = 170.2 (N*C*OAr), 165.7 (*C*O_2CH_3), 152.4 (-NCH_3*C*ONH-), 149.2 (*C*-6), 138.5 (Ar*C*), 137.7 (Ar*C*), 134.1 (Ar*C*), 129.2 (2C, Ar*C*H), 128.7 (2C, Ar*C*H), 128.5 (2C, Ar*C*H), 128.1 (Ar*C*H), 126.4 (2C, Ar*C*H), 109.6 (*C*-5), 53.4 (*C*H-4), 51.9 (O*C*H_3), 31.2 (N*C*H_3-1), 16.3 (*C*H_3-6); **HRMS**(ESI): calcd. for $C_{21}H_{20}ClN_2O_4^+$ ($[M + H]^+$): 399.1106; found: 399.1121.

General procedure for the synthesis of N3-Acylated DHPMs (5) and Thione (13)

A stirred mixture of **1** or **12** (0.40 mmol) and anhydrous THF (4.0 mL) was degassed under vacuum and saturated with argon (by an Ar-filled balloon) three times. Then the reaction mixture was cooled to 0 °C with an ice bath and *n*-BuLi (230 μL of a 2.0 M solution in *n*-hexane, 0.46 mmol) was added slowly. After 15 min at 0 °C, the ice bath was removed allowing the reaction to warm up till room temperature for another 15 min. Then, oxidant **8** (82 mg, 0.20 mmol), catalyst **C6** (22 mg, 0.04 mmol) and 4Å MS were added under an argon environment. Aldehyde **2** (0.2 mmol) was finally added, and the reaction was stirred for 16 h at room

temperature. The resulting solution was quenched with 0.5 M HCl (5 mL) and partially concentrated under vacuum to reduce the amount of THF. The crude of the reaction was extracted with DCM (3 × 15 mL), dried (anhydrous Na_2SO_4), and concentrated. Elution of the resulting residue from a column of silica with the suitable elution system afforded **5** or **13**.

Methyl (*R,E*)-3-Cinnamoyl-1,6-dimethyl-2-oxo-4-phenyl-1,2,3,4-tetrahydropyrimidine-5-carboxylate (5aa)

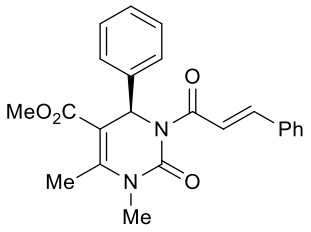

Column chromatography on silica gel with 3:1 cyclohexane:EtOAc afforded **5aa** (42 mg, 55%) as a pale yellow oil. $[\alpha]_D^{25}$ +49.7 (*c* 0.3 in CH_3OH); **Chiral HPLC analysis** Chiralpak IA (95:5 *n*-Hexane:IPA, flow rate 1.0 mLmin^{-1}, 254 nm, 25 °C) t_R (*S*): 26.0, t_R (*R*): 29.6 min, 17:83 *er*; **^{1}H NMR** (300 MHz, $CDCl_3$) δ = 7.84 (d, *J* 15.6 Hz, 1H, C=CH), 7.62 – 7.54 (m, 2H, *ArH*CH=C), 7.48 – 7.35 (m, 4H, *ArH*CH=C and C=CH), 7.32 – 7.26 (m, 5H, ArH-4), 6.76 (s, 1H, H-4), 3.77 (s, 3H, CO_2CH_3), 3.22 (s, 3H, NCH_3-1), 2.59 (s, 3H, CH_3-6); **^{13}C NMR** (101 MHz, $CDCl_3$) δ = 167.1 (N*C*O-3), 165.8 (*C*O_2CH_3), 149.3 (-NCH_3*C*ONH-), 144.6 (PhCH=*C*H), 142.8 (*C*-6), 138.9 (Ar*C*), 134.9 (Ar*C*), 130.1 (Ar*C*H), 128.8 (2C, Ar*C*H), 128.6 (2C, Ar*C*H), 128.3 (2C, Ar*C*H), 127.9 (Ar*C*H), 126.3 (2C, Ar*C*H), 120.2 (Ph*C*H=CH), 109.1 (*C*-5), 51.8 (O*C*H_3), 51.4 (*C*H-4), 31.3 (N*C*H_3-1), 16.2 (*C*H_3-6); **HRMS**(ESI): calcd. for $C_{23}H_{23}N_2O_4^+$ ([M + H]$^+$): 391.1652; found: 391.1638.

Methyl (*R,E*)-4-(3-Bromophenyl)-3-cinnamoyl-1,6-dimethyl-2-oxo-1,2,3,4-tetrahydropyrimidine-5-carboxylate (5ba)

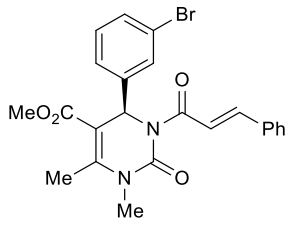

Column chromatography on silica gel with 3.5:1 cyclohexane:EtOAc afforded **5ba** (63 mg, 68%) as a pale yellow oil. $[\alpha]_D^{25}$ +35.6 (*c* 0.5 in CH_3OH); **Chiral HPLC analysis** Chiralpak IA (95:5 *n*-Hexane:IPA, flow rate 1.0 mLmin^{-1}, 254 nm, 25 °C) t_R(*S*): 22.6, t_R(*R*): 25.8 min, 28:72 *er*; **^{1}H NMR** (300 MHz, $CDCl_3$) δ = 7.84 (d, *J* 15.6 Hz, 1H, C=CH), 7.63 – 7.53 (m, 2H, *ArH*CH=C), 7.49 – 7.27 (m, 6H, *ArH*CH=C, Ar-4 and C=CH), 7.25 – 7.07 (m, 2H, ArH-4),

6.72 (s, 1H, H-4), 3.77 (s, 3H, CO_2CH_3), 3.22 (s, 3H, NCH_3-1), 2.60 (s, 3H, CH_3-6); **^{13}C NMR** (101 MHz, $CDCl_3$) δ = 167.0 (N*C*O-3), 165.5 (*C*O_2CH_3), 152.3 (-NCH_3*C*ONH-), 149.8 (*C*-6), 145.0 (PhCH=*C*H), 141.2 (Ar*C*), 134.8 (Ar*C*), 131.1 (Ar*C*H), 130.2 (2C, Ar*C*H), 129.6 (Ar*C*H), 128.8 (2C, Ar*C*H), 128.4 (2C, Ar*C*H), 125.1 (Ar*C*H), 122.8 (Ar*C*), 119.9 (Ph*C*H=CH), 108.3 (*C*-5), 51.9 (O*C*H_3), 51.0 (*C*H-4), 31.4 (N*C*H_3-1), 16.2 (*C*H_3-6); **HRMS**(ESI): calcd. for $C_{23}H_{22}BrN_2O_4^+$ ([M + H]$^+$): 469.0757; found: 469.0774.

Methyl (*R,E*)-4-(4-Chlorophenyl)-3-cinnamoyl-1,6-dimethyl-2-oxo-1,2,3,4-tetrahydropyrimidine-5-carboxylate (5ca)

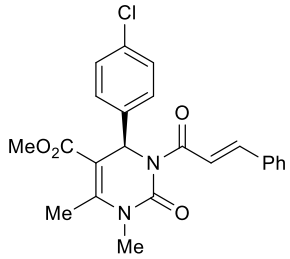

Column chromatography on silica gel with 3:1 cyclohexane:EtOAc afforded **5ca** (61 mg, 72%) as a pale yellow oil. $[\alpha]_D^{25}$ +10.3 (*c* 0.3 in CH_3OH); **Chiral HPLC analysis** Chiralpak IA (80:20 *n*-Hexane:IPA, flow rate 1.0 mLmin^{-1}, 254 nm, 25 °C) t_R(*R*): 12.3, t_R(*S*): 13.8 min, 73:27 *er*; **^{1}H NMR** (300 MHz, $CDCl_3$) δ = 7.84 (d, *J* 15.6 Hz, 1H, C=CH), 7.62 – 7.52 (m, 2H, *ArH*CH=C), 7.45 – 7.34 (m, 4H, *ArH*CH=C and C=CH), 7.30 – 7.26 (m, 1H, ArH-4), 7.25 – 7.18 (m, 3H, ArH-4), 6.69 (s, 1H, H-4), 3.76 (s, 3H, CO_2CH_3), 3.22 (s, 3H, NCH_3-1), 2.59 (s, 3H, CH_3-6); **^{13}C NMR** (101 MHz, $CDCl_3$) δ = 167.2 (N*C*O-3), 165.7 (*C*O_2CH_3), 152.4 (-NCH_3*C*ONH-), 149.7 (*C*-6), 145.0 (PhCH=*C*H), 137.5 (Ar*C*), 134.9 (Ar*C*), 133.9 (Ar*C*), 130.3 (Ar*C*H), 128.9 (4C, Ar*C*H), 128.5 (2C, Ar*C*H), 128.0 (2C, Ar*C*H), 120.1 (Ph*C*H=CH), 108.7 (*C*-5), 52.0 (O*C*H_3), 51.1 (*C*H-4), 31.4 (N*C*H_3-1), 16.3 (*C*H_3-6); **HRMS**(ESI): calcd. for $C_{23}H_{22}ClN_2O_4^+$ ([M + H]$^+$): 425.1263; found: 425.1244.

Methyl (*S,E*)-4-(2-Chlorophenyl)-3-cinnamoyl-1,6-dimethyl-2-oxo-1,2,3,4-tetrahydropyrimidine-5-carboxylate (5da)

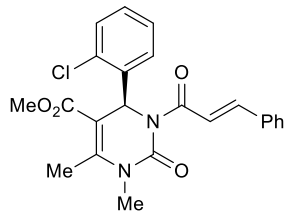

Column chromatography on silica gel with 3:1 cyclohexane:EtOAc afforded **5da** (34 mg, 41%) as a pale yellow oil. $[\alpha]_D^{25}$ +12.5 (*c* 0.4 in CH_3OH); **Chiral HPLC analysis** Chiralpak IA (85:15

n-Hexane:IPA, flow rate 1.0 mLmin^{-1}, 254 nm, 25 °C) t_R(*R*): 13.2, t_R(*S*): 17.2 min, 19:81 *er*; **^{1}H NMR** (300 MHz, $CDCl_3$) δ = 7.78 (d, *J* 15.6 Hz, 1H, C=CH), 7.59 – 7.51 (m, 2H, *ArH*CH=C), 7.45 (d, *J* 15.6 Hz, 1H, C=CH), 7.40 – 7.31 (m, 4H, *ArH*CH=C and Ar-4), 7.23 – 7.14 (m, 3H, ArH-4), 6.89 (s, 1H, H-4), 3.74 (s, 3H, CO_2CH_3), 3.33 (s, 3H, NCH_3-1), 2.52 (s, 3H, CH_3-6); **^{13}C NMR** (75 MHz, $CDCl_3$) δ = 167.2 (N*C*O-3), 166.0 (*C*O_2CH_3), 152.9 (-NCH_3*C*ONH-), 147.9 (*C*-6), 145.0 (PhCH=*C*H), 137.6 (Ar*C*), 135.3 (Ar*C*), 133.8 (Ar*C*), 131.0 (Ar*C*H), 130.4 (Ar*C*H), 129.6 (Ar*C*H), 129.1 (2C, Ar*C*H), 128.7 (2C, Ar*C*H), 128.5 (Ar*C*H), 127.5 (Ar*C*H), 120.6 (Ph*C*H=CH), 109.3 (*C*-5), 52.0 (O*C*H_3), 51.5 (*C*H-4), 31.6 (N*C*H_3-1), 16.6 (*C*H_3-6); **HRMS**(ESI): calcd. for $C_{23}H_{22}ClN_2O_4^+$ ([M + H]$^+$): 425.1263; found: 425.1246.

Methyl (*R,E*)-3-Cinnamoyl-4-(4-methoxyphenyl)-1,6-dimethyl-2-oxo-1,2,3,4-tetrahydropyrimidine-5-carboxylate (5ea)

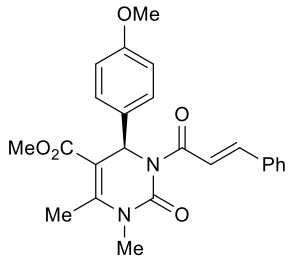

Column chromatography on silica gel with 2.5:1 cyclohexane:EtOAc afforded **5ea** (42 mg, 50%) as a pale yellow oil. $[\alpha]_D^{25}$ +67.5 (*c* 0.2 in CH_3OH); **Chiral HPLC analysis** Chiralpak IA (90:10 *n*-Hexane:IPA, flow rate 1.0 mLmin^{-1}, 254 nm, 25 °C) t_R(*S*): 23.5, t_R(*R*): 28.2 min, 16:84 *er*; **^{1}H NMR** (300 MHz, $CDCl_3$) δ = 7.83 (d, *J* 15.6 Hz, 1H, C=CH), 7.64 – 7.52 (m, 3H, *ArH*CH=C), 7.44 – 7.36 (m, 3H, *ArH*CH=C and C=CH), 7.20 (d, *J* 8.6 Hz, 2H, ArH-4), 6.82 (d, *J* 8.6 Hz, 2H, ArH-4), 6.70 (s, 1H, H-4), 3.77 (s, 3H, CO_2CH_3), 3.75 (s, 3H, ArO*C*H_3), 3.23 (s, 3H, NCH_3-1), 2.59 (s, 3H, CH_3-6); **^{13}C NMR** (101 MHz, $CDCl_3$) δ = 167.1 (N*C*O-3), 165.8 (*C*O_2CH_3), 159.2 (Ar*C*), 144.8 (-NCH_3*C*ONH-), 144.5 (*C*-6), 134.9 (PhCH=*C*H), 132.8 (Ar*C*), 130.8 (Ar*C*), 130.1 (Ar*C*H), 128.9 (Ar*C*H), 128.7 (Ar*C*H), 128.6 (Ar*C*H), 128.5 (Ar*C*H), 128.4 (Ar*C*H), 128.3 (Ar*C*H), 127.8 (Ar*C*H), 122.1 (Ar*C*H), 120.3 (Ph*C*H=CH), 114.0 (*C*-5), 55.2 (ArO*C*H_3), 51.8 (O*C*H_3), 51.1 (*C*H-4), 31.3 (N*C*H_3-1), 16.1 (*C*H_3-6); **HRMS**(ESI): calcd. for $C_{24}H_{25}N_2O_5^+$ ([M + H]$^+$): 421.1758; found: 421.1739.

Methyl (*S,E*)-3-Cinnamoyl-4-(furan-2-yl)-1,6-dimethyl-2-oxo-1,2,3,4-tetrahydropyrimidine-5-carboxylate (5fa)

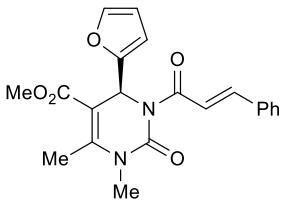

Column chromatography on silica gel with 4:1 cyclohexane:EtOAc afforded **5fa** (39 mg, 52%) as a pale yellow oil. $[\alpha]_D^{25}$ +12.5 (*c* 0.2 in CH_3OH); **Chiral HPLC analysis** Chiralpak IA (90:10 *n*-Hexane:IPA, flow rate 1.0 mLmin^{-1}, 254 nm, 25 °C) t_R(*S*): 19.1, t_R(*R*): 22.6 min, 62:38 *er*; **^{1}H NMR** (300 MHz, $CDCl_3$) δ = 7.82 (d, *J* 15.6 Hz, 1H, C=CH), 7.60 – 7.53 (m, 2H, *ArH*CH=C), 7.45 – 7.33 (m, 4H, *ArH*CH=C and C=CH), 7.32 – 7.27 (m, 1H, ArH-4), 6.74 (s, 1H, H-4), 6.29 – 6.24 (m, 1H, ArH-4), 6.20 (d, *J* 3.3 Hz, 1H, ArH-4), 3.76 (s, 3H, CO_2CH_3), 3.29 (s, 3H, NCH_3-1), 2.58 (s, 3H, CH_3-6); **^{13}C NMR** (101 MHz, $CDCl_3$) δ = 166.9 (N*C*O-3), 165.5 (*C*O_2CH_3), 152.5 (-NCH$_3$*C*ONH-), 151.7 (Ar*C*), 150.2 (*C*-6), 144.9 (PhCH=*C*H), 142.9 (Ar*C*), 135.2 (Ar*C*H), 130.4 (Ar*C*H), 129.0 (2C, Ar*C*H), 128.6 (2C, Ar*C*H), 120.5 (PhCH=*C*H), 110.4 (Ar*C*H), 107.6 (Ar*C*H), 106.7 (*C*-5), 52.0 (O*C*H$_3$), 46.9 (*C*H-4), 31.6 (N*C*H$_3$-1), 16.4 (*C*H$_3$-6); **HRMS**(ESI): calcd. for $C_{21}H_{21}N_2O_5^+$ ([M +H]$^+$): 381.1445; found: 381.1429.

Ethyl (*R,E*)-3-Cinnamoyl-1,6-dimethyl-2-oxo-4-phenyl-1,2,3,4-tetrahydropyrimidine-5-carboxylate (5ga)

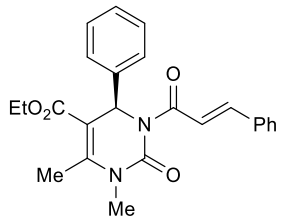

Column chromatography on silica gel with 3:1 cyclohexane:EtOAc afforded **5ga** (46 mg, 57%) as a pale yellow oil. $[\alpha]_D^{25}$ +33.9 (*c* 0.13 in CH_3OH); **Chiral HPLC analysis** Chiralpak IA (90:10 *n*-Hexane:IPA, flow rate 1.0 mLmin^{-1}, 254 nm, 25 °C) t_R(*S*): 13.6, t_R(*R*): 15.9 min, 23:77 *er*; **^{1}H NMR** (300 MHz, $CDCl_3$) δ = 7.83 (d, *J* 15.6 Hz, 1H, C=CH), 7.62 – 7.55 (m, 2H, *ArH*CH=C), 7.48 – 7.32 (m, 4H, *ArH*CH=C and C=CH), 7.30 – 7.26 (m, 5H, ArH-4), 6.74 (s, 1H, H-4), 4.35 – 4.14 (m, 2H, $CO_2CH_2CH_3$), 3.22 (s, 3H, NCH_3-1), 2.58 (s, 3H, CH_3-6), 1.29 (t, *J* 7.1 Hz, 3H, $CO_2CH_2CH_3$);**^{13}C NMR** (101 MHz, $CDCl_3$) δ = 167.3 (N*C*O-3), 165.4 (*C*O_2CH_3), 150.0 (-NCH$_3$*C*ONH-), 144.7 (PhCH=*C*H), 139.1 (*C*-6), 135.0 (Ar*C*), 130.2 (2C, Ar*C*H), 128.9 (2C, Ar*C*H), 128.7 (Ar*C*H), 128.6 (Ar*C*H), 128.4 (2C, Ar*C*H), 127.9 (Ar*C*H), 126.4 (2C, Ar*C*H), 120.4 (PhCH=*C*H), 109.7 (*C*-5), 60.9 ($CO_2CH_2CH_3$), 51.8 (*C*H-4), 31.4

(N*C*H$_3$-1), 16.3 (*C*H$_3$-6), 14.3 (CO$_2$CH$_2$*C*H$_3$); **HRMS**(ESI): calcd. for $C_{24}H_{25}N_2O_4^+$ ([M + H]$^+$): 405.1809; found: 405.1827.

Methyl (*R,E*)-3-Cinnamoyl-6-methyl-2-oxo-1,4-diphenyl-1,2,3,4-tetrahydropyrimidine-5-carboxylate (5ha)

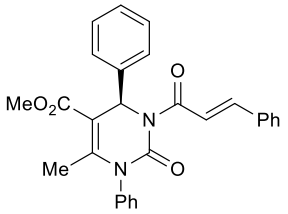

Column chromatography on silica gel with 5:1 cyclohexane:EtOAc afforded **5ha** (52 mg, 58%) as a pale yellow oil. $[\alpha]_D^{25}$ –8.2 (*c* 0.6 in CH$_3$OH); **Chiral HPLC analysis** Chiralpak IA (90:10 *n*-Hexane:IPA, flow rate 1.0 mLmin^{-1}, 254 nm, 25 °C) t_R(*R*): 11.4, t_R(*S*): 15.9 min, 57:43 *er*; **^{1}H NMR** (300 MHz, CDCl$_3$) δ = 7.88 (d, *J* 15.6 Hz, 1H, C=CH), 7.62 – 7.55 (m, 2H, *Ar*CH=C), 7.51 (d, *J* 15.6 Hz, 1H, C=CH), 7.48 – 7.26 (m, 12H, NAr-1 and Ar-4), 7.07 (bs, 1H, NAr-1), 6.90 (s, 1H, H-4), 3.81 (s, 3H, CO$_2$CH$_3$), 2.19 (s, 3H, CH$_3$-6); **^{13}C NMR** (101 MHz, CDCl$_3$) δ = 167.2 (N*C*O-3), 165.8 (*C*O$_2$CH$_3$), 151.9 (-NPh*C*ONH-), 149.5 (*C*-6), 145.0 (PhCH=*C*H), 139.4 (Ar*C*), 136.9 (Ar*C*), 134.9 (Ar*C*), 130.2 (Ar*C*H), 129.4 (2C, Ar*C*H), 129.2 (Ar*C*H), 128.9 (4C, Ar*C*H), 128.7 (2C, Ar*C*H), 128.4 (2C, Ar*C*H), 128.0 (Ar*C*H), 126.4 (2C, Ar*C*H), 120.1 (PhCH=*C*H), 109.7 (*C*-5), 51.9 (O*C*H$_3$), 51.8 (*C*H-4), 17.9 (*C*H$_3$-6); **HRMS**(ESI): calcd. for $C_{28}H_{25}N_2O_4^+$ ([M + H]$^+$): 453.1809; found: 453.1789.

Methyl (*R,E*)-1-Benzyl-3-cinnamoyl-6-methyl-2-oxo-4-phenyl-1,2,3,4-tetrahydropyrimidine-5-carboxylate (5ia)

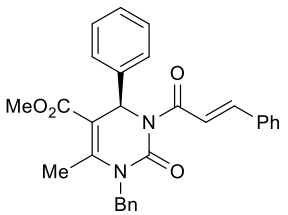

Column chromatography on silica gel with 6:1 cyclohexane:EtOAc afforded **5ia** (57 mg, 62%) as a pale yellow oil. $[\alpha]_D^{25}$ +22.5 (*c* 0.6 in CH$_3$OH); **Chiral HPLC analysis** Chiralpak IA (90:10 *n*-Hexane:IPA, flow rate 1.0 mLmin^{-1}, 254 nm, 25 °C) t_R(*S*): 17.3, t_R(*R*): 19.4 min, 22:77 *er*; **^{1}H NMR** (300 MHz, CDCl$_3$) δ = 7.89 (d, *J* 15.5 Hz, 1H, C=CH), 7.63–7.56 (m, 2H, *ArH*CH=C), 7.44 (d, *J* 15.6 Hz, 1H, C=CH), 7.40–7.34 (m, 3H, *ArH*CH=C), 7.29–7.08 (m, 8H, ArH-4 and NCH$_2$*ArH*-1), 6.80 (s, 1H, H-4), 6.71 (d, *J* 7.3 Hz, 2H, NCH$_2$*ArH*-1), 5.43 (d, *J* 16.5 Hz, 1H, N*C*H$_2$Ar-1), 4.61 (d, *J* 16.4 Hz, 1H, N*C*H$_2$Ar-1), 3.77 (s, 3H, CO$_2$CH$_3$), 2.50 (s, 3H, CH$_3$-6);

^{13}C NMR (101 MHz, $CDCl_3$) δ = 167.3 (N*C*O-3), 166.0 (*C*O_2CH_3), 149.3 (-NAr*C*ONH-), 144.9 (PhCH=*C*H), 139.0 (*C*-6), 136.4 (Ar*C*), 135.0 (2C, Ar*C*), 130.3 (Ar*C*H), 128.9 (2C, Ar*C*H), 128.8 (2C, Ar*C*H), 128.7 (2C, Ar*C*H), 128.5 (2C, Ar*C*H), 127.9 (Ar*C*H), 127.5 (Ar*C*H), 126.8 (2C, Ar*C*H), 126.5 (2C, Ar*C*H), 120.2 (PhCH=*C*H), 107.6 (*C*-5), 52.0 (*C*H-4), 51.4 (O*C*H_3), 46.7 (*C*H_2Ph), 16.3 (*C*H_3-6); **HRMS**(ESI): calcd. for $C_{29}H_{27}N_2O_4^+$ ([M + H]$^+$): 467.1965; found: 467.1946.

Methyl (*R*,*E*)-1-Benzyl-3-cinnamoyl-6-methyl-2-oxo-4-propyl-1,2,3,4-tetrahydropyrimidine-5-carboxylate (5ja)

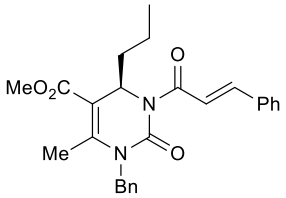

Column chromatography on silica gel with 6:1 cyclohexane:EtOAc afforded **5ja** (50 mg, 58%) as a pale yellow oil. $[\alpha]_D^{25}$+5.5 (*c* 0.2 in CH_3OH); **Chiral HPLC analysis** Chiralpak IA (90:10 *n*-Hexane:IPA, flow rate 1.0 mLmin^{-1}, 254 nm, 25 °C) t_R(*S*): 14.1, t_R(*R*): 17.8 min, 29:71 *er*; **^{1}H NMR** (300 MHz, $CDCl_3$) δ = 7.78 (d, *J* 15.6 Hz, 1H, C=CH), 7.58 – 7.51 (m, 2H, *ArH*C=CH), 7.40 – 7.27 (m, 9H, *ArH*C=CH, NCH_2*ArH*-1 and C=CH), 5.59 (t, *J* 7.0 Hz, 1H, H-4), 5.30 (d, *J* 16.3 Hz, 1H, N*C*H_2Ar-1), 4.85 (d, *J* 16.0 Hz, 1H, N*C*H_2Ar-1), 3.75 (s, 3H, CO_2CH_3), 2.47 (s, 3H, CH_3-6), 1.45–1.36 (m, 4H, *C*H_2*C*$H_2$$CH_3$), 0.84 (t, *J* 7.2 Hz, 3H, CH_2CH_2*C*H_3); **^{13}C NMR** (101 MHz, $CDCl_3$) δ = 167.0 (N*C*O-3), 165.9 (*C*O_2CH_3), 152.9 (-NAr*C*ONH-), 147.4 (*C*-6), 144.1 (PhCH=*C*H), 136.8 (Ar*C*), 135.0 (Ar*C*), 130.0 (Ar*C*H), 128.8 (2C, Ar*C*H), 128.7 (2C, Ar*C*H), 128.3 (2C, Ar*C*H), 127.7 (Ar*C*H), 127.1 (2C, Ar*C*H), 120.3 PhCH=*C*H), 111.1 (*C*-5), 51.6 (O*C*H_3), 49.3 (*C*H-4), 46.9 (*C*H_2Ph), 36.1 (*C*$H_2CH_2CH_3$), 18.4 (CH_2*C*H_2CH_3), 16.2 (*C*H_3-6), 13.9 (CH_2*C*H_3); **HRMS**(ESI): calcd. for $C_{26}H_{29}N_2O_4^+$ ([M +H]$^+$): 433.2122; found: 433.2139.

Methyl (*R*,*E*)-3-(3-(4-Methoxyphenyl)acryloyl)-1,6-dimethyl-2-oxo-4-phenyl-1,2,3,4-tetrahydropyrimidine-5-carboxylate (5ab)

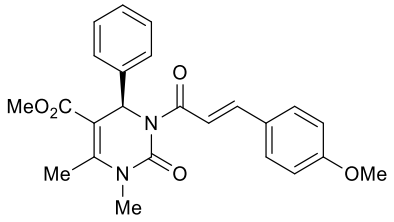

Column chromatography on silica gel with 3:1 cyclohexane:EtOAc afforded **5ab** (50 mg, 60%) as a pale yellow oil. $[\alpha]_D^{25}$ +10.1 (*c* 0.2 in CH_3OH); **Chiral HPLC analysis** Chiralpak IA (90:10 *n*-Hexane:IPA, flow rate 1.0 mLmin^{-1}, 254 nm, 25 °C) t_R(*R*): 31.3, t_R(*S*): 33.1 min, 53:47 *er*; **^{1}H NMR** (300 MHz, $CDCl_3$) δ = 7.82 (d, *J* 15.6 Hz, 1H, C= CH), 7.53 (d, *J* 8.7 Hz, 2H, *ArH*CH=C), 7.37 – 7.26 (m, 6H, C=CH and ArH-4), 6.89 (d, *J* 8.8 Hz, 2H, *ArH*CH=C), 6.77 (s, 1H, H-4), 3.84 (s, 3H, CO_2CH_3), 3.77 (s, 3H, ArO*C*H$_3$), 3.21 (s, 3H, NCH_3-1), 2.58 (s, 3H, CH_3-6); **^{13}C NMR** (101 MHz, $CDCl_3$) δ = 167.2 (N*C*O-3), 165.8 (*C*O_2CH_3), 161.3 (Ar*C*), 149.4 (-NCH$_3$*C*ONH-), 144.6 (PhCH=*C*H), 139.0 (*C*-6), 130.1 (2C, Ar*C*H), 128.6 (2C, Ar*C*H), 127.8 (Ar*C*H), 127.7 (2C, Ar*C*), 126.3 (2C, Ar*C*H), 117.7 (PhCH=*C*H), 114.2 (2C, Ar*C*H), 109.0 (*C*-5), 55.3 (PhOCH_3), 51.8 (O*C*H$_3$), 51.3 (*C*H-4), 31.3 (N*C*H$_3$-1), 16.1 (*C*H$_3$-6); **HRMS**(ESI): calcd. for $C_{24}H_{25}N_2O_5^+$ ([M + H]$^+$): 421.1758; found: 421.1741.

Methyl (*R*,*E*)-3-(3-(4-Chlorophenyl)acryloyl)-1,6-dimethyl-2-oxo-4-phenyl-1,2,3,4-tetrahydropyrimidine-5-carboxylate (5ac)

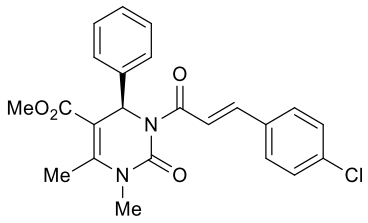

Column chromatography on silica gel with 4:1 cyclohexane:EtOAc afforded **5ac** (46 mg, 55%) as a yellowish oil. $[\alpha]_D^{25}$ +24.2 (*c* 0.2 in CH_3OH); **Chiral HPLC analysis** Chiralpak IA (90:10 *n*-Hexane:IPA, flow rate 1.0 mLmin^{-1}, 254 nm, 25 °C) t_R(*S*): 22.9, t_R(*R*): 24.9 min, 37:63 *er*; **^{1}H NMR** (300 MHz, $CDCl_3$) δ = 7.77 (d, *J* 15.6 Hz, 1H, C=CH), 7.50 (d, *J* 8.5 Hz, 2H, *ArH*CH=C), 7.44 – 7.26 (m, 7H, C=CH, *ArH*CH=C and ArH- 4), 7.25 – 7.18 (m, 1H, ArH-4), 6.75 (s, 1H, H-4), 3.77 (s, 3H, CO_2CH_3), 3.21 (s, 3H, NCH_3-1), 2.58 (s, 3H, CH_3-6); **^{13}C NMR** (101 MHz, $CDCl_3$) δ = 166.9 (N*C*O-3), 165.8 (*C*O_2CH_3), 152.7 (-NCH$_3$*C*ONH-), 149.4 (*C*-6), 143.1 (PhCH=*C*H), 138.86 (Ar*C*), 136.1 (Ar*C*), 133.5 (Ar*C*), 129.6 (2C, Ar*C*H), 129.1 (2C, Ar*C*H), 128.7 (2C, Ar*C*H), 128.0 (Ar*C*H), 126.4 (2C, Ar*C*H), 120.9 (PhCH=*C*H), 109.2 (*C*-5), 51.9 (*C*H-4), 51.6 (O*C*H$_3$), 31.4 (N*C*H$_3$-1), 16.3 (*C*H$_3$-6); **HRMS**(ESI): calcd. for $C_{23}H_{22}ClN_2O_4^+$ ([M + H]$^+$): 425.1263; found: 425.1246.

Methyl (*R*)-3-Cinnamoyl-1,6-dimethyl-4-phenyl-2-thioxo-1,2,3,4-tetrahydropyrimidine-5-carboxylate (13)

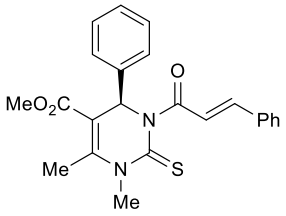

Column chromatography on silica gel with 5:1 cyclohexane:EtOAc afforded **13** (64 mg, 79%) as a pale yellow oil. $[\alpha]_D^{25}$ +12.2 (*c* 0.6 in CH_3OH); **Chiral HPLC analysis** Chiralpak IA (95:5 *n*-Hexane:IPA, flow rate 1.0 mLmin^{-1}, 254 nm, 25 °C) t_R(*R*): 17.8, t_R(*S*): 18.7 min, 58:42 *er*; **^{1}H NMR** (300 MHz, $CDCl_3$) δ = 7.70 (d, *J* 15.5 Hz, 1H, C=CH), 7.57 – 7.49 (m, 2H, *ArH*CH=C), 7.44 – 7.35 (m, 4H, *ArH*CH=C and C=CH), 7.33 – 7.26 (m, 5H, ArH-4), 6.64 (s, 1H, H-4), 3.79 (s, 3H, CO_2CH_3), 3.50 (s, 3H, NCH_3-1), 2.62 (s, 3H, CH_3-6); **^{13}C NMR** (101 MHz, $CDCl_3$) δ = 178.8 (-NAr*C*SNH-), 169.1 (N*C*O-3), 165.5 (*C*O_2CH_3), 147.8 (*C*-6), 141.3 (PhCH=*C*H), 137.9 (Ar*C*), 135.2 (Ar*C*), 130.0 (Ar*C*H), 128.9 (2C, Ar*C*H), 128.6 (2C, Ar*C*H), 128.4 (2C, Ar*C*H), 128.1 (Ar*C*H), 126.4 (2C, Ar*C*H), 121.8 (PhCH=*C*H), 113.8 (*C*-5), 52.8 (*C*H-4), 52.2 (O*C*H_3), 37.8 (N*C*H_3-1), 16.9 (*C*H_3-6); **HRMS**(ESI): calcd. for $C_{23}H_{23}N_2O_3S^+$ ([M + H]$^+$): 407.1424; found: 407.1409.

Methyl (*R*)-3-(3,3-Diphenylpropanoyl)-1,6-dimethyl-2-oxo-4-phenyl-1,2,3,4-tetrahydropyrimidine-5-carboxylate (14)

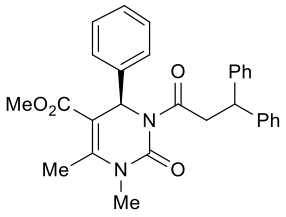

A mixture of DHPM **5aa** (39 mg, 0.1 mmol), TfOH (50 µL, 0.56 mmol), benzene (22 µL, 0.24 mmol) and DCM (0.5 mL) was stirred at room temperature for 2 h. The mixture was poured into ice water (3 mL) and extracted with DCM (3 x 10 mL). The combined extracts were washed with water (5 mL), saturated aqueous solution of $NaHCO_3$ (5 mL), water again (5 mL), dried (anhydrous Na_2SO_4), concentrated, and eluted from a column of silica gel with 3:1 cyclohexane:EtOAc to afford **14** as a white amorphous solid (25 mg, 55%). $[\alpha]_D^{25}$ +45.2 (*c* 0.2 in CH_3OH); **Chiral HPLC analysis** Chiralpak IA (80:20 *n*-Hexane:IPA, flow rate 1.0 mLmin^{-1}, 254 nm, 25 °C) t_R(*S*): 15.9, t_R(*R*): 17.2 min, 20:80 *er*; **^{1}H NMR** (300 MHz, $CDCl_3$) δ = 7.31 – 7.26 (m, 5H, ArH), 7.23 – 7.21 (m, 5H, ArH), 7.18 – 7.03 (m, 5H, ArH), 6.55 (s, 1H, H-4), 4.64 (t, *J* 7.8 Hz, 1H, Ar_2CH-), 3.76 (d, *J* 8.4 Hz, 2H, Ar_2CHCH_2-), 3.70 (s, 3H, CO_2CH_3),

3.12 (s, 3H, NCH_3-1), 2.49 (s, 3H, CH_3-6); **^{13}C NMR** (101 MHz, $CDCl_3$) δ = 173.1 (N*C*O-3), 165.6 (*C*O_2CH_3), 152.4 (-NCH_3*C*ONH-), 149.0 (*C*-6), 143.8 (Ar*C*), 143.6 (Ar*C*), 138.7 (Ar*C*), 128.5 (2C, Ar*C*H), 128.4 (2C, Ar*C*H), 128.3 (2C, Ar*C*H), 127.9 (2C, Ar*C*H), 127.8 (2C, Ar*C*H), 127.7 (2C, Ar*C*H), 126.4 (Ar*C*H), 126.3 (Ar*C*H), 126.2 (Ar*C*H), 108.6 (*C*-5), 51.7 (O*C*H_3), 50.8 (*C*H-4), 47.7 (Ar_2CH*C*H_2-), 43.0 (Ar_2*C*H-), 31.2 (N*C*H_3-1), 16.1 (*C*H_3-6); **HRMS**(ESI): calcd. for $C_{29}H_{29}N_2O_4^+$ ([M + H]$^+$): 469.2122; found: 469.2102.

Recycle of Oxidant 8

The alcohol resulting from oxidant **8** reduction (3,3′,5,5′-tetra-*tert*-butyl-[1,1′-biphenyl]-4,4′-diol) was recovered by column chromatography after each run of Table 3. The subsequent oxidation to **8** was performed stirring the 3,3′,5,5′-tetra-*tert*butyl-[1,1′-biphenyl]-4,4′-diol (578 mg, 1.41 mmol) with **11** (80 mg, 0.14 mmol) in THF (10 mL) under air atmosphere (1 atm, balloon) for 16 h. Filtration over a pad of Celite and subsequent concentration under reduced pressure afforded **8** as a dark red amorphous solid (572 mg, 88%).[13,14]

Procedure for the synthesis of N3-acylated DHPM 5aa with ETMs system

A stirred mixture of **1aa** (104 mg, 0.40 mmol) and anhydrous THF (4.0 mL) was degassed under vacuum and saturated with argon (by an Ar-filled balloon) three times. Then the reaction mixture was cooled at 0 °C with an ice bath and *n*-BuLi (230 μL of a 2.0 M solution in *n*-hexane, 0.46 mmol) was added slowly. After 15 min at 0 °C, the ice bath was removed allowing the reaction to warm up till room temperature for another 15 min. Then, oxidant **8** (20 mg, 0.05 mmol), iron(II) phthalocyanine **11** (11 mg, 0.02 mmol), catalyst **C6** (22 mg, 0.04 mmol) and 4Å MS were added under an argon environment. Aldehyde **2a** (25 μL, 0.20 mmol) was finally added and the reaction was stirred for 16 h at room temperature. The resulting solution was quenched with 0.5 M HCl (5.0 mL) and partially concentrated under vacuum to reduce the amount of THF. The crude of the reaction was extracted with DCM (3 x 15 mL), dried (anhydrous Na_2SO_4), and concentrated. Elution of the resulting crude mixture from a column of silica gel with 3:1 cyclohexane:EtOAc afforded **5aa** as a pale yellow oil (31 mg, 20%). **Chiral HPLC analysis** Chiralpak IA (95:5 *n*-Hexane:IPA, flow rate 1.0 mLmin^{-1}, 254 nm, 25 °C) t_R(*S*): 26.0, t_R(*R*): 29.6 min, 22:78 *er*.

Racemization test of N3-acylated DHPM 5aa

N-3 acylated DHPM **5aa** (76 mg, 0.2 mmol, 1.0 equiv.) and *n*-BuLi (1.0 mmol, 5.0 equiv.) were dissolved in anhydrous THF (2.0 mL, 0.1 M) in presence of 4Å MS and the mixture was degassed under vacuum and saturated with argon (by an Ar-filled balloon) three times. The

reaction solution was stirred for 16 h at room temperature after which time the resulting solution was cooled down to 0 °C and quenched with HCl 0.5 M (5.0 mL). Reaction product was extracted with DCM (5.0 x 10 mL), dried over Na_2SO_4 and concentrated under reduced pressure. The product **5aa** was re-isolated *via* column chromatography on silica gel with 3:1 cyclohexane:EtOAc (68 mg, 90%). **Chiral HPLC analysis** Chiralpak IA (95:5 *n*-Hexane:IPA, flow rate 1.0 $mLmin^{-1}$, 254 nm, 25 °C) t_R(*S*): 26.0, t_R(*R*): 29.6 min, 17:83 *er.* Original sample: 83:17 *er*; re-isolated sample: 83:17 *er*.

Procedure for the synthesis of N3-acylated DHPM 5aa with NHC/hydroxamic acid co-catalysis approach

A stirred mixture of **1aa** (52 mg, 0.2 mmol) and anhydrous THF (2.0 mL) was degassed under vacuum and saturated with argon (by an Ar-filled balloon) three times. Then the reaction mixture was cooled at 0 °C with an ice bath and *n*-BuLi (125 μL of a 2.0 M solution in *n*-hexane, 0.25 mmol) was added slowly. After 15 min at 0 °C, the ice bath was removed allowing the reaction to warm up till room temperature for another 15 min. Then, oxidant **8** (82 mg, 0.2 mmol), catalyst **C1** (6 mg, 0.02 mmol), hydroxamic acid co-catalyst **A** (6 mg, 0.02 mmol) and 4Å MS were added under an argon environment. Aldehyde **2a** (25 μL, 0.2 mmol) was finally added and the reaction was stirred for 16 h at room temperature. The resulting solution was quenched with 0.5 M HCl (3.0 mL) and partially concentrated under vacuum to reduce the amount of THF. The crude of the reaction was extracted with DCM (3 x 15 mL), dried (anhydrous Na_2SO_4), and concentrated. The product **5aa** was isolated *via* column chromatography on silica gel with 3:1 cyclohexane:EtOAc (53 mg, 69%). **Chiral HPLC analysis** Chiralpak IA (95:5 *n*-Hexane:IPA, flow rate 1.0 $mLmin^{-1}$, 254 nm, 25 °C) t_R(*S*): 26.0, t_R(*R*): 29.6 min, 47:53 *er*.

Procedure for the assignment of the absolute configuration of DHPMs

A stirred mixture of **1g** (55 mg, 0.20 mmol) and anhydrous THF (2.0 mL) was degassed under vacuum and saturated with argon (by an Ar-filled balloon) three times. Then the reaction mixture was cooled at 0 °C with an ice bath and *n*-BuLi (125 μL of a 2.0 M solution in *n*-hexane, 0.25 mmol) was added slowly. After 15 min at 0 °C, the ice bath was removed allowing the reaction to warm up till room temperature for another 15 min. Then, oxidant **8** (82 mg, 0.20 mmol), catalyst **C6** (22 mg, 0.04 mmol) and 4Å MS were added under an argon environment. Aldehyde **2a** (25 μL, 0.20 mmol) was finally added and the reaction was stirred for 16 h at room temperature. The resulting solution was quenched with 0.5 M HCl (5 mL) and partially concentrated under vacuum to reduce the amount of THF. The crude of the reaction was

extracted with DCM (3 x 15 mL), dried (anhydrous Na_2SO_4), and concentrated. Elution of the resulting crude mixture from a column of silica gel with 3:1 cyclohexane:EtOAc afforded first **5ga** as a pale yellow oil (23 mg, 29%) and then with 1:1 cyclohexane:EtOAc compound **1g** (36 mg, 65%).

Ethyl 1,6-Dimethyl-2-oxo-4-phenyl-1,2,3,4-tetrahydropyrimidine-5-carboxylate (1g)

$[\alpha]_D^{25}$ −8.0 (*c* 0.2 in CH_3OH) {Lit.[25] (>99:1 *er*) $[\alpha]_D^{20}$ −40 (*c* 0.2 in CH_3OH)}; **Chiral HPLC analysis** Chiralpak IA (90:10 *n*-Hexane:IPA, flow rate 1.0 mLmin^{-1}, 254 nm, 25 °C) t_R(*S*): 16.1, t_R(*R*): 20.5 min, 40:60 *er*.

Ethyl (*R,E*)-3-Cinnamoyl-1,6-dimethyl-2-oxo-4-phenyl-1,2,3,4-tetrahydropyrimidine-5-carboxylate (5ga)

$[\boldsymbol{\alpha}]_D^{25}$+33.9 (*c* 0.13 in CH_3OH); **Chiral HPLC analysis** Chiralpak IA (90:10 *n*-Hexane:IPA, flow rate 1.0 mLmin^{-1}, 254 nm, 25 °C) t_R(*S*): 13.6, t_R(*R*): 15.9 min, 23:77 *er*.

7.5 References and notes

1. a) C. O. Kappe, *Eur. J. Med. Chem.* **2000**, *35*, 1043–1052; b) J.-P. Wan, Y. Pan, *Mini-Rev. Med. Chem.* **2012**, *12*, 337–349.
2. B. E. Evans, K. E. Rittle, M. G. Bock, R. M. DiPardo, R. M. Freidinger, W. L. Whitter, G. F. Lundell, D. F. Veber, P. S. Anderson, R. S. L. Chang, V. J. Lotti, D. J. Cerino, T. B. Chen, P. J. Kling, K. A. Kunkel, J. P. Springer, J. Hirshfield, *J. Med. Chem.* **1988**, *31*, 2235–2246.
3. For reviews, see: a) L.-Z. Gong, X.-H. Chen, X.-Y. Xu, *Chem. Eur. J.* **2007**, *13*, 8920–8926; b) Suresh, J. S. Sandhu, *ARKIVOC* **2012**, 66–133; c) M. M. Heravi, S. Asadi, B. M. Lashkariani, *Mol. Diversity* **2013**, *17*, 389–407; d) E. Marcantoni, M. Petrini, *Adv. Synth. Catal.* **2016**, *358*, 3657–3682; e) H. Nagarajaiah, A. Mukhopadhyay, J. N. Moorthy, *Tetrahedron Lett.* **2016**, *57*, 5135–5149; f) M. M. Heravi, R. Moradi, L. Mohammadkhani, B. Moradi, *Mol. Diversity* **2018**, *22*, 751–767.
4. a) Greenhalgh, M. D.; Taylor, J. E.; Smith, A. D. *Tetrahedron* **2018**, *74*, 5554; b) H. B. Kagan, J. C. Fiaud, J. C. In *Topics in Stereochemistry* **1988**, *18*, 249−330.and references quoted therein. For selected reviews on DKR, see: c) Ward, R. S. *Tetrahedron: Asymmetry* **1995**, *6*, 1475; d) Pellissier, H. *Tetrahedron* **2003**, *59*, 8291; e) Pellissier, H. *Tetrahedron* **2008**, *64*, 1563; f) Pellissier, H. *Chirality from Dynamic Kinetic Resolution*; The Royal Society of Chemistry: Cambridge, **2011**; g) Pellissier, H. *Tetrahedron* **2011**, *67*, 3769; h) Pellissier, H. *Adv. Synth. Catal.* **2011**, *353*, 659; i) Nakano, K.; Kitamura, M. In *Separation of Enantiomers: Synthetic Methods, 1st ed*; Todd, M., Ed.; Wiley-VCH: Weinheim, **2014**, 161; j) Kreituss, I.; Bode, J. W. *Acc. Chem. Res.* **2016**, *49*, 2807; k) Pellissier, H. *Tetrahedron* **2016**, *72*, 3133; l) Li, P.; Hu, X.; Dong, X.-Q.; Zhang, X. *Molecules* **2016**, *21*, 1327.
5. a) B. Schnell, W. Krenn, K. Faber, C. O. Kappe, *J. Chem. Soc., Perkin Trans. 1* **2000**, 4382–4389; b) B. Schnell, U. T. Strauss, P. Verdino, K. Faber, C. O. Kappe, *Tetrahedron: Asymmetry* **2000**, *11*, 1449–1453; c) D. R. Sidler, N. Barta, W. Li, E. Hu, L. Matty, N. Ikemoto, J. S. Campbell, M. Chartrain, K. Gbewonyo, R. Boyd, E. G. Corley, R. G. Ball, R. D. Larsen, P. J. Reider, *Can. J. Chem.* **2002**, *80*, 646–652; d) Poonam, A. K. Prasad, C. Mukherjee, G. Shakya, G. K. Meghwanshi, J. Wengel, R. K. Saxena, V. S. Parmar, *Pure Appl. Chem.* **2005**, *77*, 237–243; e) A. K. Prasad, C. Mukherjee, S. K. Singh, R. Brahma, R. Singh, R. K. Saxena, C. E. Olsen, V. S. Parmar, *J. Mol. Catal. B* **2006**, *40*, 93–100.
6. a) J. A. Joule, K. Mills, *Heterocyclic Chemistry*; 4th ed.; Blackwell: Oxford, **2000**; b) T. Eicher, S. Hauptmann, *The Chemistry of Heterocycles*; Wiley- VCH: Weinheim, **2003**; c) A. R. Katrizky, A. F. Pozharskii, *Handbook of Heterocyclic Chemistry*; 2nd ed.; Pergamon: Amsterdam, **2000**.
7. a) K. S. Atwal, G. C. Rovnyak, S. D. Kimball, D. M. Floyd, S. Moreland, B. N. Swanson, J. Z. Gougoutas, J. Schwartz, K. M. Smillie, M. F. Malley, *J. Med. Chem.* **1990**, *33*, 2629–2635; b) G. C. Rovnyak, K. S. Atwal, A. Hedberg, S. D. Kimball, S. Moreland, J. Z. Gougoutas, B. C. O'Reilly, J. Schwartz, M. F. Malleys, *J. Med. Chem.* **1992**, *35*, 3254–3263.
8. J. C. Barrow, P. G. Nantermet, H. G. Selnick, K. L. Glass, K. E. Rittle, K. F. Gilbert, T. G. Steele, C. F. Homnick, R. M. Freidinger, R. W. Ransom, P. Kling, D. Reiss, T. P. Broten, T. W. Schorn, R. S. L. Chang, S. S. OMalley, T. V. Olah, J. D. Ellis, A. Barrish, K. Kassahun, P. Leppert, D. Nagarathnam, C. Forray, *J. Med. Chem.* **2000**, *43*, 2703–2718.
9. a) C. O. Kappe, *Tetrahedron* **1993**, *49*, 6937–6963; b) H. Namazi, Y. R. Mirzaei, H. Azamat, *J. Heterocycl. Chem.* **2001**, *38*, 1051–1054; c) D. Dallinger, N. Yu. Gorobets, C. O. Kappe, *Org. Lett.* **2003**, *5*, 1205–1208.
10. Selected reviews: a) H. U. Vora, P. Wheeler, T. Rovis, *Adv. Synth. Catal.* **2012**, *354*, 1617–1639; b) C. E. I. Knappke, A. Imami, A. J. von Wangelin, *ChemCatChem* **2012**, *4*, 937–941; c) S. De Sarkar, A. Biswas, R. C. Samanta, A. Studer, *Chem. Eur. J.* **2013**, *19*, 4664–4678;a) J. Mahatthananchai, J. W. Bode, *Acc. Chem. Res.* **2014**, *47*, 696–707; b) M. H. Wang, K. A. Scheidt, *Angew. Chem. Int. Ed.* **2016**, *55*, 14912–14922; *Angew. Chem.* **2016**, *128*, 15134–15145.

11. For recent reviews, see: a) Z. Wang, D. Pan, T. Li, Z. Jin, *Chem. Asian J.***2018**, *13*, 2149–2163; b) C. De Risi, O. Bortolini, G. Di Carmine, D. Ragno, A. Massi, *Synthesis* **2019**, *51*, 1871–1891.
12. K. Lee, H. Kim, J. Hong, *Angew. Chem. Int. Ed.* **2012**, *51*, 5735–5738; *Angew. Chem.* **2012**, *124*, 5833–5836.
13 G. Di Carmine, D. Ragno, A. Brandolese, O. Bortolini, D. Pecorari, F. Sabuzi, A. Mazzanti, A. Massi, *Chem. Eur. J.* **2019**, *25*, 7469–7474.
14. D. Ragno, G. Di Carmine, A. Brandolese, O. Bortolini, P. P. Giovannini, G.Fantin, M. Bertoldo, A. Massi, *Chem. Eur. J.* **2019**, *25*, 14701–14710.
15 a) J. W. Bode, S. S. Sohn, *J. Am. Chem. Soc.* **2007**, *129*, 13798–13799; b) H. U. Vora, T. Rovis, *J. Am. Chem. Soc.* **2007**, *129*, 13796–13797; c) P.-C. Chiang, Y. Kim, J. W. Bode, *Chem. Commun.* **2009**, 4566–4568; d) S. De Sarkar, A. Studer, *Org. Lett.* **2010**, *12*, 1992–1995; e) M. Binanzer, S.-Y. Hsieh, J. W. Bode, *J. Am. Chem. Soc.* **2011**, *133*, 19698–19701; f) S. Iwahana, H. Iida, E. Yashima, *Chem. Eur. J.* **2011**, *17*, 8009–8013; g) B. Zhang, P. Feng, Y. Cui, N. Jiao, *Chem. Commun.* **2012**, *48*, 7280–7282; h) P. Wheeler, H. U. Vora, T. Rovis, *Chem. Sci.* **2013**, *4*, 1674–1679; i) C. A. Gondo, J. W. Bode, *Synlett* **2013**, *24*, 1205–1210; j) R. W. M. Davidson, M. J. Fuchter, *Chem. Commun.* **2016**, *52*, 11638–11641; k) R. A. Green, D. Pletcher, S. G. Leach, R. C. D. Brown, *Org. Lett.* **2016**, *18*, 1198–1201; l) S. Premaletha, A. Ghosh, S. Joseph, S. R. Yetra, A. T. Biju, *Chem. Commun.* **2017**, *53*, 1478–1481; m) V. Kumar, S. J. Connon, *Chem. Commun.* **2017**,*53*, 10212–10215.
16 a) N. T. Reynolds, J. Read de Alaniz, T. Rovis, *J. Am. Chem. Soc.* **2004**, *126*, 9518–9519; b) S. Dong, M. Frings, D. Zhang, Q. Guo, C. G. Daniliuc, H. Cheng, C. Bolm, *Chem. Eur. J.* **2017**, *23*, 13888–13892.
17. a) G.-Q. Li, Y. Li, L. Dai, S. You, *Org. Lett.* **2007**, *9*, 3519–3521; b) N. Duguet, C. D. Campbell, A. M. Z. Slawin, A. D. Smith, *Org. Biomol. Chem.* **2008**, *6*, 1108–1113; c) K. Thai, L. Wang, T. Dudding, F. Bilodeau, M. Gravel, *Org. Lett.* **2010**, *12*, 5708–5711; d) C. Zheng, X. Liu, C. Ma, *J. Org. Chem.* **2017**, *82*, 6940–6945.
18 a) S. Dong, M. Frings, H. Cheng, J. Wen, D. Zhang, G. Raabe, C. Bolm, *J. Am. Chem. Soc.* **2016**, *138*, 2166–2169; b) A. Porey, S. Santra, J. Guin, *Asian J. Org. Chem.* **2016**, *5*, 870–873.
19. M. Wang, Z. Huang, J. Xu, Y. R. Chi, *J. Am. Chem. Soc.* **2014**, *136*, 1214– 1217.
20. L. Ta, H. Sundeń, *Chem. Commun.* **2018**, *54*, 531–534.
21. L. Ta, A. Axelsson, H. Sundeń, *J. Org. Chem.* **2018**, *83*, 12261–12268.
22. D. Ragno, A. Zaghi, G. Di Carmine, P. P. Giovannini, O. Bortolini, M. Fogagnolo, A. Molinari, A. Venturini, A. Massi *Org. Biomol. Chem*., **2016**, *14*, 9823.
23. For selected examples of NHC-catalysed reactions in the presence of a Lewis acid additive, see: a) D. E. A. Raup, B. Cardinal-David, D. Holte, K. A. Scheidt, *Nat. Chem.* **2010**, *2*, 766–771; b) D. T. Cohen, K. A. Scheidt, *Chem. Sci.* **2012**, *3*, 53–57; c) J. Mo, X. Chen, Y. R. J. Chi, *J. Am. Chem. Soc.* **2012**, *134*, 8810–8813; d) J. Dugal-Tessier, E. A. O'Bryan, T. B. H. Schroeder, D. T. Cohen, K. A. Scheidt, *Angew. Chem. Int. Ed.* **2012**, *51*, 4963–4967; *Angew. Chem.* **2012**, *124*, 5047–5051; e) Y. Zhang, Y. Lu, W. Tang, T. Lu, D. Du, *Org. Biomol. Chem.* **2014**, *12*, 3009–3015; f) S. Bera, R. C. Samanta, C. G. Daniliuc, A. Studer, *Angew. Chem. Int. Ed.* **2014**, *53*, 9622–9626; *Angew. Chem.* **2014**, *126*, 9776–9780.
24. J. Piera, J.-E. Bäckvall, *Angew. Chem. Int. Ed.* **2008**, *47*, 3506–3523; *Angew. Chem.* **2008**, *120*, 3558–3576.
25. a) A. Axelsson, A. Antoine-Michard, H. Sundeń, *Green Chem.* **2017**, *19*, 2477–2481. For selected example of direct use of air as oxidant, see: b) D. Xie, D. Shen, Q. Chen, J. Zhou, X. Zeng, G. Zhong, *J. Org. Chem.* **2016**, *81*, 6136–6141.
26. For the assignment of the absolute configuration: K. Singh, K. Singh, H. Kaur, *Tetrahedron* **2012**, *68*, 6169–6176.
27. N. D. Zakusilo, D. S. Ryabukhin, I. A. Boyarskaya, O. S. Yuzikhin, A. V. Vasilyev, *Tetrahedron* **2015**, *71*, 102–108.

28. a) G. C. Rovnyak, S. D. Kimball, B. Beyer, G. Cucinotta, J. D. DiMarco, J. Gougoutas, A. Hedberg, M. Malley, J. P. McCarthy, R. Zhang, S. Moreland *J. Med. Chem*. **1995**, *38*, 119−129; b) B. Jauk, T. Pernat, C. O. Kappe *Molecules* **2000**, *5,* 227−239.
29. a) N. A. White, T. Rovis, *J. Am. Chem. Soc.* **2014**, *136*, 14674–1467; b) D. A. Di Rocco, T. Rovis, *J. Am. Chem. Soc.* **2012**, *134*, 8094–8097.
30. a) D. B. Zlatković, N. S. Radulović, *RSC Adv.* **2016**, *6*, 115058–115067; b) G. Di Carmine, D. Ragno, O. Bortolini, P. P. Giovannini, A. Mazzanti, A. Massi, M. Fogagnolo, *J. Org. Chem.* **2018**, *83*, 2050–2057.
31. a) N. October, N. D. Watermeyer, V. Yardley, T. J. Egan, K. Ncokazi, K. Chibale, *ChemMedChem* **2008**, *3*, 1649–1653; b) K. Singh, D. Arora, D. Falkowski, Q. Liu, R. S. Moreland, *Eur. J. Org. Chem.* **2009**, *2009*, 3258–3264; c) S. Lou, B. M. Taoka, A. Ting, S. E. Schaus, *J. Am. Chem. Soc.* **2005**, *127*, 11256–11257.
32. H. Salehi, Q.-X. Guo, *Chin. J. Chem.* **2005**, *23*, 91–97.
33. A. A. A. Abdel-Fattah, *Synthesis* **2003**, *15*, 2358–2362.

8. Sequential Kinetic Resolution of (±)-1,2- and (±)-1,3-diols using solid-supported Isothiourea in flow-mode conditions

The research activity presented in this chapter is the result of a placement at the University of St Andrews (UK) completed under the supervision of Professor Andrew D. Smith.

8.1 Introduction

The ever-increasing necessity to synthesise highly enantioenriched compounds has brought chemists to a deep rational design of catalysts structure joined by a fine-tuning research of all the reaction parameters. However, this process could be not only time consuming but also limits the applicability of the performed procedure. Therefore, the use of other approaches could turn out to be an alternative option to laborious and expensive catalyst fine-tuning. In this regard, the Horeau's principle,[1] which is responsible for the improvement of enantioselectivity in some reactions which rely on polyfunctionalized substrates, could play a basic role. Accordingly, this phenomenon easily find application in natural product synthesis and asymmetric catalysis.[2] Nowadays, although many research groups are exploiting Horeau's principle in the context of enantioselective catalysis involving poly-functional substrates,[3] others still consider it as an anecdotal phenomenon. Indeed, the possibility to detect this principle could help to understand and interpretate some experimental results, opening a window on novel synthetic opportunities. A representative example on the application of this powerful amplification involves a synergistic sequential kinetic resolution (SKR) of (±)-*syn*-1,2-diols[4] and (±)-*anti*-1,3-diols.[5] In 2017, Bressy's group developed a SKR process to access both enantiomers of (±)-*anti*-1,3-diol with high yields and enantioselectivities.[5] The protocol uses the commercially available Isothiourea Lewis base catalyst, HyperBTM,[6] and it is based on two enantioselective acylation reactions (Scheme 1).[5] Later, in 2019, Smith's group proposed a similar process aimed to obtain highly enantioenriched 1,2-diols.[4] In particular, optimal selectivities were obtained using a readily prepared and commercially available HyperBTM[6] organocatalyst and reagents (isobutyric anhydride, Hünig's base) at 0 °C, making this KR process operationally simple to perform (Scheme 1).

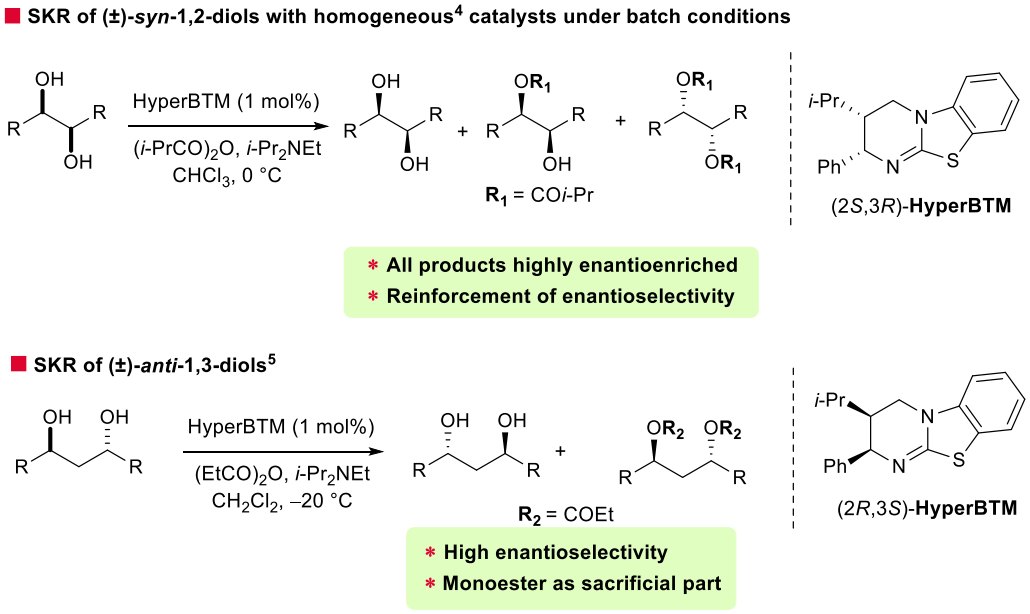

Scheme 1. Previous works on Synergistic Sequential Kinetic Resolution (SKR) of (±)-*syn*-1,2-diols and (±)-*anti*-1,3-diols under homogeneous batch conditions.

According to the collected results of the above reported SKR processes, these substrates have proved to appear well-suited to exploit Horeau's principle by applying two subsequent enantioselective acylation transformation. Chiral 1,2-diols are attractive compounds which have found applications as organocatalysts, ligands and chiral auxiliaries.[7] Additionally, they are present in a range of bioactive compounds and are also used as intermediates in organic synthesis.[7,8] The most common powerful methods to synthetize chiral 1,2-diols are pinacol coupling of aldehydes,[7,9] reduction of ketones[7,10] hydrolysis of epoxides[7,11] and enantioselective Sharpless dihydroxylation of alkenes.[7,12] However, these methods generally use toxic and expensive transition metals as stoichiometric reagents or catalysts. In analogy, chiral 1,3-diols are usually obtained through the preparation of an enantioenriched β-hydroxyketone followed by its *anti*-diastereoselective reduction.[13] However, the synthesis of chiral 1,3-diols is limited to few methods, rarely catalytic.[14] Hence, the definition of a Kinetic Resolution (KR) process, which provides access to enantioenriched compounds, represents a potentially attractive alternative, requiring only a simply modulation of the reaction conversion.[7,8,15] Indeed, both developed processes which take advantage of the additive Horeau's amplification represented a valid option to access highly enantioenriched compounds. Due to the bis-alcohol functionality presented in both (±)-*syn*-1,2-diols and (±)-*anti*-1,3-diols, two KR processes can be in operation. Hence, four rate constants could be identified, k_1 and k_2 for the first KR, and k_3 and k_4 for the second KR. If $k_1 > k_2$ and $k_3 > k_4$, the enantiomer of monoester preferentially generated in the 1st KR is also preferentially acylated in the 2nd KR. In principle, this allows the generation of both the diester (from two successive KRs) and diol in high enantiopurity and with opposite

absolute configuration (Figure 1). Both the enantiopurity and the absolute configuration of the monoester product has found to be highly dependent upon reaction conversion. Indeed, its configuration will match that of the diester at low conversion, and the diol at high conversion, while at the inflection point between these two extremes, the monoester is racemic. Moreover, the relative yields of diester, diol and monoester will be dependent upon the relative magnitude of the combined rate constants for the 1st KR process relative to the 2nd KR process. If both KR processes are reasonably selective, then this can be simplified as the relationship between the largest rate constant for each KR step (k_1 vs k_3). In relation to the two reported examples which involves (±)-*syn*-1,2-diols and (±)-*anti*-1,3-diols, assumptions on the relative rates of each KR process could be made based on the product distribution. For the sequential KR of (±)-1,2-*syn*-diol it can be estimated the relative rates of the two KR steps were significantly different, with the 1st KR being ~8 times that of the 2nd KR.[4] Indeed, the increased steric hindrance associated with the α-ester substituent introduced following the first acylation event might be considered responsible for this difference in the acylation step. Therefore, diol and diester can be isolated in both high yield and enantiopurity, and necessitates the sequential KR being driven to higher conversion to access highly enantiomerically enriched material. The KR of (±)-*anti* -1,3-diols instead is characterized by two KR steps which displayed the same sense of enantiodiscrimination.[5] Based on the product distribution, it can be estimated that the relative rates of each KR process are close to parity (i.e. $k_1 \approx k_3$).

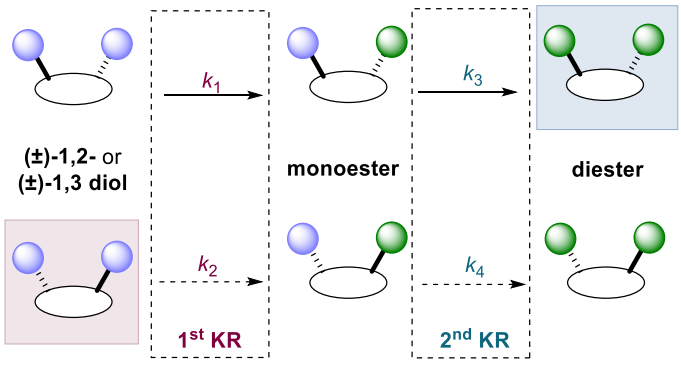

Figure 1. Horeau amplification in the sequential double acylative KR of C_2-symmetric (±)-diols.

Although incredibly powerful, organocatalysed processes usually require relatively high loadings of the catalyst, which is typically discarded at the end of the reaction. Therefore, the immobilization of the organocatalyst on a heterogeneous support could represent an alternative way to overtake the former drawback, leading to unaltered catalyst activity and high stability.[16,17] Moreover, if the process is conducted under continuous-flow conditions the benefits arising from the new reaction set-up could be remarkable. Indeed, in the context of flow chemistry, organocatalysis[18] has caught attention of numerous chemists and offers

significant opportunities in terms of invention of new transformations or re-optimization of well-established reactions.[17] This goal was recently addressed through the development of a polymer-supported Isothiourea (PS-HyperBTM) catalyst **1**, which was applied for the KR of alcohols in batch and flow-mode conditions. Pleasantly, no reduction in either activity or selectivity was observed upon recycling.[19,20] Application of this continuous-flow technology for several kinds of secondary alcohol (benzylic, allylic, propargylic alcohols, cycloalkanols[19–21]) and tertiary alcohols[22] were therefore targeted, inspiring a novel application in SKR processes. Indeed, a preliminary investigation on the synergistic sequential kinetic resolution of (±)-*syn*-1,2-diols has been also performed in batch conditions in the presence of a supported HyperBTM, showing unaltered results respect to the homogenous counterpart.[20] Hence, the possibility to conduct the SKR of (±)-*syn*-1,2-diols and (±)-*anti*-1,3-diols in flow-mode conditions represents a thought-provoking task. In this way, the beneficial influence of the Horeau's principle could be additionally widened by the use of a supported catalyst in more environmentally friendly and eco-sustainable conditions (Scheme 2).

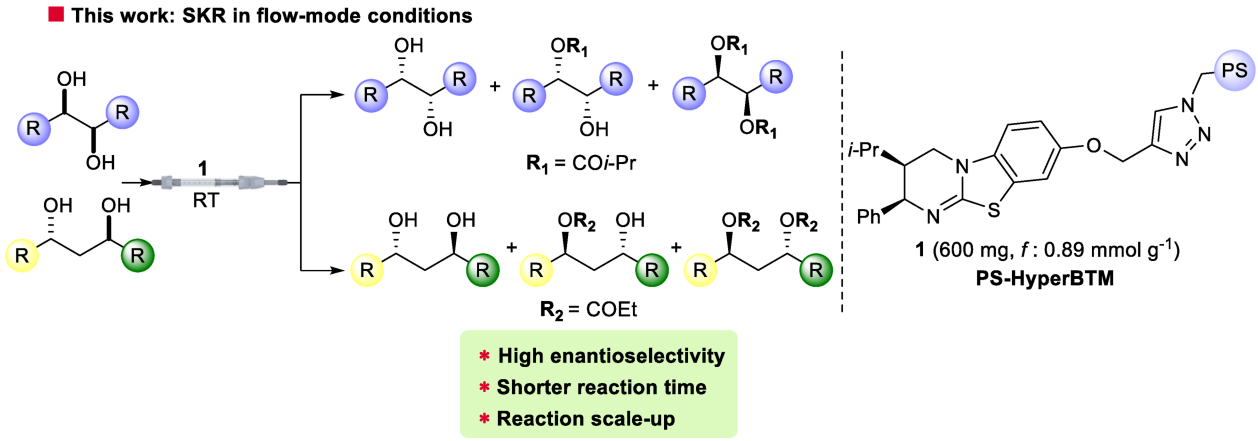

Scheme 2. This work: SKR performed under flow-mode conditions.

8.2 Results and discussion

Initial studies focused on the KR of (±)-1,2-diphenylethane-1,2-diol **2a** using isobutyric anhydride as the acylating agent and *i*-Pr$_2$EtN as the base in the same ratio as previously optimized in the homogeneous[4] and heterogeneous[20] conditions. A packed bed microreactor with PS-HyperBTM **1** has been prepared and the flow-set up used is represented in Table 1. Reaction optimization was conducted on 0.5 mmol scale and was targeted through variation of the operative conditions such as flow rate, concentration of the substrate and different flow set-up (Table 1). The use of 1.50 equiv. of isobutyric anhydride allowed isolation of monoester (1*R*,2*R*)-**3a** and diester (1*R*,2*R*)-**4a** along with the recovered diol (1*S*,2*S*)-**2a** in good

enantiopurity (entry 1). Encouraged by this first results, further experiments were conducted with the aim to increase the selectivity of the process driving the reaction to higher conversion. Differently with respect to works reported in literature, in the present case the calculation of the selectivity represents an effortful process. Indeed, as two KR processes are in operation, is not possible to calculate, using Kagan's equation, an *s* value that represents the whole process. Indeed, the *s* value should be calculated for each kinetic resolution step, i.e. for the kinetic resolution of the racemic (±)-*syn*-1,2-diols which lead to the formation of the monoester and the selectivity of the process which involves the KR of a racemic monoester **3**. In some cases, this laborious process has been simplified considering only the conversion and the enantiomeric purity of the final product for the calculation of the *s* value, however, this does not represent a meaningful metric as, in the present situation case, the selectivity is strictly dependent on the reaction conversion (as two KR processes are in operation). For this reason, the *s* value[12a] of all the processes is not reported while the optimization study was focused on the conversion into the diester and on the comparison of the products enantioselectivity. According to the study previously conducted on this sequential KR,[4] the reaction optimization was therefore evaluated by aiming for ~50% conversion to diester. Lowering the flow rate to 0.05 mL min^{-1} led to an increase of enantioselectivity of both the monoester **3a** and the diester **4a** (entry 2), while with an even slower flow rate (0.04 mL min^{-1}, entry 3) the conversion of the diol turned out to be too high though accompanied by high enantioselectivity of both products **3a** and **4a**. Later, the influence of the concentration was investigated too. However, the use of a concentrated solution was hampered by the low solubility of the diols in chloroform at concentration higher than 0.2 M whereas halving the concentration of all the three reagents (entry 4), led to an increase of the yield towards the monoester **3a**. Further studies were thus focused on the increasing of the amount of anhydride and base leading to almost full conversion of diol **2a** into the diester **4a** and monoester **3a** (entry 5), while a slightly increase gave an improved selectivity (entry 6) compared to the first experiment. Lastly, different flow set-ups were also investigated to understand if the simultaneous presence in the same syringe of the anhydride and base with possibly traces of water could lead to the formation of carboxylic acid, reducing the available amount of anhydride (entries 7 − 9). Globally, no change upon varying the flow-mode set-up were detected. To note, a control experiment in batch conditions without the presence of the catalyst, showed that when the diol, the anhydride and the base are put together for about two hours a small quantity of monoester is formed, thus preventing the use of this flow set-up for the experiment. Finally, the optimized reaction conditions reported in entry 6 have been applied to a 2 mmol scale to verify the yield of the process (entry 10). Overall, this process allowed isolation of (1*R*,2*R*)-**4a** in 47% yield and 94:6 *er* and the (1*S*,2*S*) enantiomer of both diol **2a** and

monoester **3a** in a combined 41% yield and >99:1 *er* and 98:2 *er*, respectively. However, as some substrates reported in the reaction scope showed a non-complete solubility in $CHCl_3$ the addition of the anhydride in the same syringes turned out to be beneficial in order to obtain a homogenous solution. Consequently, the benchmark reaction was also conducted on 2 mmol scale using this flow-mode set up (entry 11) and furnishing analogues results with respect to the ones obtained in entry 10.

Table 1. Optimization study for the sequential kinetic resolution of (±)-**2a** in flow-mode.[a]

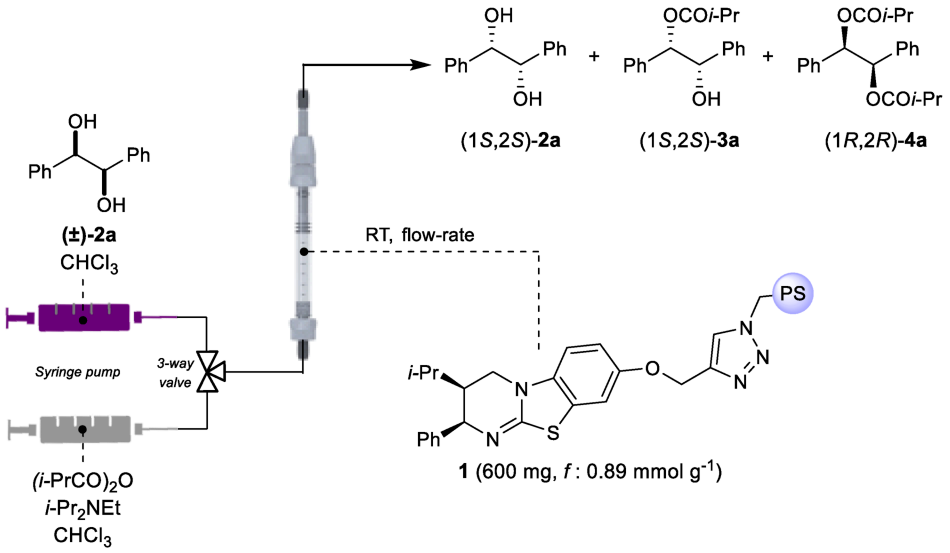

Entry	(±)-**2a** [M]	$(i\text{-PrCO})_2O$ [M]	$i\text{-Pr}_2NEt$ [M]	Product Ratio (**2a**:**3a**:**4a**)[b]	**2a** *er* (1*S*,2*S*): (1*R*,2*R*)[c]	**3a** *er* (1*S*,2*S*): (1*R*,2*R*)[c]	**4a** *er* (1*R*,2*R*): (1*S*,2*S*)[c]
1	0.2	0.3	0.32	17:39:44	99:1	85:15	95:5
2[d]	0.2	0.3	0.32	12:39:49	>99:1	92:8	97:3
3[e]	0.2	0.3	0.32	4:43:53	-	98:2	93:7
4	0.1	0.15	0.16	10:44:46	>99:1	75:25	94:6
5	0.2	0.4	0.44	1:40:59	-	>99:1	75:25
6	**0.2**	**0.35**	**0.35**	**7:41:52**	**99:1**	**97:3**	**90:10**
7[f]	0.2	0.3	0.32	14:39:47	99:1	88:12	96:4
8[g]	0.2	0.3	0.32	9:39:52	>99:1	96:4	94:6
9[h]	0.2	0.3	0.32	10:45:45	99:1	89:11	94:6
10[i]	**0.2**	**0.35**	**0.35**	**7:41:52**	**>99:1 (3%)**[j]	**98:2 (38%)**[j]	**94:6 (47%)**[j]
11[i,f]	**0.2**	**0.35**	**0.35**	**7:40:53**	**>99:1 (3%)**[j]	**98:2 (35%)**[j]	**94:6 (48%)**[j]

[a]Conditions: (±)-**2a** (0.5 mmol), RT, flow rate 0.1 mL min^{-1}. [b]Determined by ^1H NMR spectroscopic analysis of the crude reaction product. [c]Determined by CSP-HPLC analysis. [d]Flow rate 0.05 mL min^{-1}. [e]Flow rate 0.04 mL min^{-1}. [f]Flow set-up: diol and anhydride in one syringe and base in the other one. [g]Flow set-up: all the reagents together in one syringe. [h]Flow set-up: diol and base in one syringe and anhydride in the other one. [i]Conditions: (±)-**2a** (2.0 mmol). RT, flow rate 0.1 mL min^{-1}. [j]Isolated yield.

At this point, aware of the influence of the Horeau's principle for the improvement of the enantioselectivity,[1] the KR of the racemic monoester **3a** under flow-mode conditions was additionally explored (Scheme 3). Thus, the KR of (±)-**3a** was achieved with an *s* value of 38 when 0.85 equiv. of $(i\text{-PrCO})_2O$ were used, with the corresponding monoester **4a** being isolated

with 95:5 *er* and the monoester **3a** with 82:18 *er*. Indeed, the recovered monoester **3a** showed an *er* value lower than that obtained by using a sequential KR procedure (98:2 *er*), thus confirming the beneficial effect of the Horeau's amplification.

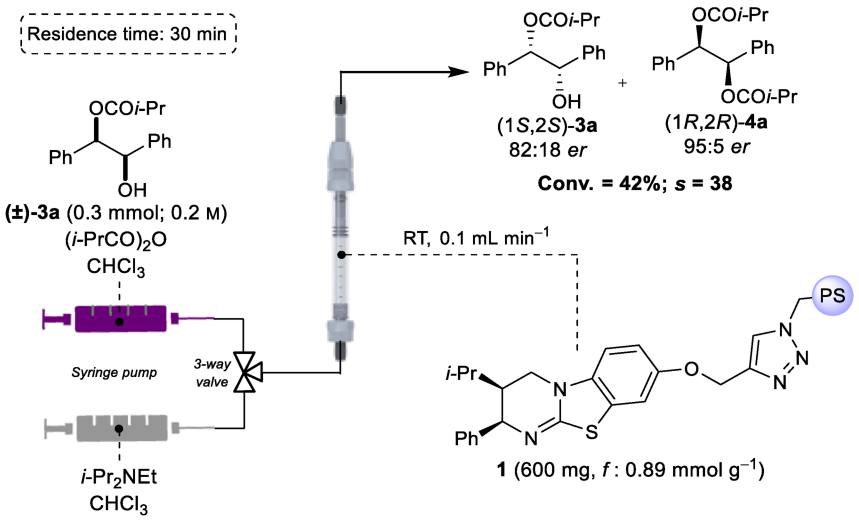

Scheme 3. Flow-mode KR of monoester (±)-**3a**. Conversion and *er* were determined by chiral HPLC analysis. Selectivity factors (*s*) was calculated using monoester *er* and reaction conversion (see ref. 15a).

Finally, the generality of this sequential KR process in flow was investigated using a selection of electronically and sterically differentiated (±)-*syn*-1,2-diols (Scheme 4). The optimized procedure (Table 1, entry 11) has thus been applied to (±)-1,2-diarylethane-1,2-diol derivatives with both electron-withdrawing and electron-donating groups on the aryl units. Compounds **2b-2d** were all resolved with excellent selectivity furnishing results comparable with those obtained using the homogeneous catalyst.[4] Moreover, the KR of compound **2d** provided products with higher enantioselectivity than the substrates **2b** and **2c** bearing electron-withdrawing groups. These results are in agreement with those previously observed for the homogenous catalyst and with the selectivity trends recorded for the KR of secondary benzylic alcohols.[22] This behaviour is attributed to the increased stability of the positively charged acylated catalyst intermediate in the acylation transition state due to the presence of more electron-rich aromatic substituent.[22] The applicability of the disclosed procedure was also extended to substrates bearing a naphthyl substituent. However, the substrate **2e** presented low solubility in the optimized reaction conditions forcing the use of a different solvent system. The mixture 1:1 THF:$CHCl_3$ turned out to be a good choice for this substrate and the double kinetic resolution process was applied without further optimization. Thus, diol **2e** and diester **4e** were recovered with high enantioselectivity (97:3 *er* and 94:6 *er*, respectively) while the monoester **3e** with moderate (70:30 *er*) as expected by the low conversion of the diol **2e** into the acylated derivative. This low conversion can be ascribed to the reduced residence time of the substrate

inside the reactor. In fact, the swelling properties of the supported catalyst depends upon the type of solvent used as observed in previous works.[20] Experimentally, the supported catalyst **1** swells less in a 1:1 THF:$CHCl_3$ mixture respect to $CHCl_3$, leading to a short residence time, thus a lower flow rate could have led to a higher conversion of the diol **2e** probably resulting in a higher enantioselectivity of monoester **3e**. Finally, the KR of (±)-1,2-diols **2f** and **2g** bearing adjacent π -donor systems were also performed, recording for both processes a moderate selectivity. The low enantioselectivity of diesters **4f** and **4g**, could be attributed to the high conversion of the starting diols (higher than 50%) due to the use of 1.75 equiv. of anhydride as required in the optimized conditions. However, no further investigations based on different ratio of acyl donor reagent have been conducted.

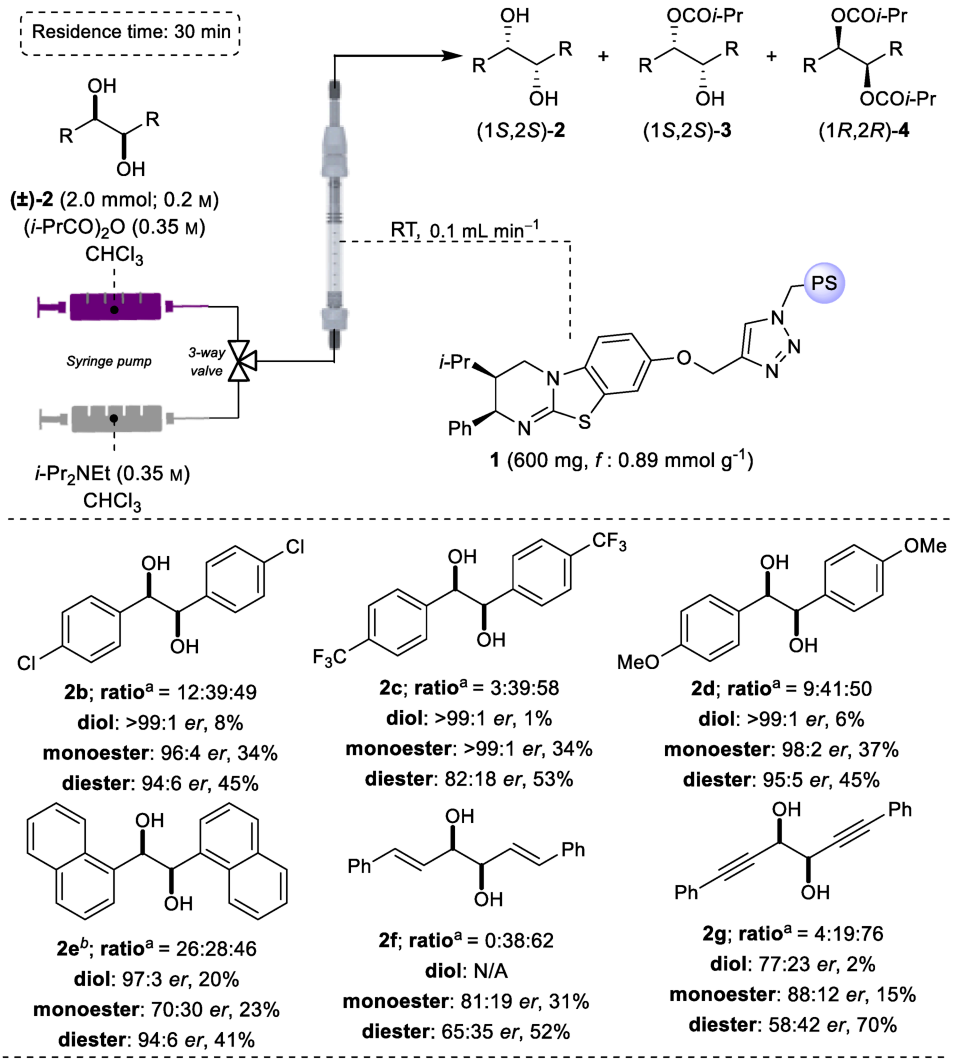

Scheme 4. Reaction scope.[a] Ratio of diol/monoester/diester determined by ^{1}H NMR spectroscopic analysis of the crude reaction product.[b] Solvent 1:1 THF:$CHCl_3$.

Considering the positive outcome of the sequential kinetic resolution of 1,2-diols in continuous flow, the process was further extended to *anti*-1,3-diols. Indeed, the double kinetic resolution

of acyclic *anti*-1,3-diols, relying on an additive Horeau's amplification, was performed with the homogeneous HyperBTM with excellent results.[5] However, the use of the same reaction conditions already optimized for the (±)-*syn*-1,2-diols was hampered due to the non-complete solubility of the substrate **5a** in $CHCl_3$. For this reason, a preliminary investigation with homogeneous organocatalyst HyperBTM has been conducted to understand the outcome of the process, influenced by variation of the solvent and the reaction temperature. In fact, the reaction in homogeneous phase was performed at −20 °C in CH_2Cl_2 as the optimal solvent. Therefore, firstly the influence of the temperature over the selectivity of the process was explored. Indeed, perform a reaction at room temperature represent a more sustainable and easy way to conduct a reaction mainly under flow-mode conditions. Pleasantly the diester **7a** has been obtained with a comparable yield and *er* (Table 3, entry 1) respect to the reaction conducted at −20°C. However, the starting (±)-**5a** was not totally soluble in CH_2Cl_2 while the use of $CHCl_3$:THF 1:1 mixture led to a homogeneous solution which is essential when a reaction is conducted with a flow-mode apparatus. The change in the solvent system did not hugely affect the outcome of the reaction, therefore the reaction conditions reported in entry 2 were chosen for the following studies in flow.

Table 3. Optimization study for SKR of (±)-**5a** with homogeneous HyperBTM.

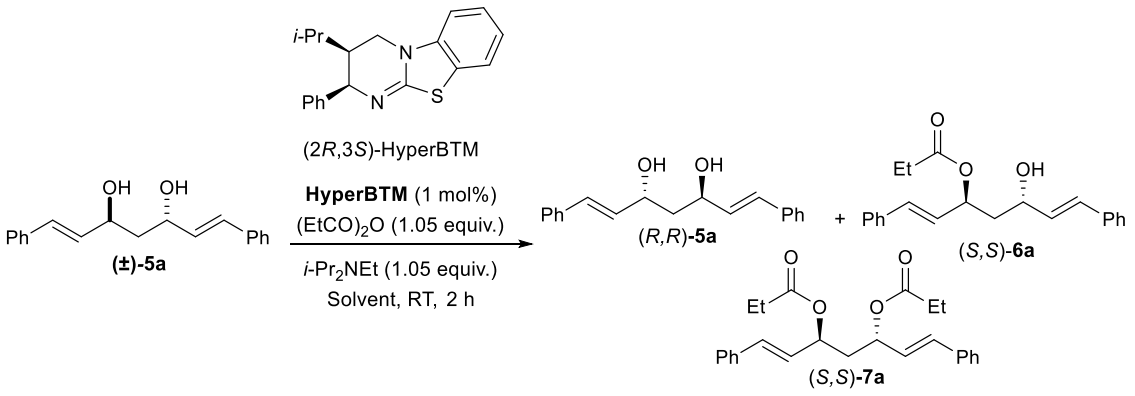

Entry	Solvent	Product Ratio (**5a**:**6a**:**7a**)[b]	**5a** *er* (*R*,*R*):(*S*,*S*)[c]	**7a** *er* (*S*,*S*):(*R*,*R*)[c]
1	CH_2Cl_2	40:8:42	99:1	90:10
2	$CHCl_3$:THF (1:1)	36:6:46	>99:1	87:13

[a]Conditions: (±)-**5a** (0.2 M), $(EtCO)_2O$ (1.05 equiv.), *i*-Pr_2NEt (1.05 equiv), RT 2 h. [b]Isolated Yield. [c]Determined by CSP-HPLC analysis.

At this point, an optimization procedure on 0.5 mmol scale in flow-mode conditions has been performed using the former optimized solvent system and targeted through variation of the operative conditions such as flow rate, concentration of the substrate and different flow set-ups (Table 4). For the sake of simplicity, in this part of the work, only the starting diol **5a** and the

corresponding diester **7a** were analysed. In fact, monoester **6a** was usually obtained with an isolated yield not higher than 20% and it was yielded as an inseparable mixture of combined *anti*- and *syn*-compounds, requiring a purification step prior to the enantioselectivity determination. This process was performed while expanding the reaction scope and the result is reported in Scheme 6. Indeed, as reported for the homogeneous process,[5] also in flow mode conditions, the *anti*-diol was contaminated by a small amount of *syn*-diol and the latter was captured as its monoester as pointed out by the lower *dr* which characterized the monoester.

Table 4. Optimization study for the SKR of (±)-*anti*-1,3-diol **5a** in flow-mode.[a]

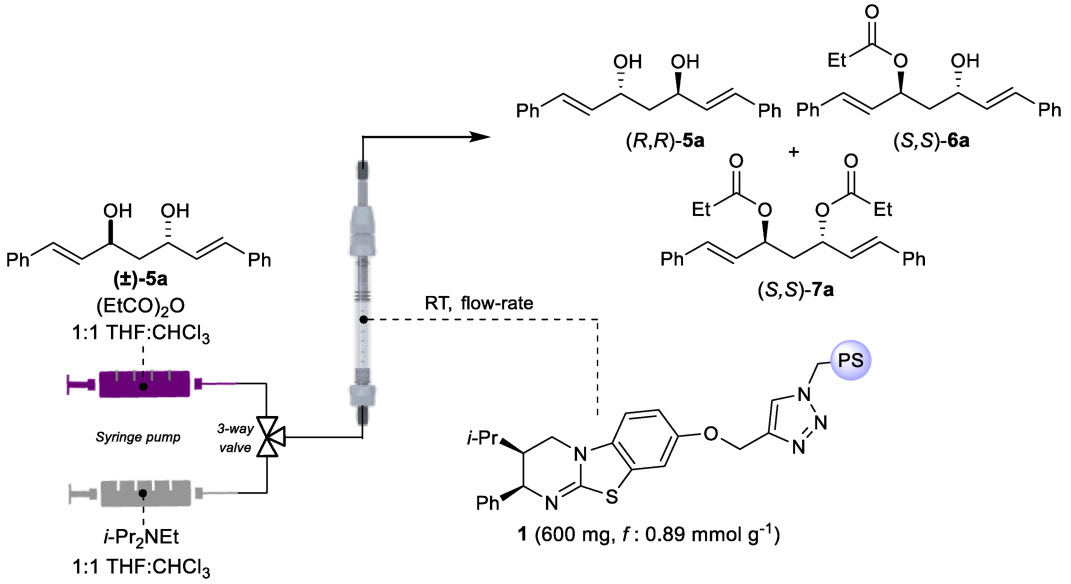

Entry	(±)-**5a** [M]	$(EtCO)_2O$ [M]	*i*-Pr_2NEt [M]	Product Ratio (**5a**:**6a**:**7a**)[b]	**5a** *er* (*R*,*R*):(*S*,*S*)[c]	**7a** *er* (*S*,*S*):(*R*,*R*)[c]
1	0.2	0.210	0.210	19:7:21[d]	99:1	89:11
2[e]	**0.1**	**0.105**	**0.105**	**39:22:39**	**98:2**	**96:4**
3[f]	0.1	0.105	0.105	39:19:42	98:2	96:4
4[g]	0.1	0.120	0.120	38:21:41	96:4	96:4
5[e,g]	0.1	0.105	0.105	38:27:35	99:1	94:6

[a]Conditions: (±)-**5a** (0.5 mmol), RT, flow rate 0.1 mL min^{-1}. [b]Determined by ^1H NMR spectroscopic analysis of the crude reaction product with 1,3,5-Trimethoxybenzene as Internal Standard (IS). [c]Determined by CSP-HPLC analysis. [d]Isolated yield. [e]Flow rate 0.2 mL min^{-1}. [f]Flow rate 0.16 mL min^{-1}. [g]Flow set-up: diol and base in one syringe and anhydride in the other one.

The first attempt of the reaction conducted in flow-mode conditions was the use of a concentrated solution of **5a** which was hampered by the low solubility of this compound (entry 1). In fact, during the flow-mode experiment, a precipitation occurred in the syringe reducing the amount of the available starting material. Therefore, the use of a diluted solution along with a higher flow rate (0.2 mL min^{-1} instead of 0.1 mL min^{-1}) turned out to be a good compromise to achieve both enantioselectivity and yield values similar to those obtained with the

homogeneous catalyst (entry 2). A slight decrease of the flow rate did not improve selectivities (entry 3) as well as the use of higher amount of anhydride and base (entry 4). Lastly, the change of the flow-mode set-up by the addition of the base along with the substrate in place of the anhydride, as expected, did not hugely affect the outcome of the process (entry 5).

At this point of the work, in order to confirm the beneficial effect of the double enantioselective acylation, the KR of racemic monoester **6a** was performed under the optimized reaction conditions (Table 4, entry 2) but with reduced amount of anhydride and base (Scheme 5).

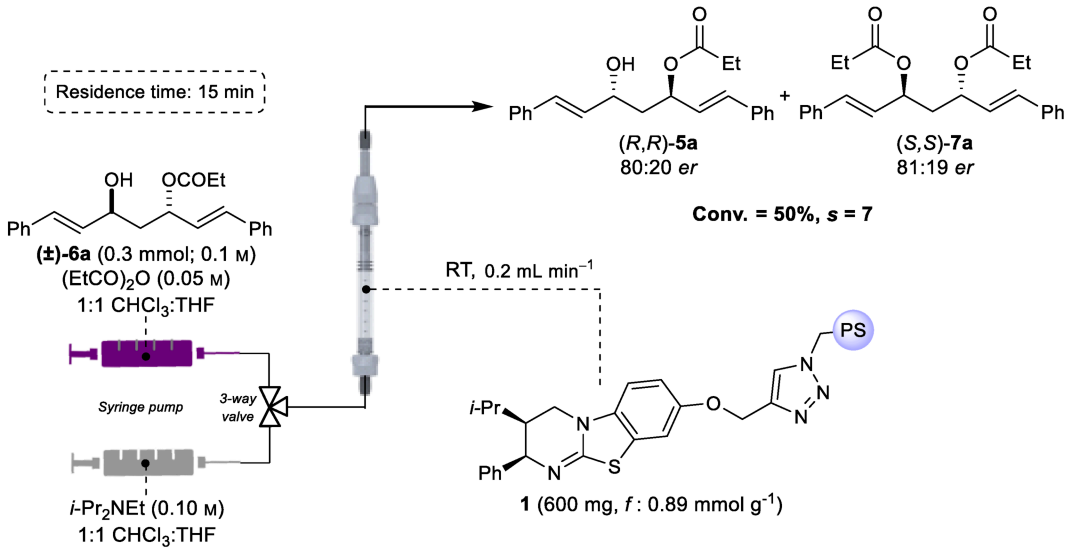

Scheme 5. Flow-mode KR of racemic monoester **6a**. Conversion and *er* were determined by chiral HPLC analysis. Selectivity factors (*s*) was calculated using monoester *er* and reaction conversion (see ref. 15a).

Similarly to the results observed for (±)-*syn*-1,2-diols, the single enantioselective step resulted in low selectivity leading to diester **7a** being recovered with 81:19 *er* (in place of 96:4 *er* detected when the SKR is performed). Later, the optimized reaction conditions (entry 2) have been applied to investigate the scope and limitations of the procedure (Scheme 6 and 7).

C_2- symmetric (±)-*anti*-1,3-diols **5** were used bearing a π-system nearby the reactive centres in the benzylic position. Diol **5b** was resolved with excellent selectivity recording better results with respect to the benchmark reaction. The introduction of electron-withdrawing and electron-donating substituent on the aryl units produced no evident changes in the process, with substrate **5c** and **5d** being resolved with good conversion and excellent enantioselectivity. To note, the KR of derivative **5c** bearing electron-donating substituents provided the diester **7c** with higher enantiomeric purity respect to the KR of the substrate **5d** bearing an electron-withdrawing group. These results can be justified as in the previous case with compound **2d** where the presence of an electron-rich aromatic substituent provides enhanced stabilization of the acylation transition state through π-cation interactions.[22] Overall, monoesters **6a**–**6d** were obtained with low *dr* respect to the corresponding diol and diester and with low

enantioselectivity. These observations are consistent with the results obtained for the homogenous catalyst and can be rationalised by the lower rate of acylation of the small amount of the *syn*-diol which contaminated the starting material, with respect to the *anti*-diol.[5]

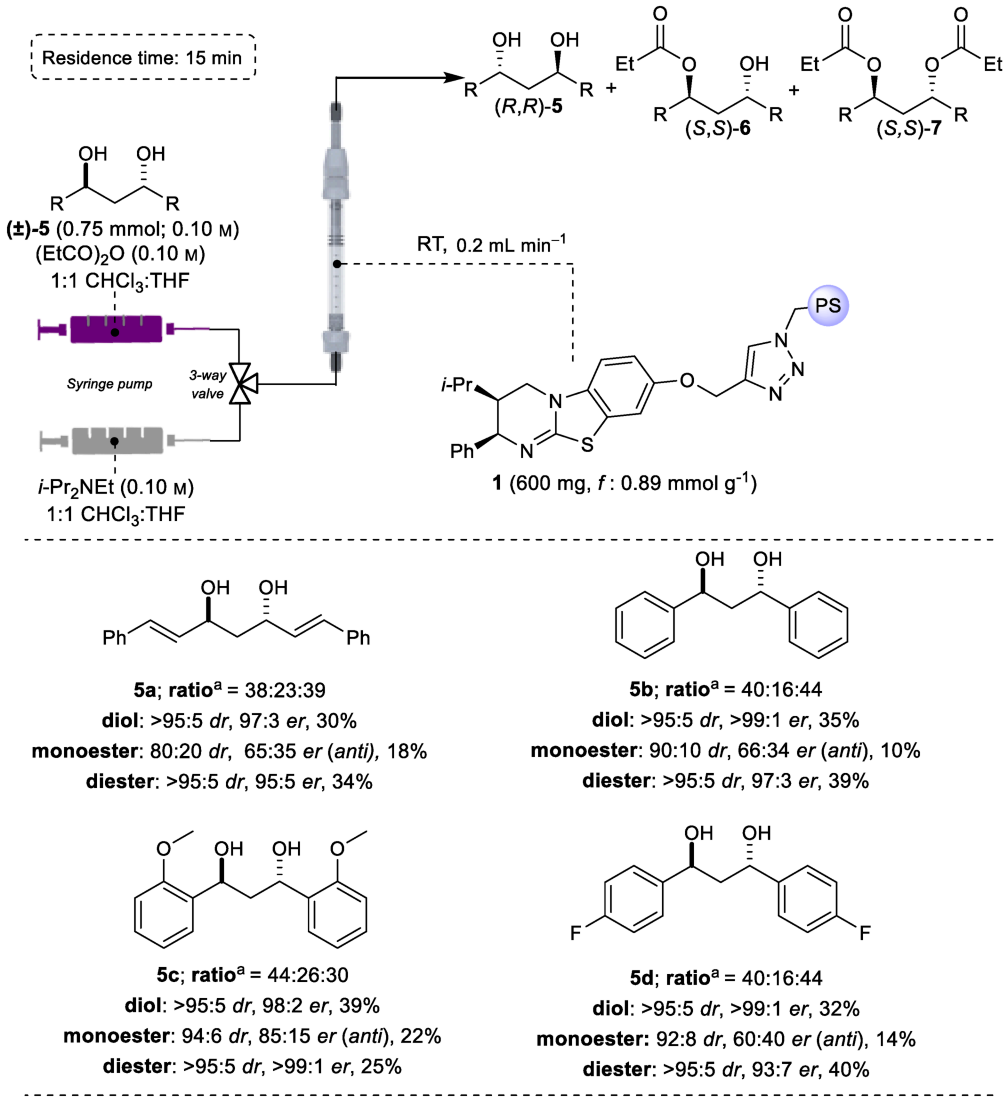

Scheme 6. Reaction scope for C_1-symmetric (±)-*anti*-1,3-diols.[a] Ratio of diol/monoester/diester determined by ^{1}H NMR spectroscopic analysis of the crude reaction product.

As this type of SKR has been successfully applied to C_1-symmetric (±)-*anti*-1,3-diols with the homogeneous catalyst, their behaviour under flow-mode conditions was investigated too (Scheme 7). If the scenario based on the Horeau's principle can be well explained in the case of symmetric 1,2-diol and symmetric 1,3-diols, when unsymmetric compounds are used the system becomes more complex. The two different acylation rates might be very different as suggested by the obtained results. Globally, compounds **5e** and **5f** were resolved with excellent selectivity, with diols **5e** and **5f** and diesters **7e** and **7f** being recovered with high enantioselectivities.

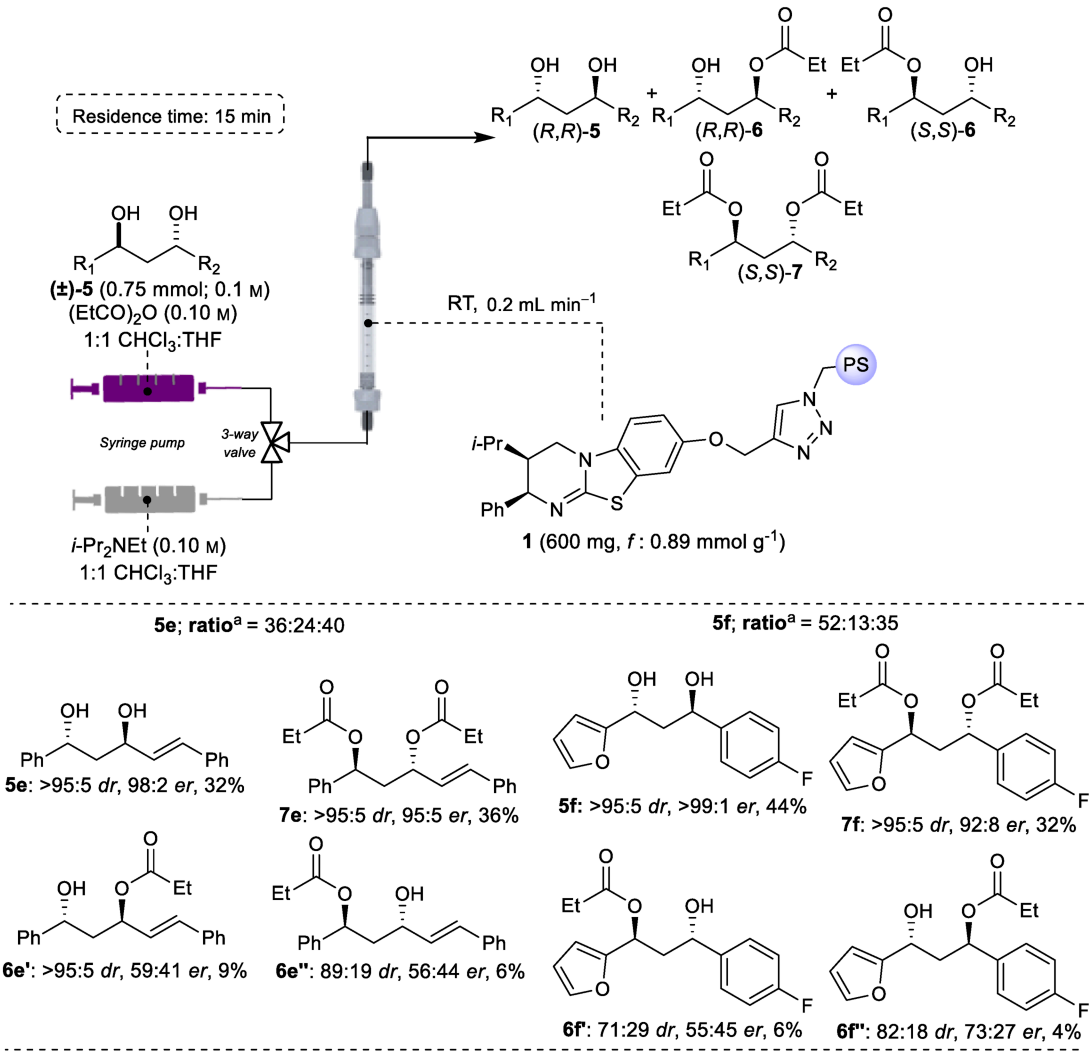

Scheme 7. Reaction scope for C_1-symmetric (±)-*anti*-1,3-diols.[a] Ratio of diol/monoester/diester determined by ^{1}H NMR spectroscopic analysis of the crude reaction product.

The corresponding monoesters **6e'** and **6e''** and **6f'** and **6f''** were all isolated with low *er* and generally, with lower *dr* with respect to the starting *anti*-1,3-diols. Noteworthy, these monoesters showed an opposite configuration: one is the same of the starting diol and the second one of the corresponding diester. These results suggest that each constitutional isomer has a different inflection point where the enantiomer of monoester switches from (*S*,*S*) to (*R*,*R*). Stopping the reaction at lower conversion both constitutional isomer of monoester would be enriched in the (*S*,*S*)-enantiomer, whilst at high conversion they would be enriched in the (*R*,*R*)-enantiomer. This behaviour is displayed in Scheme 8 and can be explained as the results of eight independent rate constants and the reaction conversion, which is controlled by the concentration of reagents, catalyst bed loading and flow-rate.

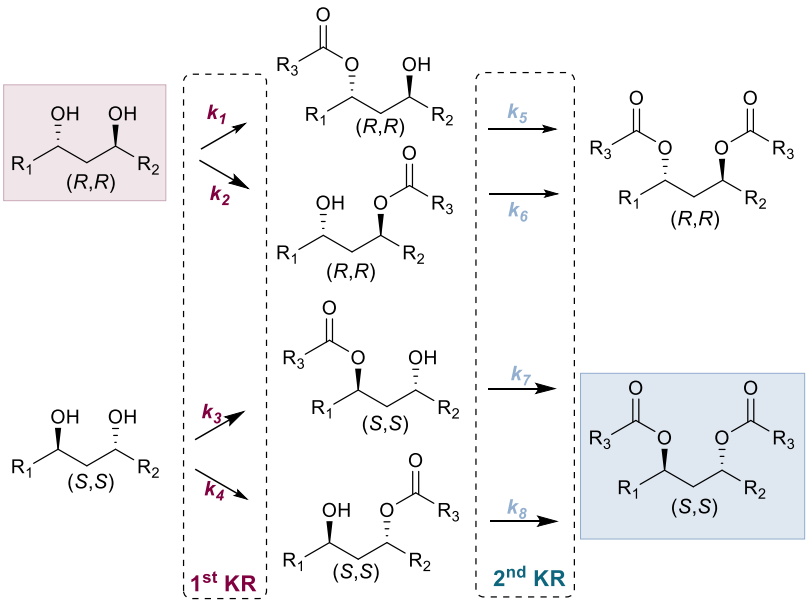

Scheme 8. Double organocatalytic Kinetic Resolution of C_1-symmetric (±)-*anti*-1,3-diols.

Lastly, a suggested acylation transition state (TS) for the fast and slow reacting enantiomers, for simple (±)-*syn*-1,2- and *(±)-anti*-1,3- diols, have been proposed to explain the enantioselectivity of these KRs. For the sake of simplicity in the following figures only one of the two reactive carbinol center has been considered for the purpose of the representation.

Building upon former studies,[22] interactions which govern enantiodiscrimination have been hypothesized. Firstly, the formation of a S•••O interaction (chalcogen bond) is considered responsible to stabilize the conformation of acylated HyperBTM exhibiting *syn* coplanarity of the 1,5-O and S atom. Secondly, the benzene ring of the catalyst supplies π- π and cation-π stabilizing interactions with the aromatic part of the (±)-*syn*-1,2-diol **2a** favoring the (*R*,*R*)-substrate. The (*S*,*S*)-enantiomer is considered to be less reactive due to steric repulsion among the *i*-Pr group and the R substituent of the secondary alcohol (Figure 2).

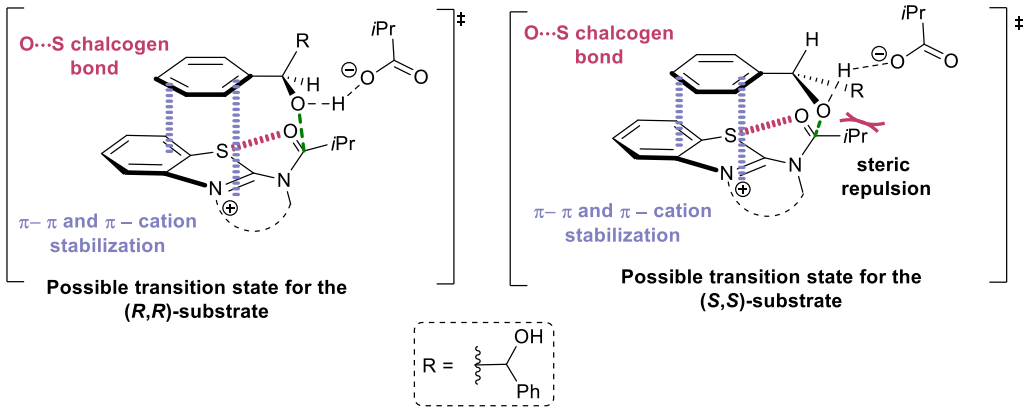

Figure 2. Suggested acylation TSs for the fast and slow reacting enantiomers of (±)-*syn*-1,2-diols.

Similarly, a supplies π- π and π-cation stabilizing interactions can also be found in the suggested transition state which involve the (±)-*anti*-1,3-diol **5a**. However, in this case, the presence of steric repulsion, which occur in the (*R*,*R*)-substrate among the phenyl group of the catalyst and the R group of the secondary alcohol, could decrease the stabilization of this TS, thus favouring the reactivity of the enantiomer (Figure 3).

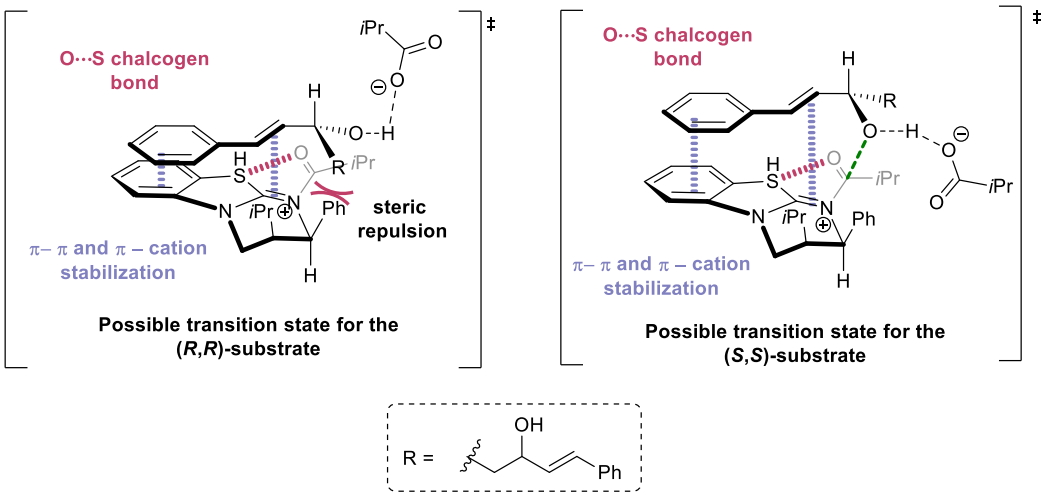

Figure 3. Suggested acylation TSs for the fast and slow reacting enantiomers of (±)-*anti*-1,3-diols.

Although these models account for the sense of asymmetric induction in these kinetic resolutions, they are currently speculative as further investigations are needed to better understand the geometry of the transition state.

8.3 Conclusion

In conclusion, a double organocatalytic kinetic resolution of (±)-*syn*-1,2-diols and (±)-*anti*-1,3-diols under flow-mode conditions has been presented. Excellent results in terms of isolated yield and enantioselectivity have been obtained for both processes. It worth to note that the developed procedure has been conducted at room temperature, in place of low temperature as for the reaction performed with the homogeneous catalyst.[4,5] The use of room temperature makes the process operationally simple to perform and the use of a flow-mode system makes the overall method more environmentally sustainable. Moreover, the flow-mode conditions led to an increase of the productivity, accompanied by an easily scale-up thanks to the use of a packed bed reactor which has proved to work for more than 100 h without loss of efficiency.[24]

8.4 Experimental section

General procedure

Reactions involving moisture sensitive reagents were carried out in flame-dried glassware under an argon or nitrogen atmosphere using standard vacuum line techniques and using anhydrous solvents. Anhydrous solvents (THF) were obtained from an anhydrous solvent system (purified using an alumina column, Mbraun SPS-800). All other reactions were performed in standard glassware with no precautions to exclude air or moisture. Solvents and commercial reagents were used as supplied without further purification unless otherwise stated.

'in vacuo' refers to the use of either a Büchi Rotavapor R-200 with a Büchi V-491 heating bath and Büchi V-800 vacuum controller, a Büchi Rotavapor R-210 with a Büchi V-491 heating bath and Büchi V-850 vacuum controller, a Heidolph Laborota 4001 with vacuum controller, an IKA RV10 rotary evaporator with a IKA HB10 heating bath and ILMVAC vacuum controller, or an IKA RV10 rotary evaporator with a IKA HB10 heating bath and Vacuubrand CVC3000 vacuum controller. Rotary evaporator condensers are fitted to Julabo FL601 Recirculating Coolers filled with ethylene glycol and set to –5 °C. Analytical thin layer chromatography was performed on pre-coated aluminium plates (Kieselgel 60 F_{254} silica). TLC visualisation was carried out with ultraviolet light (254 nm), followed by staining with a 1% aqueous $KMnO_4$ solution. Manual column chromatography was performed in glass columns fitted with porosity 3 sintered discs over Kieselgel 60 silica using the solvent system stated. HPLC analyses were obtained using either a Shimadzu HPLC consisting of a DGU-20A5 degassing unit, LC-20AT liquid chromatography pump, SIL-20AHT autosampler, CMB-20A communications bus module, SPD-M20A diode array detector and a CTO-20A column oven; or a Shimadzu HPLC consisting of a DGU-20A5R degassing unit, LC-20AD liquid chromatography pump, SIL-20AHT autosampler, SPD-20A UV/Vis detector and a CTO-20A column oven. Separation was achieved using DAICEL CHIRALCEL OD-H and OJ-H columns or DAICEL CHIRALPAK ID, IC and AS-H columns. All HPLC traces of enantiomerically-enriched compounds were compared with authentic racemic spectra. ^{1}H, ^{13}C, and ^{19}F nuclear magnetic resonance (NMR) spectra were acquired on either a Bruker Avance II 400 (^{1}H 400 MHz; ^{13}C 101 MHz; ^{19}F 377 MHz, ^{19}F 377 MHz) or a Bruker Avance II 500 (^{1}H 500 MHz; ^{13}C 126 MHz; ^{19}F 470 MHz) spectrometer at ambient temperature in the deuterated solvent stated. All chemical shifts are quoted in parts per million (ppm) and referenced to the residual solvent peak. All coupling constants, *J*, are quoted in Hz. NMR peak assignments of monoester **6** were confirmed using 2D ^{1}H–^{13}C heteronuclear single quantum coherence (HSQC) and 2D ^{1}H–^{13}C heteronuclear multiple-bond correlation spectroscopy (HMBC). Absolute configuration of monoester **6** were

determined following hydrolysis to the corresponding diol and through CSP-HPLC analysis. Melting points were recorded on an Electrothermal 9100 melting point apparatus and are uncorrected. Optical rotations were measured on a Perkin Elmer Precisly/Model-341 polarimeter operating at the sodium D line with a 100 mm path cell at 20 °C.

Infrared spectra were recorded on a Shimadzu IRAffinity-1 Fourier transform IR spectrophotometer fitted with a Specac Quest ATR accessory (diamond puck). Spectra were recorded of either thin films or solids, with characteristic absorption wave numbers (vmax) reported in cm^{-1}. Continuous flow experiments: the catalyst resin was packed into an Omnifit column [borosilicate glass; length = 100 mm (70 mm adjustable bed height); internal diameter = 10 mm; maximum bed volume 5.6 mL]. A Gilson 305 HPLC pump was used to pump solvent for column equilibration and regeneration. A Legato 200 series syringe pump (World Precision Instruments) was used to deliver solutions of reagents.

For the kinetic resolution, selectivity factors (*s*) were calculated according to Kagan's equation: $s = \ln((1-\text{Conv.})(1-ee_{rsm}))/\ln((1-\text{Conv.})(1+ee_{rsm})) = \ln(1-\text{Conv.}(1+ee_{prod}))/\ln(1-\text{Conv.}(1-ee_{prod}))$, wherein Conv. is conversion of the reaction, ee_{prod} is the enantiomeric excess of diester product and ee_{rsm} is the enantiomeric excess of the recovered monoester. Conversions (Conv.) were calculated by the following equation: $\text{Conv.} = ee_{rsm}/(ee_{prod}+ee_{rsm})$.[12a]

Synthesis of (±)-1,2-Diol, monoesters (±)-3, and diesters (±)-4

(±)-1,2-Diols **2a-2g,** monoesters (±)-**3** and diesters (±)-**4** were synthesized following a literature procedure.[4] Spectral data were in accordance with the literature.[25,26]

Synthesis of (±)-1,3-Diols and monoester (±)-6a

(±)-1,3-Diols **5** and monoester (±)-**6a** were synthesised following a literature procedure.[5] Spectral data were in accordance with the literature.[5]

General procedure of Kinetic Resolution (±)-1,2-Diols 2 in flow-mode conditions

A packed bed reactor consisting of a vertically-mounted Omnifit glass chromatography column [borosilicate glass; length = 100 mm (70 mm adjustable bed height); internal diameter = 10 mm; maximum bed volume 5.6 mL], with a glass cooling jacket was loaded with PS-HyperBTM resin (600 mg; f = 0.89 mmol g^{-1}). The resin was allowed to swell to its maximum volume by pumping $CHCl_3$ at 1 mL min^{-1} for 30 min at room temperature using a Gilson 305 HPLC pump. Two syringes were used to inject reagents using a Legato 200 series syringe pump by World Precision Instruments. The first syringe was filled with a solution of the appropriate diol (2.0 mmol, 1.0 equiv.) and $(i\text{-PrCO})_2O$ (3.5 mmol, 1.75 equiv.) in $CHCl_3$ (10 mL total

volume) and the second syringe with *i*-Pr_2NEt (3.5 mmol, 1.75 equiv.) in $CHCl_3$ (10 mL total volume). Both solutions were injected at 50 μL min^{-1}, mixed in a T-type mixing chamber, and passed through the reactor at a combined flow rate of 100 μL min^{-1}. After complete addition of the reagents from the syringes, a Gilson 305 HPLC pump was connected, and $CHCl_3$ was pumped at 100 μL min^{-1} for 30 min to ensure elution of the products. A solution of 10% MeOH in $CHCl_3$ was then pumped at 200 μL min^{-1} for 30 min to wash the column and avoid cross contamination. The column was then prepared for the next KR by pumping $CHCl_3$ at 200 μL min^{-1} for 30 min. The mixture was diluted with CH_2Cl_2 and washed sequentially with HCl (1 M), saturated $NaHCO_3$ and brine. The organic layer was dried (Na_2SO_4), filtered and concentrated to give the crude products which were purified by column chromatography.

Hydrolysis of diesters and monoesters

In some instances it was difficult to find conditions to separate the enantiomers of diesters or monoesters by HPLC using a chiral support, and therefore these products were hydrolysed to the diol prior to HPLC analysis: $LiOH•H_2O$ (3 equiv.) was added to a solution of the diester or monoester (1 equiv.) in MeOH (0.3 M) and allowed to stir at 50 °C until completion, based on TLC analysis. The mixture was diluted with EtOAc and washed sequentially with HCl (1 M), saturated $NaHCO_3$ and brine. The organic layer was dried (Na_2SO_4), filtered and concentrated to give the diol product.

Kinetic Resolution of (±)-1,2-diphenylethane-1,2-diol ((±)-2a)

According to the **General Procedure**, (±)-1,2-diphenylethane-1,2-diol (428 mg, 2.0 mmol) and (*i*-PrCO)$_2$O (580 μL, 3.5 mmol, 1.75 equiv.) in $CHCl_3$ (10 mL total volume), and *i*-Pr_2NEt (610 μL, 3.5 mmol, 1.75 equiv.) in $CHCl_3$ (10 mL total volume) gave crude products that were purified by column chromatography (80:20 to 60:40 Hexane:EtOAc) to give:

(1*S*,2*S*)-1,2-Diphenylethane-1,2-diol (2a)

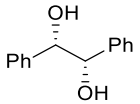

(13 mg, 3%) as a colourless solid with spectroscopic data in accordance with the literature.[4,25] **mp** 118−119 °C {Lit.[4] 121 °C}; $[\alpha]_D^{20}$ −87.1 (*c* 0.55 in $CHCl_3$) {Lit.[4] (*ent*, >99:1 er) $[\alpha]_D^{20}$ +88.0 (*c* 0.15 in $CHCl_3$)}; **Chiral HPLC analysis** Chiralpak ID (90:10 Hexane:IPA, flow rate 1.0 mL min^{-1}, 211 nm, 30 °C) t_R(1*R*,2*R*): 11.6 min, t_R(1*S*,2*S*): 14.9 min, 0.63:99.37 *er*; **^{1}H NMR** (400 MHz, $CDCl_3$) δ = 7.28 – 7.20 (m, 6H, ArH), 7.20 – 7.10 (m, 4H, ArH), 4.74 (s, 2H, C*H*OH), 2.97 – 2.74 (brs, 2H, O*H*).

(1*S*,2*S*)-2-Hydroxy-1,2-diphenylethyl isobutyrate (3a)

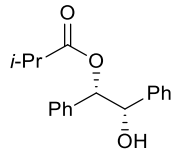

(200 mg, 35%) as a colourless solid with spectroscopic data in accordance with the literature.[26] **mp** 80−82 °C; $[\alpha]_D^{20}$ −6.2 (*c* 0.50 in $CHCl_3$) {Lit.[4] (*ent*, >99:1 *er*) $[\alpha]_D^{20}$ +2.6 (*c* 0.50 in $CHCl_3$)}; **Chiral HPLC analysis** Chiralcel OD-H (95:5 Hexane:IPA, flow rate 1 mL min^{-1}, 211 nm, 30 °C) t_R (1*S*,2*S*): 11.9 min, t_R (1*R*,2*R*): 17.5 min, 97.90:2.10 *er*; **^{1}H NMR** (400 MHz, $CDCl_3$) δ = 7.28 – 7.22 (m, 6H, ArH), 7.22 – 7.07 (m, 4H, ArH), 5.88 (d, *J* 7.1 Hz, 1H, C*H*OC(O)*i*-Pr), 4.96 (dd, *J* 7.1, 3.3 Hz, 1H, C*H*OH), 2.66 (hept, *J* 7.0 Hz, 1H, C*H*CH_3), 2.53 (d, *J* 3.6 Hz, 1H, OH), 1.19 (d, *J* 7.0 Hz, 3H, CH_3), 1.18 (d, *J* 7.0 Hz, 3H, CH_3).

(1*R*,2*R*)-1,2-Diphenylethane-1,2-diyl bis(2-methylpropanoate) (4a)

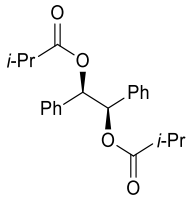

(340 mg, 48%) as a colourless solid with spectroscopic data in accordance with the literature.[26] **mp** 71−72 °C {Lit.[26] 73−74 °C}; $[\alpha]_D^{20}$ −22.9 (*c* 1.0 in $CHCl_3$) {Lit.[4] (*ent,* 97:3 *er*) $[\alpha]_D^{20}$ +20.2 (*c* 1.0 in $CHCl_3$)}; following hydrolysis to 1,2-diphenylethane-1,2-diol: **Chiral HPLC analysis** Chiralpak ID (90:10 Hexane:IPA, flow rate 1.0 mL min^{-1}, 211 nm, 30 °C) t_R(1*R*,2*R*): 12.7 min, t_R(1*S*,2*S*): 15.4 min, 94.45:5.55 *er*; **^{1}H NMR** (400 MHz, $CDCl_3$) δ = 7.27 – 7.17 (m, 6H, ArH), 7.18 – 7.07 (m, 4H, ArH), 6.07 (s, 2H, C*H*OC(O)*i*-Pr), 2.60 (hept, *J* 7.0 Hz, 2H, C*H*CH_3), 1.17 (d, *J* 7.0 Hz, 6H, CH_3), 1.16 (d, *J* 7.0 Hz, 6H, CH_3).

Kinetic Resolution of (±)-1,2-bis(4-chlorophenyl)ethane-1,2-diol ((±)-2b)

According to the **General Procedure**, (±)-1,2-bis(4-chlorophenyl)ethane-1,2-diol (567 mg, 2.0 mmol) and $(i\text{-PrCO})_2O$ (580 µL, 3.5 mmol, 1.75 equiv.) in $CHCl_3$ (10 mL total volume) and *i*-Pr_2NEt (610 µL, 3.5 mmol, 1.75 equiv.) in $CHCl_3$ (10 mL total volume) gave crude products that were purified by column chromatography (80:20 to 60:40 Hexane:EtOAc) to give:

(1*S*,2*S*)-1,2-bis(4-chlorophenyl)ethane-1,2-diol (2b)

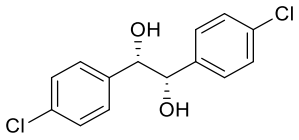

(45 mg, 8%) as a colourless solid with spectroscopic data in accordance with the literature.[27] **mp** 131−133 °C {Lit.[28] 126−128 °C}; $[\alpha]_D^{20}$ −183.0 (*c* 0.25 in $CHCl_3$) {Lit.[4] (*ent*, >99:1 *er*) $[\alpha]_D^{20}$ +112 (*c* 0.25 in $CHCl_3$)}; **Chiral HPLC analysis** Chiralpak AS-H (98:2 Hexane:IPA, flow rate 1 mL min^{-1}, 220 nm, 30 °C) t_R (1*S*,2*S*): 41.5 min, 0:100 *er*; **^{1}H NMR** (500 MHz, $CDCl_3$) δ = 7.27 – 7.18 (m, 4H, ArH), 7.09 – 7.00 (m, 4H, ArH), 4.65 (t, *J* 1.2 Hz, 2H, C*H*OH), 2.91 (q, *J* 1.2 Hz, 2H, OH).

(1*S*,2*S*)-1,2-bis(4-chlorophenyl)-2-hydroxyethyl isobutyrate (3b)

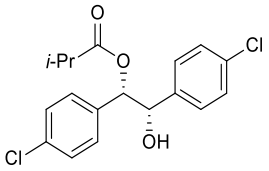

(240 mg, 34%) as a colourless solid with spectroscopic data in accordance with the literature.[4] **mp** 141−142 °C {Lit.[4] 143 °C}; $[\alpha]_D^{20}$ −34.5 (*c* 1.0 in $CHCl_3$) {Lit.[4] (*ent*, 99:1 *er*) $[\alpha]_D^{20}$ +35.0 (*c* 1.0 in $CHCl_3$)}; **Chiral HPLC analysis** Chiralpak AS-H (99.5:0.5 Hexane:IPA, flow rate 0.7 mL min^{-1}, 220 nm, 30 °C) t_R (1*S*,2*S*): 35.9 min, t_R (1*R*,2*R*): 46.7 min, 95.53:4.47 *er*; **^{1}H NMR** (400 MHz, $CDCl_3$) δ = 7.28 – 7.19 (m, 4H, ArH), 7.13 – 6.98 (m, 4H, ArH), 5.76 (d, *J* 7.3 Hz, 1H, C*H*OC(O)*i*-Pr), 4.91 (dd, *J* 7.3, 3.3 Hz, 1H, C*H*OH), 2.65 (hept, *J* 7.0 Hz, 1H, C*H*CH_3), 2.54 (d, *J* 3.4 Hz, 1H, OH), 1.20 (d, *J* 7.0 Hz, 3H, CH_3), 1.18 (d, *J* 7.0 Hz, 3H, CH_3),.

(1*R*,2*R*)-1,2-bis(4-chlorophenyl)ethane-1,2-diyl bis(2-methylpropanoate) (4b)

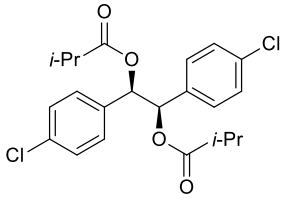

(381 mg, 45%) as a colourless oil with spectroscopic data in accordance with the literature.[4] $[\alpha]_D^{20}$ −5.3 (*c* 1.0 in $CHCl_3$) {Lit.[4] (*ent*, 95:5 *er*) $[\alpha]_D^{20}$ +4.8 (*c* 0.5 in $CHCl_3$)}; following hydrolysis to 1,2-bis(4-chlorophenyl)ethane-1,2-diol: **Chiral HPLC analysis** Chiralpak AS-H (98:2 Hexane:IPA, flow rate 1 mL min^{-1}, 220 nm, 30 °C) t_R (1*R*,2*R*): 31.0 min, t_R (1*S*,2*S*): 43.8 min, 93.62:6.38 *er*; **^{1}H NMR** (400 MHz, $CDCl_3$) δ = 7.27 – 7.17 (m, 4H, ArH), 7.12 – 7.02 (m, 4H, ArH), 5.99 (s, 2H, C*H*OC(O)*i*-Pr), 2.59 (hept, *J* 7.0 Hz, 2H, C*H*CH_3), 1.17 (d, *J* 7.0 Hz, 6H, CH_3), 1.15 (d, *J* 7.0 Hz, 6H, CH_3),.

Kinetic Resolution of (±)-1,2-bis(4-chlorophenyl)ethane-1,2-diol ((±)-2c)

According to the **General Procedure**, (±)-1,2-bis(4-(trifluoromethyl)phenyl)ethane-1,2-diol (700 mg, 2.0 mmol) and (*i*-PrCO)$_2$O (580 µL, 3.5 mmol, 1.75 equiv.) in $CHCl_3$ (10 mL total volume) and *i*-Pr$_2$NEt (610 µL, 3.5 mmol, 1.75 equiv.) in $CHCl_3$ (10 mL total volume) gave crude products that were purified by column chromatography (80:20 to 60:40 Hexane:EtOAc) to give:

(1*S*,2*S*)-1,2-bis(4-(trifluoromethyl)phenyl)ethane-1,2-diol (2c)

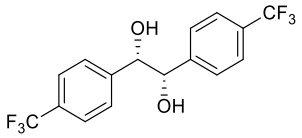

(8 mg, 1%) as a colourless solid with spectroscopic data in accordance with the literature.[26] **mp** 135−137 °C {Lit.[29] 128−130 °C}; $[\alpha]_D^{20}$ −10.7 (*c* 0.7 in $CHCl_3$) {Lit.[4] (*ent*, >99:1 *er*) $[\alpha]_D^{20}$ +41.1 (*c* 1.0 in $CHCl_3$)}; **Chiral HPLC analysis** Chiralpak AS-H (97:3 Hexane:IPA, flow rate 1 mL min^{-1}, 220 nm, 30 °C) t_R (1*R*,2*R*): 11.3 min, t_R (1*S*,2*S*): 15.6 min, 0.27:99.73 *er*; **^{1}H NMR** (500 MHz, $CDCl_3$) δ = 7.54 (d, *J* 8.1 Hz, 4H, ArH), 7.26 (d, *J* 8.0 Hz, 4H, ArH), 4.81 – 4.73 (m, 2H, C*H*OH), 2.98 (t, *J* 1.4 Hz, 2H, OH); **^{19}F NMR** (377 MHz, $CDCl_3$) δ = −62.58.

(1*S*,2*S*)-2-hydroxy-1,2-bis(4-(trifluoromethyl)phenyl)ethyl isobutyrate (3c)

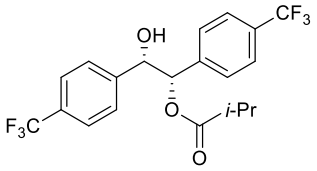

(285 mg, 34%) as a colourless solid with spectroscopic data in accordance with the literature.[26] **mp** 147−148 °C {Lit.[26] 148 °C}; $[\alpha]_D^{20}$ −4.4 (*c* 1.0 in $CHCl_3$) {Lit.[26] (96:4 *er*) $[\alpha]_D^{23}$ −1.06 (*c* 1.01 in $CHCl_3$)}; **Chiral HPLC analysis** Chiralcel OJ-H (95:5 Hexane:IPA, flow rate 1 mL min^{-1}, 220 nm, 30 °C) t_R (1*S*,2*S*): 7.7 min, 100:0 *er*; **^{1}H NMR** (400 MHz, $CDCl_3$) δ = 7.55 (dd, *J* 8.3, 2.1 Hz, 4H, ArH), 7.34 – 7.23 (m, 4H, ArH), 5.91 (d, *J* 6.6 Hz, 1H, C*H*OC(O)*i*-Pr), 5.05 (dd, *J* 6.7, 3.7 Hz, 1H, C*H*OH), 2.67 (hept, *J* 7.0 Hz, 1H, C*H*CH$_3$), 2.58 (d, *J* 3.7 Hz, 1H, OH), 1.19 (d, *J* 7.1 Hz, 6H, CH*$_3$*); **^{19}F NMR** (377 MHz, $CDCl_3$) δ = −62.61, −62.68.

(1*R*,2*R*)-1,2-bis(4-(trifluoromethyl)phenyl)ethane-1,2-diyl bis(2-methylpropanoate) (4c)

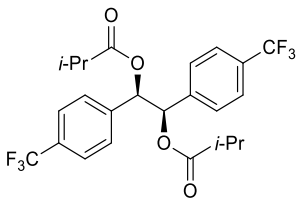

(520 mg, 53%) as a colourless solid with spectroscopic data in accordance with the literature.[26] **mp** 109−110 °C {Lit.[26] 108 °C}; $[\alpha]_D^{20}$ −9.0 (*c* 1.0 in $CHCl_3$) {Lit.[4] (*ent*, 97:3 *er*) $[\alpha]_D^{20}$ +11.0 (*c* 0.10 in $CHCl_3$)}; following hydrolysis to 1,2-bis(4-(trifluoromethyl)phenyl)ethane-1,2-diol: **Chiral HPLC analysis** Chiralpak AS-H (97:3 Hexane:IPA, flow rate 1 mL min^{-1}, 211 nm, 30 °C) t_R (1*R*,2*R*): 11.5 min, t_R (1*S*,2*S*): 15.8 min, 81.67:18.33 *er*; **^{1}H NMR** (400 MHz, $CDCl_3$) δ = 7.62 – 7.46 (m, 4H, ArH), 7.22 – 7.34 (m, 4H, ArH), 6.12 (s, 2H, C*H*OC(O)*i*-Pr), 2.69 – 2.55 (m, *J* 6.9 Hz, 2H, C*H*CH_3), 1.16 (d, *J* 7.0 Hz, 12H, CH_3); **^{19}F NMR** (377 MHz, $CDCl_3$) δ = −62.72.

Kinetic Resolution of (±)-1,2-bis(4-methoxyphenyl)ethane-1,2-diol ((±)-2d)

According to the **General Procedure**, (±)-1,2-diphenylethane-1,2-diol (548 mg, 2.0 mmol) and (*i*-PrCO)$_2$O (580 µL, 3.5 mmol, 1.75 equiv.), in $CHCl_3$ (10 mL total volume), and *i*-Pr_2NEt (610 µL, 3.5 mmol, 1.75 equiv.) in $CHCl_3$ (10 mL total volume) gave crude products that were purified by column chromatography (80:20 to 60:40 Hexane:EtOAc) to give:

(1*S*,2*S*)-1,2-bis(4-methoxyphenyl)ethane-1,2-diol (2d)

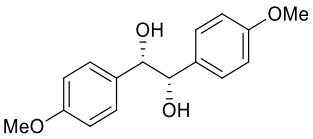

(33 mg, 6%) as a colourless solid with spectroscopic data in accordance with the literature.[30] **mp** 106−107 °C {Lit.[28] 118−119 °C}; $[\alpha]_D^{20}$ −102 (*c* 0.25 in $CHCl_3$) {Lit.[4] (*ent*, >99:1 *er*) $[\alpha]_D^{20}$ +126 (*c* 0.25 in $CHCl_3$)}; **Chiral HPLC analysis** Chiralpak ID (80:20 Hexane:IPA, flow rate 1 mL min^{-1}, 211 nm, 30 °C) t_R (1*S*,2*S*): 24.09 min, 0:100 *er*; **^{1}H NMR** (400 MHz, $CDCl_3$) δ = 7.11 – 7.02 (m, 4H, ArH), 6.84 – 6.74 (m, 4H, ArH), 4.66 (s, 2H, C*H*OH), 3.79 (s, 6H, OCH_3), 2.89 (s, 2H, OH).

(1*S*,2*S*)-2-hydroxy-1,2-bis(4-methoxyphenyl)ethyl isobutyrate (3d)

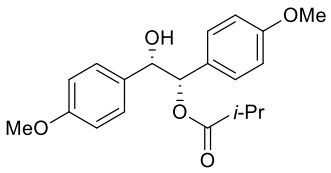

(254 mg, 37%) as a colourless solid with spectroscopic data in accordance with the literature.[4] **mp** 88−89 °C {Lit.[4] 88 °C}; $[\alpha]_D^{20}$ −26.7 (*c* 0.5 in $CHCl_3$) {Lit.[4] $[\alpha]_D^{20}$ (*ent*, 99:1 *er*) +23.6 (*c* 0.5 in $CHCl_3$)}; following hydrolysis to 1,2-bis(4-methoxyphenyl)ethane-1,2-diol: **Chiral HPLC analysis** Chiralpak ID (85:15 Hexane:IPA, flow rate 1 mL min^{-1}, 211 nm, 30 °C) t_R (1*R*,2*R*): 21.91 min, t_R (1*S*,2*S*): 36.53 min, 1.56:98.44 *er*; **^{1}H NMR** (400 MHz, $CDCl_3$) δ = 7.13

– 6.98 (m, 4H, ArH), 6.84 – 6.71 (m, 4H, ArH), 5.78 (d, *J* 7.7 Hz, 1H, C*H*OC(O)*i*-Pr), 4.89 (d, *J* 7.8 Hz, 1H, C*H*OH), 3.78 (d, *J* 3.8 Hz, 6H, OCH_3), 2.65 (hept, *J* 7.0 Hz, 1H, C*H*CH_3), 1.20 (d, *J* 7.0 Hz, 3H, CH_3), 1.18 (d, *J* 7.0 Hz, 3H, CH_3).

(1*R*,2*R*)-1,2-bis(4-methoxyphenyl)ethane-1,2-diyl bis(2-methylpropanoate) (4d)

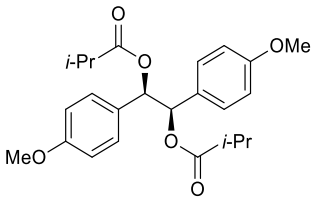

(380 mg, 45%) as a colourless oil with spectroscopic data in accordance with the literature.[26] **mp** 122−124 °C {Lit.[4] 126−128 °C}; $[\alpha]_D^{20}$ −25.0 (*c* 1.0 in $CHCl_3$) {Lit.[4] $[\alpha]_D^{20}$ (*ent*, 98:2 *er*) +19.3 (*c* 1.0 in $CHCl_3$)}; following hydrolysis to 1,2-bis(4-methoxyphenyl)ethane-1,2-diol: **Chiral HPLC analysis** Chiralpak ID (85:15 Hexane:IPA, flow rate 1 mL min^{-1}, 211 nm, 30 °C) t_R (1*R*,2*R*): 21.81 min, t_R (1*S*,2*S*): 38.61 min, 94.66:5.34 *er*; **^{1}H NMR** (400 MHz, $CDCl_3$) δ = 7.11 – 7.00 (m, 4H, ArH), 6.83 – 6.68 (m, 4H, ArH), 6.00 (s, 2H, C*H*OC(O)*i*-Pr), 3.76 (s, 6H, OCH_3), 2.58 (hept, *J* 7.0 Hz, 2H, C*H*CH_3), 1.18 (d, *J* 7.0 Hz, 6H, CH_3), 1.15 (d, *J* 7.0 Hz, 6H, CH_3).

Kinetic Resolution of (±)-1,2-di(naphthalen-1-yl)ethane-1,2-diol ((±)-2e)

According to the **General Procedure**, (±)-1,2-di(naphthalen-1-yl)ethane-1,2-diol (628 mg, 2.0 mmol) and (*i*-PrCO)$_2$O (580 µL, 3.5 mmol, 1.75 equiv.), in 1:1 $CHCl_3$:THF mixture (10 mL total volume), and *i*-Pr_2NEt (610 µL, 3.5 mmol, 1.75 equiv.) in 1:1 $CHCl_3$:THF mixture (10 mL total volume) gave crude products that by column chromatography (80:20 to 60:40 Hexane:EtOAc) to give:

(1*S*,2*S*)-1,2-di(naphthalen-1-yl)ethane-1,2-diol (2e)

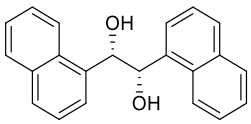

(125 mg, 20%) as a colourless solid with spectroscopic data in accordance with the literature.[26] **mp** 128−130 °C {Lit.[31] 122−124 °C}; $[\alpha]_D^{20}$ −28.6 (*c* 0.25 in $CHCl_3$) {Lit.[4] $[\alpha]_D^{24}$ (*ent*, 88:12 *er*) +40.7 (*c* 0.99 in THF)}; **Chiral HPLC** Chiralpak OJ-H (80:20 Hexane:IPA, flow rate 1 mL min^{-1}, 220 nm, 30 °C) t_R (1*S*,2*S*): 22.6 min, t_R (1*R*,2*R*): 33.7 min, 97.49:2.51 *er*; **^{1}H NMR** (500 MHz, $CDCl_3$) δ = 7.90 (dd, *J* 8.6, 1.2 Hz, 2H, ArH); 7.87 – 7.65 (m, 6H, ArH), 7.47 – 7.35 (m, 4H, ArH), 7.31 (ddd, *J* 8.3, 6.8, 1.4 Hz, 2H, ArH), 5.86 – 5.76 (m, 2H, C*H*OH), 3.00 (dd, *J* 2.1, 1.1 Hz, 2H, OH).

(1*S*,2*S*)-2-hydroxy-1,2-di(naphthalen-1-yl)ethyl isobutyrate (3e)

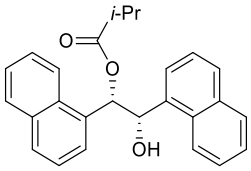

(177 mg, 23%) as a colourless oil with spectroscopic data in accordance with the literature.[4] **mp** 102−104 °C {Lit.[4] 110−111 °C}; $[\alpha]_D^{20}$ −49.4 (*c* 1.2 in $CHCl_3$) {Lit.[4] $[\alpha]_D^{20}$ (*ent*, >99:1 *er*) +57.2 (*c* 1.0 in $CHCl_3$)}; following hydrolysis to 1,2-di(naphthalen-1-yl)ethane-1,2-diol **Chiral HPLC** Chiralpak OJ-H (80:20 Hexane:IPA, flow rate 1 mL min^{-1}, 220 nm, 30 °C) t_R (1*S*,2*S*): 23.1 min, t_R (1*R*,2*R*): 33.5 min, 70.30:29.70 *er*; **^{1}H NMR** (400 MHz, $CDCl_3$) δ = 8.14 – 8.01 (m, 2H, ArH), 7.80 – 7.66 (m, 4H, ArH), 7.63 – 7.48 (m, 2H, ArH), 7.47 – 7.31 (m, 6H, ArH), 6.94 (d, *J* 6.5 Hz, 1H, C*H*OC(O)*i*-Pr), 5.95 (d, *J* 6.5 Hz, 1H, C*H*OH), 2.66 (dp, *J* 31.8, 7.0 Hz, 1H, C*H*CH_3), 1.20 (d, *J* 7.0 Hz, 3H, CH_3), 1.18 (d, *J* 7.0 Hz, 3H, CH_3).

(1*R*,2*R*)-1,2-di(naphthalen-1-yl)ethane-1,2-diyl bis(2-methylpropanoate) (4e)

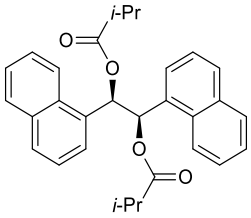

(372 mg, 41%) as a colourless solid with spectroscopic data in accordance with the literature.[26] **mp** 115−117 °C {Lit.[26] 113−114 °C}; $[\alpha]_D^{20}$ +71.2 (*c* 1.0 in $CHCl_3$) {Lit.[4] $[\alpha]_D^{20}$ (*ent*, 95:5 *er*) −67.5 (*c* 1.0 in $CHCl_3$)}; following hydrolysis to 1,2-di(naphthalen-1-yl)ethane-1,2-diol **Chiral HPLC analysis** Chiralpak OJ-H (80:20 Hexane:IPA, flow rate 1 mL min^{-1}, 220 nm, 30 °C) t_R (1*S*,2*S*): 23.9 min, t_R (1*R*,2*R*): 32.4 min, 6.41:93.59 *er*; **^{1}H NMR** (400 MHz, $CDCl_3$) δ = 8.31 – 8.11 (m, 2H, ArH), 7.77 – 7.60 (m, 4H, ArH), 7.39 (td, *J* 6.8, 5.9, 2.9 Hz, 6H, ArH), 7.24 (t, *J* 7.7 Hz, 2H, ArH), 7.11 (s, 2H, C*H*OC(O)*i*-Pr), 2.75 – 2.55 (m, 2H, C*H*CH_3), 1.22 (d, *J* 7.0 Hz, 6H, CH_3), 1.17 (d, *J* 7.0 Hz, 6H, CH_3).

Kinetic Resolution of (±)-(1*E*,5*E*)-1,6-diphenylhexa-1,5-diene-3,4-diol ((±)-2f)

According to the **General Procedure**, (±)-(1*E*,5*E*)-1,6-diphenylhexa-1,5-diene-3,4-diol (532 mg, 2.0 mmol) and (*i*-PrCO)$_2$O (580 µL, 3.5 mmol, 1.75 equiv.), in $CHCl_3$ (10 mL total volume), and *i*-Pr_2NEt (610 µL, 3.5 mmol, 1.75 equiv.) in $CHCl_3$ (10 mL total volume) gave crude products that were purified by column chromatography (80:20 to 60:40 Hexane:EtOAc) to give:

(1*E*,3*S*,4*S*,5*E*)-4-hydroxy-1,6-diphenylhexa-1,5-dien-3-yl isobutyrate (3f)

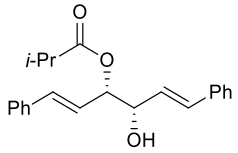

(208 mg, 31%) as a colourless solid with spectroscopic data in accordance with the literature.[4] **mp** 102−103 °C {Lit.[4] 95−96 °C}; $[\alpha]_D^{20}$ −0.6 (*c* 0.4 in $CHCl_3$) {Lit.[4] $[\alpha]_D^{20}$ (*ent,* 77:23 *er*) +0.9 (*c* 1.0 in $CHCl_3$)}; **Chiral HPLC analysis** Chiralpak IC (95:5 Hexane:IPA, flow rate 1 mL min^{-1}, 254 nm, 30 °C) t_R (3*S*,4*S*): 18.0 min, t_R (3*R*,4*R*): 22.7 min, 80.96:19.04 *er*; **^{1}H NMR** (400 MHz, $CDCl_3$) δ = 7.53 – 7.32 (m, 10H, ArH), 6.75 (dt, *J* 16.0, 1.5 Hz, 2H, PhC*H*=CH), 6.26 (ddd, *J* 16.0, 6.5, 5.2 Hz, 2H, PhCH=C*H*), 5.54 (ddd, *J* 7.0, 5.6, 1.1 Hz, 1H, C*H*OC(O)*i*-Pr), 4.53 (td, *J* 5.7, 1.5 Hz, 1H, C*H*OH), 2.66 (hept, *J* 6.8 Hz, 1H, C*H*CH_3), 1.23 (d, *J* 7.1 Hz, 3H, CH_3), 1.21 (d, *J* 7.1 Hz, 3H, CH_3).

(1*E*,3*R*,4*R*,5*E*)-1,6-diphenylhexa-1,5-diene-3,4-diyl bis(2-methylpropanoate) (4f)

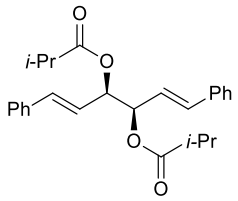

(422 mg, 52%) as a colourless solid with spectroscopic data in accordance with the literature.[4] **mp** 78−80 °C {Lit.[4] 84−85 °C}; $[\alpha]_D^{20}$ −4.57 (*c* 0.35 in $CHCl_3$) {Lit.[4] $[\alpha]_D^{20}$ (*ent*, 79:21 *er*) +10.8 (*c* 1.0 in $CHCl_3$)}; following hydrolysis to (1*E*,5*E*)-1,6-diphenylhexa-1,5-diene-3,4-diol: **Chiral HPLC analysis** Chiralpak ID (85:15 Hexane:IPA, flow rate 1 mL min^{-1}, 254 nm, 30 °C) t_R (1*S*,2*S*): 13.0 min, t_R (1*R*,2*R*): 14.7 min, 35.00:65.00 *er*; **^{1}H NMR** (400 MHz, $CDCl_3$) δ = 7.43 – 7.23 (m, 10H, ArH), 6.72 (d, *J* 15.9 Hz, 2H, PhC*H*=CH), 6.23 – 6.08 (m, 2H, PhCH=C*H*), 5.75 – 5.62 (m, 2H, C*H*OC(O)*i*-Pr), 2.71 – 2.56 (m, *J* 7.0 Hz, 2H, C*H*CH_3), 1.17 (d, *J* 7.1 Hz, 12H, C*H*$_3$).

Kinetic Resolution of (±)-1,6-diphenylhexa-1,5-diyne-3,4-diol ((±)-2g)

According to the **General Procedure**, (±)-1,6-diphenylhexa-1,5-diyne-3,4-diol (525 mg, 2.0 mmol) and (*i*-PrCO)$_2$O (580 µL, 3.5 mmol, 1.75 equiv.), in $CHCl_3$ (10 mL total volume), and *i*-Pr$_2$NEt (610 µL, 3.5 mmol, 1.75 equiv.) in $CHCl_3$ (10 mL total volume) gave crude products that were purified by by column chromatography (80:20 to 60:40 Hexane:EtOAc) to give:

(3*S*,4*S*)-1,6-diphenylhexa-1,5-diyne-3,4-diol (2g)

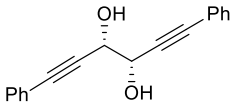

(10 mg, 2%) as a colourless solid with spectroscopic data in accordance with the literature.[4] **mp** 74−77 °C {Lit.[4] 78−79 °C}; $[\alpha]_D^{20}$ −101 (*c* 0.1 in $CHCl_3$) {Lit.[4] $[\alpha]_D^{20}$ (*ent*, >99:1 *er*) +97.2 (*c* 0.25 in $CHCl_3$)}; **Chiral HPLC analysis** Chiralcel OJ-H (80:20 Hexane:IPA, flow rate 1 mL min^{-1}, 211 nm, 30 °C) t_R (3*S*,4*S*): 13.6 min, t_R (3*R*,4*R*): 19.1 min, 77.37:22.63 *er*; **^{1}H NMR** (400 MHz, $CDCl_3$) δ = 7.53 – 7.46 (m, 4H, ArH), 7.40 – 7.31 (m, 6H, ArH), 4.77 (s, 2H, C*H*OH).

(3*S*,4*S*)-4-hydroxy-1,6-diphenylhexa-1,5-diyn-3-yl isobutyrate (3g)

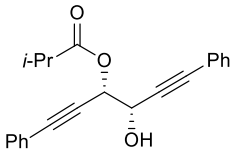

(99 mg, 15%) as a colourless solid with spectroscopic data in accordance with the literature.[4] **mp** 71−72 °C {Lit.[4] 71 °C}; $[\alpha]_D^{20}$ +12.8 (*c* 1.0 in $CHCl_3$) {Lit.[4] $[\alpha]_D^{20}$ (*ent,* 85:15 *er*) −12.2 (*c* 1.0 in $CHCl_3$)}; following hydrolysis to 1,6-diphenylhexa-1,5-diyne-3,4-diol: **Chiral HPLC analysis** Chiralcel OJ-H (80:20 Hexane:IPA, flow rate 1 mL min^{-1}, 211 nm, 30 °C) t_R (3*S*,4*S*): 12.6 min, t_R (3*R*,4*R*): 18.1 min, 88.34:11.66 *er*; **^{1}H NMR** (500 MHz, $CDCl_3$) δ = 7.55 – 7.43 (m, 4H, ArH), 7.40 – 7.30 (m, 6H, ArH), 5.86 (d, *J* 5.7 Hz, 1H, C*H*OC(O)*i*-Pr), 4.87 (d, *J* 5.7 Hz, 1H, C*H*OH), 2.72 (hept, *J* 7.0 Hz, 1H, C*H*CH_3), 1.27 (d, *J* 7.0 Hz, 3H, CH_3), 1.26 (d, *J* 7.0 Hz, 3H, CH_3).

(3*R*,4*R*)-1,6-diphenylhexa-1,5-diyne-3,4-diyl bis(2-methylpropanoate) (4g)

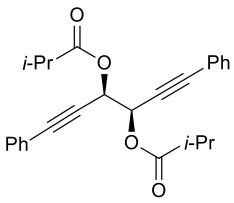

(569 mg, 70%) as a colourless oil with spectroscopic data in accordance with the literature.[4] $[\alpha]_D^{20}$ −10.4 (*c* 1.0 in $CHCl_3$) {Lit.[4] $[\alpha]_D^{20}$ (*ent*, 83:17 *er*) +39.8 (*c* 0.5 in $CHCl_3$)}; following hydrolysis to 1,6-diphenylhexa-1,5-diyne-3,4-diol: **Chiral HPLC analysis** Chiralcel OJ-H (80:20 Hexane:IPA, flow rate 1 mL min^{-1}, 211 nm, 30 °C) t_R (3*S*,4*S*): 12.6 min, t_R (3*R*,4*R*): 18.1 min, 41.64:58.36 *er*; **^{1}H NMR** (500 MHz, $CDCl_3$) δ = 7.50 – 7.43 (m, 4H, ArH), 7.40 –

7.30 (m, 6H, ArH), 6.00 (s, 2H, C*H*OC(O)*i*-Pr), 2.68 (hept, *J* 7.0 Hz, 2H, C*H*CH_3), 1.25 (d, *J* 7.0 Hz, 6H, CH_3), 1.24 (d, *J* 7.0 Hz, 6H, CH_3).

Procedure of Kinetic Resolution (±)-3a in Flow-mode conditions

A packed bed reactor consisting of a vertically-mounted Omnifit glass chromatography column [borosilicate glass; length = 100 mm (70 mm adjustable bed height); internal diameter = 10 mm; maximum bed volume 5.6 mL], with a glass cooling jacket was loaded with PS-HyperBTM resin (600 mg; f = 0.89 mmol g^{-1}). The resin was allowed to swell to its maximum volume by pumping $CHCl_3$ at 1 mL min^{-1} for 30 min at room temperature using a Gilson 305 HPLC pump. Two syringes were used to inject reagents using a Legato 200 series syringe pump by World Precision Instruments. The first syringe was filled with a solution of 2-hydroxy-1,2-diphenylethyl isobutyrate (0.3 mmol, 1.0 equiv.) and (*i*-$PrCO)_2O$ (0.26 mmol, 0.85 equiv.) in $CHCl_3$ (1.5 mL total volume) and the second syringe with *i*-Pr_2NEt (0.26 mmol, 0.85 equiv.) in $CHCl_3$ (1.5 mL total volume). Both solutions were injected at 50 µL min^{-1}, mixed in a T-type mixing chamber, and passed through the reactor at a combined flow rate of 100 µL min^{-1}. After complete addition of the reagents from the syringes, a Gilson 305 HPLC pump was connected, and $CHCl_3$ was pumped at 100 µL min^{-1} for 30 min to ensure elution of the products. A solution of 10% MeOH in $CHCl_3$ was then pumped at 200 µL min^{-1} for 30 min to wash the column and avoid cross contamination. The column was then prepared for the next KR by pumping $CHCl_3$ at 200 µL min^{-1} for 30 min. The mixture was diluted with CH_2Cl_2 and washed sequentially with HCl (1 M), saturated $NaHCO_3$ and brine. The organic layer was dried (Na_2SO_4), filtered and concentrated to give the crude products. The corresponding monoester and diester were then isolated by flash chromatography (80:20 Hexane:EtOAc).

(1*S*,2*S*)-2-Hydroxy-1,2-diphenylethyl isobutyrate (3a): **Chiral HPLC analysis** Chiralcel OD-H (95:5 Hexane:IPA, flow rate 1 mL min^{-1}, 211 nm, 30 °C) t_R (1*S*,2*S*): 11.9 min, t_R (1*R*,2*R*): 17.5 min, 82.19:17.82 *er*;

(1*R*,2*R*)-1,2-Diphenylethane-1,2-diyl bis(2-methylpropanoate) (4a): **Chiral HPLC analysis** Chiralpak ID (90:10 Hexane:IPA, flow rate 1.0 mL min^{-1}, 211 nm, 30 °C) t_R(1*R*,2*R*): 12.7 min, t_R(1*S*,2*S*): 15.4 min, 95.20:4.80 *er*.

General procedure of Kinetic Resolution (±)-1,3-Diols 5 in flow-mode conditions

A packed bed reactor consisting of a vertically-mounted Omnifit glass chromatography column [borosilicate glass; length = 100 mm (70 mm adjustable bed height); internal diameter = 10 mm; maximum bed volume 5.6 mL], with a glass cooling jacket was loaded with PS-HyperBTM resin (600 mg; f = 0.89 mmol g^{-1}). The resin was allowed to swell to its maximum

volume by pumping 1:1 THF:$CHCl_3$ mixture at 1 mL min^{-1} for 30 min at RT using a Gilson 305 HPLC pump. Two syringes were used to inject reagents using a Legato 200 series syringe pump by World Precision Instruments. The first syringe was filled with a solution of the appropriate diol (0.75 mmol, 1.0 equiv.) and $(EtCO)_2O$ (0.79 mmol, 1.05 equiv.) in 1:1 THF:$CHCl_3$ mixture (7.5 mL total volume) and the second syringe with *i*-Pr_2NEt (0.79 mmol, 1.05 equiv.) in 1:1 THF:$CHCl_3$ mixture (7.5 mL total volume). Both solutions were injected at 100 µL min^{-1}, mixed in a T-type mixing chamber, and passed through the reactor at a combined flow rate of 200 µL min^{-1}. After complete addition of the reagents from the syringes, a Gilson 305 HPLC pump was connected, and $CHCl_3$ was pumped at 200 µL min^{-1} for 30 min to ensure elution of the products. A solution of 10% MeOH in 1:1 THF:$CHCl_3$ mixture was then pumped at 200 µL min^{-1} for 30 min to wash the column and avoid cross contamination. The column was then prepared for the next KR by pumping 1:1 THF:$CHCl_3$ mixture at 200 µL min^{-1} for 30 min. The mixture was concentrated to remove THF and later diluted with CH_2Cl_2. So, it was washed sequentially with HCl (1 M), saturated $NaHCO_3$ and brine. The organic layer was dried (Na_2SO_4), filtered and concentrated to give the crude products which were purified by column chromatography.

Hydrolysis of diesters and monoesters

In some instances, it was difficult to find conditions to separate the enantiomers of diesters or monoesters by HPLC using a chiral support, and therefore these products were hydrolysed to the diol prior to HPLC analysis: $LiOH•H_2O$ (3 equiv.) was added to a solution of the diester or monoester (1 equiv.) in MeOH (0.3 M) and allowed to stir at 50 °C until completion, based on TLC analysis. The mixture was diluted with EtOAc and washed sequentially with HCl (1 M), saturated $NaHCO_3$ and brine. The organic layer was dried (Na_2SO_4), filtered and concentrated to give the diol product.

Kinetic Resolution of (±)-(1*E*,6*E*)-1,7-diphenylhepta-1,6-diene-3,5-diol ((±)-5a)

According to the **General Procedure**, (±)-(1*E*,6*E*)-1,7-diphenylhepta-1,6-diene-3,5-diol (210 mg, 0.75 mmol) and propionic anhydride (101 µL, 0.787 mmol, 1.05 equiv.), in 1:1 $CHCl_3$:THF mixture (7.5 mL total volume), and *i*-Pr_2NEt (138 µL, 0.787 mmol, 1.05 equiv.) in 1:1 $CHCl_3$:THF mixture (7.5 mL total volume) gave crude products that were purified by column chromatography (80:20 to 60:40 Hexane:EtOAc) to give:

(1*E*,3*R*,5*R*,6*E*)-1,7-diphenylhepta-1,6-diene-3,5-diol (5a)

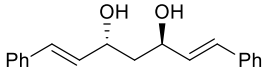

(63 mg, 30%) as a colourless solid with spectroscopic data in accordance with the literature.[5] **mp** 140−141 °C {Lit.[5] 149 °C}; $[\alpha]_D^{20}$+25.0 (*c* 1.0 in $CHCl_3$) {Lit.[5] $[\alpha]_D^{25}$ (>99:1 *er*) +16.2 (*c* 0.50, $CHCl_3$)}; **Chiral HPLC analysis** Chiralpak IC (90:10 Hexane:IPA, flow rate 1.0 mL min^{-1}, 211 nm, 30 °C) t_R(3*S,*5*S*): 12.3 min, t_R(3*R,*5*R*): 14.0 min, 3.19:96.81 *er*; **^{1}H NMR** (500 MHz, $CDCl_3$) δ = 7.42 (d, *J* 7.5 Hz, 4H, ArH), 7.35 (t, *J* 7.3 Hz, 4H, ArH), 7.27 – 7.23 (m, 2H, ArH), 6.68 (d, *J* 15.7 Hz, 2H, C*H*Ar), 6.33 (dd, *J* 15.7, 6.2 Hz, 2H, C*H*CHAr), 4.72 (s, 2H, C*H*OH), 2.57 (d, *J* 3.9 Hz, 2H, OH), 2.01 (t, *J* 5.4 Hz, 2H, C(2)H_2).

(1*E*,3S,5S,6*E*)-5-hydroxy-1,7-diphenylhepta-1,6-dien-3-yl propionate (6a)

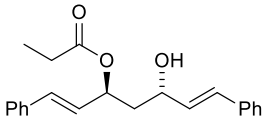

As an inseparable mixture of combined *anti* and *syn* diastereoisomers (4:1 $dr_{anti:syn}$) (45 mg, 18%) as a colourless oil with spectroscopic data in accordance with the literature.[5,31] $[\alpha]_D^{20}$ −21.5 (*c* 1.0 in $CHCl_3$).

Data for major diastereoisomer anti-**6a** in accordance with the literature:[5] following hydrolysis to (1*E*,6*E*)-1,7-diphenylhepta-1,6-diene-3,5-diol and the *anti*-diastereoisomer was purified through crystallization form hot 1:1 Toluene:Hexane: **Chiral HPLC analysis** Chiralpak IC (90:10 Hexane:IPA, flow rate 1.0 mL min^{-1}, 211 nm, 30 °C) t_R(3R*,*5*R*): 12.2 min, t_R(3*R,*5*R*): 14.0 min, 64.99:35.01 *er*; **^{1}H NMR** (400 MHz, $CDCl_3$) δ = 7.48 – 7.29 (m, 10H, ArH), 6.66 (ddd, *J* 16.0, 6.0, 1.1 Hz, 2H, PhC*H*=CH), 6.34 – 6.15 (m, 2H, PhCH=C*H*), 5.82 – 5.71 (m, 1H, C*H*OC(O)Et), 4.43 – 4.28 (m, 1H, C*H*OH), 2.62 (d, *J* 3.8 Hz, 1H, OH), 2.43 (q, *J* 7.5 Hz, 2H, CH_2CH$_3$), 2.12 – 1.87 (m, 2H, C(2)H_2), 1.24 – 1.11 (m, 3H, CH_3).

Data for minor diastereoisomer syn-**6a** in accordance with the literature:[32] **^{1}H NMR** (400 MHz, $CDCl_3$) (*selected*) δ = 5.73 – 5.59 (m, 1H, C*H*OC(O)Et), 4.51 – 4.41 (m, 1H, C*H*OH).

(1*E*,3*S*,5*S*,6*E*)-1,7-diphenylhepta-1,6-diene-3,5-diyl dipropionate (7a)

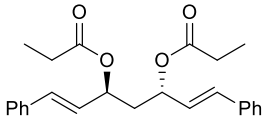

(99 mg, 34%) as a colourless solid with spectroscopic data in accordance with the literature.[5] **mp** 51−52 °C {Lit.[5] 56 °C}; $[\alpha]_D^{20}$ −5.0 (*c* 0.3 in $CHCl_3$) {Lit.[5] $[\alpha]_D^{25}$ (98:2 *er*) −44.1 (*c* 1.00, $CHCl_3$)}; **Chiral HPLC analysis** Chiralcel OJ-H (85:15 Hexane:IPA, flow rate 1.5 mL min^{-1}, 211 nm, 30 °C) t_R(3*R,*5*R*): 9.5 min, t_R(3*S,*5*S*): 13.4 min, 4.85:95.15 *er*.; **^{1}H NMR** (500 MHz, $CDCl_3$) δ = 7.47 – 7.19 (m, 10H, ArH), 6.75 – 6.57 (m, 2H, PhC*H*=CH), 6.18 (dd, *J* 15.9, 7.3 Hz, 2H, PhCH=C*H*), 5.65−5.51 (m, 2H, C*H*OC(O)Et), 2.37 (qd, *J* 7.5, 4.5 Hz, 4H, CH_2CH$_3$), 2.16 (dd, *J* 7.3, 6.6 Hz, 2H, CH_2), 1.16 (t, *J* 7.6 Hz, 6H, CH_3).

Kinetic Resolution of (±)-1,3-diphenylpropane-1,3-diol ((±)-5b)

According to the **General Procedure**, (±)-1,3-diphenylpropane-1,3-diol (171 mg, 0.75 mmol) and propionic anhydride (101 μL, 0.787 mmol, 1.05 equiv.), in 1:1 $CHCl_3$:THF mixture (7.5 mL total volume), and *i*-Pr_2NEt (138 μL, 0.787 mmol, 1.05 equiv.) in 1:1 $CHCl_3$:THF mixture (7.5 mL total volume) gave crude products that were purified by column chromatography (80:20 to 60:40 Hexane:EtOAc) to give:

(1*R*,3*R*)-1,3-diphenylpropane-1,3-diol (5b)

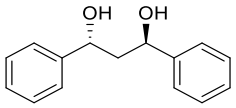

(60 mg, 35%) as a colourless solid with spectroscopic data in accordance with the literature.[5] **mp** 141−143 °C {Lit.[5] 153 °C}; $[\alpha]_D^{20}$ +75.0 (*c* 0.1 in $CHCl_3$) {Lit.[5] $[\alpha]_D^{25}$ (99:1 *er*) +115.9 (*c* 1.0, $CHCl_3$)}; **Chiral HPLC analysis** Chiralpak ID (90:10 Hexane:IPA, flow rate 1.0 mL min^{-1}, 211 nm, 30 °C) t_R(3*R,*5*R*): 11.4 min, 100:0 *er*.; **^{1}H NMR** (500 MHz, $CDCl_3$) δ = 7.41 – 7.36 (m, 8H, ArH), 7.33 – 7.29 (m, 2H, ArH), 5.01 (dd, *J* 6.3, 5.4 Hz, 2H, C*H*OH), 2.21 (dd, *J* 6.2, 5.4 Hz, 2H, C(2)H_2).

(1*S*,3*S*)-3-hydroxy-1,3-diphenylpropyl propionate (6b)

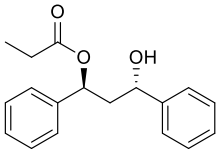

As an inseparable mixture of combined *anti* and *syn* diastereoisomers (90:10 $dr_{anti:syn}$) (24 mg, 10%) as a colourless oil. $[\alpha]_D^{20}$ −21.8 (*c* 0.45 in $CHCl_3$); following hydrolysis to 1,3-diphenylpropane-1,3-diol **Chiral HPLC analysis** Chiralpak ID (90:10 Hexane:IPA, flow rate 1.0 mL min^{-1}, 211 nm, 30 °C) t_R(3*R,*5*R*): 11.4 min, t_R(3*S,*5*S*): 14.6 min, 33.73:66.27 *er*; **IR** (neat) ν_{max}: 3447 (OH), 1754 (C=O), 1495, 1456, 1350, 1277, 1188, 1063, 1022 cm^{-1}; **HRMS** (ESI): calcd. for $C_{18}H_{20}O_3Na^+$ ([M + Na]$^+$): 307.1305; found 307.1299.

Data for major diastereoisomer anti-**6b**: **^{1}H NMR** (500 MHz, $CDCl_3$) δ = 7.42 – 7.34 (m, 8H, ArH), 7.34 – 7.29 (m, 2H, ArH), 6.11 (dd, *J* 10.3, 3.4 Hz, 1H, C*H*OC(O)Et), 4.74 (dt, *J* 9.9, 3.5 Hz, 1H, C*H*OH), 2.77 (d, *J* 3.6 Hz, 1H, OH), 2.43 (qd, *J* 7.5, 4.4 Hz, 2H, CH_2CH$_3$), 2.29 (ddd, *J* 14.6, 10.3, 3.4 Hz, 1H, C(2)H_2), 2.17 (ddd, *J* 14.5, 9.9, 3.4 Hz, 1H, C(2)H_2), 1.19 (t, *J* 7.6 Hz, 3H, CH_3); **^{13}C NMR** (126 MHz, $CDCl_3$) δ = 174.0 (CHO*C*(O)Et), 143.7 (Ar*C*), 140.4 (Ar*C*), 128.6 (4 × Ar*C*H), 128.0 (Ar*C*H), 127.7 (Ar*C*H), 126.4 (2 × Ar*C*H), 125.8 (2 × Ar*C*H), 73.0 (*C*HOC(O)Et), 70.4 (*C*HOH), 46.6 (*C*(2)H_2), 27.8 (*C*H_2CH$_3$), 9.2 (*C*H_3).

Data for minor diastereoisomer syn-**6b** in accordance with the literature:[32] **^{1}H NMR** (500 MHz, $CDCl_3$) (*selected*) δ = 5.90 (dd, *J* 7.8, 6.5 Hz, 1H, C*H*OC(O)Et), 4.65 (dd, *J* 8.4, 4.8 Hz, 1H, C*H*OH).

(1*S*,3*S*)-1,3-diphenylpropane-1,3-diyl dipropionate (7b)

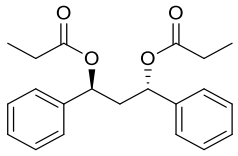

(105 mg, 39%) as a colourless oil with spectroscopic data in accordance with the literature.[5] $[\alpha]_D^{20}$ −89.4 (*c* 0.4 in $CHCl_3$) {Lit.[5] $[\alpha]_D^{25}$ (98:2 *er*) −48.9 (*c* 1.0, $CHCl_3$)}; following hydrolysis to 1,3-diphenylpropane-1,3-diol **Chiral HPLC analysis** Chiralpak ID (90:10 Hexane:IPA, flow rate 1.0 mL min^{-1}, 211 nm, 30 °C), t_R(3*R,5R*): 11.4 min, t_R(3*S,5S*): 14.5 min, 3.45:96.55 *er*; **^{1}H NMR** (500 MHz, $CDCl_3$) δ = 7.39 – 7.29 (m, 10H, ArH), 5.90 (dd, *J* 7.7, 6.5 Hz, 2H, C*H*OC(O)Et), 2.46 – 2.24 (m, 6H, CH_2CH$_3$ and C(2)H$_2$), 1.14 (t, *J* 7.5 Hz, 6H, CH$_3$).

Kinetic Resolution of (±)-1,3-bis(2-methoxyphenyl)propane-1,3-diol ((±)-5c)

According to the **General Procedure**, (±)-1,3-bis(2-methoxyphenyl)propane-1,3-diol (216 mg, 0.75 mmol) and propionic anhydride (101 μL, 0.787 mmol, 1.05 equiv.), in 1:1 $CHCl_3$:THF mixture (7.5 mL total volume), and *i*-Pr$_2$NEt (138 μL, 0.787 mmol, 1.05 equiv.) in 1:1 $CHCl_3$:THF mixture (7.5 mL total volume) gave crude products that were purified by column chromatography (80:20 to 60:40 Hexane:EtOAc) to give:

(1*R*,3*R*)-1,3-bis(2-methoxyphenyl)propane-1,3-diol (5c)

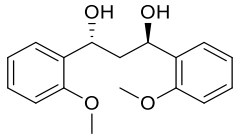

(85 mg, 39%) as a colourless solid with spectroscopic data in accordance with the literature.[5] **mp** 106−107 °C {Lit.[5] 117 °C}; $[\alpha]_D^{20}$ +84.3 (*c* 1.0 in $CHCl_3$) {Lit.[5] $[\alpha]_D^{25}$ (>99:1 *er*) +121.8 (*c* 1.0, $CHCl_3$)}; **Chiral HPLC analysis** Chiralpak ID (80:20 Hexane:IPA, flow rate 1.0 mL min^{-1}, 211 nm, 30 °C) t_R(3*R,5R*): 16.9 min, t_R(3*S,5S*): 21.1 min, 97.50:2.50 *er*; **^{1}H NMR** (400 MHz, $CDCl_3$) δ = 7.48 – 7.41 (m, 2H, ArH), 7.30 – 7.23 (m, 2H, ArH), 7.00 (td, *J* 7.5, 1.1 Hz, 2H, ArH), 6.89 (dd, *J* 8.2, 1.1 Hz, 2H, ArH), 5.23 (t, *J* 5.8 Hz, 2H, C*H*OH), 3.83 (s, 6H, OCH$_3$), 2.31 (dd, *J* 6.3, 5.3 Hz, 2H, C(2)H$_2$).

(1*S*,3*S*)-3-hydroxy-1,3-bis(2-methoxyphenyl)propyl propionate (6c)

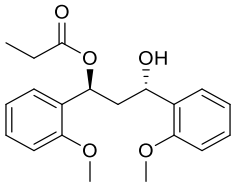

As an inseparable mixture of combined *anti* and *syn* diastereoisomers (94:6 $dr_{anti:syn}$) (56 mg, 22%) as a colourless oil. $[\alpha]_D^{20}$ −146.3 (*c* 0.6 in $CHCl_3$); following hydrolysis to 1,3-bis(2-methoxyphenyl)propane-1,3-diol **Chiral HPLC analysis** Chiralpak ID (80:20 Hexane:IPA, flow rate 1.0 mL min^{-1}, 211 nm, 30 °C) t_R(3*R,*5*R*): 16.7 min, t_R(3*S,*5*S*): 20.2 min, 14.77:85.23 *er*; **IR** (neat) ν_{max}: 3450 (OH), 2940; 1732 (C=O), 1490, 1462; 1287; 1242; 1186; 1049; 1028 cm^{-1}; **HRMS** (ESI): calcd. for $C_{20}H_{24}O_5Na^+$ ([M+Na]$^+$): 367.1516; found 367.1502.

Data for major diastereoisomer anti-**6c**: **^{1}H NMR** (400 MHz, $CDCl_3$) δ = 7.44 – 7.38 (m, 1H, ArH), 7.35 (dd, *J* 7.6, 1.8 Hz, 1H, ArH), 7.28 – 7.20 (m, 2H, ArH),1.20 (t, *J* 7.6 Hz, 3H, CH_3), 7.01 − 6.92 (m, 2H, ArH), 6.88 (ddd, *J* 8.2, 4.4, 1.1 Hz, 2H, ArH), 6.50 (dd, *J* 9.9, 3.1 Hz, 1H, C*H*OC(O)Et), 5.01 (dd, *J* 9.4, 3.5 Hz, 1H, C*H*OH), 3.87 (s, 3H, OCH_3), 3.85 (s, 3H, OCH_3), 3.20 (d, *J* 5.8 Hz, 1H, OH), 2.41 (qd, *J* 7.6, 0.9 Hz, 2H, CH_2CH$_3$), 2.11 – 2.35 (m, 2H, C(2)H_2); **^{13}C NMR** (126 MHz, $CDCl_3$) δ = 174.3 (CHO*C*(O)Et), 156.2 (Ar*C*), 156.0 (Ar*C*), 131.9 (Ar*C*), 129.4 (Ar*C*), 128.7 (Ar*C*H), 128.2 (Ar*C*H), 126.8 (Ar*C*H), 126.2 (Ar*C*H), 120.8 (Ar*C*H), 120.5 (Ar*C*H), 110.6 (Ar*C*H), 110.3 (Ar*C*H), 68.1 (*C*HOC(O)Et), 66.8 (*C*HOH), 55.5 (O*C*H$_3$), 55.3 (O*C*H$_3$), 43.1 (*C*(2)H_2), 27.9 (*C*H_2CH$_3$), 9.3 (*C*H$_3$).

Data for minor diastereoisomer syn-**6c** in accordance with the literature:[32] **^{1}H NMR** (400 MHz, $CDCl_3$) (*selected*) δ = 6.30 – 6.16 (m, 1H, C*H*OC(O)Et), 4.99 – 4.91 (m, 1H, C*H*OH).

(1*S*,3*S*)-1,3-bis(2-methoxyphenyl)propane-1,3-diyl dipropionate (7c)

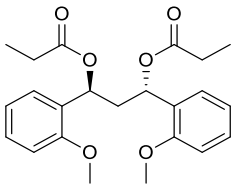

(75 mg, 25%) as a colorless oil with spectroscopic data in accordance with the literature.[5] $[\alpha]_D^{20}$ −48.0 (*c* 1.0 in $CHCl_3$) {Lit.[5] $[\alpha]_D^{25}$ (>99:1 *er*) −22.8 (*c* 1.0, $CHCl_3$)}; following hydrolysis to 1,3-bis(2-methoxyphenyl)propane-1,3-diol **Chiral HPLC analysis** Chiralpak ID (80:20 Hexane:IPA, flow rate 1.0 mL min^{-1}, 211 nm, 30 °C) t_R(3*R,*5*R*): 17.1 min, t_R(3*S,*5*S*): 20.4 min, 0.46:99.54 *er*; **^{1}H NMR** (400 MHz, $CDCl_3$) δ = 7.31 (dd, *J* 7.6, 1.8 Hz, 2H, ArH), 7.23 (ddd, *J* 8.2, 7.4, 1.8 Hz, 2H, ArH), 6.94 (td, *J* 7.5, 1.1 Hz, 2, ArH), 6.85 (dd, *J* 8.2, 1.1 Hz, 2H, ArH), 6.33 (dd, *J* 7.3, 5.9 Hz, 2H, C*H*OC(O)Et), 3.85 (s, 6H, OCH_3), 2.39 (qd, *J* 7.5, 3.2 Hz, 4H, CH_2CH$_3$), 2.27 (dd, *J* 7.3, 5.9 Hz, 2H, C(2)H_2), 1.18 (t, *J* 7.6 Hz, 6H, CH_3).

Kinetic Resolution of (±)-1,3-bis(4-fluorophenyl)propane-1,3-diol ((±)-5d)

According to the **General Procedure**, (±)-1,3-bis(4-fluorophenyl)propane-1,3-diol (198 mg, 0.75 mmol) and propionic anhydride (101 μL, 0.787 mmol, 1.05 equiv.), in 1:1 $CHCl_3$:THF mixture (7.5 mL total volume), and *i*-Pr_2NEt (138 μL, 0.787 mmol, 1.05 equiv.) in 1:1 $CHCl_3$:THF mixture (7.5 mL total volume) gave crude products that were purified by column chromatography (80:20 to 60:40 Hexane:EtOAc) to give:

(1*R*,3*R*)-1,3-bis(4-fluorophenyl)propane-1,3-diol (5d)

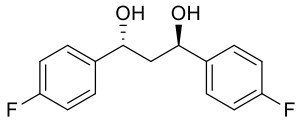

(65 mg, 32%) as a colourless solid with spectroscopic data in accordance with the literature.[5] **mp** 115−117 °C {Lit.[5] 121.5 °C}; $[\alpha]_D^{20}$ +50.6 (*c* 1.0 in $CHCl_3$) {Lit.[5] $[\alpha]_D^{25}$ (>99:1 *er*) +73.5 (*c* 1.0, $CHCl_3$)}; **Chiral HPLC analysis** Chiralcel OJ-H (80:20 Hexane:IPA, flow rate 1.0 mL min^{-1}, 211 nm, 30 °C) t_R(3*R,5R*): 6.4 min, t_R(3*S,5S*): 7.3 min, 99.49:0.51 *er*; **^{1}H NMR** (400 MHz, $CDCl_3$) δ = 7.39 – 7.31 (m, 4H, ArH), 7.11 – 7.02 (m, 4H, ArH), 4.99 (t, *J* 5.8 Hz, 2H, C*H*OH), 2.14 (dd, *J* 6.3, 5.3 Hz, 2H, C(2)H_2); **^{19}F NMR** (377 MHz, $CDCl_3$) δ = −115.02.

(1*S*,3*S*)-1,3-bis(4-fluorophenyl)-3-hydroxypropyl propionate (6d)

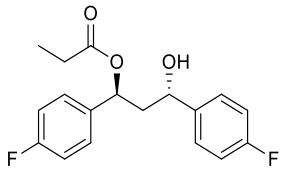

As an inseparable mixture of combined *anti* and *syn* diastereoisomers (92:8 $dr_{anti:syn}$) (34 mg, 14%) as a colourless oil. $[\alpha]_D^{20}$ −5.9 (*c* 0.45 in $CHCl_3$); following hydrolysis to 1,3-bis(4-fluorophenyl)propane-1,3-diol **Chiral HPLC analysis** Chiralcel OJ-H (80:20 Hexane:IPA, flow rate 1.0 mL min^{-1}, 211 nm, 30 °C) t_R(3*R,5R*): 6.4 min, t_R(3*S,5S*): 7.3 min, 40.40:59.60 *er*; **IR** (neat) ν_{max}: 3447 (OH), 1732 (C=O), 1605; 1510, 1223; 1186; 1157 cm^{-1}; **HRMS** (ESI): calcd. for $C_{18}H_{18}O_3F_2Na^+$ ([M+Na]$^+$): 343.1116; found 343.1105.

Data for major diastereoisomer anti-**6d**: **^{1}H NMR** (400 MHz, $CDCl_3$) δ = 7.42 – 7.31 (m, 4H, ArH), 7.11 – 6.99 (m, 4H, ArH), 6.06 (dd, *J* 10.3, 3.4 Hz, 1H, C*H*OC(O)Et), 4.71 (dd, *J* 9.8, 3.5 Hz, 1H, C*H*OH), 2.78 (bs, 1H, OH), 2.42 (qd, *J* 7.5, 3.9 Hz, 2H, C$H_2$$CH_3$), 2.24 (ddd, *J* 14.5, 10.2, 3.5 Hz, 1H, C(2)H_2), 2.11 (ddd, *J* 14.5, 9.8, 3.4 Hz, 1H, C(2)H_2), 1.18 (t, *J* 7.6 Hz, 3H, CH_3); **^{13}C NMR** (126 MHz, $CDCl_3$) δ = 174.5 (CHO*C*(O)Et), 163.4 (d, $^1J_{C\text{-}F}$ 246.2 Hz Ar*C*), 161.3 (d, $^1J_{C\text{-}F}$ 246.2 Hz, Ar*C*), 139.3 (d, $^4J_{C\text{-}F}$ 3.0 Hz, Ar*C*), 136.1 (d, $^4J_{C\text{-}F}$ 3.1 Hz, Ar*C*), 128.2 (d, $^3J_{C\text{-}F}$ 8.2 Hz, 2 × Ar*C*H), 127.4 (d, $^3J_{C\text{-}F}$ 8.1 Hz, 2 × Ar*C*H), 115.5 (dd, $^2J_{C\text{-}F}$ 16.9 Hz,

2 × Ar*C*H), 9.1 (*C*H$_3$), 115.3 (dd, $^2J_{C\text{-}F}$ 16.9 Hz, 2 × Ar*C*H), 72.3 (*C*HOC(O)Et), 69.7 (*C*HOH), 46.6 (*C*(2)H$_2$), 27.8 (*C*H$_2$CH$_3$); **^{19}F NMR** (377 MHz, CDCl$_3$) δ = −113.90, −114.81.

Data for minor diastereoisomer syn-**6d** in accordance with the literature:[32] **^{1}H NMR** (400 MHz, CDCl$_3$) (*selected*) δ = 5.87 (t, *J* 7.1 Hz, 1H, C*H*OC(O)Et), 4.60 (dd, *J* 8.5, 4.8 Hz, 1H, C*H*OH); **^{19}F NMR** (377 MHz, CDCl$_3$) δ = −113.79, −114.46.

(1*S*,3*S*)-1,3-bis(4-fluorophenyl)propane-1,3-diyl dipropionate (7d)

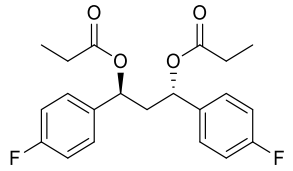

(113 mg, 40%) as a colourless oil with spectroscopic data in accordance with the literature.[5] $[\alpha]_D^{20}$ −66.1 (*c* 0.6 in CHCl$_3$) {Lit.[5] $[\alpha]_D^{25}$ (99:1 *er*) −68.4 (*c* 1.0, CHCl$_3$)}; following hydrolysis to 1,3-bis(4-fluorophenyl)propane-1,3-diol **Chiral HPLC analysis** Chiralcel OJ-H (80:20 Hexane:IPA, flow rate 1.0 mL min^{-1}, 211 nm, 30 °C) t$_R$(3*R,5R*): 6.5 min, t$_R$(3*S,5S*): 7.4 min, 6.72:93.28 *er*; **^{1}H NMR** (400 MHz, CDCl$_3$) δ = 7.37 – 7.30 (m, 4H, ArH), 7.08 – 7.00 (m, 4H, ArH), 5.88 – 5.79 (m, 2H, C*H*OC(O)Et), 2.43 – 2.25 (m, 6H, C*H*$_2$CH$_3$ and C(2)H$_2$), 1.13 (t, *J* 7.5 Hz, 6H, CH$_3$); **^{19}F NMR** (377 MHz, CDCl$_3$) δ = −113.71.

Kinetic Resolution of (±)-1,5-diphenylpent-4-ene-1,3-diol ((±)-5e)

According to the **General Procedure**, (±)-1,5-diphenylpent-4-ene-1,3-diol (191 mg, 0.75 mmol) and propionic anhydride (101 µL, 0.787 mmol, 1.05 equiv.), in 1:1 CHCl$_3$:THF mixture (7.5 mL total volume), and *i*-Pr$_2$NEt (138 µL, 0.787 mmol, 1.05 equiv.) in 1:1 CHCl$_3$:THF mixture (7.5 mL total volume) gave crude products that were purified by column chromatography (80:20 to 60:40 Hexane:EtOAc) to give:

(1*R*,3*R*,*E*)-1,5-diphenylpent-4-ene-1,3-diol (5e)

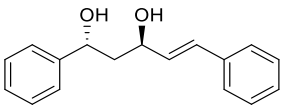

(60 mg, 32%) as a white solid with spectroscopic data in accordance with the literature.[5] **mp** 106−107 °C {Lit.[5] 106 °C}; $[\alpha]_D^{20}$ −13.5 (*c* 1.0 in CHCl$_3$) {Lit.[5] $[\alpha]_D^{25}$ (>99:1 *er*) −11.8 (*c* 1.0, CHCl$_3$)}; **Chiral HPLC analysis** Chiralcel OD-H (80:20 Hexane:IPA, flow rate 1.0 mL min^{-1}, 254 nm, 30 °C) t$_R$(3*S,5S*): 10.5 min, t$_R$(3*R,5R*): 17.5 min, 1.91:98.09 *er*; **^{1}H NMR** (400 MHz, CDCl$_3$) δ = 7.45 – 7.32 (m, 10H, ArH), 6.66 (dd, *J* 15.9, 1.4 Hz, 1H, PhC*H*=CH), 6.34 (dd, *J* 15.9, 6.1 Hz, 1H, PhCH=C*H*), 5.12 (dd, *J* 8.5, 3.4 Hz, 1H, C(1)*H*OH), 4.69 – 4.55 (m, 1H, C(3)*H*OH), 2.17 (ddd, *J* 14.6, 8.5, 3.5 Hz, 1H, C(2)H$_2$), 2.06 (ddd, *J* 14.5, 7.7, 3.3 Hz, 1H, C(2)H$_2$).

(3*R*,5*R*,*E*)-5-hydroxy-1,5-diphenylpent-1-en-3-yl propionate (6e')

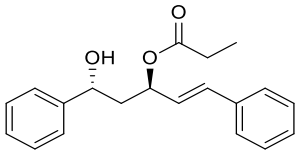

(21 mg, 9%) as a pale yellow oil. $[\alpha]_D^{20}$ −5.6 (*c* 0.25 in $CHCl_3$); following hydrolysis to 1,5-diphenylpent-4-ene-1,3-diol **Chiral HPLC analysis** Chiralcel OD-H (80:20 Hexane:IPA, flow rate 1.0 mL min^{-1}, 211 nm, 30 °C) t_R(3*S,*5*S*): 10.4 min, t_R(3*R,*5*R*): 18.1 min, 40.75:59.25 *er*; **IR** (neat) ν_{max}: 3447 (OH), 3028, 1732 (C=O), 1494, 1450, 1273, 1186, 1080, 1066 cm^{-1}; **^{1}H NMR** (400 MHz, $CDCl_3$) δ = 7.44 – 7.29 (m, 10H, ArH), 6.66 (d, *J* 15.9 Hz, 1H, PhC*H*=CH), 6.21 (dd, *J* 15.9, 7.0 Hz, 1H, PhCH=C*H*), 5.76 (qd, *J* 6.8, 1.1 Hz, 1H, C*H*OC(O)Et), 4.82 – 4.66 (m, 1H, C*H*OH), 2.43 (q, *J* 7.5 Hz, 2H, C$H_2$$CH_3$), 2.25 – 2.05 (m, 2H, C(2)H_2), 1.21 (t, *J* 7.6 Hz, 3H, CH_3); **^{13}C NMR** (126 MHz, $CDCl_3$) δ = 174.7 (CHO*C*(O)Et), 143.7 (Ar*C*), 136.2 (Ar*C*), 132.4 (Ph*C*H=CH), 128.6 (4 × Ar*C*H), 128.1 (PhCH=*C*H), 127.7 (Ar*C*H), 127.3 (Ar*C*H), 126.6 (2 × Ar*C*H), 125.8 (2 × Ar*C*H), 71.9 (*C*HOC(O)Et), 70.3 (*C*HOH), 44.6 (*C*(2)H_2), 27.9 (*C*$H_2$$CH_3$), 9.2 (*C*$H_3$); **HRMS** (ESI): calcd. for $C_{20}H_{22}O_3Na$ ([M+Na]$^+$): 333.1461; found 333.1457.

(1*S*,3*S*,*E*)-3-hydroxy-1,5-diphenylpent-4-en-1-yl propionate (6e'')

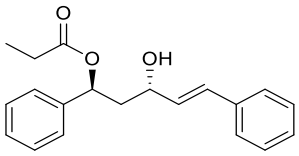

As an inseparable mixture of combined *anti* and *syn* diastereoisomers (89:11 $dr_{anti:syn}$) (14 mg, 6%) as a pale yellow oil. $[\alpha]_D^{20}$ +23.6 (*c* 0.25 in $CHCl_3$); following hydrolysis to 1,5-diphenylpent-4-ene-1,3-diol **Chiral HPLC analysis** Chiralcel OD-H (80:20 Hexane:IPA, flow rate 1.0 mL min^{-1}, 211 nm, 30 °C) t_R(3*S,*5*S*): 10.5 min, t_R(3*R,*5*R*): 18.4 min, 56.02:43.98 *er*; **IR** (neat) ν_{max}: 3429 (OH), 1754 (C=O), 1494, 1450, 1275, 1186, 1080, 1068 cm^{-1}; **HRMS** (ESI): calcd. for $C_{20}H_{22}O_3Na^+$ ([M+Na]$^+$): 333.1461; found 333.1459.

Data for major diastereoisomer anti-**6e''**: **^{1}H NMR** (500 MHz, $CDCl_3$) δ = 7.43 – 7.36 (m, 8H, ArH), 7.36 – 7.30 (m, 2H, ArH), 6.71 – 6.60 (m, 1H, PhC*H*=CH), 6.30 – 6.21 (m, 1H, PhCH=C*H*), 6.08 (dd, *J* 10.2, 3.6 Hz, 1H, C*H*OC(O)Et), 4.39 − 4.30 (m, 1H, CHOH), 2.26 – 2.17 (m, 1H, OH), 2.43 (qd, *J* 7.6, 4.9 Hz, 2H, CH_2CH_3), 2.05 (ddd, *J* 14.4, 9.5, 3.6 Hz, 1H, C(2)H_2), 1.17 (t, *J* 7.5 Hz, 3H, CH_3); **^{13}C NMR** (126 MHz, $CDCl_3$) δ = 174.6 (CHO*C*(O)Et), 140.4 (Ar*C*), 136.6 (Ar*C*), 131.1 (PhCH=*C*H), 130.4 (Ph*C*H=CH), 128.6 (4 × Ar*C*H), 128.1 (Ar*C*H), 127.7 (Ar*C*H), 126.5 (2 × Ar*C*H), 126.4 (2 × Ar*C*H), 72.8 (*C*HOC(O)Et), 68.9 (*C*HOH), 44.7 (*C*(2)H_2), 27.8 (*C*$H_2$$CH_3$), 9.1 (*C*$H_3$).

Data for minor diastereoisomer syn-**6e''**: **^{1}H NMR** (500 MHz, $CDCl_3$) *(selected)* δ = 6.56 (d, *J* 16.0 Hz, 1H, PhC*H*=CH), 6.00 (dd, *J* 7.7, 6.5 Hz, 1H, C*H*OC(O)Et), 4.32 – 4.23 (m, 1H, C*H*OH); **^{13}C NMR** (126 MHz, $CDCl_3$) *(selected)* δ = 73.6 (*C*HOC(O)Et), 70.1 (*C*HOH).

(1*S*,3*S*,*E*)-1,5-diphenylpent-4-ene-1,3-diyl dipropionate (7e)

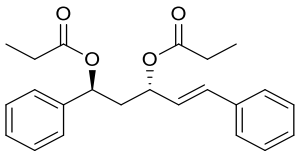

(100 mg, 36%) as a pale yellow oil with spectroscopic data in accordance with the literature.[5] $[\alpha]_D^{20}$ −53.2 (*c* 1.0 in $CHCl_3$) {Lit.[5] $[\alpha]_D^{25}$ (98:2 *er*) −53.12 (*c* 1.0, $CHCl_3$)}; following hydrolysis to 1,5-diphenylpent-4-ene-1,3-diol **Chiral HPLC analysis** Chiralcel OD-H (80:20 Hexane:IPA, flow rate 1.0 mL min^{-1}, 211 nm, 30 °C) t_R(3*S,*5*S*): 10.5 min, t_R(3*R,*5*R*): 18.0 min, 94.91:5.09 *er*; **^{1}H NMR** (400 MHz, $CDCl_3$) δ = 7.41 – 7.30 (m, 10H, ArH), 6.72 – 6.55 (m, 1H, PhC*H*=CH), 6.15 (dd, *J* 15.9, 7.3 Hz, 1H, PhCH=C*H*), 5.90 (dd, *J* 9.7, 4.5 Hz, 1H, C(3)*H*OC(O)Et), 5.58 (td, *J* 8.8, 4.7 Hz, 1H, C(1)*H*OC(O)Et), 2.44 – 2.17 (m, 6H, CH_2CH$_3$ and C(2)H$_2$), 1.15 (dt, *J* 15.2, 7.5 Hz, 6H, CH$_3$).

Kinetic Resolution of (±)-1-(4-fluorophenyl)-3-(furan-2-yl)propane-1,3-diol ((±)-5f)

According to the **General Procedure**, (±)-1-(4-fluorophenyl)-3-(furan-2-yl)propane-1,3-diol (177 mg, 0.75 mmol) and propionic anhydride (101 µL, 0.787 mmol, 1.05 equiv.), in 1:1 $CHCl_3$:THF mixture (7.5 mL total volume), and *i*-Pr$_2$NEt (138 µL, 0.787 mmol, 1.05 equiv.) in 1:1 $CHCl_3$:THF mixture (7.5 mL total volume) gave crude products that were purified by column chromatography (80:20 to 60:40 Hexane:EtOAc) to give:

(1*R*,3*R*)-1-(4-fluorophenyl)-3-(furan-2-yl)propane-1,3-diol (5f)

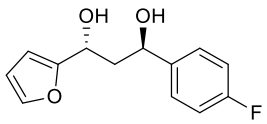

(77 mg, 44%) as a pale yellow solid with spectroscopic data in accordance with the literature.[5] **mp** 141−144 °C {Lit.[5] 139 °C}; $[\alpha]_D^{20}$ +29.7 (*c* 0.5 in $CHCl_3$) {Lit.[5] $[\alpha]_D^{25}$ (97:3 *er*) +7.8 (*c* 0.5, $CHCl_3$)}; **Chiral HPLC analysis** Chiralcel ID (90:10 Hexane:IPA, flow rate 1.0 mL min^{-1}, 211 nm, 30 °C) t_R(3*R,*5*R*): 11.0 min, t_R(3*S,*5*S*): 12.8 min, 99.73:0.27 *er*.; **^{1}H NMR** (500 MHz, $CDCl_3$) δ = 7.41 (dd, *J* 1.8, 0.9 Hz, 1H, ArH), 7.39 – 7.34 (m, 2H, ArH), 7.09 – 7.04 (m, 2H, ArH), 6.37 (dd, *J* 3.3, 1.8 Hz, 1H, ArH), 6.30 (dt, *J* 3.3, 0.8 Hz, 1H, ArH), 5.09 – 4.96 (m, 2H, C(1)*H*OH and C(3)*H*OH), 2.36 – 2.17 (m, 2H, C(2)H$_2$), 2.16 – 2.00 (m, 2H, O*H*); **^{19}F NMR** (471 MHz, $CDCl_3$) δ = −115.04.

(1*S*,3*S*)-1-(4-fluorophenyl)-3-(furan-2-yl)-3-hydroxypropyl propionate (6f')

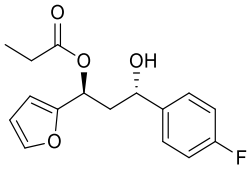

As an inseparable mixture of combined *anti* and *syn* diastereoisomers (71:29 $dr_{anti:syn}$) (14 mg, 6%) as a pale yellow oil. $[\alpha]_D^{20}$ −15.7 (*c* 0.07 in $CHCl_3$); following hydrolysis to 1-(4-fluorophenyl)-3-(furan-2-yl)propane-1,3-diol **Chiral HPLC analysis** Chiralcel ID (90:10 Hexane:IPA, flow rate 1.0 mL min^{-1}, 211 nm, 30 °C) t_R(3*R,*5*R*): 11.1 min, t_R(3*S,*5*S*): 12.8 min, 45.34:54.66 *er*; **IR** (neat) ν_{max}: 3447 (OH), 2984, 1732 (C=O), 1605, 1510, 1221, 1182, 1157, 1067, 1013 cm^{-1}; **HRMS** (ESI): calcd. for $C_{16}H_{17}O_4FNa^+$ ($[M+Na]^+$) 315.1009; found 315.0997.

Data for major diastereoisomer anti-**6f'**:**^{1}H NMR** (500 MHz, $CDCl_3$) δ = 7.41 (dd, *J* 1.8, 0.9 Hz, 1H, ArH), 7.38 – 7.32 (m, 2H, ArH), 7.11 − 6.96 (m, 2H, ArH), 6.46 – 6.24 (m, 2H, ArH), 6.15 (dd, *J* 10.1, 3.7 Hz, 1H, C(3)*H*OC(O)Et), 4.69 (dt, *J* 9.8, 3.6 Hz, 1H, C(1)*H*OH), 2.49 – 2.34 (m, 3H, C$H_2$$CH_3$ and C(2)H_2), 2.25 (ddd, *J* 14.4, 9.9, 3.8 Hz, 1H, C(2)H_2), 1.18 (t, *J* 7.6 Hz, 3H, CH_3); **^{13}C NMR** (126 MHz, $CDCl_3$) δ = 174.7 (CHO*C*(O)Et), 161.2 (d, $^1J_{C\text{-}F}$ 245.6 Hz, Ar*C*), 152.2 (Ar*C*), 142.7 (Ar*C*H), 139.2 (d, $^4J_{C\text{-}F}$ 3.0 Hz, Ar*C*), 127.4 (d, $^3J_{C\text{-}F}$ 8.1 Hz, 2 × Ar*C*H), 115.3 (d, $^2J_{C\text{-}F}$ 21.4 Hz, 2 × Ar*C*H), 110.3 (Ar*C*H), 108.5 (Ar*C*H), 69.4 (*C*(1)HOH), 65.9 (*C*(3)HOC(O)Et), 42.5 (*C*(2)H_2), 27.6 (*C*$H_2$$CH_3$), 9.1 (*C*$H_3$); **^{19}F NMR** (471 MHz, $CDCl_3$) δ = −114.90.

Data for minor diastereoisomer syn-**6f'**: **^{1}H NMR** (500 MHz, $CDCl_3$) *(selected)* δ = 6.04 (t, *J* 7.2 Hz, 1H, C(3)*H*OC(O)Et), 4.64 (dd, *J* 8.6, 4.7 Hz, 1H, C(1)*H*OH); **^{13}C NMR** (126 MHz, $CDCl_3$) *(selected)* δ = 71.0 (*C*(1)HOH), 66.5 (*C*(3)HOC(O)Et), 45.0 (*C*(2)H_2); **^{19}F NMR** (471 MHz, $CDCl_3$) δ = −114.65.

(1*R*,3*R*)-3-(4-fluorophenyl)-1-(furan-2-yl)-3-hydroxypropyl propionate (6f'')

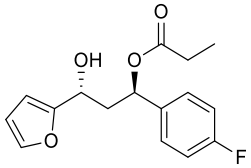

As an inseparable mixture of combined *anti* and *syn* diastereoisomers (82:18 $dr_{anti:syn}$) (9 mg, 4%) as a pale yellow oil. $[\alpha]_D^{20}$ +24.5 (*c* 0.1 in $CHCl_3$); following hydrolysis to 1-(4-fluorophenyl)-3-(furan-2-yl)propane-1,3-diol **Chiral HPLC analysis** Chiralcel ID (90:10 Hexane:IPA, flow rate 1.0 mL min^{-1}, 211 nm, 30 °C) t_R(3*R,*5*R*): 11.1 min, t_R(3*S,*5*S*): 12.8 min, 72.97:27.03 *er*; **IR** (neat) ν_{max}: 3439 (OH), 1732 (C=O), 1606, 1510, 1223, 1182, 1157, 1080,

1065, 1011 cm^{-1}; **HRMS** (ESI): calcd. for $C_{16}H_{17}O_4FNa^+$ ($[M+Na]^+$): 315.1009; found 315.0995.

Data for major diastereoisomer anti-**6f''**: **^{1}H NMR** (500 MHz, $CDCl_3$) δ = 7.40 (dd, *J* 1.8, 0.8 Hz, 1H, ArH), 7.38 – 7.33 (m, 2H, ArH), 7.09 – 7.02 (m, 2H, ArH), 6.38 – 6.33 (m, 1H, ArH), 6.28 (dt, *J* 3.2, 0.8 Hz, 1H, ArH), 6.04 (dd, *J* 10.3, 3.6 Hz, 1H, C(3)*H*OC(O)Et), 4.75 (dt, *J* 9.2, 4.2 Hz, 1H, C(1)*H*OH), 2.70 (d, *J* 4.9 Hz, 1H, OH), 2.47 – 2.34 (m, 3H, C$H_2$$CH_3$ and C(2)H_2), 2.26 (ddd, *J* 14.4, 9.7, 3.6 Hz, 1H, C(2)H_2), 1.16 (t, *J* 7.5 Hz, 3H, CH_3); **^{13}C NMR** (126 MHz, $CDCl_3$) δ = 174.4 (CHO*C*(O)Et), 162.4 (d, $^1J_{C\text{-}F}$ 246.6 Hz, Ar*C*), 155.6 (Ar*C*), 142.2 (Ar*C*H), 136.2 (d, $^4J_{C\text{-}F}$ 3.2 Hz, Ar*C*), 128.2 (d, $^3J_{C\text{-}F}$ 8.2 Hz 2 ×Ar*C*H), 115.5 (d, $^2J_{C\text{-}F}$ 21.5 Hz, 2 ×Ar*C*H), 110.3 (Ar*C*H), 106.2 (Ar*C*H), 72.0 (*C*(3)HOC(O)Et), 64.0 (*C*(1)HOH), 42.6 (*C*(2)H_2), 27.7 (*C*$H_2$$CH_3$), 9.1 (*C*$H_3$); **^{19}F NMR** (471 MHz, $CDCl_3$) δ = −113.95

Data for minor diastereoisomer syn-**6f''**: **^{1}H NMR** (500 MHz, $CDCl_3$) *(selected)* δ = 5.89 (t, *J* 7.2 Hz, 1H, C(3)*H*OC(O)Et), 4.61 (dd, *J* 8.3, 5.4 Hz, 1H, C(1)*H*OH); **^{13}C NMR** *(selected)* (126 MHz, $CDCl_3$) δ = 72.8 (*C*(3)HOC(O)Et), 64.9 (*C*(1)HOH); **^{19}F NMR** (471 MHz, $CDCl_3$) δ = −113.85.

(1*S*,3*S*)-1-(4-fluorophenyl)-3-(furan-2-yl)propane-1,3-diyl dipropionate (7f)

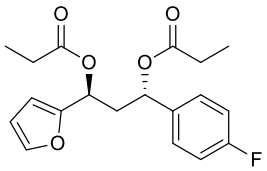

(82 mg, 32%) as a yellow oil with spectroscopic data in accordance with the literature.[5] $[\alpha]_D^{20}$ −88.8 (*c* 1.2 in $CHCl_3$) {Lit.[5] $[\alpha]_D^{25}$ (98:2 *er*) −135.3 (*c* 1.0, $CHCl_3$)}; following hydrolysis to 1,5-diphenylpent-4-ene-1,3-diol **Chiral HPLC analysis** Chiralcel ID (90:10 Hexane:IPA, flow rate 1.0 mL min^{-1}, 211 nm, 30 °C) t_R(3*R,*5*R*): 11.1 min, t_R(3*S,*5*S*): 12.8 min, 7.98:92.02 *er*; **^{1}H NMR** (500 MHz, $CDCl_3$) δ = 7.40 (t, *J* 1.3 Hz, 1H, ArH), 7.37 – 7.30 (m, 2H, ArH), 7.09 – 7.01 (m, 2H, ArH), 6.35 (d, *J* 1.4 Hz, 2H, ArH), 6.03 – 5.93 (m, 1H, C(3)*H*OC(O)Et), 5.86 – 5.79 (m, 1H, C(1)*H*OC(O)Et), 2.57 – 2.44 (m, 2H, C(2)H_2), 2.42 – 2.27 (m, 4H, C$H_2$$CH_3$), 1.13 (q, *J* 7.5 Hz, 6H, CH_3); **^{19}F NMR** (471 MHz, $CDCl_3$) δ = −113.79.

Procedure of Kinetic Resolution (±)-6a in flow-mode conditions

A packed bed reactor consisting of a vertically-mounted Omnifit glass chromatography column [borosilicate glass; length = 100 mm (70 mm adjustable bed height); internal diameter = 10 mm; maximum bed volume 5.6 mL], with a glass cooling jacket was loaded with PS-HyperBTM resin (600 mg; *f* = 0.89 mmol g^{-1}). The resin was allowed to swell to its maximum volume by pumping 1:1 THF:$CHCl_3$ mixture at 1 μL min^{-1} for 30 min at RT using a Gilson 305

HPLC pump. Two syringes were used to inject reagents using a Legato 200 series syringe pump by World Precision Instruments. The first syringe was filled with a solution of (±)-(1*E*,6*E*)-5-hydroxy-1,7-diphenylhepta-1,6-dien-3-yl propionate (0.3 mmol, 1.0 equiv.) and $(EtCO)_2O$ (0.17 mmol, 0.55 equiv.) in 1:1 THF:$CHCl_3$ mixture (3.0 mL total volume) and the second syringe with *i*-Pr_2NEt (0.17 mmol, 0.55 equiv.) in 1:1 THF:$CHCl_3$ mixture (3.0 mL total volume). Both solutions were injected at 100 μL min^{-1}, mixed in a T-type mixing chamber, and passed through the reactor at a combined flow rate of 200 μL min^{-1}. After complete addition of the reagents from the syringes, a Gilson 305 HPLC pump was connected, and $CHCl_3$ was pumped at 200 μL min^{-1} for 30 min to ensure elution of the products. A solution of 10% MeOH in 1:1 THF:$CHCl_3$ mixture was then pumped at 200 μL min^{-1} for 30 min to wash the column and avoid cross contamination. The column was then prepared for the next KR by pumping 1:1 THF:$CHCl_3$ mixture at 200 μL min^{-1} for 30 min. The mixture was concentrated to remove THF and later diluted with CH_2Cl_2. So, it was washed sequentially with HCl (1 M), saturated $NaHCO_3$ and brine. The organic layer was dried (Na_2SO_4), filtered and concentrated to give the crude products. The corresponding monoester and diester were then isolated by flash chromatography (90:10 Hexane:EtOAc).

(1*E*,3*R*,5*R*,6*E*)-5-hydroxy-1,7-diphenylhepta-1,6-dien-3-yl propionate (6a): **Chiral HPLC analysis** Chiralpak IC (90:10 Hexane:IPA, flow rate 1.0 mL min^{-1}, 211 nm, 30 °C) t_R(3R,5*R*): 12.2 min, t_R(3*R*,5*R*): 14.0 min, 19.38:80.62 *er*;

(1*E*,3*S*,5*S*,6*E*)-1,7-diphenylhepta-1,6-diene-3,5-diyl dipropionate (7a): **Chiral HPLC analysis** Chiralcel OJ-H (85:15 Hexane:IPA, flow rate 1.5 mL min^{-1}, 211 nm, 30 °C) t_R(3*R*,5*R*): 9.5 min, t_R(3*S*,5*S*): 13.4 min, 80.11:19.89 *er*.

8.5 References and notes

1. J.-P. Vigneron, M. Dhaenes, A. Horeau, *Tetrahedron* **1973**, *29*, 1055−1059.
2. Selected publications: a) A. J. Wagner, J. G. David, S. D. Rychnovsky, *Org. Lett.* **2011**, *13*, 4470−4473; b) M. A. Perry, J. V. Trinidad, S. D. Rychnovsky, *Org. Lett*. **2013**, *15*, 472−475; c) A. J. Wagner, S. D. Rychnovsky, *J. Org. Chem.* **2013,** *78*, 4594−4598; d) A. Burtea, S. D. Rychnovsky, *Org. Lett.* **2017**, *19*, 4195−4198; e) A. S. Burns, C. C. Ross, S. D. Rychnovsky, *J. Org. Chem.* **2018**, *83*, 2504−2515.
3. Some representative examples: a) G. A. Crispino, P. T. Ho, K. B. Sharpless, *Science,* **1993**, *259*, 64−66; b) J. A. Enquist, B. M. Stoltz, *Nature.* **2008**, *453*, 1228−1231; c) N. J. Green, A. L. Lawrence, G. Bojase, A. C. Willis, M. N. Paddon-Row, M. S. Sherburn, *Angew. Chem. Int. Ed.,* **2013**, *125*, 8491−8494; d) K. Mori, Y. Ichikawa, M. Kobayashi, Y. Shibata, M. Yamanaka, T. Akiyama, *J. Am. Chem. Soc.* **2013**, *135*, 3964−3970.
4. S. Harrer, M. D. Greenhalgh, R. M. Neyyappadath, A. D. Smith, *Synlett,* **2019**, *30*, 1555−1560.
5. J. Merad, P. Borkar, F. Caijo, J.-M. Pons, J.-L. Parrain, O. Chuzel, C. Bressy, *Angew. Chem. Int. Ed*., **2017**, *56*, 16052−16056.
6. L. C. Morrill, J. Douglas, T. Lebl, A. M. Z. Slawin, D. J. Fox, A. D. Smith *Chem. Sci.* **2013**, *4*, 4146−4155.
7. H. Yang, W. -H. Zheng, *Tetrahedron Lett.* **2018**, *59*, 583−591.
8. J. I. Murray, Z. Heckenast, A. C. Spivey, In *Lewis Base Catalysis in Organic Synthesis, Vol. 2*; E. Vedejs, S. E. Denmark, Ed. Wiley-VCH: Weinheim, **2016**, 459.
9. (a) A. Chatterjee, N. N. Joshi, *Tetrahedron* **2006**, *62*, 12137−12158. (b) N. Takenaka, G. -Y. Xia, H. Yamamoto, *J. Am. Chem. Soc.***2004**, *126*, 13198−13199. (c) H. Yang, H. Wang, C. Zhu, *J. Org. Chem.* **2007**, *72*, 10029−10034.
10. (a) K. R. K. Prasad, N. N. Joshi, *J. Org. Chem.* **1996**, *61*, 3888−3889. (b) K. Murata, K. Okano, M. Miyagi, H. Iwane, R. Noyori, T. Ikariya, *Org. Lett.* **1999**, *1*, 1119−1121. (c) T. Ohkuma, N. Utsumi, M. Watanabe, K. Tsutsumi, N. Arai, K. Murata, *Org. Lett.* **2007**, *9*, 2565−2567. (d) R. Kadyrov, R. M. Koenigs, C. Brinkmann, D. Voigtlaender, M. Rueping, *Angew. Chem. Int. Ed.* **2009**, *48*, 7556−7559.
11. (a) M. Tokunaga, J. F. Larow, F. Kakiuchi, E. N. Jacobsen, *Science* **1997**, *277*, 936−938. (b) L. P. Nielsen, C. P. Stevenson, D. G. Blackmond, E. N. Jacobsen, *J. Am. Chem. Soc.* **2004**, *126*, 1360−1362. (c) M. R. Monaco, S. Prévost, B. List, *Angew. Chem. Int. Ed.***2014**, *53*, 8142−8145. (d) S. Matsunaga, J. Das, J. Roels, E. M. Vogl, N. Yamamoto, T. Iida, K. Yamaguchi, M. Shibasaki, *J. Am. Chem. Soc.* **2000**, *122*, 2252−2260. (e) L. Zhao, B. Han, Z. Huang, M. Miller, H. Huang, D. S. Malashock, Z. Zhu, A. Milan, D. E. Robertson, D. P. Weiner, M. J. Burk, *J. Am. Chem. Soc.* **2004**, *126*, 11156−11157.
12. (a) H. C. Kolb, M. S. VanNieuwenhze, K. B. Sharpless, *Chem. Rev.* **1994**, *94*, 2483−2547; (b) A. B. Zaitsev, H. Adolfsson, *Synthesis* **2006**, 1725−1756.
13. For the two major reductive methods, see: a) D. A. Evans, K. T. Chapman, E. M. Carreira, *J. Am. Chem. Soc.* **1988**, *110*, 3560−3578; b) D. A. Evans, A. H. Hoveyda, *J. Am. Chem. Soc.* **1990**, *112*, 6447−6449.
14. a) M. Kitamura, T. Ohkuma, S. Inoue, N. Sayo, H. Kumobayashi, S. Akutagawa, T. Ohta, H. Takaya, R. Noyori, *J. Am. Chem. Soc*. **1988**, *110*, 629−631; b) A. K. Dilger, V. Gopalasamuthiram, S. D. Burke, *J. Am. Chem. Soc.* **2007**, *129*, 16273−16277; c) Y. Lu, I. S. Kim, A. Hassan, D. J. Del Vall, M. J. Krische, *Angew. Chem. Int. Ed.* **2009**, *48*, 5018−5021; *Angew. Chem.* **2009**, *121*, 5118−5121; Aldol-Tischenko process: a) C. M. Mascarenhas, S. P. Miller, P. S. White, J. P. Morken, *Angew. Chem. Int. Ed.* **2001**, *40*, 601−603; *Angew. Chem.* **2001**, *113*, 621−623; b) V. Gnanadesikan, Y. Horiuchi, T. Ohshima, M. Shibasaki, *J. Am. Chem. Soc.* **2004**, *126*, 7782−7783; c) B. Martín-Matute, M. Edin, J.-E. Bäckvall, *Chem. Eur. J*. **2006**, *12*, 6053−6061.
15. (a) H. B. Kagan, J. C. Fiaud, J. C. In *Topics in Stereochemistry* **1988**, *18*, 249−330; (b) C.-S. Chen, Y. Fujimoto, G. Girdaukas, C. J. Shi, *J. Am. Chem. Soc.* **1982**, *104*, 7294−7299; (c)

M. D. Greenhalgh, J. E. Taylor, A. D. Smith, *Tetrahedron* **2018**, *74*, 5554−5560; (d) J. M. Keith, J. F. Larrow, E. N. Jacobsen, *Adv. Synth. Catal.* **2001**, *343*, 5−26.
16. C. De Risi, O. Bortolini, A. Brandolese, G. Di Carmine, D. Ragno, A. Massi, *React. Chem. Eng.*, **2020**, *5*, 1017−1052.
17. a) M. Benaglia, A. Puglisi, F. Cozzi, *Chem. Rev.* **2003**, *103*, 3401–3429; b) A. F. Trindade, P. M. P. Gois, C. A. M. Alfonso, *Chem.Rev.* **2009**, *109*, 418–514; c) T. E. Kristensen, T. Hansen, Eur. *J. Org. Chem.* **2010**, 3179–3204; d) B. Altava, M. I. Burguete, E. Garcia-Verdugo, S. V. Luis, *Chem. Soc. Rev.* **2018**, *47*, 2722–2771; d) C. Rodríguez-Escrich, M. A. Pericàs, *Eur. J. Org. Chem.* **2015**, 1173–1188; e) C. Rodríguez-Escrich, M. A. Pericàs, *Chem. Rec.* **2019**, *19*, 1872–1890; f) T. Yu, Z. Ding, W. Nie, J. Jiao, H. Zhang, Q. Zhang, C. Xue, X. Duan, Y. M. A. Yamada, P. Li, *Chem. Eur. J.* **2020**, *26*, 5729–5747.
18. For selected reviews on organocatalysis, see: (a) A. Sinibaldi, V. Nori, A. Baschieri, F. Fini, A. Arcadi, A. Carlone, *Catalysts*, **2019**, *9*, 928−963; (b) V. D. G. Oliveira, M. F. D. C. Cardoso, L. D. S. M. Forezi, *Catalysts*, **2018**, *8*, 605−634; (c) P. Vogel, Y.-H. Lam, A. Simon, K. N. Houk, *Catalysts*, **2016**, *6*, 128−193; (d) J. Aleman, S. Cabrera, *Chem. Soc. Rev.*, **2013**, *42*, 774−793; (e) S. Bertelsen, K. A. Jørgensen, *Chem. Soc. Rev.*, **2009**, *38*, 2178−2189; (f) D. W. C. MacMillan, *Nature*, **2008**, *455*, 304−308; (g) P. Melchiorre, P. Marigo, A. Carlone, G. Bartoli, *Angew. Chem., Int. Ed.*, **2008**, *47*, 6138−6171; (h) P. I. Dalko, L. Moisan, *Angew. Chem., Int. Ed*., **2004**, *43*, 5138−5175.
19. R. M. Neyyappadath, R. Chisholm, M. D. Greenhalgh, C. Rodriguez-Escrich, M. A. Pericàs, G. Hähner, A. D. Smith, *ACS Catal.* **2018**, *8*, 1067–1075.
20. a) R. M. Neyyappadath, R. Chisholm, M. D. Greenhalgh, C. Rodríguez-Escrich, M. A. Pericàs, G. Hähner, A. D. Smith, *ACS Catal.,* **2018**, *8*, 1067−1075; b) N. R. Guha, R. M. Neyyappadath, M. D. Greenhalgh, R. Chisholm, S. M. Smith, M. L. McEvoy, C. M. Young, C. Rodríguez-Escrich, M. A. Pericàs, G. Hähner, A. D. Smith, *Green Chem.* **2018**, *20*, 4537–4546; c) J. Lai, R. M. Neyyappadath, A. D. Smith, M. A. Pericàs, *Adv. Synth. Catal.* **2020**, *362*, 1370–1377.
21. M. D. Greenhalgh, S. M. Smith, D. M. Walden, J. E. Taylor, Z. Brice, E. R. T. Robinson, C. Fallan, D. B. Cordes, A. M. Z. Slawin, H. C. Richardson, M. A. Grove, P. H.-Y. Cheong, A. D. Smith, *Angew. Chem. Int. Ed.,* **2018**, *57*, 3200−3206.
22. For representative examples see: a) V. B. Birman, X. Li, *Org. Lett.*, **2006**, *8*, 1351−1354; b) V. B. Birman, L. Guo, *Org. Lett.*, **2006**, *8*, 4859−4861; c) I. Shiina, K. Nakata, *Tetrahedron Lett.,* **2007**, *48*, 8314−8317; d) V. B. Birman, X. Li, *Org. Lett.*, **2008**, *10*, 1115−1118; e) Q. Hu, H. Zhou, X. Geng, P. Chen, *Tetrahedron*, **2009**, *65*, 2232−2238; f) I. Shiina, K. Nakata, K. Ono, M. Sugimoto, A. Sekiguchi, *Chem. Eur. J.,* **2010**, *16*, 167−172; g) D. Belmessieri, C. Joannesse, P. A. Woods, C. MacGregor, C. Jones, C. D. Campbell, C. P. Johnston, N. Duguet, C. Concellón, R. A. Bragg, A. D. Smith, *Org. Biomol. Chem*., **2011**, *9*, 559−570; h) X. Li, H. Jiang, E. W. Uffman, L. Guo, Y. Zhang, X. Yang, V. B. Birman*, J. Org. Chem.*, **2012**, *77*, 1722−1737; i) K. Nakata, K. Gotoh, K. Ono, K. Futami, I. Shiina, *Org. Lett*., **2013**, *15*, 1170−1173; j) I. Shiina, K. Ono and T. Nakahara, *Chem. Commun*., **2013**, *49*, 10700−10702; k) S. F. Musolino, O. S. Ojo, N. J. Westwood, J. E. Taylor, A. D. Smith, *Chem. Eur. J.*, **2016**, *22*, 18916−18922; l) S. Qu, S. M. Smith, V. Laina-Martín, R. M. Neyyappadath, M. D. Greenhalgh, A. D. Smith, *Angew. Chem. Int. Ed.* **2020**, *59*, 2–9.
23. X. Li, H. Jiang, E. W. Uffman, L. Guo, Y. Zhang, X. Yang, V. B. J. Birman, *Org. Chem.*, **2012**, *77*, 1722−1737.
24. The efficiency of the packed bed catalyst has been evaluated prior to start the study and at the end of the work, by conducting a KR of (±)-1-phenyethanol as reported in ref. 20a.
25. E.Jahn, J. Smrček, R. Pohl, I. Cisařovà, P. G Jones, U. Jahn, *Eur.J. Org. Chem.,* **2015**, *35*, 7785−7798.
26. K. Fujii, K. Mitsudo, H. Mandai, S. Suga, *Adv. Synth. Catal.*, **2017**, *359*, 2778−2788.
27. L. Zhao, B. Han, Z. Huang, M. Miller, H. Huang, D. S. Malashock, Z. Zhu, A. Milan, D. E. Robertson, D. P. Weiner, M J. Burk, *J. Am. Chem. Soc*., **2004**, *126*, 11156−11157.

28. S. Satishkumar, M. Periasamy, *Indian Journal of Chemistry*, **2008**, *47B*, 1080−1083.
29. M. Periasamy, S. S. Kumar, N. S. Kumar, *Tetrahedron Letters*, **2008**, *49*, 4416−4419.
30. H. Kronenwetter, J. Husek, B. Etz, A. Jones, R. Manchanayakage, *Green Chem.*, **2014**, *16*, 1489−1495.
31. Y.-G. Li, Q.-S. Tian, J. Zhao, Y. Feng, M.-J. Li, T.-P. You, *Tetrahedron Asymmetry*, **2004**, *15*, 1707−1710.
32. J. Merad, P. Borkar, T. B. Yenda, C. Roux, J.-M. Pons, J.-L. Parrain, O. Chuzel, C. Bressy, *Org. Lett*., **2015**, *17*, 2118−2121.

9. Conclusion

This thesis describes the application of Lewis base organocatalysts for the development of new synthetic routes to access molecules with added-value. Overall, the results obtained are summarised below.

At the onset of this work, a deep insight into the oxidative esterification procedure promoted by NHC catalysts has been provided. As reported in Chapter 3, the investigation of a model glycerol esterification, has permitted the identification of the best performing triazolium pre-catalyst which has later been immobilized onto silica and polystyrene supports. The latter proved to be more efficient, thus leading to the synthesis of a novel class of MAG-derivatives starting from bio-based aldehydes (furfural, 5-hydroxymethylfurfural, citronellal, and vanillin) with high conversions and selectivities in batch and flow-mode approaches using the green solvent Me-THF (Figure 1). Parallelly, the same study has been extended to the oxidative esterification of solketal with a comparable level of efficiency.

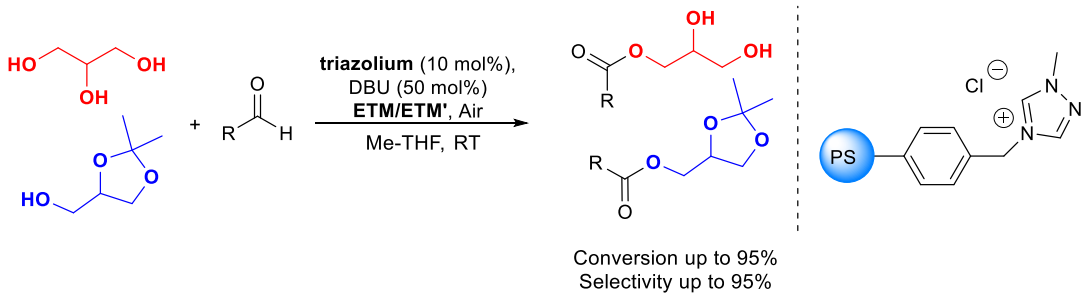

Figure 1. Esterification of glycerol and solketal by oxidative NHC-catalysis under heterogeneous batch and flow conditions.

Encouraged by these results, the valorisation of renewable chemicals has also been extended to HMF to access the valuable bio-based 5-hydroxymethyl-2-furancarboxylic acid (HMFCA). In analogy to the above-described work, a polystyrene-supported triazolylidene catalyst is capable to promote the sequential oxidative esterification of HMF leading to a key oligomeric intermediate, which can be easily elaborated into HMFCA and its ester and amide derivatives through a one-pot two-step protocol (Chapter 4, Figure 2). Furthermore, the direct conversion under batch and flow-mode conditions of HMF and furfural with suitable nucleophiles has also been exploited to expand the set of bio-based chemicals.

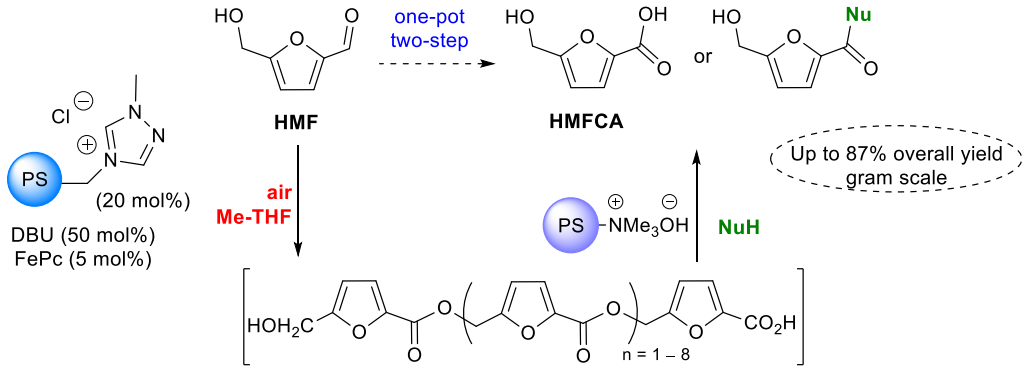

Figure 2. Aerobic oxidation of 5-hydroxymethylfurfural to 5-hydroxymethyl-2-furancarboxylic acid by heterogeneous NHC-catalysis.

The disclosed synthesis of HMF oligomeric intermediate inspired the application of a new organocatalytic protocol for the production of polyesters and polyamides as intriguing alternative to known polycondensation procedures (Chapter 5 and 6). These novel strategies for the synthesis of both polyesters and polyamides relies on the polycondensation of dialdehydes and diols or diamine, respectively (Figure 3). In the first case, an effective preparation of a series of synthetically relevant bio-based polyesters from furanic monomers, glycerol, and isosorbide has been proposed. Additionally, the compatibility of the obtained oligoesters with a subsequent NHC-catalysed chain-elongation step to achieve PEs with higher molecular weight has been proved as well. Differently, the preparation of PAs required the addition of hexafluoro-2-proponal (HFIP) as a nucleophilic additive to guarantee the oligomer growth. The mild polyamidation conditions (room temperature) together with the simple recovery of both external oxidant and HFIP may represent operational advantages of the proposed methodology. Furthermore, in this case, a subsequent chain-elongation step to achieve PAs with higher molecular weight has been investigated with a positive outcome. Finally, a significant benefit of the disclosed iterative amine-to-aldehyde condensation may consist in the utilization of readily available dialdehyde monomers including those belonging to the furanic platform, allowing an easy access to known and novel bio-based PAs for the development of environmentally benign macromolecular materials.

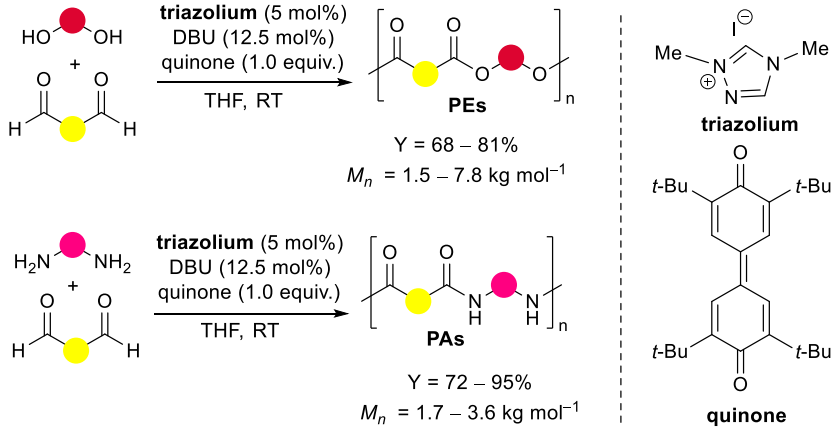

Figure 3. Oxidative NHC-catalysis as organocatalytic platform for the synthesis of polyester and polyamide oligomers.

In summary, the above reported studies underly the challenging applications of NHC Lewis base organocatalysts to create new synthetic opportunities to access molecule with added-value. The upgrading of biomass compounds has been deeply investigated along with the research of eco-sustainable procedures. For this reason, the choice of heterogeneous catalysts along with green solvents under mild conditions emerged crucial for alternative green routes.

The methodology described in Chapter 7 represents the first example of asymmetric N-acylation strategy based on oxidative NHC-catalysis leading to N3-acylated DHPMs in enantioenriched form (Figure 4). Although the enantioselectivity of the process was moderate, the use of aldehydes as mild acylating agents appear well-suited for the (stereo)chemical decoration of the DHPM nucleus and, in general, for the direct N-acylation of molecules containing the ureido functionality. Moreover, the disclosed methodology opened to investigations on the kinetic resolution promoted by NHC catalyst based on N-acylation of biologically and pharmaceutically interesting molecules.

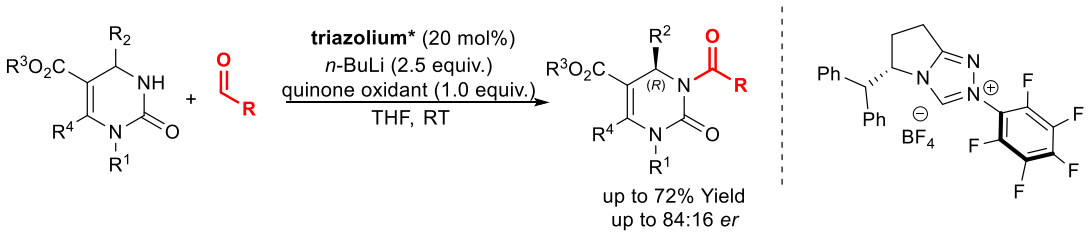

Figure 4. Enantioselective N-acylation of Biginelli dihydropyrimidines by oxidative NHC-catalysis.

Lastly, in Chapter 8 is reported a new application of Lewis base organocatalysts, a polystyrene supported isothiourea, able to promote enantioselective acylations in flow-mode conditions. Accordingly, a sequential organocatalytic kinetic resolution of (±)-*syn*-1,2-diols and (±)-*anti*-1,3-diols has been developed (Figure 5). Excellent results in terms of

enantioselectivities and isolated yield have been obtained for both processes. Additionally, the reported procedure has been conducted at room temperature making the process operationally simple to perform and the use of a flow-mode system makes the overall procedure more environmentally sustainable.

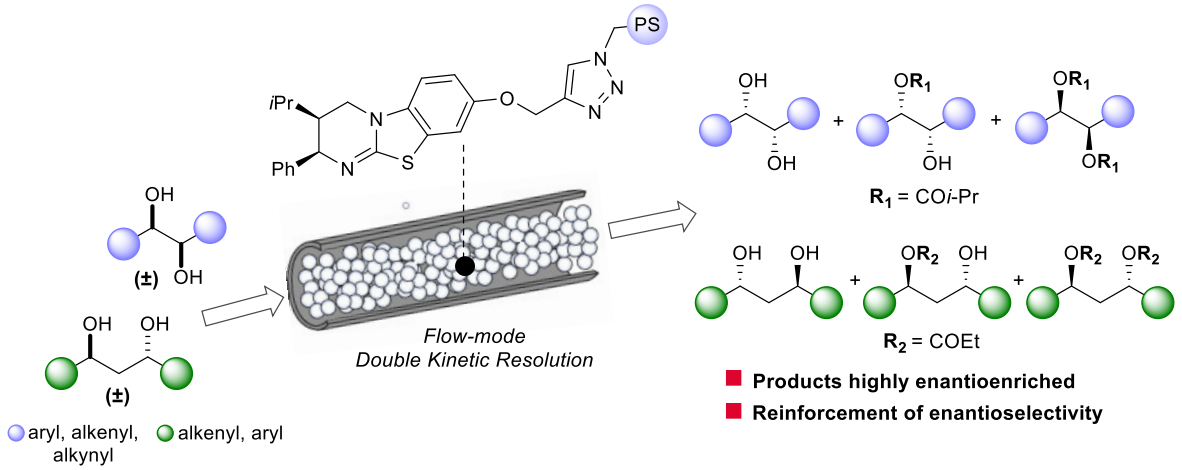

Figure 5. Organocatalytic sequantial kinetic resolution of (±)-*syn*-1,2- and (±)-*anti*-1,3-diols using solid-supported isothiourea in flow-mode conditions.

In conclusion, this PhD thesis helps to shed light on new applications of homogeneous and heterogeneous Lewis base organocatalysts, broadening the available synthetic routes to access added-value molecules thus paving the way for further progress in this field.

“Ai posteri l’ardua sentenza”

(A. Manzoni, V maggio)